

# **PENOBSCOT RIVER MERCURY STUDY**

## **Chapter 11**

### **Distribution and biogeochemical controls on net methyl mercury production in Penobscot River marshes and sediments 2009-2012**

**Submitted to Judge John Woodcock  
United States District Court (District of Maine)**

**April 2013**

By: C.C. Gilmour<sup>1</sup>, T. Bell<sup>1</sup>, A. Bullock<sup>1</sup>, A. Graham<sup>1</sup>, A. Maizel<sup>1</sup>, G. Reidel<sup>1</sup>, G. Riedel<sup>1</sup>,  
and A.D Kopec<sup>2</sup>

1. Smithsonian Environmental Research Center, Edgewater, MD
2. Penobscot River Mercury Study

## SECTION 1. STUDY DESIGN, SAMPLING AND METHODS

### 1.1 Overview of Study Design

From 2009-2011, a survey of Penobscot sediments and marsh soils was conducted to evaluate the distribution and biogeochemical controls on net methyl mercury (Hg) in the Penobscot River ecosystem. The main goals of the study were to:

- Define the habitats within the Penobscot River system where Hg contamination is most efficiently converted to methyl Hg, and
- Understand the biogeochemical drivers of net methyl Hg production in the Penobscot system

The study approach was to intensively examine the geochemical indicators of methyl Hg production, including Hg methylation rate constants, at a suite of study areas along the salinity and Hg contamination gradients of the Penobscot. The study was confined to the tidal river reach between Bangor and Fort Point. The study focused on marsh soils and river sediments/mud flats, as these have been repeatedly identified as the main zones of methyl Hg production and accumulation in estuarine systems. Although anoxic bottom waters may also contribute to methyl Hg production in some estuaries and coastal zones, Penobscot River bottom waters do not currently become anoxic during the summer, although they once did.

The study focused on the key drivers of methyl Hg production, which are Hg concentration, the bioavailability of Hg for methylation, and the activity of Hg-methylating bacteria. Biogeochemical indicators of Hg bioavailability include sulfur and iron chemistry, dissolved and bulk organic matter, Hg partitioning between solid and aqueous phases, microbial electron acceptors, and redox status.

*Initial surveys in August 2009 and May 2010.* Study sites were selected and included marsh soils, tidal mud flats and bottom sediments. The study areas selected were based on initial surveys by Normandeau Associates and the Penobscot River team, allowing the team to build a larger data set through time that includes both Normandeau and Smithsonian Environmental Research Center (SERC) sampling events. In late summer 2009, a survey of four marsh complexes along the river was conducted, plus a bottom sediment transect in the main stem of the river upstream of Fort Point. In each of the marsh complexes, samples were collected across a gradient from the tidal mud flat to the upper marsh. In the large Mendall Marsh complex, additional study sites were added on the main west and south platforms. Multiple replicate sediment and soils cores were taken in each habitat, and a variety of biogeochemical parameters in soils/sediments and pore waters were examined with depth. The survey was repeated in May/June 2010 to help evaluate the seasonality of methyl Hg production and accumulation. Two additional bottom sediment sites were sampled in 2010.

*Distribution of methyl Hg across high marsh platforms at Mendall Marsh.* As the study progressed, it became apparent that the large marsh platforms in the Mendall Marsh complex are sites of high Hg accumulation and exceptional methyl Hg production and accumulation. Over time, the study focused more on this area. During summer 2011 a

wider surveys of habitats in the Mendall complex was conducted, including sites on the main east, west and south platforms. In addition to biogeochemistry, this survey focused on the relationships between marsh plant community structure, marsh elevation and MeHg, and included site surveys of marsh vegetation done by Drs. Aram Calhoun (University of Maine) and Dianne Kopec, (PRMS). Elevation data was obtained from a LIDAR survey of the marsh.

*Influence of daily and monthly tides on methyl Hg.* In May and June of 2011, we evaluated the influence of diel and monthly tides on MeHg at a few selected sites on the Mendall Marsh west platform.

*Remediation study in Mendall Marsh study plots.* Study plots were established on the west Mendall Marsh platform in September 2010 for a test of in-situ soil amendments as potential Hg remediation options. Detailed design and results of that study are provided in a separate report. The control sites for the study plots are included in the data presented in this report.

## **1.2 Study Sites and Dates**

Table 11-1.1 gives an overview of sampling sites and dates. The full set of sampling sites with locations is given in the data appendices (Sites Table).

Four marsh complexes spanning a salinity range from <2 to >25 psu were sampled in August 2009 and again in May/June 2010 (Figure 11-1.1). Marshes W10 and W17 are fringing marshes along the main Penobscot River. Marsh complex W26 is along the upper Orland River. Marsh W21 is the large Mendall Marsh complex along the Marsh River. Bald Hill Cove (W10) is in the oligohaline reach of the Penobscot, while W17, W21 and W26 are mesohaline (see salinities at sampling in Figure 11-1.2).

The fringing marshes (W10, W17 and W26) are narrow marshes in which the distance from the river to the trees is generally <100 yards. They have a generally smooth elevation gradient from the mud flats to the trees; there may be a small lip near the water edge of plant growth. In each of these areas we sampled up to four habitats – mud flats, low marsh, mid-marsh and high marsh. Mud flats (MF) were sampled within walking distance seaward from the edge of vegetation, generally <20 m out. Low marsh (LM) was the vegetated area below any lip in the marsh surface (if it existed) or the closest vegetation to the river (within ~5 m). High marsh (HM) was the highest elevation marsh below the trees and large shrubs. Mid-marsh (MM) and low marsh (LM) habitats were in between, in the main portion of the marsh with emergent vegetation. The high marsh areas tended to be driest, with some woody/shrubby vegetation. Not all habitats were available in all of the marshes; and it was not always possible to obtain pore water from the high marsh sites because they were dry.

Mendall Marsh (W21) is a large marsh complex on the Marsh River, a sub-estuary of the Penobscot. Mendall Marsh is comprised of 3 main marsh platforms (east, west, south), plus additional marsh area. Each platform is at least 0.4 km wide (distance between the river and trees), and at least 10 hectares in size. The total marsh area of the complex is >50 ha. Sites MF, LM, MM and HM were established on the bank of the

main west platform, all within ~20 yards of the Marsh River. These initial sites surveys did not include any sites on the main marsh platforms at Mendall Marsh. In August 2009, we established new sites on the main west marsh platforms. These were resampled in May/June 2010. Some west Mendall marsh sites were sampled again in fall 2010, summer and fall 2011, and fall 2012 in association with *in-situ* soil amendment trials begun in fall 2010. A sampling of some of these sites in early April of 2011 was done to help evaluate methyl Hg levels during colder months. Sites on the Mendall Marsh platforms are technically high marsh sites. In this report they are often labeled “marsh platform” to separate them from the higher and dried HM sites at W10, W17, and W26. The HM site in at W21 is on high berm at the edge of the west platform of Mendall Marsh.

In 2011, a wider survey of soils in Mendall Marsh was conducted. During summer 2011, surveys of 15 additional sites in the Mendall complex were conducted in July and August, including sites on the main east, west and south platforms. The vegetation at each of these sites was assessed by Drs. Aram Calhoun (University of Maine) and Dianne Kopec (PRMS). Maps of these study sites are shown in the results section.

Bottom sediments were sampled along a transect inside of Fort Point Cove (previously named the E-01 transect) in Aug. 2009 and May/June 2010. The study was initially designed to sample bottom sediments along the full salinity gradient of the river. We attempted to retrieve bottom sediments along and upstream from Verona Island using a variety of small coring devices that could be deployed from a small boat and winch, including small box corers, gravity cores and a small Ponar dredge. After multiple sampling attempts, and examination of river bottom sonar, we concluded that the river bottom is mainly rocky, probably scoured, and not accumulating soft sediment. Therefore, we were not able to sample this type of bottom with available equipment. However, without accumulating sediment, the river bottom is an unlikely location for methyl Hg production. We had also planned to sample mud flats at different depth below mean high tide, but were generally unable to obtain samples with available equipment. While we were able to access mud flats just below the vegetation line by walking out on the mud flats and sampling by hand, safety precluded walking very far out on the mud flats at low tide. We were able to sample two sites with particularly soft bottoms from a boat in June 2010. These were mud bank sites on the east side of Verona Island (ES11, in 3' of water) and near the Marsh River, (OB1, in 15' of water).

<b>Table 11-1.1: Marsh areas and sediments sampled, with dates and habitats sampled within each area. MF=mud flats; LM=low marsh; MM=mid marsh; HM=high marsh. Sites PB-E01, PB-E03 and PB-E05 are the same as PRMS sites E01-1, E01-3 and E01-5 (see Chapter 11b).</b>			
<b>Marsh Complexes</b>	<b>Name</b>	<b>Dates Sampled</b>	<b>Habitats Sampled</b>
W10	Bald Hill Cove	Aug 2009	MF, LM, MM, HM
		May/June 2010	LM, MM
W17		Aug 2009	MF, LM, MM, HM
		May/June 2010	LM, MM

**Table 11-1.1: Marsh areas and sediments sampled, with dates and habitats sampled within each area. MF=mud flats; LM=low marsh; MM=mid marsh; HM=high marsh. Sites PB-E01, PB-E03 and PB-E05 are the same as PRMS sites E01-1, E01-3 and E01-5 (see Chapter 11b).**

Marsh Complexes	Name	Dates Sampled	Habitats Sampled
W21	Mendall Marsh	August 2009	MF, LM, MM, HM, West Platform (3 sites)
		May/June 2010	LM, MM, HM, West Platform (3 sites) South Platform (1 sites)
		September 2010	West Platform (2 sites)
		October 2010	West Platform (2 sites)
		April 2011	LM, HM, West Platform (4 sites) South Platform (1 site)
		June 2011	West Platform (4 sites) East Platform (5 sites) South Platform (3 sites)
		July 2011	West Platform (6sites) East Platform (8 sites) South Platform (3 sites)
		Sept ember 2011	West Platform (2 sites)
		September 2012	West Platform (2 sites)
		August 2009	MF, LM, MM
<b>Sediments</b>			
E0 Transect	Inside Fort Point	August 2009	PB-E01, PB-E03, PB-E05
		May/June 2010	PB-E01, PB-E03
Frankfort Flats		May/June 2010	OB-1
East side of Verona island		May/June 2010	ES-11
Notes: Marsh habitat types vary somewhat between the fringing marshes (W10, W17 and W26) and the large Mendall Marsh complex (W21); see text.			

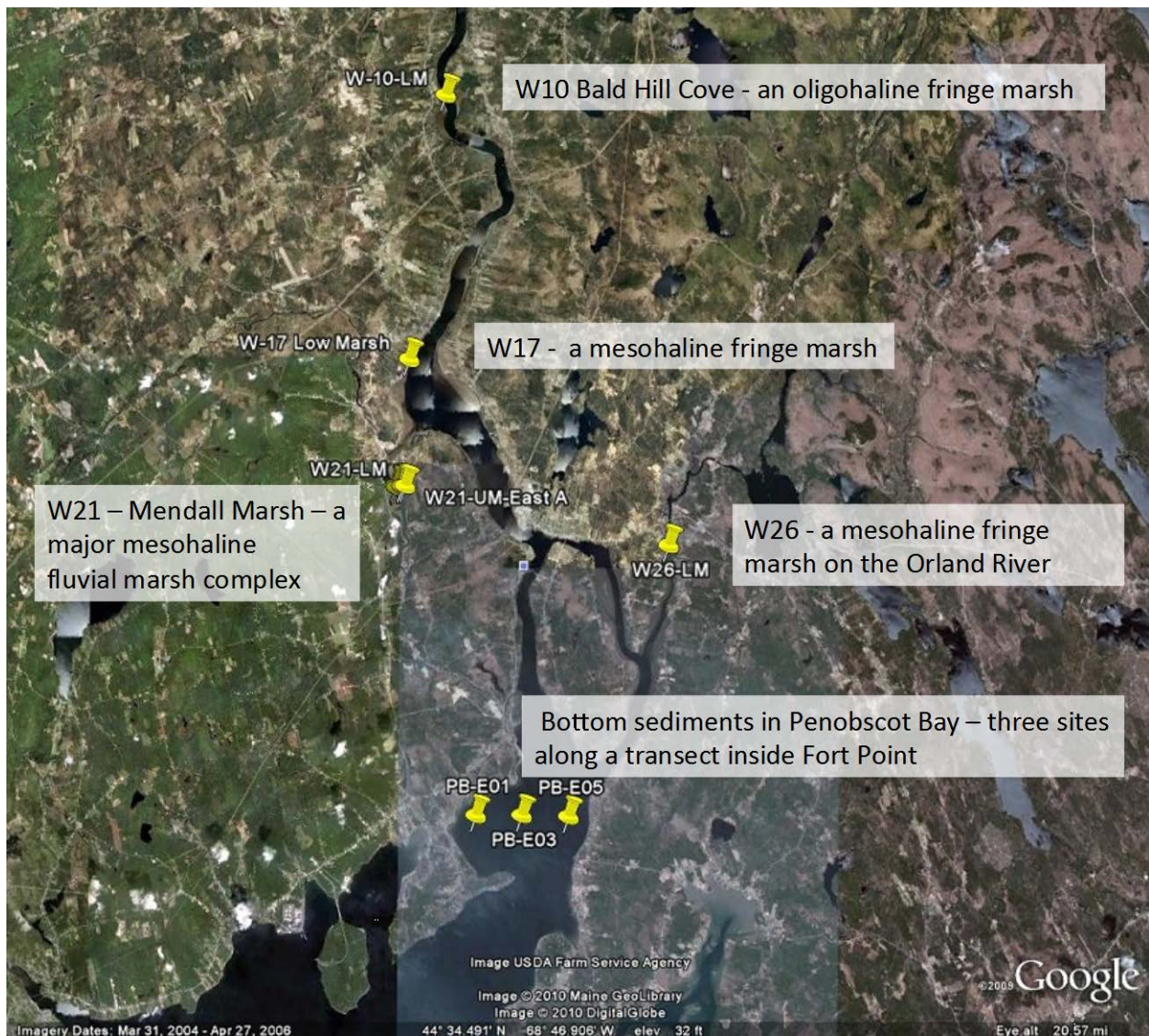


Figure 11-1.1. Study sites areas, fall 2009 and June 2010.

### 1.3 Sampling Design and Methods

This section provides an overview of sampling methods by sampling date. Detailed sampling methods are provided in SERC SOPs, which are available from the project.

#### 1.3.1 August 2009 and May/June 2010

These surveys were designed to evaluate methyl Hg concentrations and production rates across habitat types, salinity, and sediment or soil depth. The salinity range of the sites sampled is shown in Figure 11-1.2.

*Sampling.* At each study site during each survey, up to 20 sediment or soil cores were sampled simultaneously in order to measure a suite of parameters with depth in solids and in interstitial waters. The total number of sites sampled in August 2009 was 21. The total number of sites sampled in May/June 2010 was 15.

Marsh and mud flat study sites were accessed on foot from road access points or more often by boat. In marshes and mud flats, cores were sampled by hand into multiple 4.8 cm ID core tubes. The method is detailed in SERC SOP "Sediment And Soil Sampling Using Hand Coring Techniques." To summarize, clear core tubes were pushed or twisted into the soil or sediment, capped with a rubber stopper and removed. Generally, 15-20 cores were collected at each site, over an area of about a square meter. All cores were pushed into place before any were removed. A bottom stopper was pushed into place during removal. Overlying water was left on cores until processing. Cores were placed in a rack fitted into a cooler. Cores to be used for microbial rate activity measurements were kept at ambient marsh surface soil temperature; cores to be used for chemical measurements were iced. Sediments and soils were generally sampled on a morning low tide when there was no overlying water on the marsh or mud flat. Samples were processed the same day.

Sediment sites in Penobscot Bay (E0 transect) and River (OB1 and ES11) were sampled from a small boat. Shallow site E01-1 was sampled using an Ekman box corer. Sites E01-3 and E01-5 were sampled using a Van Veen dredge. Once deployed and recovered on the boat, the dredge material was subsampled from the open dredge using 4.8 cm core tubes. This sampling gear limited the depth of samples, often to only 3 cm, depending on how far the dredge penetrated bottom material.

Basic field parameters collected included surface soil temperature (~2 cm depth), air temperature, soil surface pH, and water depth where needed. Soil pH was measured with a calibrated Oakton pH spear (designed for wet solid samples).

*Sample processing.* Cores were returned to the Winterport field laboratory within two hours of sampling and processed immediately. To preserve redox-sensitive analytes, all cores were sectioned and processed inside an O<sub>2</sub>-free glove bag. In August 2009, the depths examined were 0-3, 3-6, 6-9 and 9-12 cm below the surface of the sediment or soil, where sample was available. In May/June 2010, the 9-12 cm depth interval was dropped because it was apparent that most methyl Hg production and accumulation was in shallower depths.

Table 11-1.2 is a full list of parameters measured in bulk sediments; Table 11-1.3 is the parameter list for pore waters. Sample preservation methods are given in Tables 11a-1.4. Each parameter measured was taken from composite sections or pore waters from 3 or more cores. For bulk parameters, three cores sections were combined in a sampling cup or bag (depending on the analysis). Air was removed from bags and samples were frozen immediately in freezers in the Winterport laboratory. Prior to analysis, these bulk samples were thawed and homogenized in a glove bag at SERC. A duplicate field sample was taken for each analyte group (with separate sample numbers) roughly every 10th sample.

Pore waters were separated from core sections in the Winterport laboratory within a few hours of sampling, by centrifugation followed by filtration. Details are in SOP "Extraction Of Pore Water From Sediment Cores By Centrifugation." Basically, core sections were placed in centrifuge jars inside the glove bag, where they were tared and sealed. Generally, sections from the same depth interval from 2-3 cores were combined in one

jar to provide a composite sample with enough volume for all desired analyses. Sealed jars were removed from the glove bag and centrifuged; then brought back into the glove bag for filtration. All of the pore water from each depth interval was combined prior to filtration, so that all analytes are taken from the same parcel of combined pore water. Sulfide samples were placed in sulfide-antioxidant buffer inside the glove bag. Pore water pH was measured immediately on extracted pore water with a calibrated pH probe. Other samples were preserved immediately as indicated. Filter blanks were taken and preserved using the same methods, filtering SERC DI water concomitantly in the Winterport field laboratory. A duplicate field sample was taken for each analyte group (with separate sample numbers) roughly every 10th sample, where sufficient sample volume was available.

*Methylation rate constant measurements* were made in triplicate intact cores from each site, following methods in Mitchell et al. 2008 and Hollweg et al. 2009. Potential Hg methylation rate constants were measured using spike additions of enriched  $^{201}\text{Hg}$  (98.11% purity). A  $200\text{ mg ml}^{-1}$  stock solution of  $^{201}\text{Hg}$  (as  $\text{HgCl}$ ) was diluted with overlying water from each site and left to equilibrate for one hour prior to injection into the soil cores. 100 mL of the solution was then injected at 1 cm intervals in each core through silicon septa. Injections were made as spatially uniform as possible throughout each section by manipulating the syringe during injection. Target  $^{201}\text{Hg}$  addition levels were  $100\text{ ng/g}$ ; the  $^{201}\text{Hg}$  spike was measured explicitly in each sample and used to calculate rate constants. Soil cores were then incubated in the dark at ambient surface soil temperatures, for 6 h in August 2009, or 3 h in June 2010. Incubations were ended by sectioning and freezing of the soil. Since newly introduced Hg may be more bioavailable for Hg(II)-methylation than ambient Hg, rate constants can only be considered as potentials. Prior to analysis, soil sections were thawed and homogenized.

Non-contaminating, Hg clean techniques were used through all stages of sample collection, storage, handling and analysis. Samples were collected using methods that minimized contamination through the use of clean sampling equipment, sample containers, gloves, and plastic bags to prevent sample contact with unclean surfaces. Sample integrity was carefully maintained throughout the sampling process, from field collection to delivery of samples to the laboratory. All samples were stored away from sunlight to limit the effect of photo degradation, biological activity and assure sample integrity. Samples were individually numbered and tracked.

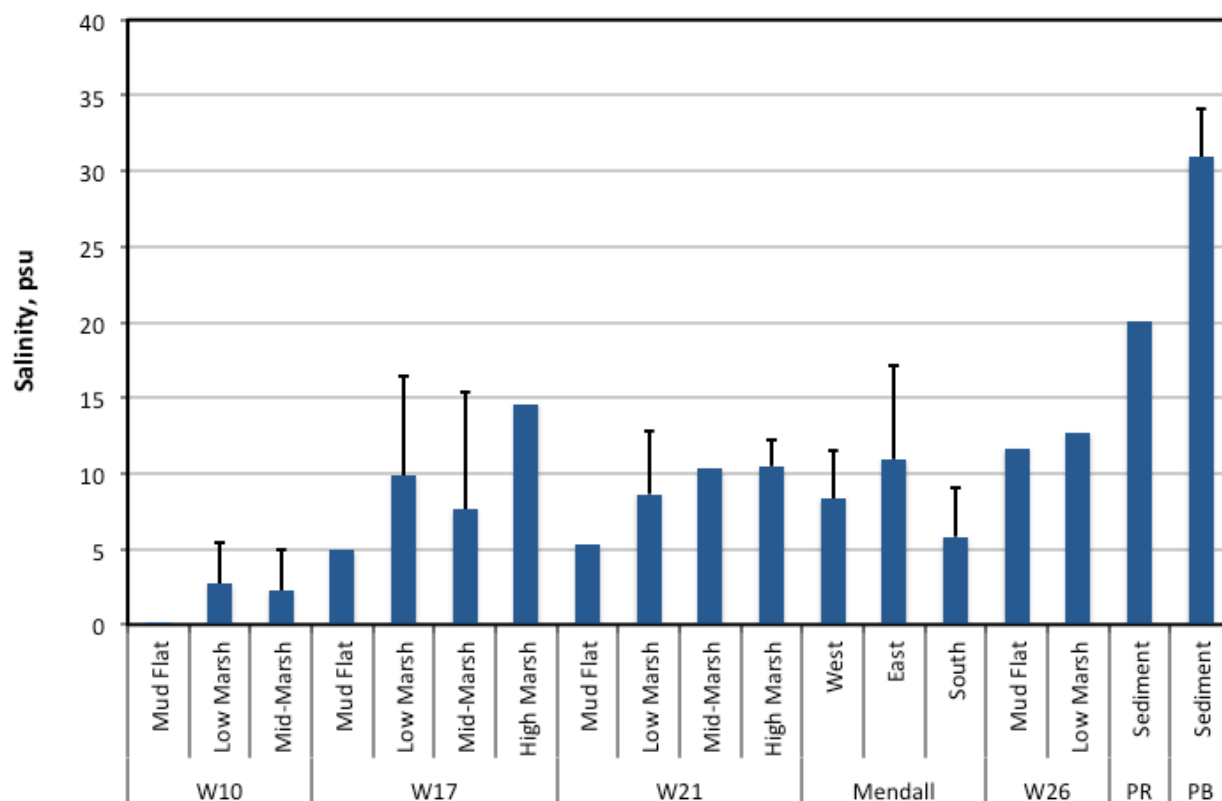


Figure 11-1.2. Average salinities of each major marsh complex and sediment area sampled in August 2009 and May/June 2010. Salinities were derived from the measured chloride content of pore waters, and averaged across all surficial samples taken in the area during the sampling trip.

### 1.3.2 Remediation plot sampling in Fall 2010, 2011 and 2012

Two sites on the Mendall west marsh platform (W21-UM-West-A W21-UM-Central-B) were used in a plot study of potential in situ remediation approaches. Data from controls were used in the results of this report. Sampling details for this study are provided in a separate report. To summarize, the study focused only on the soil surface; so samples were collected from one depth only at each site (0-3 cm composite cores for solids; and a composite pore water sample centered on a 5 cm depth). Samples were collected for all of the parameters listed in Tables 11a-1.2 and 11a-1.3, however, methylation rate constants were not measured.

Small surface soil cores were collected by hand using sharpened stainless-steel cork borers (2 cm diameter X 9 cm depth), and cut to 3 cm depth. Four cores from each plot were composited for analysis. Soil interstitial waters (pore waters) were collected for the plot study using stainless steel push point sippers (<http://www.mheproducts.com>). Use of the sippers in SERC projects is described in detail in SOP: "Extraction Of Pore Water From *In-Situ* Sediments Using Push Points." Sippers were pushed into soils to 5 cm depth. In each plot, pore waters were extracted from 4 locations. At each location, the first 10 ml of sample was wasted as a rinse, and then next 20 ml were retained. Volumes taken from each insertion of the sipper were limited to 20 ml per to make sure

that pore waters were withdrawn only from the top few cm of soils. Pore water samples from each plot were composited for analysis.

Sulfide samples were filtered and immediately preserved in sulfide-antioxidant buffer in the field. The remaining pore water samples were kept in 60 cc syringes (without headspace) on ice in coolers in the dark until they were filtered and processed in the Winterport laboratory. All four samples were composited for filtration and analysis. Sample filtration and preservation usually occurred in the afternoon, after morning collection.

### 1.3.3 April 2011

Solid 0-3 cm core samples were taken at 7 sites in west Mendall Marsh in early spring 2011 to evaluate methyl Hg concentrations during this season. Samples were collected using cork-borers as described above. Four cores were composited from each site. Methylation rate measurements were not made, nor were pore waters sampled.

### 1.3.4 Summer 2011 marsh survey

This survey also focused on surface soils. Sampling methods and samples collected were the same as the remediation plot sampling described above.

<b>Table 11-1.2: Parameters measured in soil solids. For the remediation plot studies, all samples were taken from 0-3 cm depth cores. For other sites, multiple depths were often sampled. All core samples were place in coolers on ice in the field, and frozen in bags with air excluded within hours of collection.</b>	
<b>Parameter</b>	<b>Units</b>
Bulk density, wet	g wet wt./cc
Bulk density, dry	g dry wt./cc
Porosity	ml/cc
Loss on ignition (LOI)	%
Total Hg	ng/g dry wt.
Methyl Hg	ng/g dry wt.
Acid-volatile sulfides (AVS)	μmoles/g dry wt.
Chromium-reducible sulfides (CRS)	μmoles/g dry wt.
Extractable Fe(II)	μmoles/g dry wt.
Extractable Fe(III)	μmoles/g dry wt.
Elemental Analysis (Al, Ca, Fe, K, Mg, Mn, Na, P, S, Si)	mg/g dry wt.

**Table 11-1.3: Parameters measured in soil pore waters. Pore waters were collected from centrifuged core sections and from sippers in the field. Depths varied.**

Parameter	Units
Total Hg	ng/L
Methyl Hg	ng/L
Sulfide	μM
Anions (Br, Cl, F, NO <sub>2</sub> , NO <sub>3</sub> , PO <sub>4</sub> , SO <sub>4</sub> )	μM
Nutrients (NH <sub>4</sub> , NO <sub>2</sub> +NO <sub>3</sub> , PO <sub>4</sub> )	μM
Dissolved organic carbon (DOC)	mg C/L
DOC spectral properties:	
Absorbance @ 280 nm (aCDOM 280)	m <sup>-1</sup>
Absorbance @ 440 nm (aCDOM 440)	m <sup>-1</sup>
Spectral slope, 275-295 nm	nm <sup>-1</sup>
Spectral slope, 300-700 nm	nm <sup>-1</sup>
Spectral slope, 350-400 nm	nm <sup>-1</sup>
Slope ratio (275-295/350-400)	unitless
Elemental Analysis (Al, Ca, Fe, K, Mg, Mn, Na, P, S, Si)	mg/L

**Table 11-1.4: Filtration and preservation methods for parameters measured in soil porewaters. All samples were filtered with Whatman GD/X filters (0.45 micron).**

Parameter	Preservation	Storage
Total Hg	0.5% HCl, refrigerate	PETG bottles,
Methyl Hg	0.5% HCl, refrigerate	PETG bottles,
Sulfide	Sulfide anti-oxidant buffer	50 ml polypro tubes, analyze same day
Anions	Refrigerate	15 ml polypro tubes
Nutrients	Freeze	7 ml autosampler vials
DOC	Refrigerate until spectral properties measured (24-48 h), then freeze	15 ml polypro tubes
DOC spectral properties	Refrigerate	Analyze within 48 h

<b>Table 11-1.4: Filtration and preservation methods for parameters measured in soil porewaters. All samples were filtered with Whatman GD/X filters (0.45 micron).</b>		
<b>Parameter</b>	<b>Preservation</b>	<b>Storage</b>
Elemental Analysis	0.5% HCl, refrigerate	15 ml polypro tubes

#### **1.4 Analytical Methods**

Sample preparation and analysis methods are summarized in Table 11-1.5 and given in detail in the SOPs listed in the table.

*Notes on nutrient analysis.* Ammonium, phosphate and sometimes nitrate + nitrite were measured using colorimetric method at either SERC or the University of Maryland Chesapeake Biological Lab (Nutrient Analytical Services Lab). Nitrate and nitrite were also measured separately in all pore water samples by ion chromatography at SERC, with comparable detection limits to the colorimetric samples. All data are reported for comparison. For Aug 2009 pore water samples, NH<sub>4</sub> and PO<sub>4</sub> were analyzed at SERC using. Nitrate and nitrite were measured by IC. For May/June 2010 samples, NH<sub>4</sub> and PO<sub>4</sub> were not analyzed, but nitrate and nitrite were measured by IC. For all subsequent pore water samples, NH<sub>4</sub>, NO<sub>3</sub>+NO<sub>2</sub>, and PO<sub>4</sub> were measured by CBL Analytical Nutrient Services and nitrate and nitrite were measured separately by IC at SERC.

*Spectral analysis of dissolved organic matter.* The character of dissolved organic matter (DOM) in pore water was assessed using proxy measures related to the UV spectrophotometric analysis of chromophoric dissolved organic matter (CDOM). These parameters included specific UV absorbance at 280 nm (SUVA<sub>280</sub>) and the absorbance slope ratio (S<sub>R</sub>), defined by Helms et al. (2008). To characterize the DOM in our samples, UV absorbance was measured at wavelengths between 270 and 750 nm using clean 1 cm quartz cells on a Cary 4E UV visible spectrophotometer. SUVA<sub>280</sub> was calculated by dividing the UV absorbance measured at 280 nm by the concentration of DOC in the sample (units of L mg<sup>-1</sup> m<sup>-1</sup>). S<sub>R</sub> was calculated by dividing the fitted UV-absorbance slope between 275 and 295 nm by that between 350 and 400 nm (Helms et al. 2008). Both measures can be used as a first approximation of the molecular weight of DOM in the range of approximately 500–4000 (Chin et al. 1994; Helms et al. 2008). SUVA<sub>280</sub> is also related to percent aromaticity (Chin et al. 1994).

**Table 11-1.5: Sample preparation and analysis methods. All sample preparation and analysis performed at SERC except nutrients, some of which were analyzed by the Nutrient Analytical Services Laboratory at the University of Maryland Chesapeake Biological Laboratory. CBL SOPs are available at: <http://nasl.cbl.umces.edu/>.**

Parameter	Sample Preparation Method	SERC Sample Prep SOP	Sample Analysis Method	Reference	SERC Analytical SOP
Filtered total Hg in water			Oxidation, Purge And Trap, And Cold Vapor Atomic Fluorescence Spectrometry or ICP-MS	EPA 1631	total Hg FIAS-ICP-MS or HgT Tekran 2600
Filtered methyl Hg in water	Distillation	Methyl Hg Distillation Method	Ethylation, GC, CVAF or ICP-MS	EPA 1630	Methyl Hg ET-GC-ID-ICPMS or Methyl Hg MERX ET-GC-ID-ICPMS
Total Hg in solids	Hot acid digest	Sediment and Tissue Digestion for Total Hg	Oxidation, Purge And Trap, And Cold Vapor Atomic Fluorescence Spectrometry or ICP-MS	EPA 1631	total Hg FIAS-ICP-MS
Methyl Hg in solids	Distillation	Methyl Hg Distillation Method	Ethylation, GC, CVAF or ICP-MS	EPA 1630	Methyl Hg ET-GC-ID-ICPMS or Methyl Hg MERX ET-GC-ID-ICPMS
Filterable sulfide	Preserve in fresh anti-oxidant buffer		Ion selective electrode	Brouwer and Murphy 1994; Standard Methods 4500G	Analysis Of Dissolved Sulfide Ion In Aqueous Media Using Sulfide Anti-Oxidant Buffer And Sulfide Selective Electrode
Anions			Ion Chromatography	EPA 300.0A	Analysis Of Inorganic Anions In Aqueous Biogeochemical Samples By Ion Chromatography
<b>Nutrients</b>					

**Table 11-1.5: Sample preparation and analysis methods. All sample preparation and analysis performed at SERC except nutrients, some of which were analyzed by the Nutrient Analytical Services Laboratory at the University of Maryland Chesapeake Biological Laboratory. CBL SOPs are available at: <http://nasl.cbl.umces.edu/>.**

Parameter	Sample Preparation Method	SERC Sample Prep SOP	Sample Analysis Method	Reference	SERC Analytical SOP
NH <sub>4</sub>			phenol/hypochlorite method	Solorzano 1969; EPA Method 350.1	
NO <sub>2</sub> +NO <sub>3</sub>			cadmium reduction	EPA Method 352.3	
PO <sub>4</sub>			molybdate/ascorbic acid method	EPA Method 365.1	
DOC			Shimadzu - catalytically-aided platinum 680°C combustion	Suzuki et al. 1992	Determination Of DOC By High Temperature Catalytic Oxidation And Quantification By A Non-Dispersive Infrared Detector
DOC spectral properties			uv/vis spectrophotometry	Weishaar et al. 2003	
Elemental Analysis (Al, Ca, Fe, K, Mg, Mn, Na, P, S, Si)	Porewaters		ICP-AES	Lichte et al. 1987; EPA 200.7	Analysis of Trace Elements By Inductively Couple Plasma – Atomic Emission Spectrophotometry
	Solids	Open Vessel Digestion of Siliceous Sediment Samples for Elemental Analysis			
Acid-volatile sulfides (AVS)			Cold-acid (6N HCl) distillation, sulfide trapping in SAOB, detection by selective ion probe	Fossing and Jorgensen 1989; Brouwer and Murphy 1994; Gilmour et al. 1998	Determination Of Acid-Volatile And Chromium-Reducible Sulfides From Sediments By Sequential Distillation, With SAOB Trapping And Determination Using Sulfide Selective Electrode

**Table 11-1.5: Sample preparation and analysis methods. All sample preparation and analysis performed at SERC except nutrients, some of which were analyzed by the Nutrient Analytical Services Laboratory at the University of Maryland Chesapeake Biological Laboratory. CBL SOPs are available at: <http://nasl.cbl.umces.edu/>.**

Parameter	Sample Preparation Method	SERC Sample Prep SOP	Sample Analysis Method	Reference	SERC Analytical SOP
Chromium-reducible sulfides (CRS)			Hot-acid (1M Cr(II) in concentrated HCl) distillation, sulfide trapping in SAOB, detection by selective ion probe	Fossing and Jorgensen 1989; Brouwer and Murphy 1994; Gilmour et al. 1998	Same as AVS
Extractable Fe(II)/Fe(III)	0.5 M HCl extraction and hydroxylamine (NH <sub>2</sub> OH) oxidation		Ferrozine-HEPES/UV spectrophotometry at 562 nm	Stookey 1970; Lovley and Phillips 1986	Extraction and Analysis of Reactive Iron in Sediments and Soils by Colorimetric Ferrozine Analysis

## 1.5 QA/QC Overview

*Sample logs and sample numbering.* All project samples were given a unique identifier in the field, and recorded in electronic and paper sample logs. Sample numbers begin with a project identifier (in this case “PB”) followed by a two-digit year and a four digit sequential unique number (Example: PB10-6583). Sample logs and sample labels were generally pre-printed before field trips and amended as needed during sampling and fieldwork. Hard copies of sample logs are kept in ring-binders in the lab; these pages include hand-written notes from field sample processing. “Rite in the Rain” field notebooks were also kept, recording field data like GPS locations, visual observations, dates and times of sampling, etc. All samples were shipped or carried directly to SERC, by SERC or project personnel.

*Project database.* Sample logs were uploaded to a project database, maintained in ACCESS. Sample location and status were recorded and updated in the DB as samples were stored, and analysis proceeded. Once analysis was complete, datasets including full QC were formatted and uploaded to the project database. The database has been maintained by a manager who does not conduct project analyses. Data and QC were obtained for these reports by querying the project database. Collection of ongoing QC data in the DB allows project personnel an overview of QC behavior through time.

*File backups.* All files including raw instrument data, analytical files in Excel, and the project database, are maintained on Smithsonian servers. These are mirrored, and

backed up frequently (at least daily). Additional copies of files backups are maintained on lab hard drives.

*QC strategy for sampling and analysis.* In summary, the QC strategy for all analytes measured at SERC for this study (and all projects) is 5% to 10% blanks, lab duplicates and CRMs (where available). Multiple types of blanks may be obtained depending on the analyte, including field blanks. At least 5% of samples are also duplicated in the field. Analytical QA/QC is provided in detail in separately available method SOPs (listed in Table 11-1.5).

<b>Table 11-1.6: QC summary for filter-passing methyl Hg analysis at SERC. Notes: lab duplicates were not included for samples &lt; 1 ng/L. No CRM is available for methyl Hg in water at appropriate concentration. No spike recoveries calculated, sample analysis was done using isotope dilution (ID), in which a spike is added to every samples and used to calculated samples concentrations.</b>					
<b>QC Parameter</b>	<b>Min. Frequency</b>	<b>Target QC goal</b>	<b>n</b>	<b>Average</b>	<b>Standard Deviation</b>
Total # of samples			316		
# of analytical runs			16		
Batch size	Daily run	1 - 30 samples per normal batch		22.1	8.3
Distillation Blank (ng/L)	1 per batch of each appropriate type	≤ MDL	44	0.012	0.010
Lab Blank (ng/L)	1 per batch of each appropriate type	≤ MDL	25	0.09	0.06
IPC/OPR	Initial and final and 1 per 10 samples	90-110% of nominal value	51	100.8%	9.9%
Laboratory Duplicate/Analytical Duplicates	1 per 20 samples	RPD ± 20%	29	13.9%	17.8%
QCS (Standard from alternate source)	1 per batch	80-120% of nominal value	26	96.5%	12.7%
Spike Recovery	1 per 10 samples	80-120%			

**Table 11-1.7: QC summary for filter-passing total Hg analysis at SERC. Notes: lab duplicates were not included for samples < 5 ng/L.**

QC Parameter	Min. Frequency	Target QC goal	n	Average	Standard Deviation
Total # of samples			321		
# of analytical runs			15		
Batch size	Daily run	1 - 30 samples per normal batch		23.2	7.3
Lab Blank (ng/L)	1 per batch of each appropriate type	≤ MDL	47	0.21	0.26
OPR	Initial and final + 1 per 10 samples	90-110% of nominal value	53	104.1%	10.8%
Laboratory Duplicate/Analytical Duplicates	1 per 20 samples	RPD ± 20%	31	4.1%	4.2%
QCS (Standard from alternate source)	1 per batch	80-120% of nominal value	25	99.0%	16.9%
Spike Recovery	1 per 10 samples	80-120%	79	95.8%	16.4%

**Table 11-1.8: QC summary for methyl Hg-solid analysis at SERC.**

QC Parameter	Min. Frequency	Target QC goal	n	Average	Standard Deviation
Total # of samples			349		
# of analytical runs			15		
Batch size	Daily run	1 - 30 samples per normal batch		23	7
Distillation Blank	1 per batch of each appropriate type	≤ MDL	12	0.076	0.042
Ethylation Blank			31	0.044	0.084

**Table 11-1.8: QC summary for methyl Hg-solid analysis at SERC.**

<b>QC Parameter</b>	<b>Min. Frequency</b>	<b>Target QC goal</b>	<b>n</b>	<b>Average</b>	<b>Standard Deviation</b>
IPC/OPR	Initial and final and 1 per 10 samples	90-110% of nominal value	59	99.96%	8.89%
Laboratory Duplicate/Analytical Duplicates	1 per 20 samples	RPD $\pm$ 20%	38	8.2%	9.2%
CRM (if available)	1 per 20 samples	$\pm$ 20% Certified range	42	102.3%	20.0%
QCS (Standard from alternate source)	1 per batch	80-120% of nominal value	13	102.2%	23.1%

**Table 11-1.9: QC summary for total Hg-solid analysis at SERC.**

<b>QC Parameter</b>	<b>Min. Frequency</b>	<b>Target QC goal</b>	<b>n</b>	<b>Average</b>	<b>Standard Deviation</b>
Total # of samples			289		
# of analytical runs			7		
Batch size	Daily run	1 - 30 samples per normal batch		36.1	16.7
Lab Blank (ng/L)	1 per batch of each appropriate type	≤ MDL	31	0.0045	0.0046
Digestion Blank (ng/L)			21	0.0071	0.0097
IPC/OPR	Initial	90-110% of nominal value	33	100.9%	5.2%
Laboratory Duplicate/Analytical Duplicates	1 per 20 samples	RPD ± 20%	22	7.7%	9.9%
CRM (if available)	1 per 20 samples	± 20% Certified range	36	103.4%	5.9%
QCS (Standard from alternate source)	1 per batch	80-120% of nominal value	8	102.8%	5.3%
Spike Recovery	1 per 10 samples	80-120%	65	98.6%	7.7%

## **SECTION 2. RESULTS**

### **2.1 AUGUST 2009/MAY 2010 SURVEYS**

Extensive surveys of sediments and soils in the Penobscot River, including riverine tidal marshes, in August 2009 and again in May and June 2010, provided a comprehensive look at the spatial distribution of methyl Hg production and accumulation in the system. This in-depth look at the biogeochemistry of methyl Hg production in the Penobscot ecosystem provided information on the distribution of methyl Hg and methyl Hg production across different types of sites and salinities, and with depth in sediments and soils.

The graphics in this section present data from those surveys in a number of ways, highlighting results on different time and space scales. The full data set is available in excel files, including are tables providing averages and standard deviations by site, habitat and season.

This section presents raw and synthesized data, including trends through time and space. A comparison of Penobscot River total and methyl Hg data with other ecosystems is in Section 3. An analysis of the biogeochemical controls on Hg and methyl Hg based on these data is presented in Section 4.

The graphics presented are sometimes grouped by sampling area or by habitat. Sampling “areas” are defined here as the four main marsh complexes studied (and their adjacent mud flats), plus the sediment transect in Penobscot Bay. These areas are mapped in Figure 11-1.1. They are:

- W10 (Bald Hill Cove) an oligohaline riverine marsh above Orrington
- W17 a mesohaline marsh riverine marsh just upstream from the Marsh River
- W21 the large Mendall Marsh complex along the South Marsh River
- W26, a marsh on the upper Orland River
- OB1 and ES11 - river bottom sediments only
- E01 transect, bottom sediments in Fort Point Cove in Penobscot Bay

Target habitats in each complex were mud flat (MF), lower marsh (LM), mid-marsh (MM) and upper marsh (UM). These designations are appropriate for the fringing marsh complexes W10, W17 and W26, where the marshes grow across a relatively smooth elevation change back from the water. More detail can be found in the Study Sites section, above. For the Mendall Marsh (W21) samples, we also added a “marsh platform” habitat that better represents the extensive, relatively flat marshes along the South Marsh River. It’s important to note that LM, MM and HM samples for W21 were taken along the bank of the South Marsh River, rather than on the platform itself, following the sampling locations of earlier surveys.

During the August 2009 and May/June 2010 surveys, sediment and soil core samples were sectioned at 3 cm intervals (generally in 4 intervals up to 12 cm) to evaluate the depth distribution of various parameters. In bottom sediments and in many marshes, methyl Hg production and accumulation are maximal at or near the surface. However, few studies of macrotidal systems, high salinity marshes, or high energy sediments like Penobscot mud flats have been done, so it was important to look at the depth distribution of methyl Hg here.

Graphics in this section focus on depth profiles. Summary graphics across all sites and dates sampled are below in Section 2.3.

### **2.1.1 Depth profiles of individual parameters, by site and date.**

*Hg and methyl Hg in solids and pore water.* Figures 11-2.1 and 11-2.2 show depth profiles of total Hg, methyl Hg, MeHg as a percent of total Hg (% methyl Hg), and methylation rate constants in bulk sediments and soils from the August 2009 and May/June 2010 surveys, respectively. Profiles are grouped by habitat type, from lowest elevation on the left, to highest on the right. Thus the panel on the top left compares depth profiles for the mud flat sites in each of the 5 study areas. Similar plots for pore water Hg and methyl Hg are shown in Figures 11-2.3 and 11-2.4. Depth profiles of sediment:water partition coefficients are in Figures 11-2.5 and 11-2.6. Partition coefficients were calculated as the concentration in the bulk phase (in ng/kg) divided by the concentration in pore water (in ng/L).

These Hg and methyl Hg depth profiles highlight key trends:

- methyl Hg concentrations and methyl Hg as percent of total Hg (% methyl Hg) were usually highest at or near the sediment or soil surface for almost all sites and habitats, and often declined sharply with depth. This was true of both the bulk phase and pore waters. Hg methylation rate constants were also generally highest at the surface. This finding is consistent with most aquatic sediments and marsh soils studied.
- Total Hg concentrations in surface sediments and marsh soils varied among the sites examined by roughly an order of magnitude. Methyl Hg concentrations, and % methyl Hg vary somewhat more (also see bar graphs with averages by site and date (Figure 11-2.33) and by area and habitat in (Figure 11-2.46).
- Depth profiles of total Hg in mud flats were often flat, probably because of significant physical mixing of this environment. Methyl Hg profiles in mud flats also had less pronounced changes with depth than in the marsh habitats.
- In marsh environments (above low marsh) total Hg often increased with depth, perhaps reflecting a history of declining Hg input to marsh soils over time, or dilution of surface soils with fresh organic matter from marsh plants. Marshes act as sediment traps for particles from the main river.
- The % methyl Hg values in Penobscot marsh soils were exceptionally high in comparison with other freshwater and estuarine marshes (see Section 3

“Comparisons with Other Ecosystems”). Methyl Hg as a % of total Hg was highest in surface soils in the mesohaline marshes in the central river – W17 and W21.

- Sediment:water partition coefficients were often lowest at the surface, but depth trends varied.

Methyl Hg may account for more than half of total Hg in pore waters, especially in marsh habitats. In evaluating these data, we have sometimes presented inorganic Hg concentrations (shown as Hgi) calculated from the total Hg concentration minus the methyl Hg concentration. The very high fraction of Hg in pore waters as methyl Hg is an unusual feature of the Penobscot system.

*Depth profiles of other bulk constituents.* Depth profiles in marsh soils reflect early diagenesis of organic and inorganic materials accreting in the marsh. Soils are generally anaerobic at or very near the soil surface, and become more reducing at depth. However, plant roots can mitigate anoxia at small and heterogeneous scales. Depth profiles in mud flats reflect a physically more energetic environment, in which mud flat materials may mix down 10's of cm on some tides. The biogeochemistry of sediments and soils can help us to identify areas of high methylation in the Penobscot system, help identify the drivers of methyl Hg accumulation in the system and how they compare with other ecosystems, and help predict how they might react to changed conditions or remediation.

*Iron-sulfur chemistry in solids.* Because of the well-established links between Hg biogeochemistry and sulfur, we measured concentrations of key solid phase and pore water iron and sulfide compounds. Acid-volatile sulfides (AVS) are Fe mono-sulfides and other poorly crystalline FeS minerals. Chromium-reducible sulfides (CRS) are more crystalline, primarily pyrite ( $\text{FeS}_2$ ). Depth profiles of AVS and CRS (Figures 11-2.7 and 11-2.8) show the diagenetic progression from poorly crystalline FeS at the surface toward pyrite at depth. At all depths, even in surface soils, CRS concentrations were much higher than AVS, reflecting the sulfidic and reducing conditions of salt marshes and tidal mud flats, and the availability of sufficient Fe for FeS precipitation. We also measured the total concentrations of S in samples from May/June 2010 (Figure 11-2.11). Sulfur in AVS+CRS represented on average about half of the total S in sediments and soils. The remaining S is most likely reduced S in organic matter (measured total S concentrations were much higher than the amount of S contributed by sulfate in pore waters).

We measured HCl-extractable Fe(II) and Fe(III) in the bulk phase as a measure of redox, and also to help assess the bulk speciation of Fe in soils (Figures 11-2.9 and 11-2.10). Concentrations of extractable Fe(III) were often below detection limits, indicating reducing, anoxic sediments or soils. Extractable Fe(III) was generally only found in the surface interval sampled, and then often at concentrations below extractable Fe(II). The more oxidized conditions where Fe(III) was found at the surface included the Penobscot Bay sediments, which were sandy and low in organic matter (hence low sediment oxygen demand and high oxygen diffusion rates into sediments), mud flats (highly mixed environments), and some very dry high marsh sites. We also measured the total

concentrations of Fe (Figures 11-2.9 and 11-2.10). On average, only about a third of total Fe is buried as FeS minerals. Unlike sulfur, iron in vegetation is an unimportant source to marsh soils. Fe may be buried as non-reactive iron-oxyhydroxide minerals (especially associated with clays) or Fe in various forms sorbed to organic matter.

In Figure 11-2.11, the degree of pyritization is the fraction of “reactive” iron found as pyrite. Reactive iron is the sum of HCl-extractable Fe plus the Fe in pyrite – which is the redox reactive Fe pool. Reactive Fe in Penobscot soils and sediments is generally highly pyritized; and the degree increase with depth in sediments. As more detailed discussion of Fe-S chemistry and how it impacts Hg bioavailability of methylation is given below.

*Depth profiles of pore water constituents.* Figures 11-2.12 to 11-2.14 show depth profiles of individual pore water constituents - pH, anions, nutrients and dissolved organic carbon (DOC) for August 2009 and May/June 2010 surveys. Figure 11-2.15 shows the same data in a different way, providing a comparison of many parameters for many of the study sites. Key trends in these data were:

*pH.* Pore water pH varied among habitats (Figure 11-2.12 and 11-2.13), with the highest values in marine sediments and mud flats, and lowest values generally in marshes. Pore water pH often increased slightly with depth, probably via alkalinity generation from microbial sulfate reduction.

*Sulfide.* Pore water sulfide varied dramatically with habitat and depth (Figures 11-2.12 and 11-2.15). The range in observed concentrations was at least 5 orders magnitude. Because of that, most sulfide graphics are presented on log scales. Sulfide concentrations generally increase with sediment or soil depth. Although sulfide production may be strongest at or near the surface, sulfide in surface sediments can be oxidized, removed by precipitation or sorption, or diffuse into overlying water.

*Sulfate.* Sulfate is supplied to pore waters by diffusion from overlying water, and by reoxidation of reduced S in sediments. Sulfate concentrations in pore waters vary with the salinity of overlying river water. In pore waters, observed sulfate concentration varied over at least 4 orders of magnitude. Sulfate depth profiles were generally flat in high salinity sediments and soils. Sulfate was only significantly depleted at depth at the lowest salinity site (W10). As in most salt marsh soils and marine sediments, sulfate is probably the dominant terminal electron acceptor for anaerobic microbial activity. The very high concentrations of sulfate in mesohaline and marine waters were not limiting for microbial sulfate reduction at most sites. Thus, variations in sulfate reduction activity would be expected to be linked to availability of organic substrates.

*Dissolved organic matter.* DOC is produced in sediments and soils from root exudates and the remineralization of deposited organic matter. DOC varied from a few mg C/L to well over 100 mg C/L. Marsh soil pore waters generally supported the highest concentrations of DOC, but were highly variable. DOC was often depleted at surface, probably due to loss through diffusive efflux.

*Ammonium*. Ammonium (Figure 11-2.14) in sediments and soils arises from the mineralization of organic matter. Ammonium accumulation is indicative of strong microbial activity, leading to reducing conditions. Concentrations generally increase with depth, reaching almost mM concentrations in a few samples.

*Nitrate* concentrations are uniformly low, rarely exceeding 10  $\mu\text{M}$ , which would strongly limit microbial denitrification, as is common in marine and estuarine sediments and soils.

*Phosphate* accumulated to 50-100  $\mu\text{M}$  concentrations in mud flats and silty, often sparsely vegetated low marsh sediments (another indication of low redox) but was highly depleted in marsh soils where it is probably limiting for plant growth.

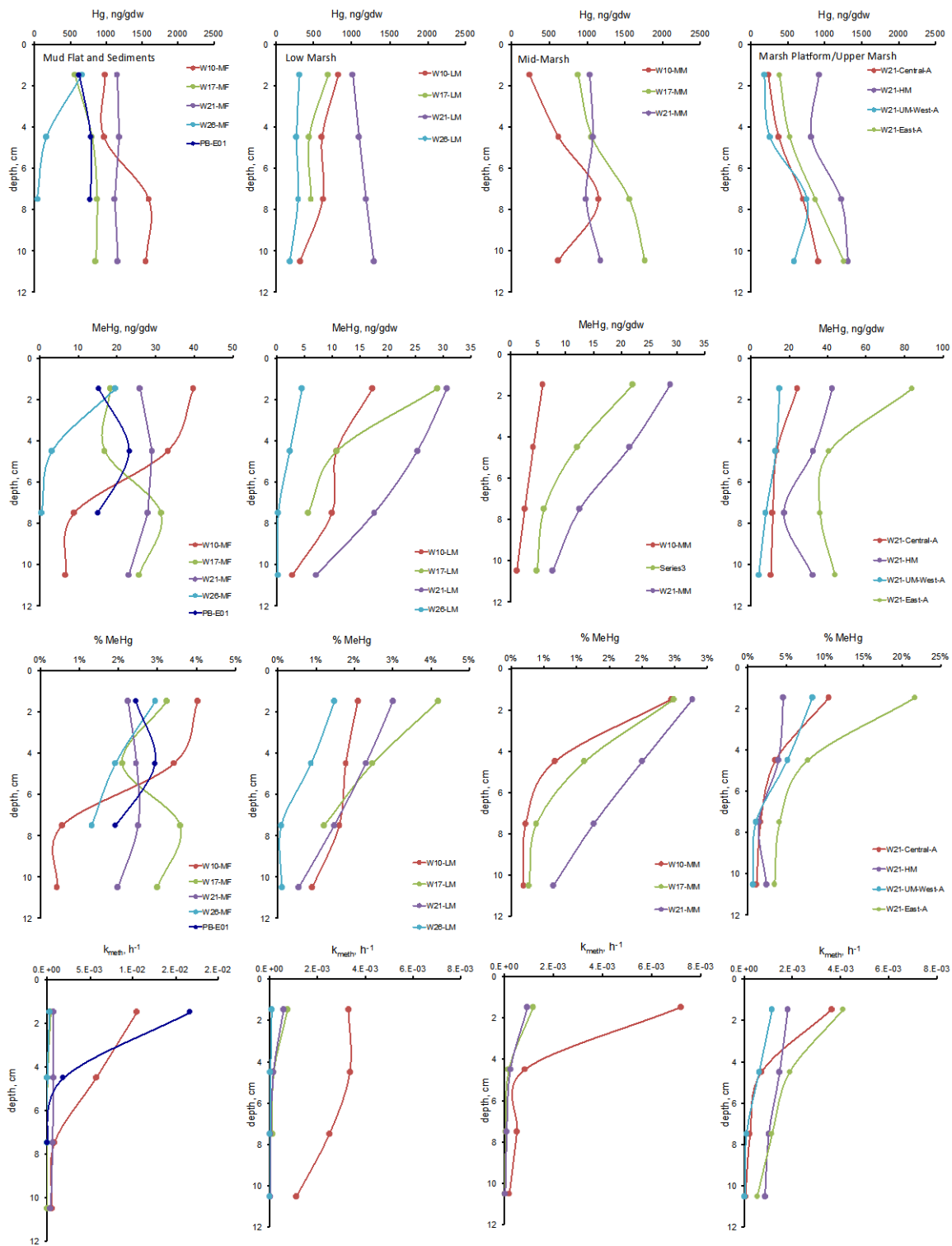
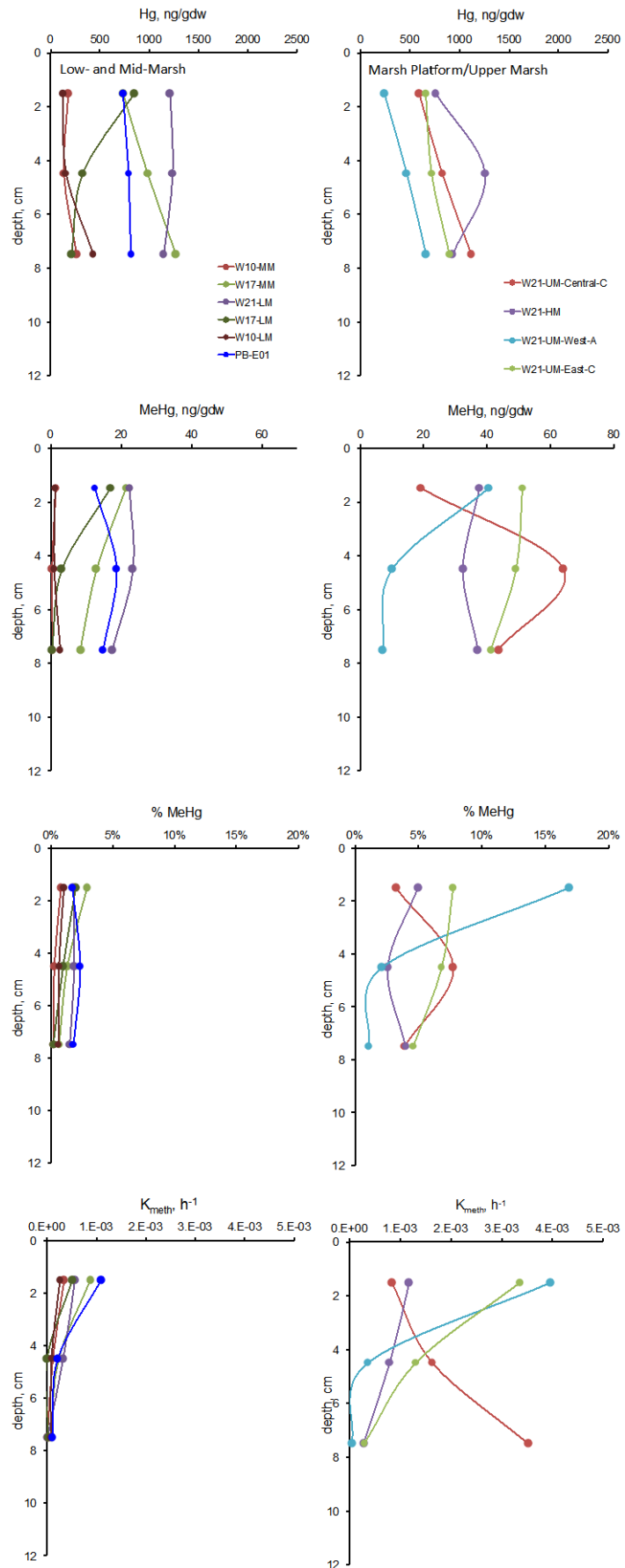


Figure 11-2.1. Depth profiles of total Hg (top), methyl Hg (top middle) and % methyl Hg (methyl Hg as a % of total Hg; bottom middle) and methylation rate constants ( $k_{\text{meth}}$ ) for sediment and marsh sites sampled in August 2009. Sites are grouped by habitat type, from lowest elevation on the left, to highest on the right. Thus the panel on the top left compares depth profiles for the mud flat sites sampled within each of the 5 study areas. Note that the axis scales are the same across graphs for each parameter (except  $k_{\text{meth}}$ ), for easier comparison.

Figure 11-2.2. Depth profiles of total Hg (top), methyl Hg (top middle) and % methyl Hg (methyl Hg as a % of total Hg; bottom middle) and methylation rate constants ( $k_{\text{meth}}$ ) for sites sampled in May/June 2010. Sites are grouped by habitat type, from lowest elevation on the left, to highest on the right. Thus the panel on the top left compares depth profiles for the mud flat sites sampled within each of the 5 study areas. Note that the axis scales are the same across graphs for each parameter (except  $k_{\text{meth}}$ ), for easier comparison.



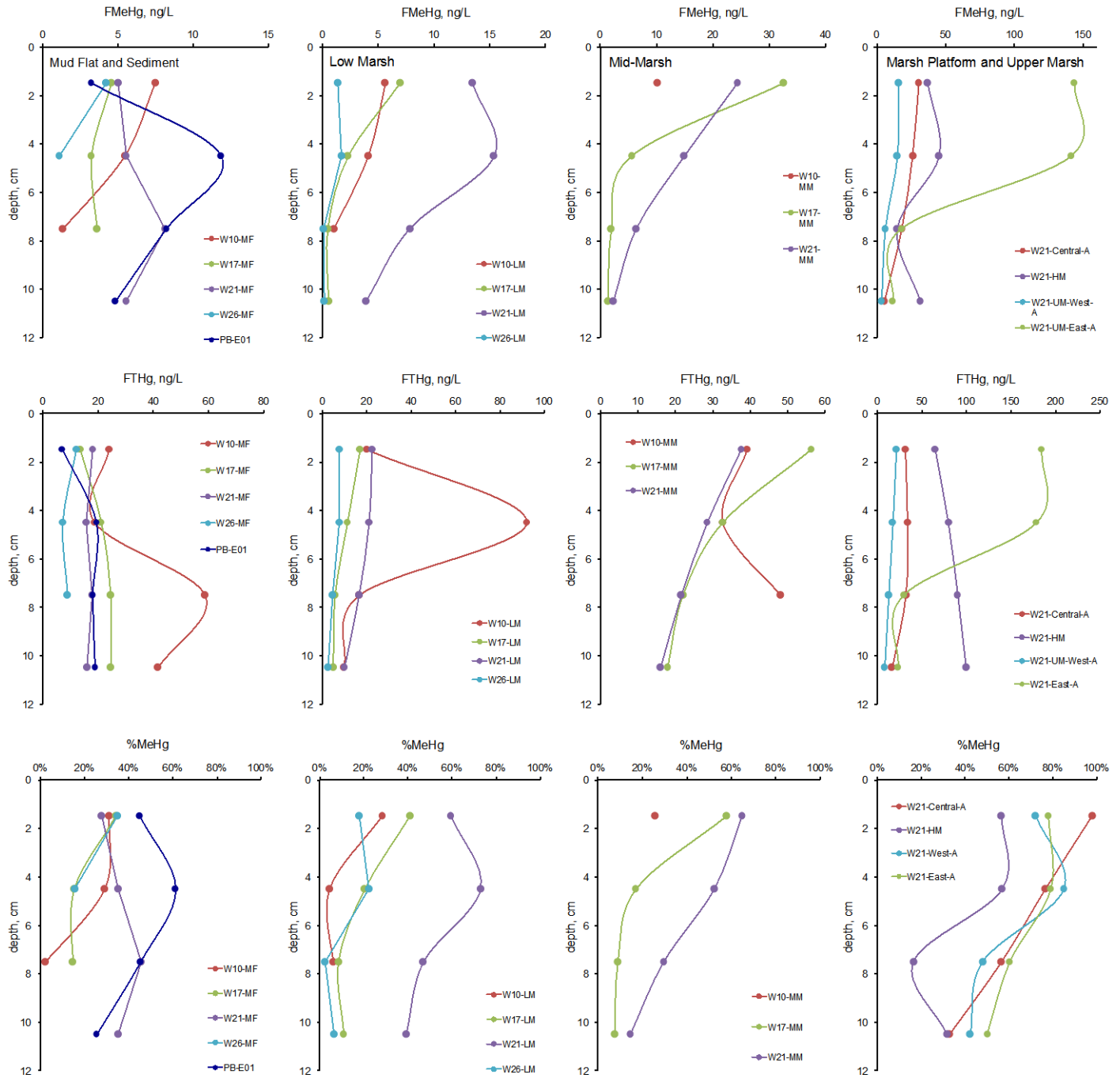
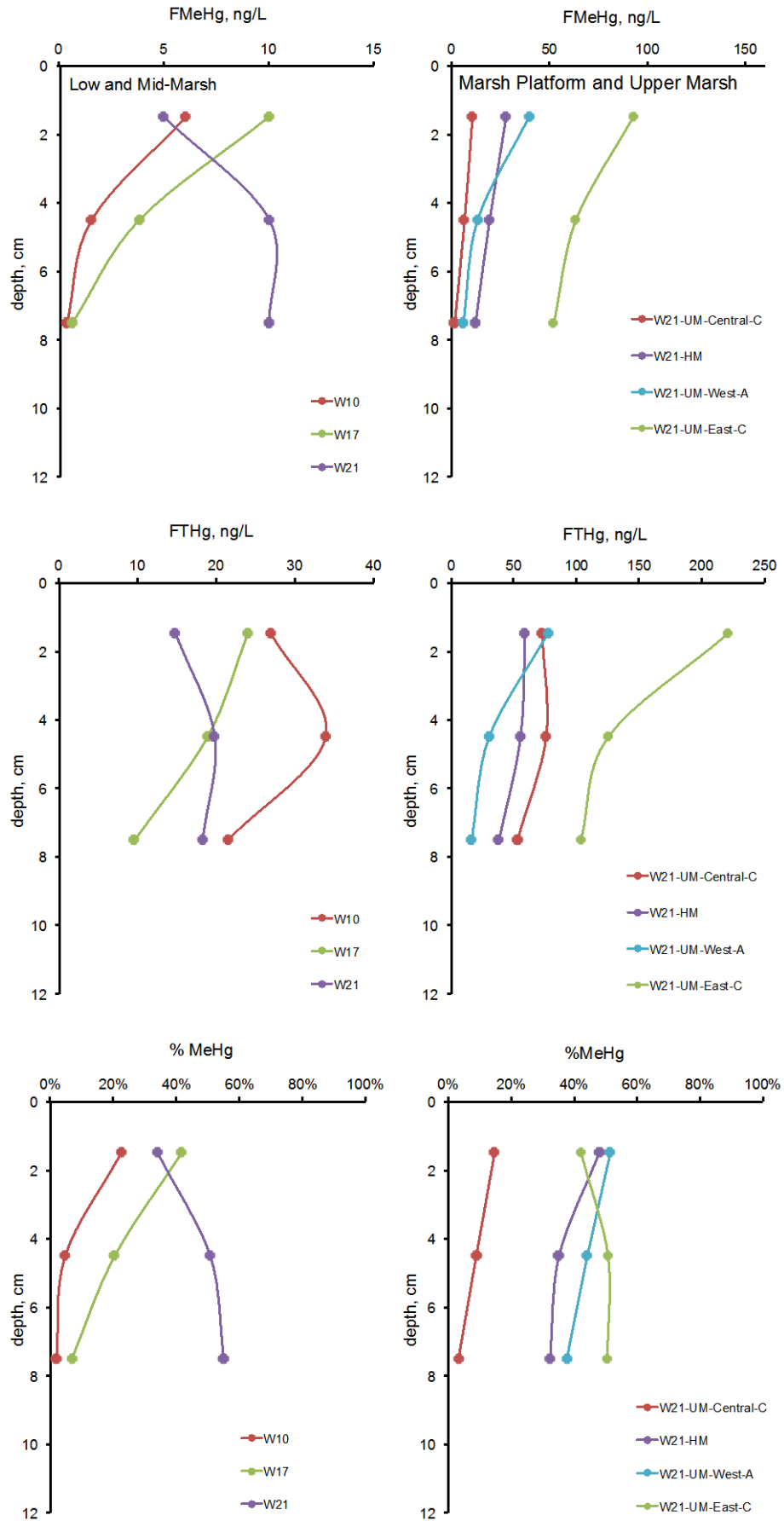


Figure 11-2.3. Depth profiles of total filterable Hg (top), methyl Hg (top middle) and % methyl Hg (methyl Hg as a % of total Hg; bottom middle) for sediment and marsh sites sampled in August 2009. Sites are grouped by habitat type, from lowest elevation on the left, to highest on the right. Thus the panel on the top left compares depth profiles for the mud flat sites sampled within each of the 5 study areas. Note that the scales differ across habitats for filter-passing total Hg and filter-passing methyl Hg.

Figure 11-2.4. Depth profiles of total filterable Hg (top), methyl Hg (top middle) and % methyl Hg (methyl Hg as a % of total Hg; bottom middle) for sediment and marsh sites sampled in May/June 2010. Sites are grouped by habitat type, from lowest elevation on the left, to highest on the right. Thus the panel on the top left compares depth profiles for the mud flat sites sampled within each of the 5 study areas. Note that the scales differ across habitats for filter-passing total Hg and filter-passing methyl Hg.



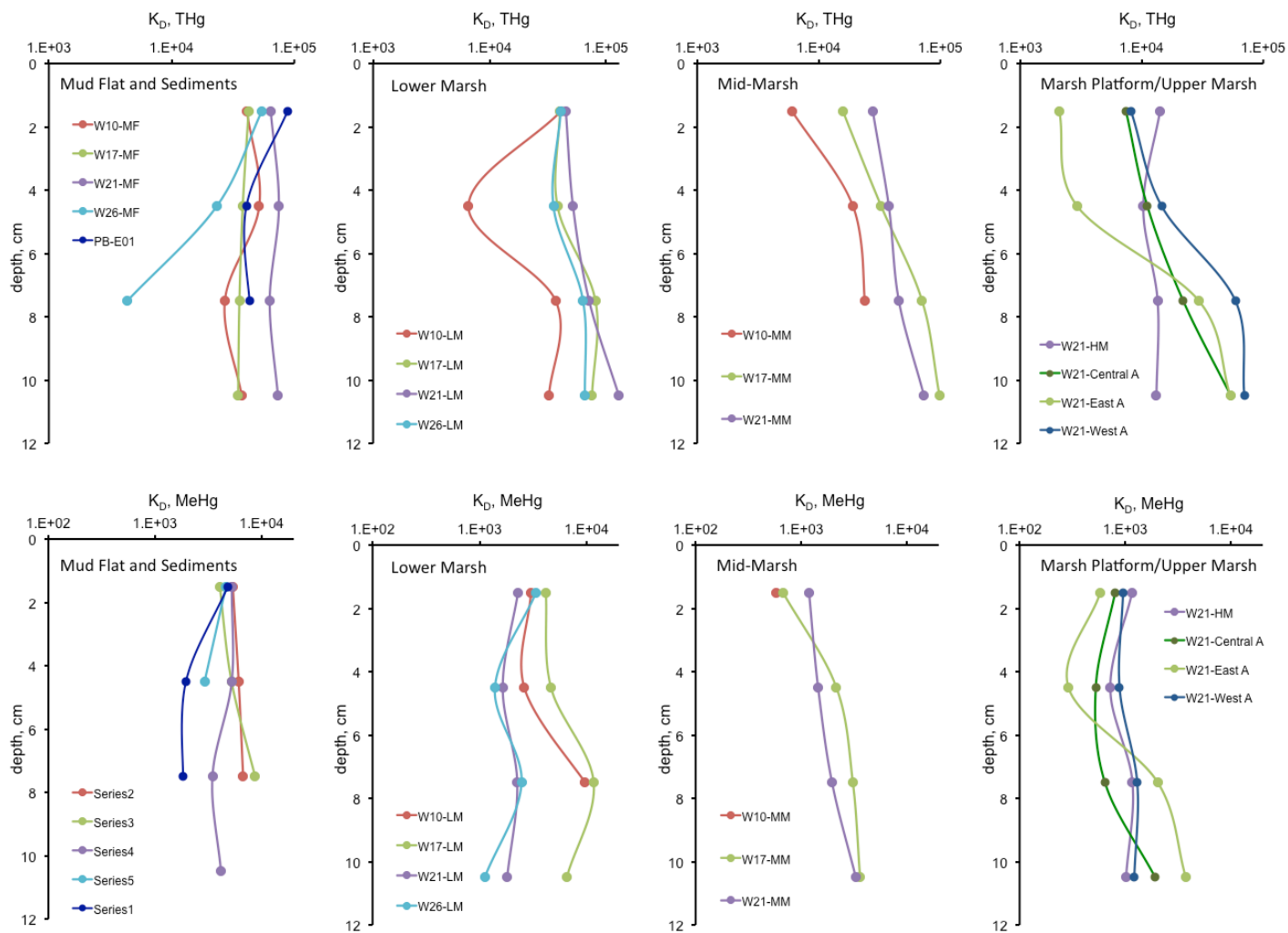
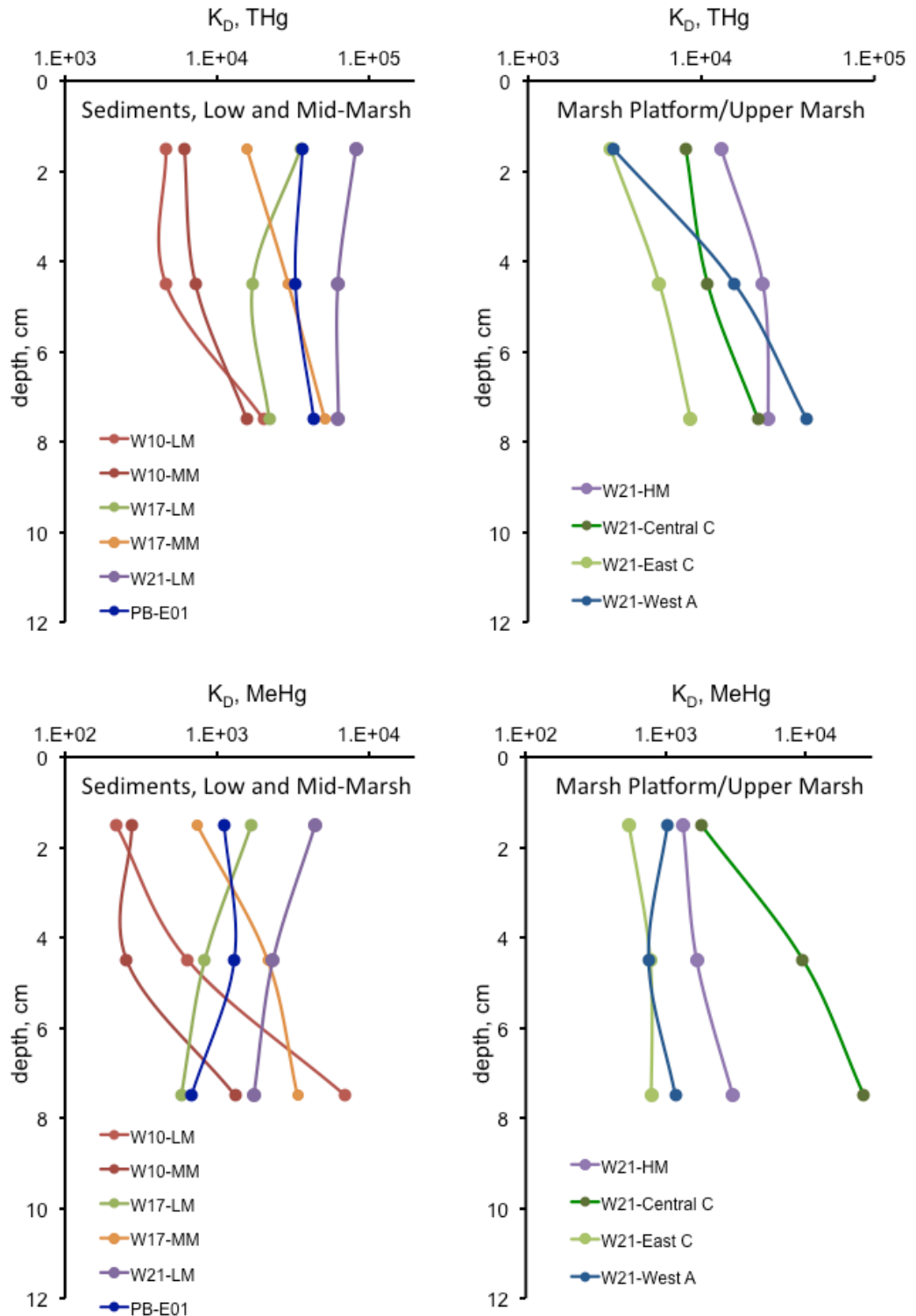


Figure 11-2.5. Depth profiles of sediment:water partition coefficients for total Hg (top) and methyl Hg (bottom) for sediment and marsh sites sampled in August 2009.

Figure 11-2.6. Depth profiles of sediment:water partition coefficients for total Hg (top) and methyl Hg (bottom) for sediment and marsh sites sampled in May/June 2010.



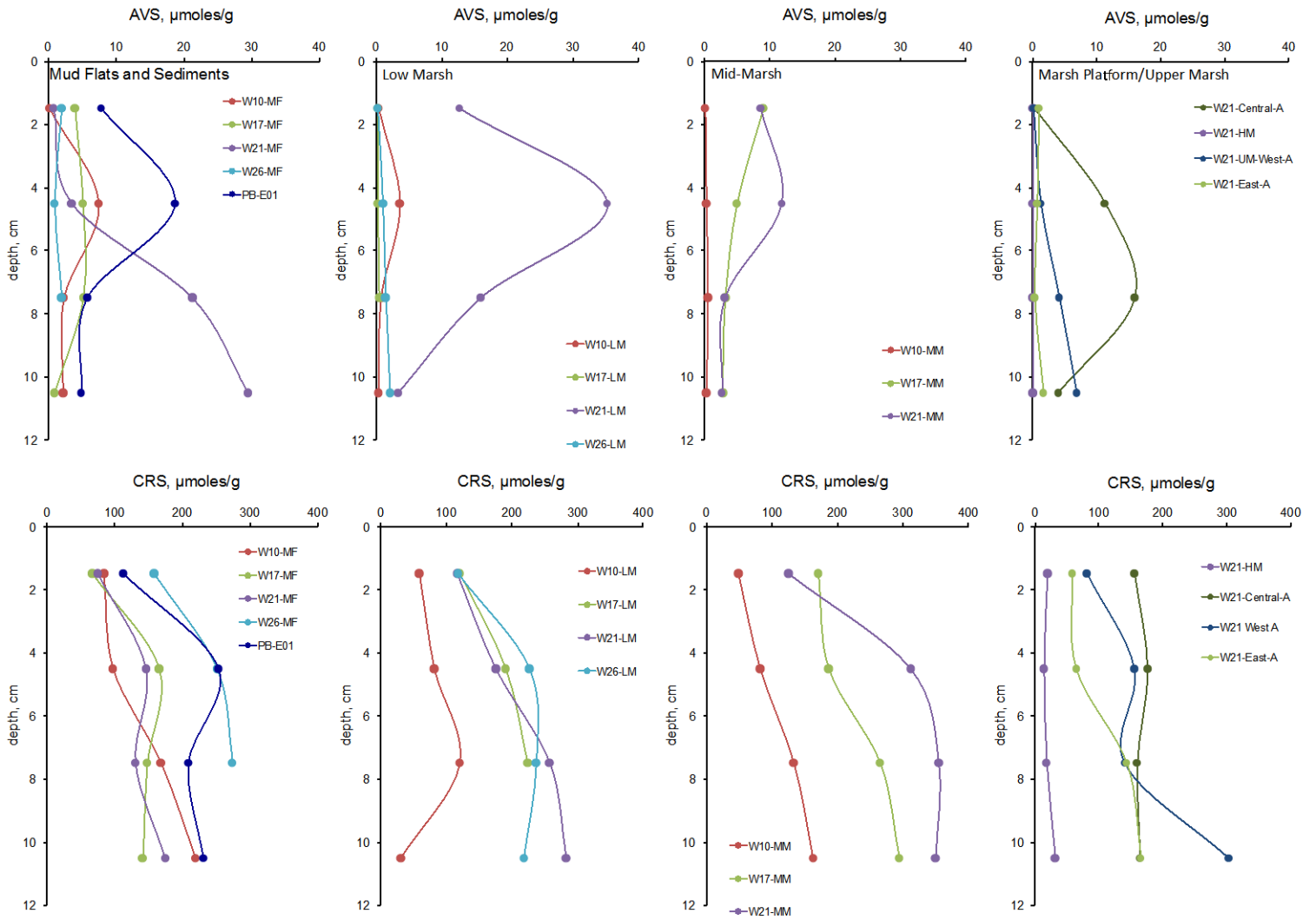


Figure 11-2.7. Depth profiles of acid-volatile sulfide (AVS; top) and chromium-reducible sulfide (CRS; middle) for sediment and marsh sites sampled in August 2009. Sites are grouped by habitat type, from lowest elevation on the left, to highest on the right.

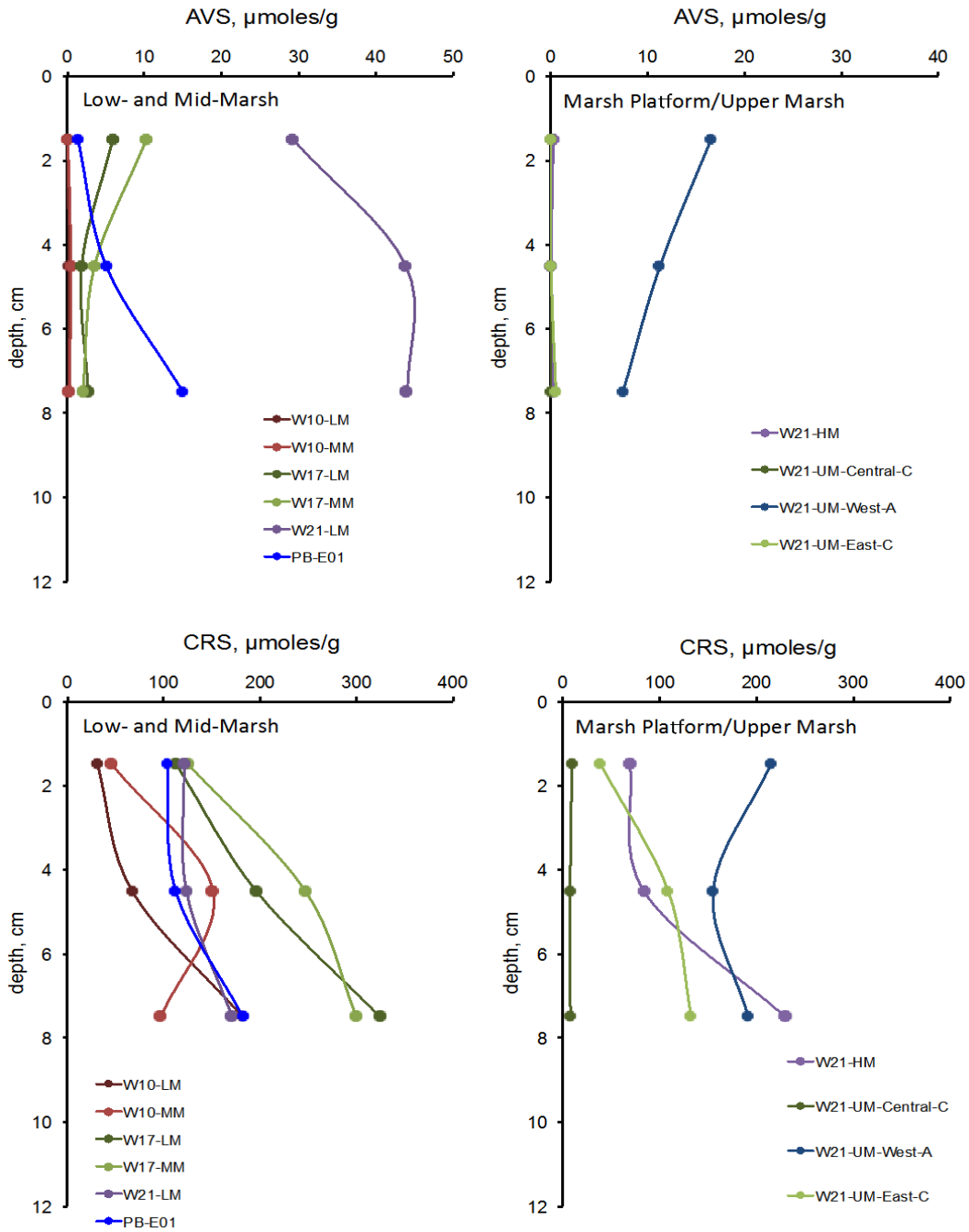


Figure 11-2.8. Depth profiles of acid-volatile sulfide (AVS; top) and chromium-reducible sulfide (CRS; middle) for sediment and marsh sites sampled in May/June 2010. Sites are grouped by habitat type, from lowest elevations on the left, to highest on the right.

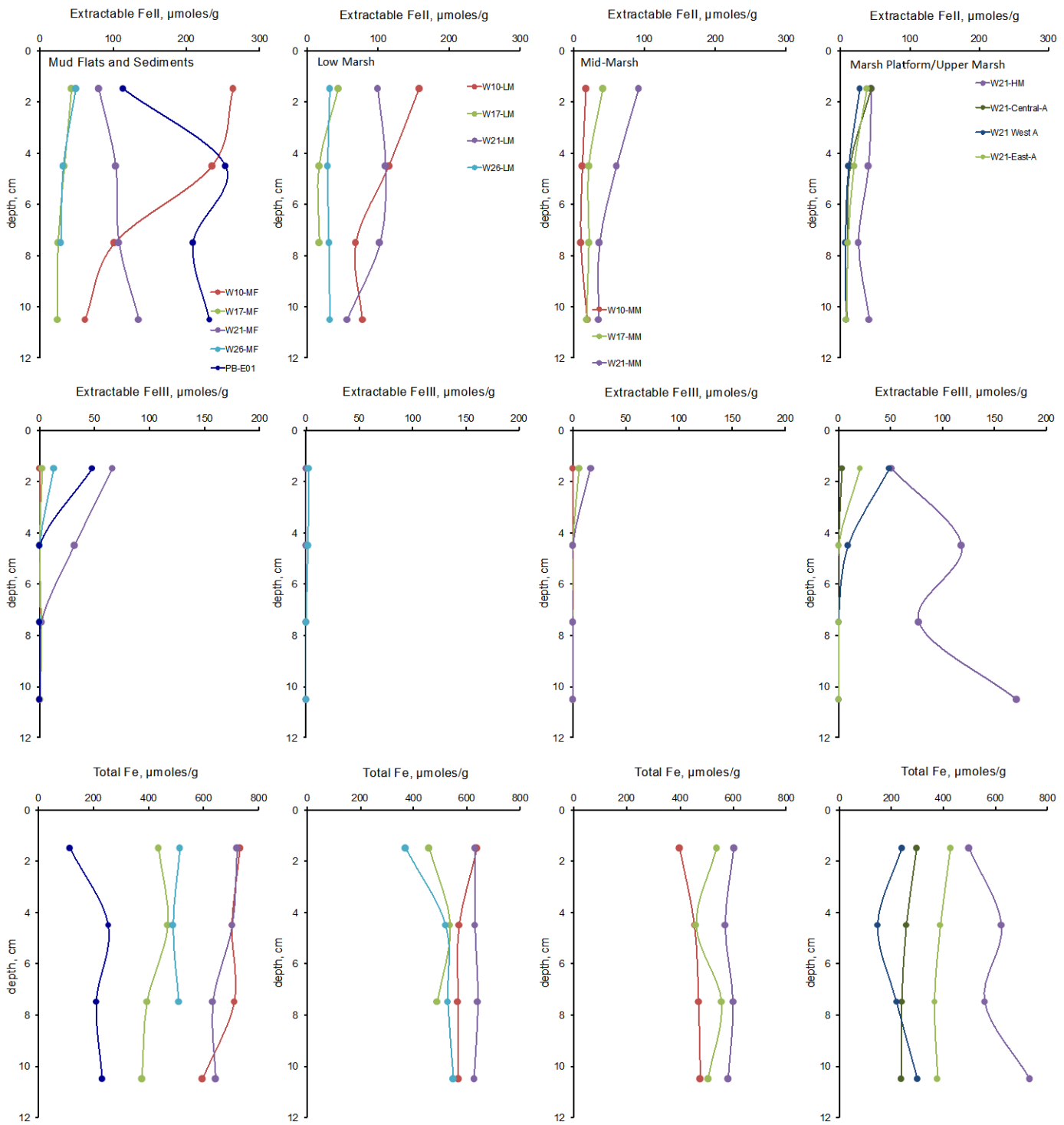


Figure 11-2.9. Depth profiles of extractable Fe(II) (top), Fe(III) (middle) and total Fe (bottom) for sediment and marsh sites sampled in August 2009. Sites are grouped by habitat type, from lowest elevation on the left, to highest on the right.

Figure 11-2.10. Depth profiles of extractable Fe(II) (top), Fe(III) (middle) and total Fe (bottom) for sediment and marsh sites sampled in May/June 2010. Sites are grouped by habitat type, from lowest elevation on the left, to highest on the right.

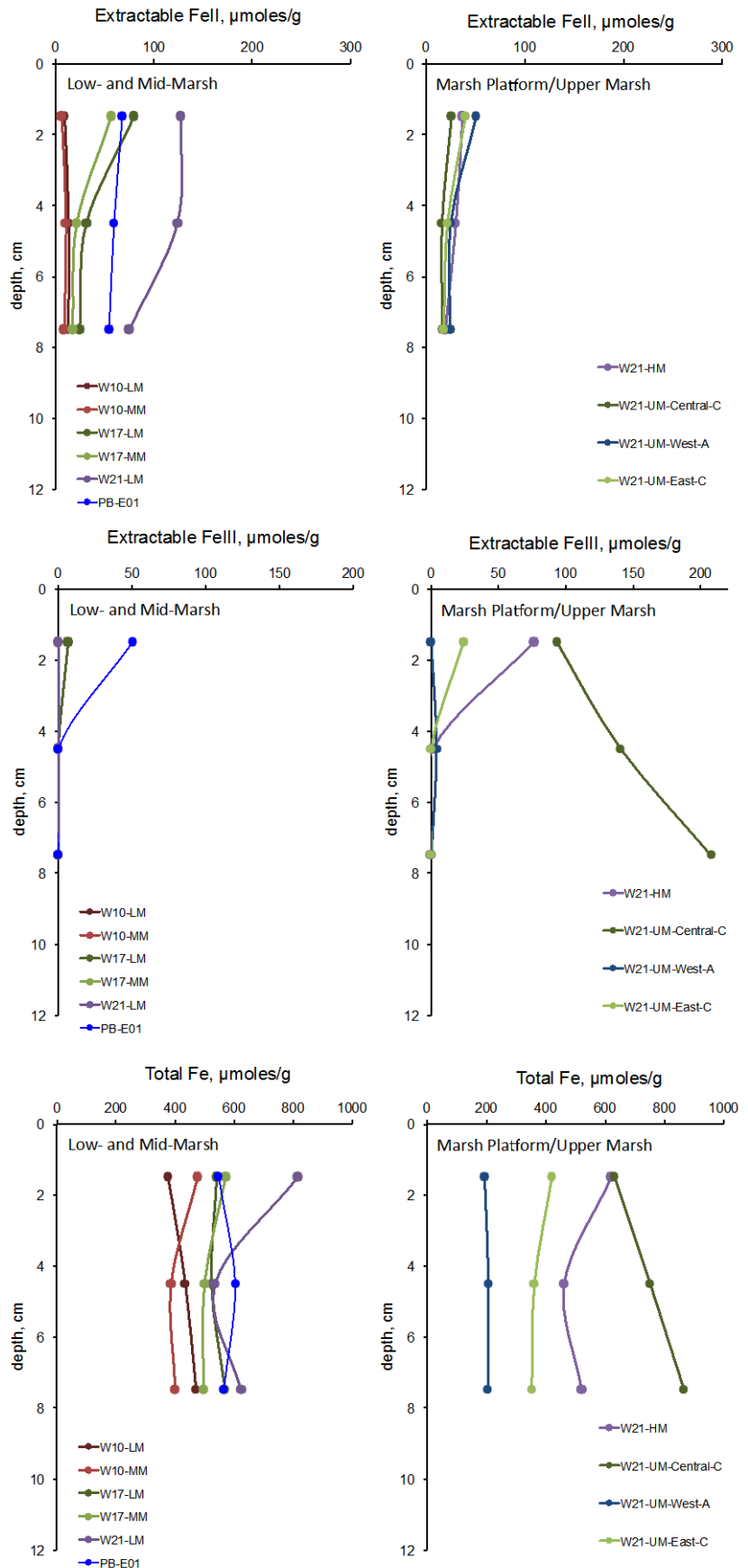
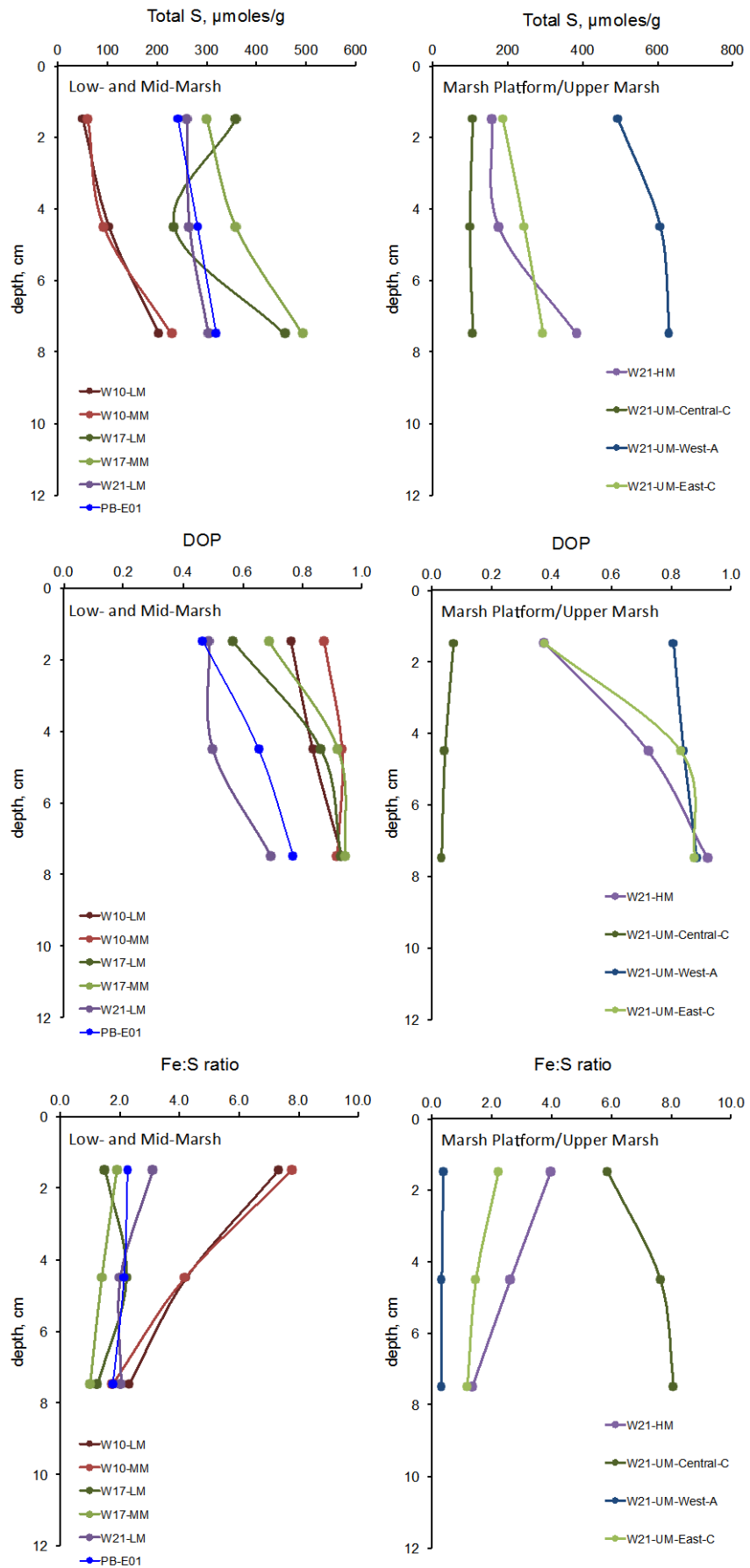


Figure 11-2.11. Depth profiles of total S (top), degree of pyritization of reactive Fe (DOP middle) and ratio of total Fe to total S (bottom) for sediment and marsh sites sampled in May/June 2010.



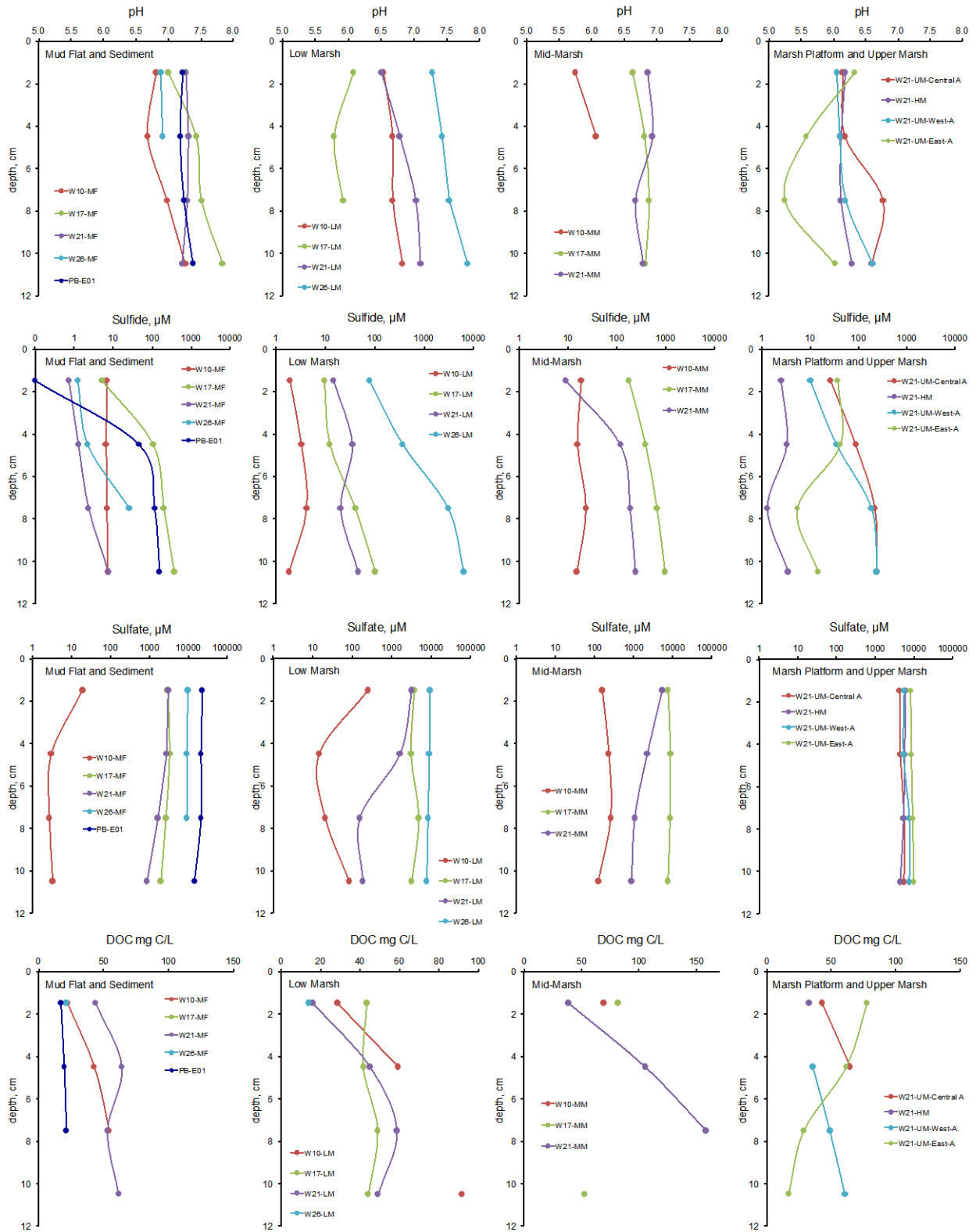
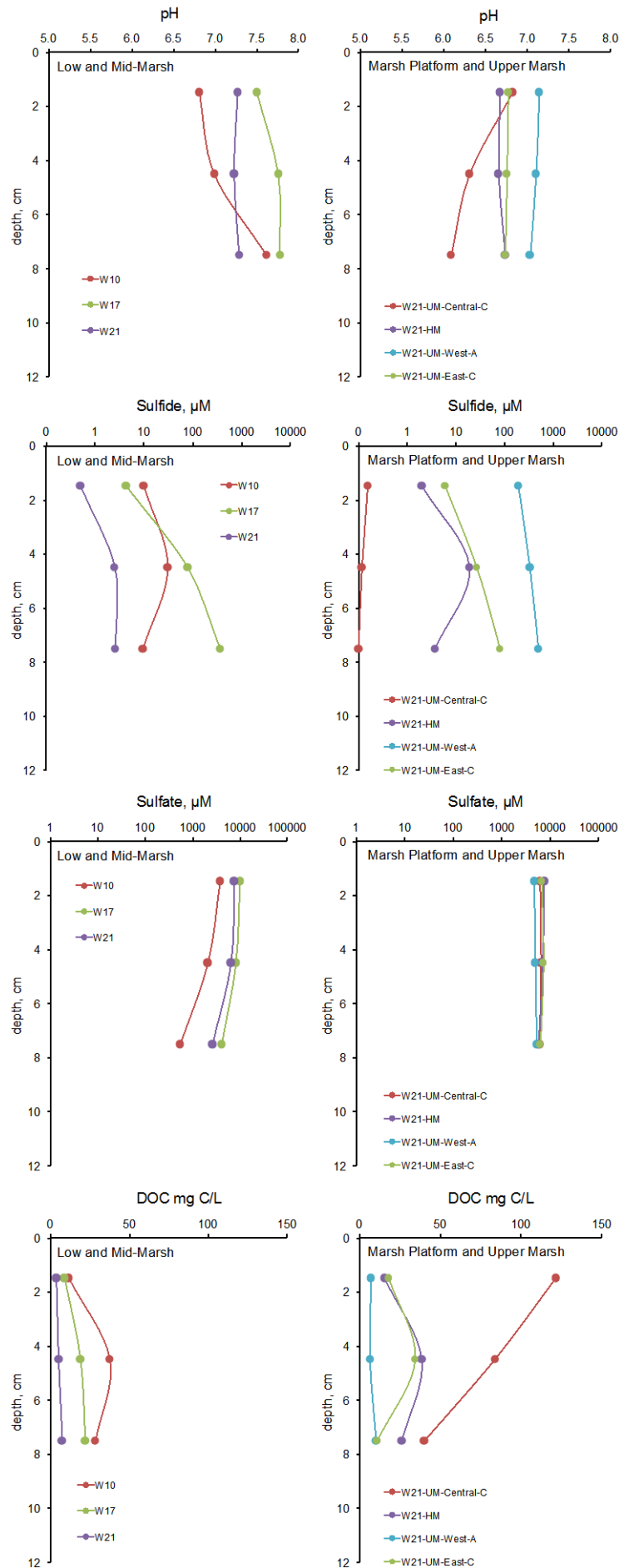


Figure 11-2.12. Depth profiles of pore water constituents, by parameter: pH (top), sulfate and sulfide (middle) and DOC (bottom) for sediment and marsh sites sampled in August 2009.

Figure 11-2.13. Depth profiles of pore water constituents, by parameter: pH (top), sulfate and sulfide (middle) and DOC (bottom) for sediment and marsh sites sampled in May/June 2010. Sites are grouped by habitat type.



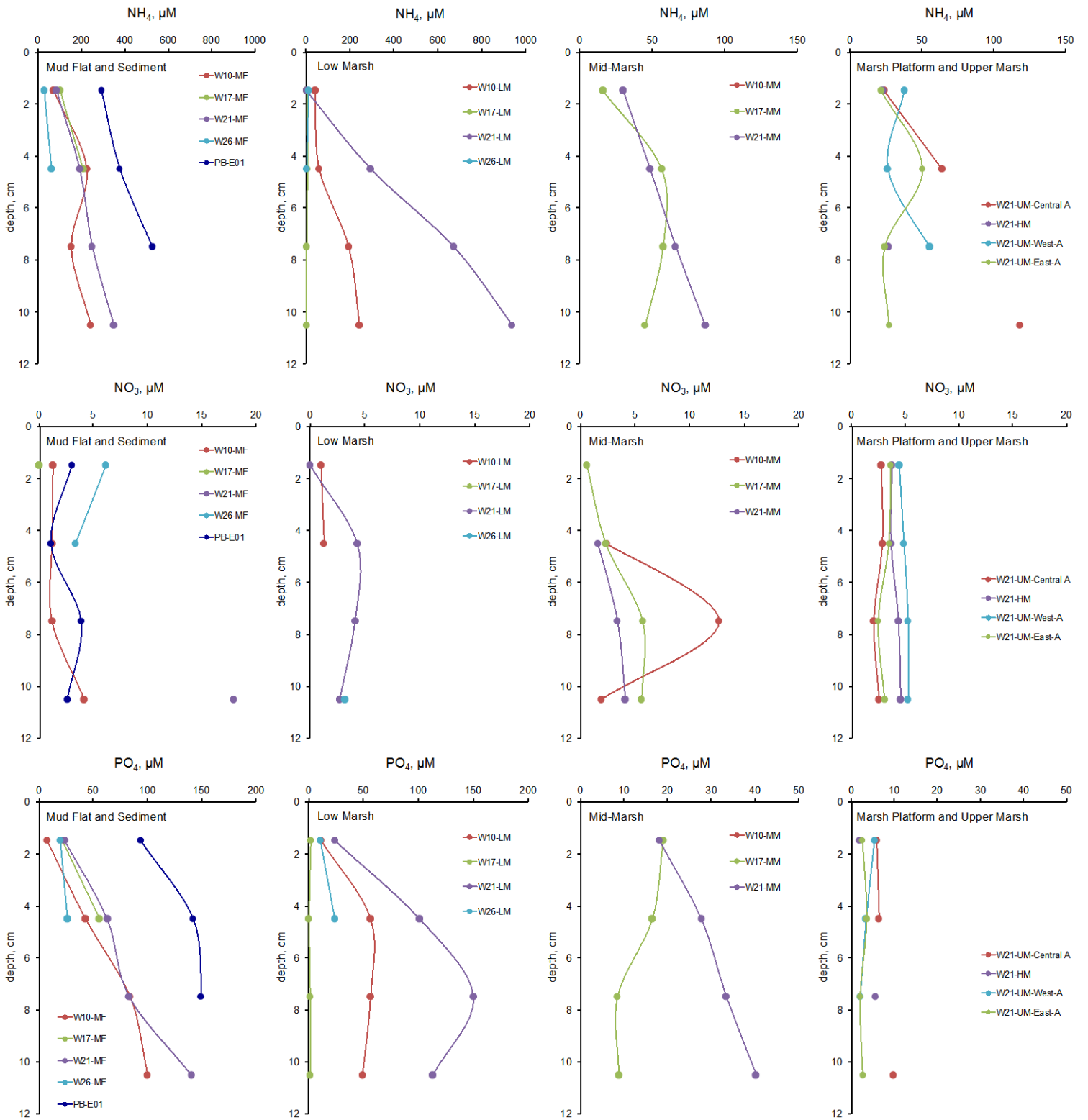


Figure 11-2.14. Depth profiles of pore water nutrients for sediment and marsh sites sampled in August 2009. Note that scales vary.

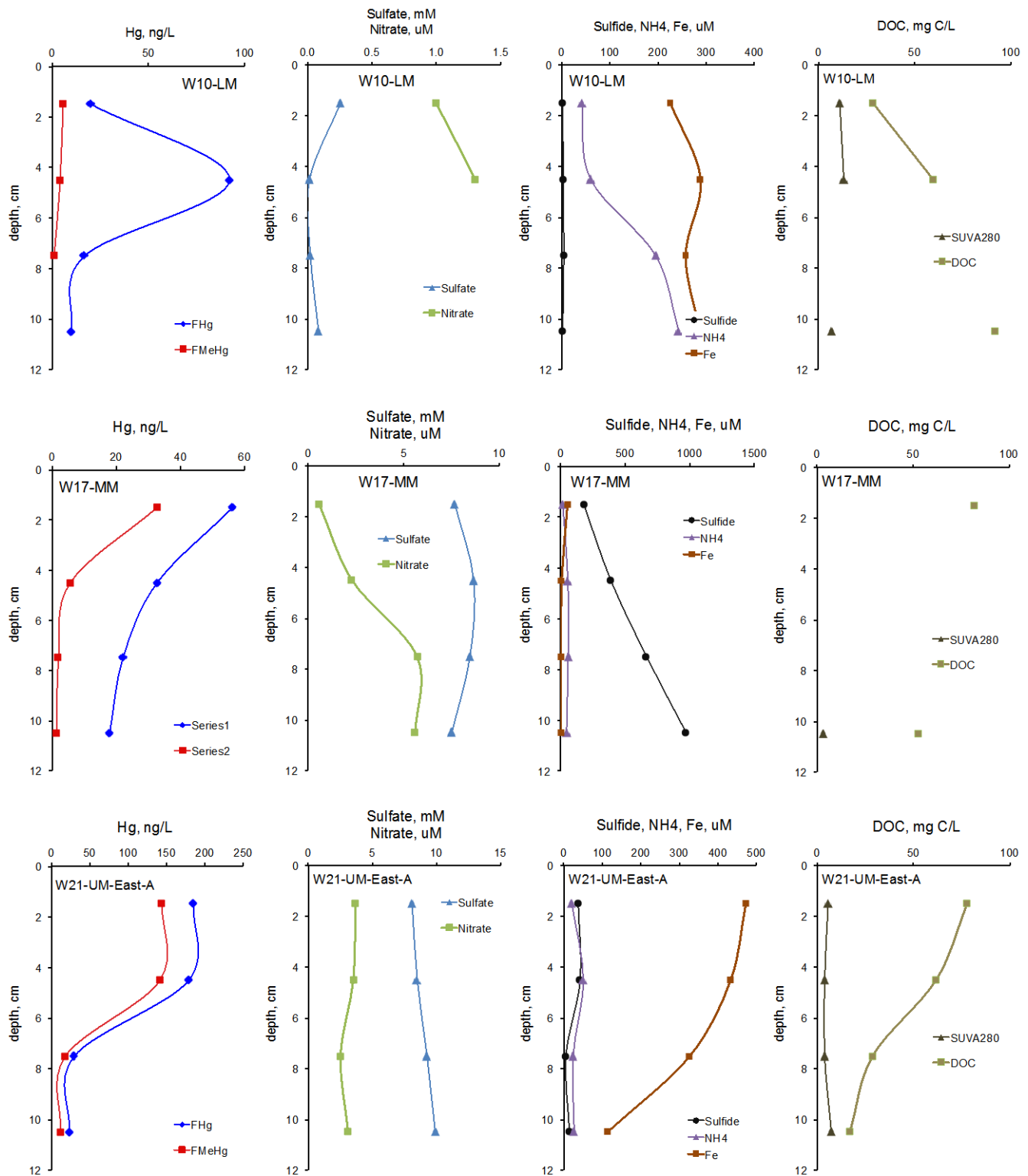


Figure 11-2.15. Example depth profiles, comparing pore water constituents, for each marsh complex examined, all from August 2009. Note the different scales across sites.

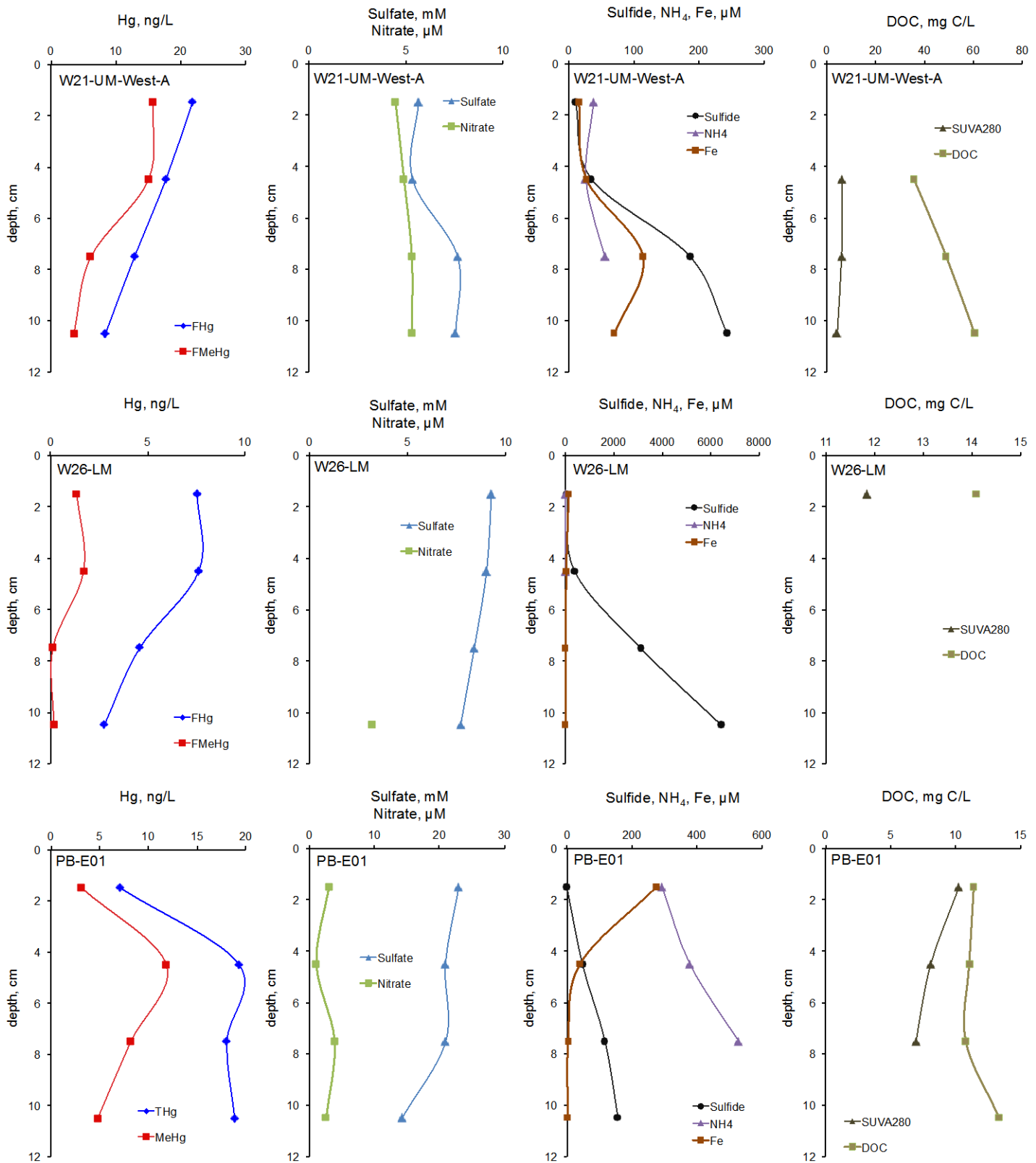


Figure 11-2.15 (cont). Example depth profiles of pore water constituents for each marsh complex examined, all from August 2009. Note the different scales across sites.

### 2.1.2 Depth profiles - comparison by habitat

The average depth profiles (across all sampling dates) for % methyl Hg and  $k_{\text{meth}}$  in solid material for each habitat are shown in Figure 11-2.16 along with averages for bulk density and loss on ignition. Because Hg and methyl Hg concentrations vary substantially along the river, it is not appropriate to average their absolute concentrations by habitat. The comparisons highlight the higher, on average, %methyl Hg in high marsh and marsh platform soils than in sediments and mud flats. The pattern of higher % methyl Hg in habitats with higher organic matter content (% LOI) and lower bulk density is apparent. Methylation rate constants and % methyl Hg are consistently higher in surface sediments and soils (Figure 11-2.16) across habitats. This was the case even though the profiles of % LOI were straight up and down. So while % LOI was a general predictor of methylation activity when comparing sites (see Section 4), it was not a predictor of the decrease in activities with depth. Surface soils have a small pool of labile carbon that turns over rapidly and doesn't add substantially to the general level of organic material at the site. Additionally, strong redox gradients and changes with tide contribute to high methylation rates in near-surface soils.

Figure 11-2.17 and 11-2.18 are similar to Figure 11-2.16 but for pore waters, not solid material. They show average pore water concentrations of some parameters for each habitat type, highlighting the decrease in pH from sediment to high marsh; the generally higher % methyl Hg in surface soils and in high marsh/marsh platform soils, and the very low nitrate concentrations across the system.

Dissolved organic matter (DOM) can have a profound influence on Hg complexation and bioavailability. Recent research in our lab and others has highlighted the role of both DOC concentration and DOC chemical character in Hg partitioning and bioavailability. Figure 11-2.18 compares the concentration and spectral characteristics of DOC across habitats. Not surprisingly, DOC concentrations are highest in marsh soils. The specific UV absorbance at 280 nm (SUVA<sub>280</sub>) and slope ratios (ratio of spectral slopes in certain wavelength regions) provide proxy measures of DOM molecular weight and aromaticity. The profiles of these spectral parameters show differences in the character of DOC among habitats and with depth.

SUVA<sub>280</sub>, an indicator of aromaticity in the DOC, was the parameter that showed the most obvious decrease with depth, although this was not the case in all habitats (Figure 11-2.18). For all the DOC spectral parameters, there were general differences among the habitat types, indicating that the quality of DOC differed among these habitat types. Relationships between DOC concentration, character and Hg chemistry and bioavailability are discussed below.

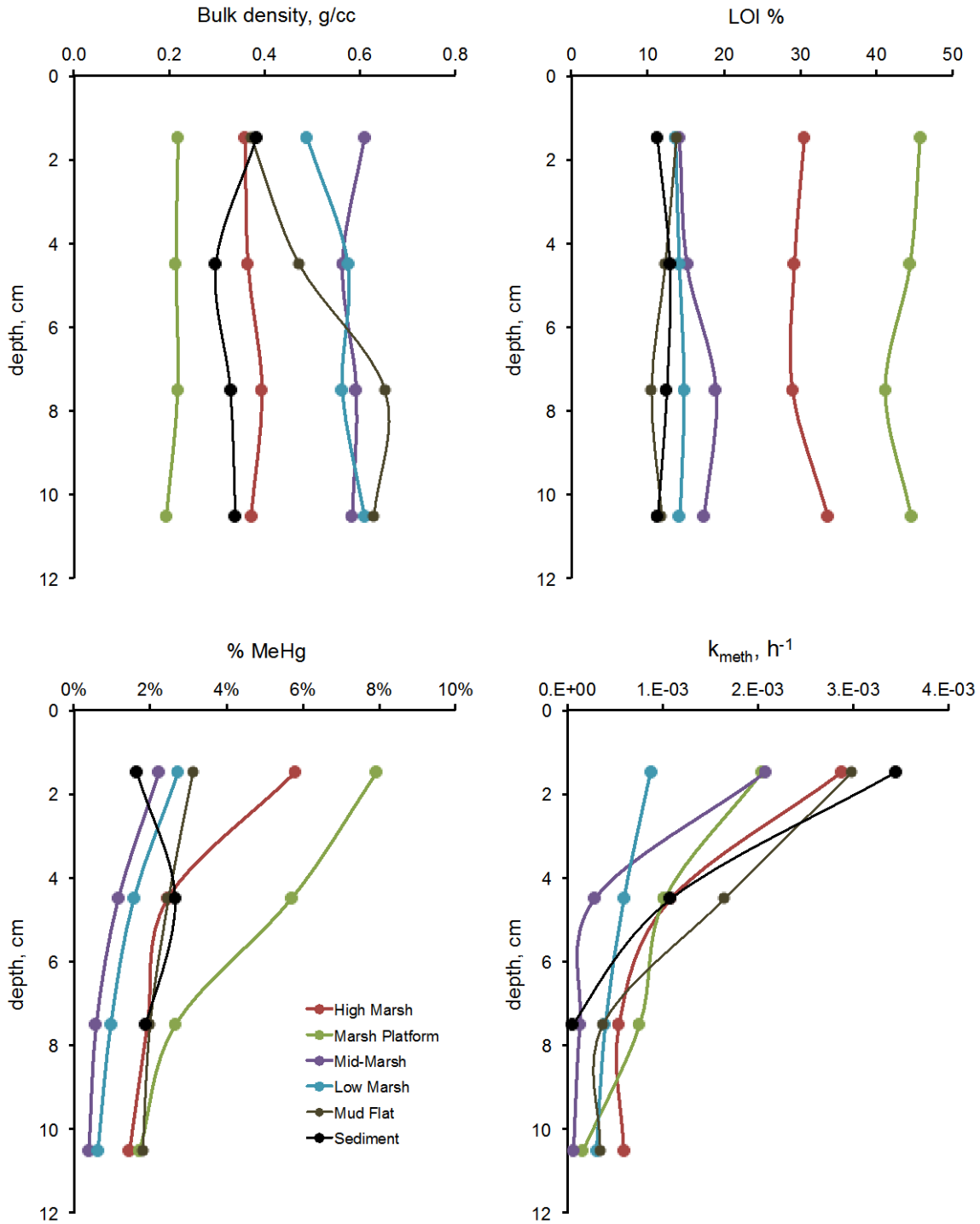


Figure 11-2.16. Average depth profiles by habitat of bulk density, % LOI, bulk % methyl Hg and methylation rate. Profiles shown are averages by habitat type across all sites and sampling dates. Error bars are omitted for clarity, but can be found in data appendices.

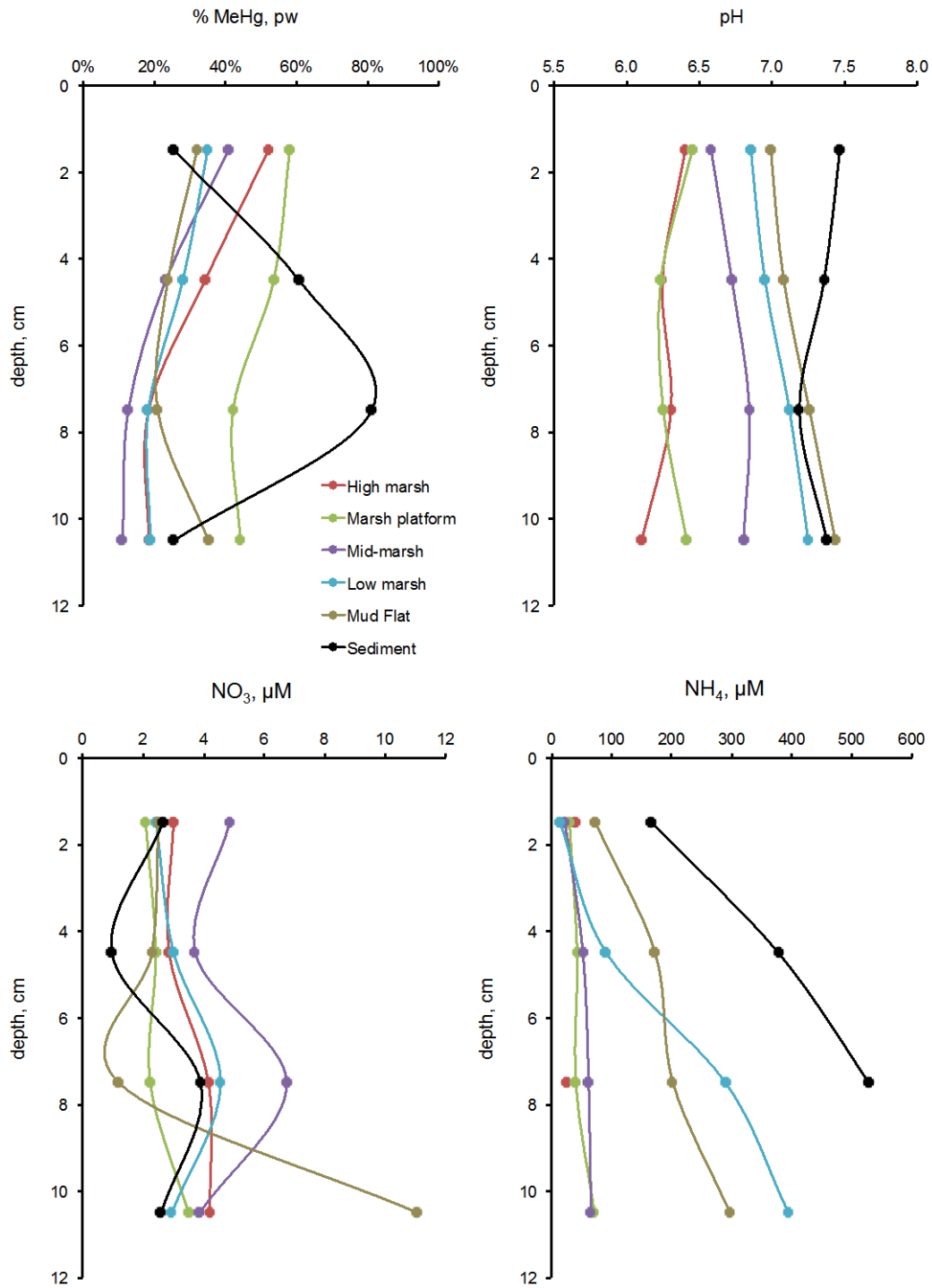


Figure 11-2.17. Average depth profiles of % methyl Hg in pore water, pore water pH, nitrate and ammonia. Profiles shown are averages for each habitat type across all sites and sampling dates. Error bars are omitted for clarity, but can be found in data appendices.

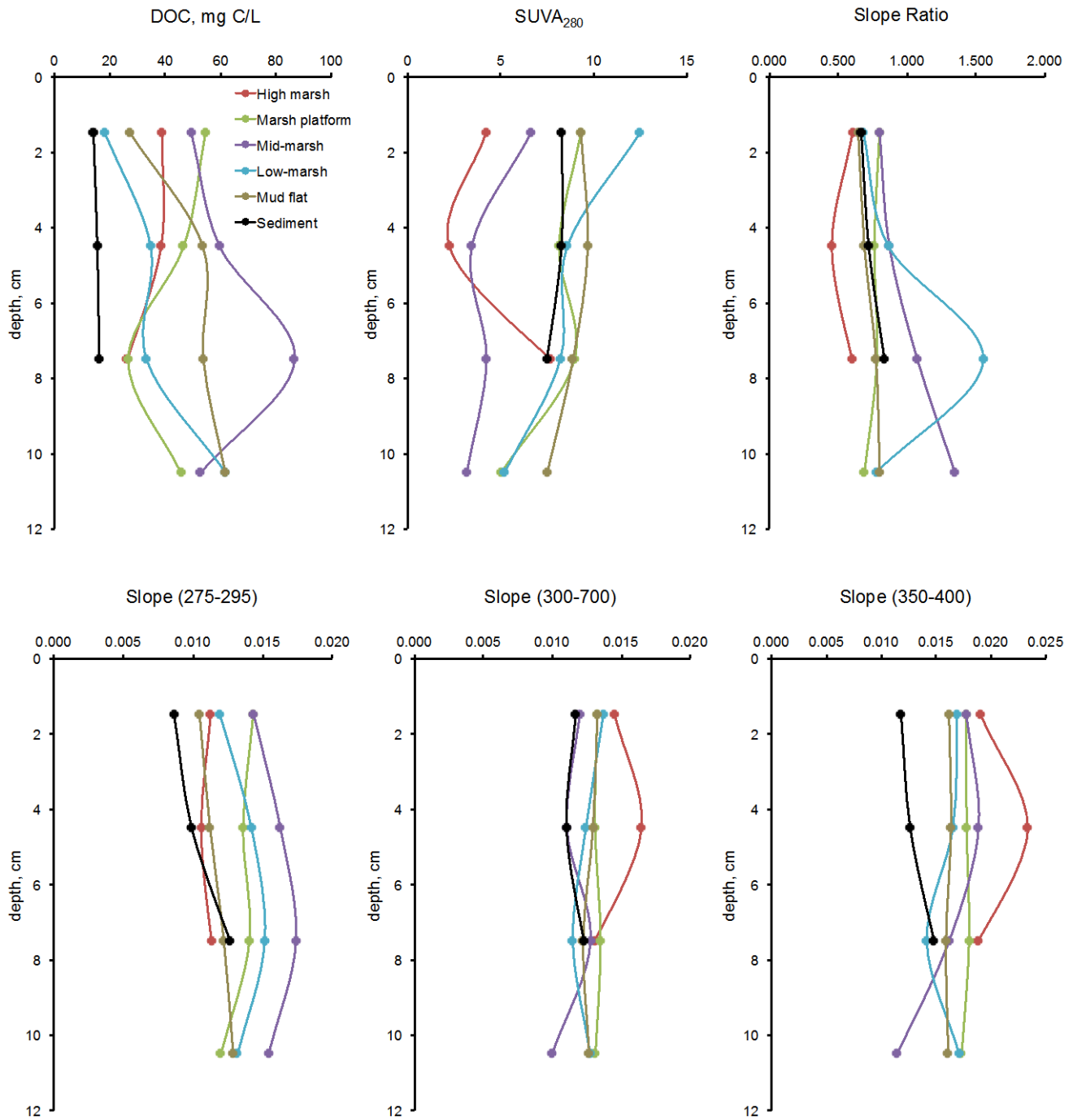


Figure 11-2.18. Average pore water depth profiles of DOC and spectral parameters. Profiles shown are averages by habitat type across all sites and sampling dates. Error bars are omitted for clarity, but can be found in data appendices.

## 2.2 Summer 2011 Mendall Marsh Survey

In early June and late July of 2011, an expanded survey of soils in the Mendall Marsh was conducted. Surveys of methyl Hg in Penobscot sediments and soils in 2009 and 2010 showed that the high marsh platforms of Mendall Marsh are sites of particularly high methyl Hg accumulation relative to other sites in the Penobscot estuary (see Section 4) and relative to many other ecosystems (see Section 3). The Mendall Marsh complex is the largest marsh complex along the tidal Penobscot River. It is situated along the river reach south of Orrington where sediments are highly contaminated with Hg.

One goal of the marsh survey was to more fully evaluate the initial finding of particularly high methyl Hg concentrations in the marsh. Other goals of the 2011 marsh survey included:

- identify hot spots within the marsh
- evaluate the drivers of high methyl Hg in the Mendall marsh complex
- link hot spots to vegetation, elevation, or site chemistry.

These objectives were based on the idea that hot spots of methyl Hg accumulation in the marsh might be identified and targeted for remediation, protection or monitoring.

In 2009 and 2010, a few sites in Mendall Marsh were sampled on the large west platform of the marsh (the part of the marsh that runs along Rt. 1A), plus one site in the southern part of the marsh complex near where Rt. 174 crosses the South Marsh River. In 2011, 15 additional sites were sampled, including sites on both of the large marsh platforms near the mouth on each side of the South Marsh River (here called the east and west platforms) and in the southern part of the marsh complex, further upstream. Ten sites were sampled in early June. In late July, the sites were resampled, and 5 more sites were added.

Figure 11-2.19 shows the additional sites surveyed in 2011. Sampling focused on surface soils (0-3 cm depth) and pore waters. Based on the volume sampled, we estimate that pore waters were extracted from roughly the top 5 cm of soil. Soil and pore water Hg and methyl Hg were measured, along with a suite of geochemical parameters. Dianne Kopec conducted most of the sampling, and Aram Calhoun provided identification of the vegetation at each site.

Figures 11-2.20 to 11-2.22 show that average Hg and methyl Hg concentrations at these sites in 2011, and the dominant vegetation type, on maps of the west, east and south portions of the Mendall Marsh complex. A summary of marsh data and controls on methyl Hg in marsh soils is provided below.



Figure 11-2.19. Overview of site locations in the summer 2011 survey of soils in Mendall Marsh (map from Google Earth).

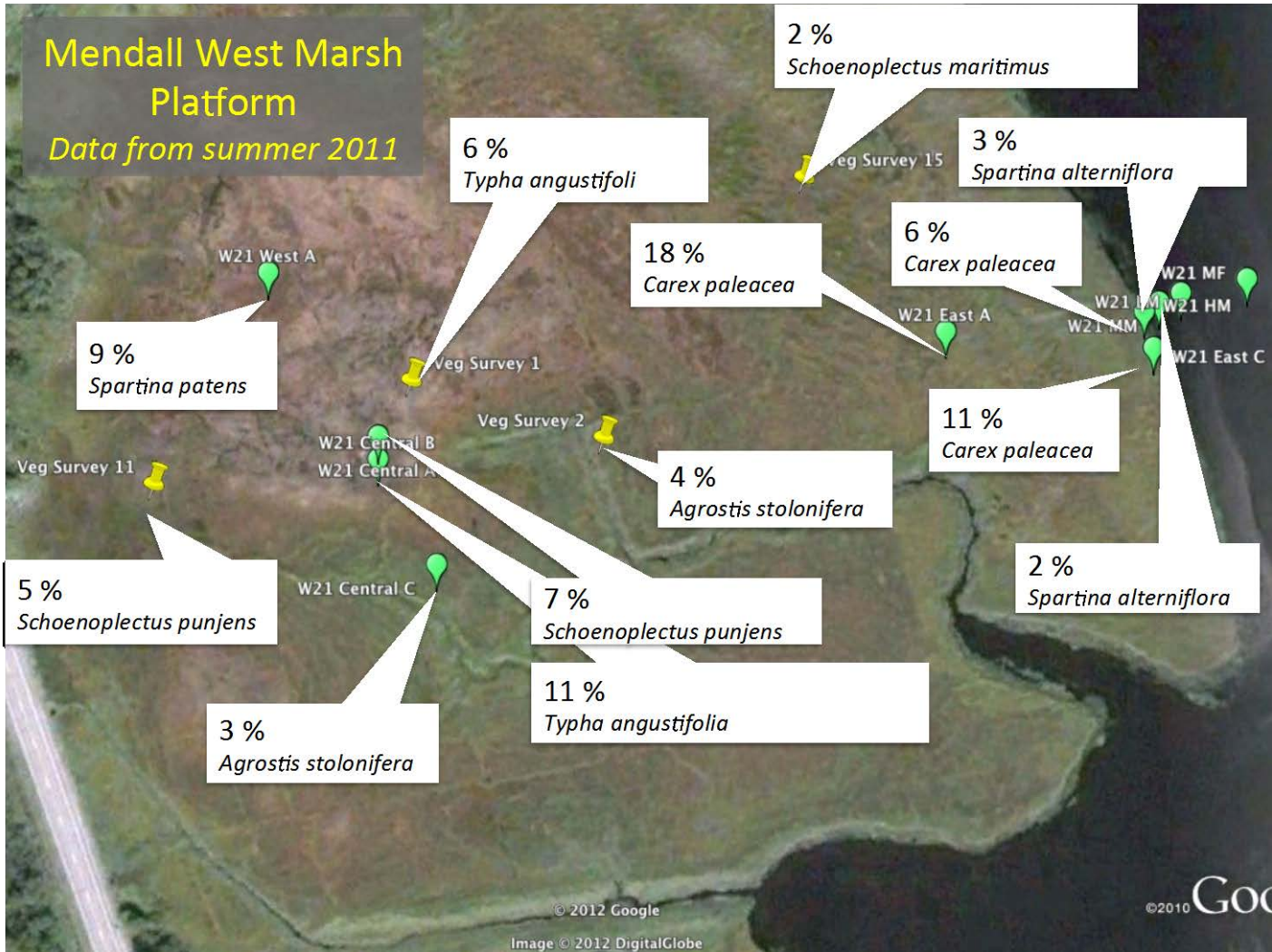


Figure 11-2.20. % methyl Hg in surface soils in Mendall Marsh, west platform, summer 2011. Data shown are averages of all samples (generally n= 2 to 3). The dominant vegetation for each sampling site is also listed.

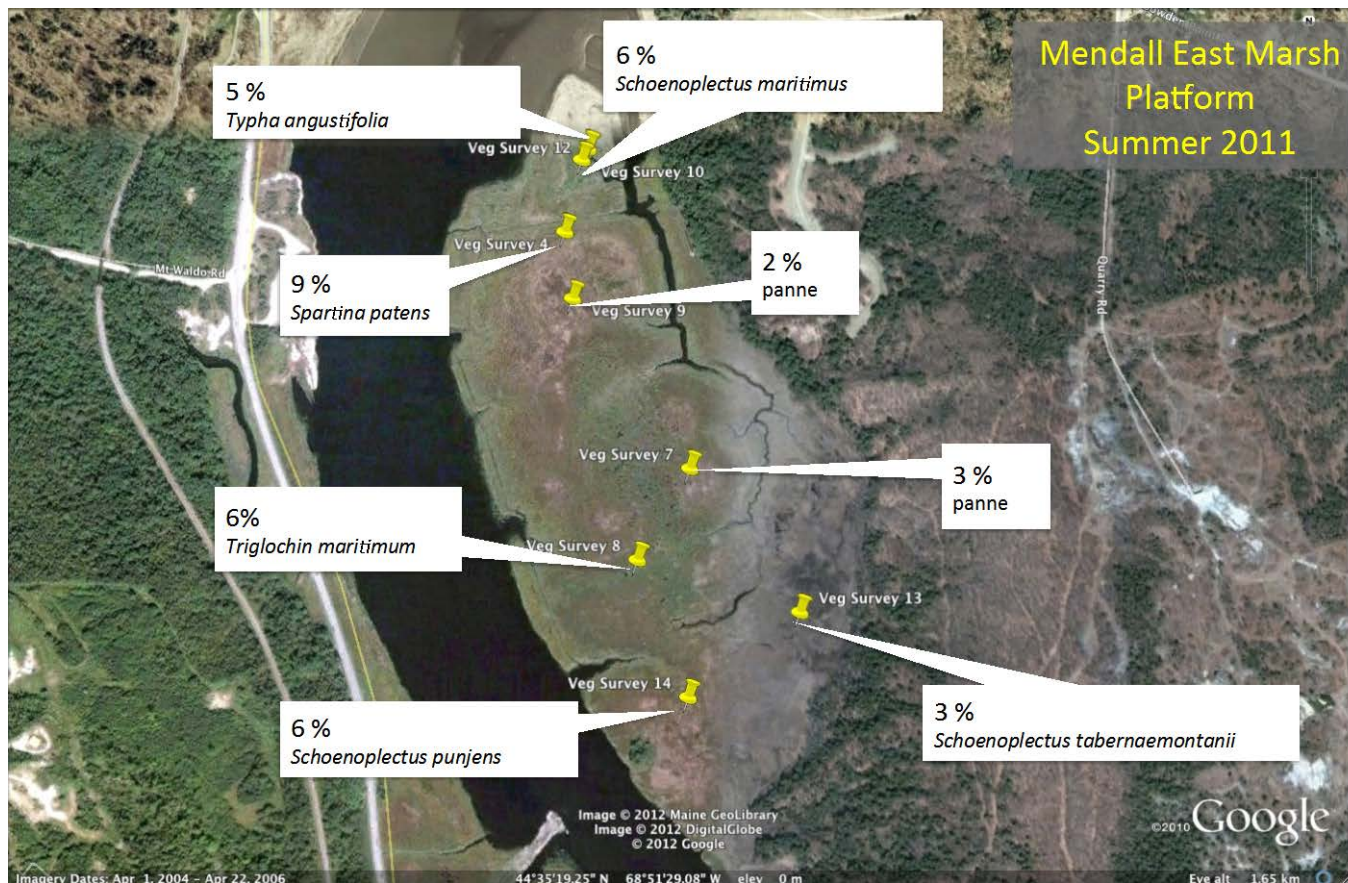


Figure 11-2.21. % methyl Hg in surface soils in Mendall Marsh, east platform, summer 2011. Data shown are averages of all samples (generally n= 1 to 2). The dominant vegetation for each sampling site is also listed.

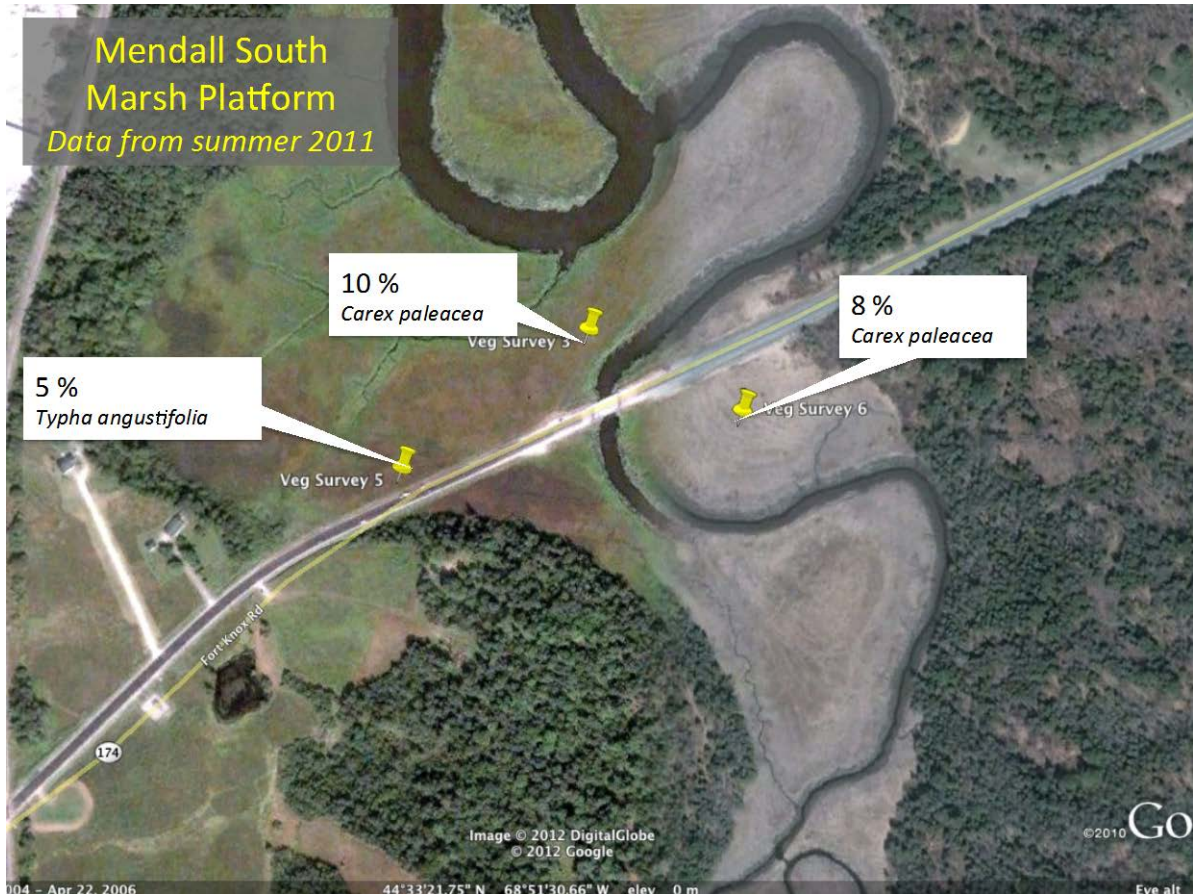


Figure 11-2.22. % methyl Hg in surface soils in Mendall Marsh, south marsh complex, summer 2011. Data shown are averages of all samples (generally n= 2 to 3). The dominant vegetation for each sampling site is also listed.

### 2.3 Summary Of Hg And Methyl Hg Distributions In Mendall Marsh

The detailed 2011 survey of Mendall Marsh confirmed the high accumulation of methyl Hg in high marsh soils of the complex, and extended the data to a larger range of habitats within the marsh. The survey showed that high levels of methyl Hg are found in all of the major Mendall Marsh complex platforms, not just the west platform where high methyl Hg was initially identified. The survey also identified certain vegetation complexes as most prone to methyl Hg accumulation.

Figure 11-2.23 shows the average values of total Hg, methyl Hg and % methyl Hg in surface (0-3) soils, and Figure 11-2.24 shows the same for surficial (0-5 cm) pore waters, for all of the Mendall marsh sites sampled, across all years (2009-2011). The detailed 2011 survey of Mendall Marsh confirmed the high accumulation of methyl Hg in high marsh soils of the complex, and identified certain vegetation complexes as most prone to methyl Hg accumulation. The survey showed that high levels of methyl Hg are found in all of the major Mendall Marsh complex platforms, not just the west platform where high methyl Hg was initially identified.

Spatially, % methyl Hg was highly variable across the marsh platforms. Although there was variability among sampling dates at individual sample sites, % methyl Hg varied more spatially than temporally (see bar graphs of % methyl Hg by site and season in Figure 11-2.33 below). However, in context with sediments and soils in other ecosystems, methyl Hg and % methyl Hg are substantially elevated across the Mendall complex relative to other parts of the Penobscot system, and most other ecosystems (see Sections 3 and 4).

The 2011 marsh survey was designed to sample a wider and range of vegetation types, based on the hypothesis that vegetation types are linked to elevation and average water table height, which could also be a determinant of Hg and methyl Hg concentrations.

The average elevation of dominant plant communities is shown in Figure 11-2.25. *Spartina alterniflora* (tall *Spartina*) was the dominant plant at the river edge below the marsh platform. The average elevation on the marsh platform varied by less than half a meter among vegetation types. Cosmopolitan bulrush (*Schoenoplectus maritimus*), arrow grass (*Triglochin maritimum*) and creeping bentgrass (*Agrostis stolonifera*) were dominants at the lowest elevations; Cattail (*Typha angustifolia*) at the highest. Table 11-2.1 lists the dominant plant species in Mendall Marsh.

Total Hg in marsh surface soils was highest at the marsh edge by the river, at elevations below the main platform, and on the berm at the marsh edge (Figure 11-2.25). Total Hg concentrations in the surface soils of the high marsh platform were roughly half of concentrations in the mud and berm at the edge of the marsh, where *S. alterniflora* grows. Bulk density is higher in the low and mid marsh (Figure 11-2.26), as are concentrations of crustal metals (see data appendices), reflecting the silt/mud nature of the marsh edges. Soils on the high marsh platform are much higher in organic matter content than marsh edges, because of higher root mass and accretion of plant material into peat (Figure 11-2.26). The concentration of crustal metals (e.g. Fe, Al, Mg) in high marsh soils is roughly half of that in the lower marsh. However, the mineral

content of high marsh soils is highly variable by vegetation type, perhaps due to the growth rate of the marsh in different vegetation regimes, the ability of different vegetation to trap particulates suspended in river water, or distance from the Marsh River.

Total Hg concentrations in marsh soils are well predicted by the mineral content of soils (represented by bulk density, Fe and Al in Figure 11-2.27a), and are inversely correlated with soil organic matter content. Thus, accumulation of Hg in marsh surface soils seems to depend on the rate of accretion of river particulates in marsh soils, and the dilution of that mineral matter by plant growth and organic matter accumulation in surface soils. Within surface marsh soils, total Hg accounts for about 40% of the variability in bulk methyl Hg, based on linear regression of the log transformed variables (Figure 11-2.27b). Because total Hg is an important driver of methyl Hg in the marsh, the factors that impact Hg accumulation are important when considering remediation options.

Methyl Hg concentrations, and methyl Hg as percentage of total Hg in soils were highest in the vegetation types dominant at middle elevations in the marsh (Figure 11-2.28). The highest % methyl Hg values in soil were found at sites dominated by *Carex paleacea* (Salt marsh sedge). Slightly lower % methyl Hg values were found at sites dominated by *Spartina patens* (Salt hay grass or short *Spartina*) or *Schoenoplectus*



*Carex paleacea*. Photo from Biopix.eu

*punjens* (Three-square). These species were found at intermediate elevations in the marsh. The % methyl Hg was usually below 3% in pannes (open areas) and in tall *Spartina* stands (*S. alterniflora*), which are found in the lower marsh. As is typical of tidal marsh platforms, elevation changes across the marsh are heterogeneous, and don't follow a smooth increase with distance from the river.

Pore water Hg and methyl Hg concentrations were concomitantly highest at middle elevations (Figure 11-2.29), and sediment:water partition coefficients for Hg were low (Figure 11-2.30). These sites of highest % methyl Hg were generally high in solid organic matter content, and had high pore water DOM content. The DOM at these sites was also generally more aromatic (based on SUVA<sub>280</sub>) than other sites (Figure 11-2.31). These sites were also often highly sulfidic.

The correspondence between % methyl Hg and measured geochemical parameters across the marsh sites can be used to try and identify the drivers and locations of highest methyl Hg production and accumulation. There was strong correlation between % methyl Hg in surface soils and measured methylation rates ( $r^2 = 0.60$  for  $n = 23$ ) and the sediment:water partition coefficient for total Hg (0.29). Surface soil % methyl Hg was

weakly but significantly correlated with porosity, and inversely correlated with total Hg. There was no significant correlation between % methyl Hg and pH, salinity, or pore water sulfide. However, % methyl Hg was significantly correlated with colloidal FeS in porewaters (see Section 4 for more biogeochemical information).

The main driver of bioaccumulation and risk may be the concentration of methyl Hg in pore water, and/or the partition coefficient for methyl Hg between solid and aqueous phase in soils (Gilmour et al. in review). Methyl Hg concentrations in pore waters are a strong function of the  $K_D$  for total Hg (Figure 11-2.32b). Thus high methylation rates, and high bioavailability of methyl Hg for uptake may both be functions of the weak partitioning of Hg and methyl Hg to the solid phase in Penobscot marshes, relative to many other ecosystems. Biogeochemical controls on partitioning behavior are explored in depth in Sections 3 and 4.

The association of high methyl Hg with certain elevations and types of vegetation may allow targeting of remediation options to particular areas within the Mendall Marsh. However, these areas are heterogeneously distributed across the marsh, and may be difficult to survey. Based on the survey, LIDAR elevation maps, and personal observations, the areas of high methyl Hg are widespread across the marsh platforms, and not confined to small areas. Further, although we can identify sub-areas with particularly high % methyl Hg, methyl Hg levels in most areas of the marsh are elevated above those found in many other ecosystems.

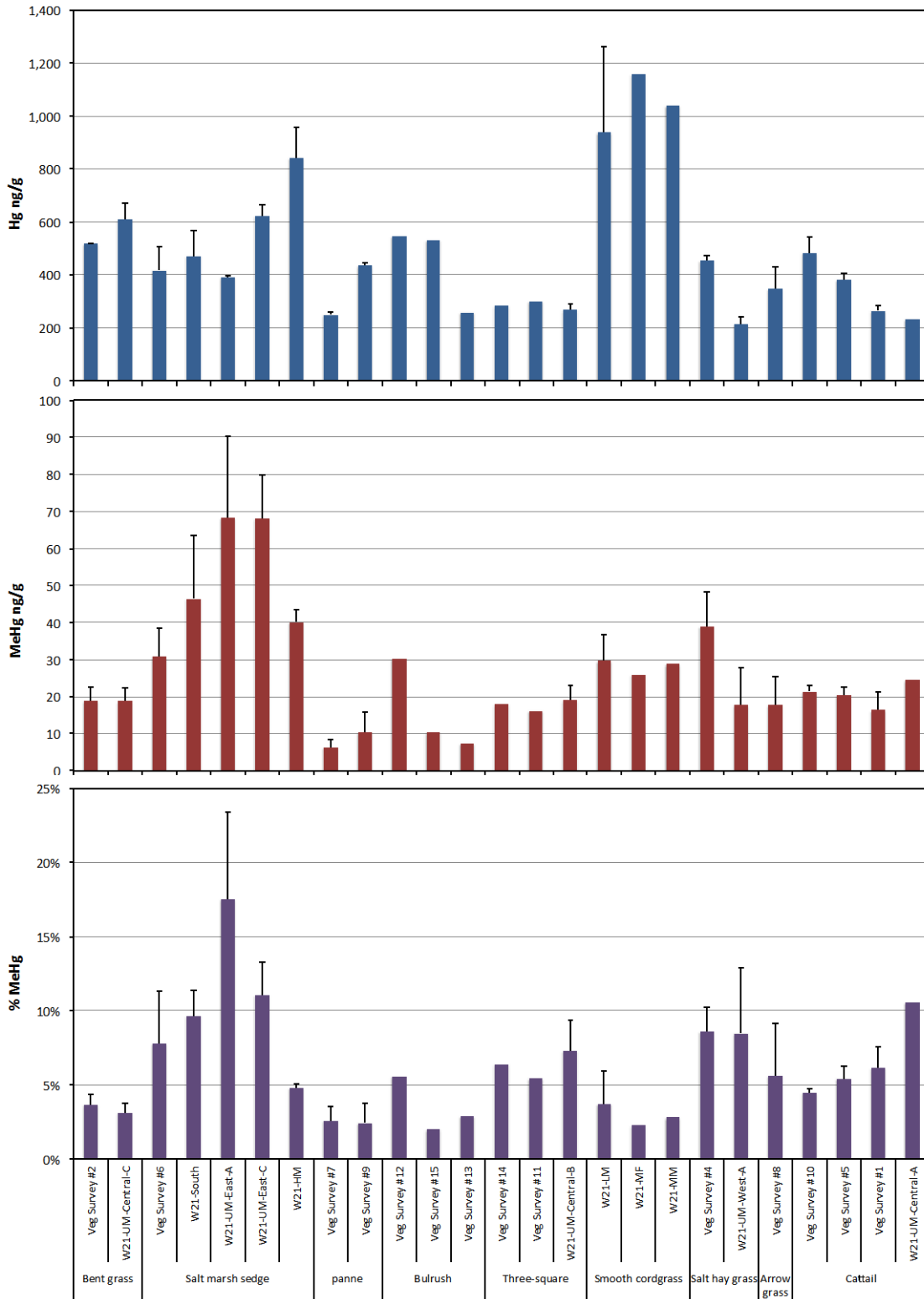


Figure 11-2.23. Total Hg (top), methyl Hg (middle) and methyl Hg as a percent of total Hg (% methyl Hg, bottom) in Mendall Marsh surface soils (0-3 cm) by vegetation type. Bars are averages, with standard deviations, of all samples collected in June-September in all years. April data were not included in this comparison as April values tended to be higher, but were not available for all sites. Sites without error bars were only sampled once.

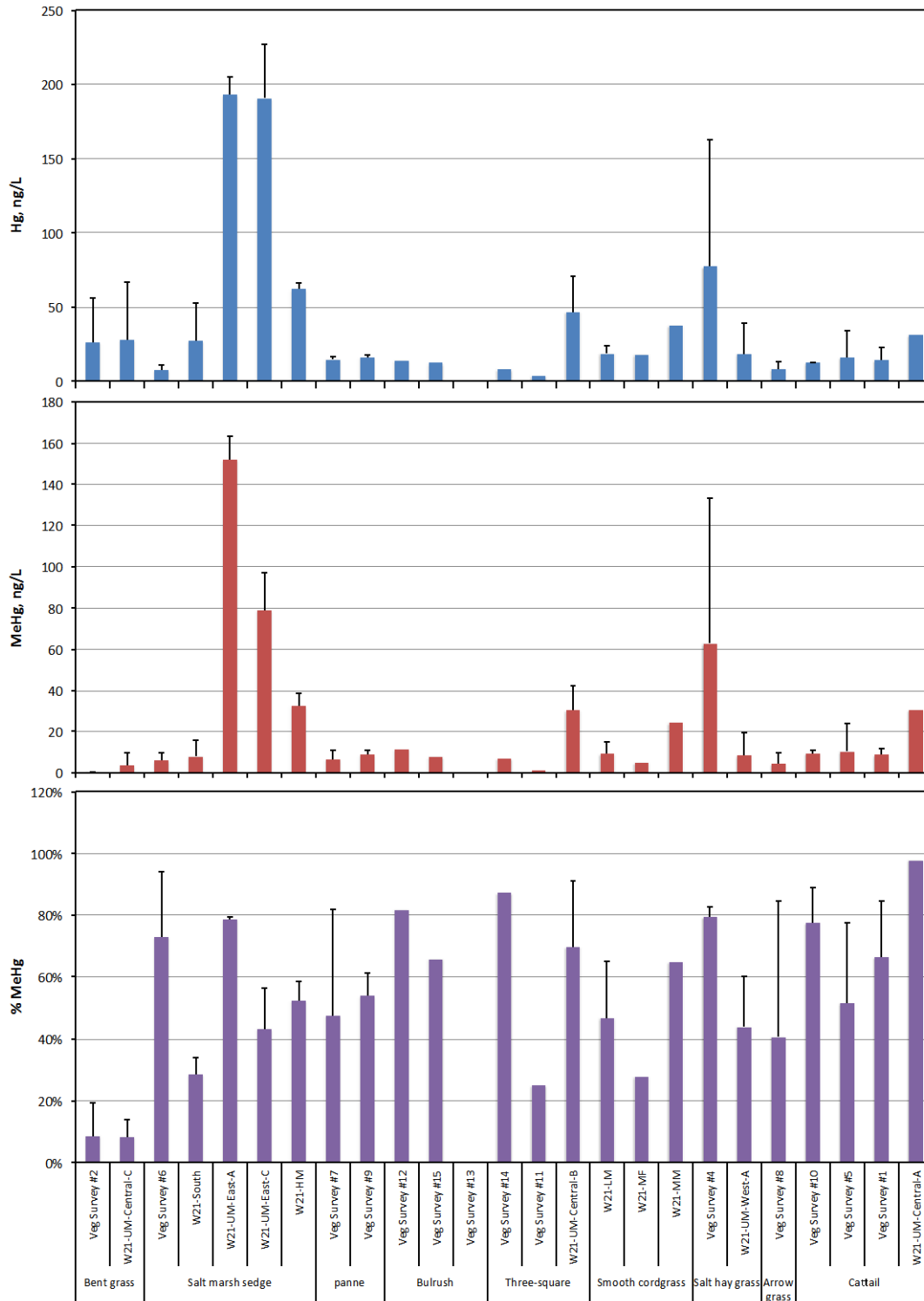


Figure 11-2.24. Total Hg (top), methyl Hg (middle) and methyl Hg as a percent of total Hg (% methyl Hg, bottom) in Mendall Marsh surface pore water (0-5 cm) by vegetation type. Bars are averages, with standard deviations, of all samples collected in June-September in all years. April data were not included in this comparison as April values tended to be higher, but were not available for all sites. Sites without error bars were only sampled once.

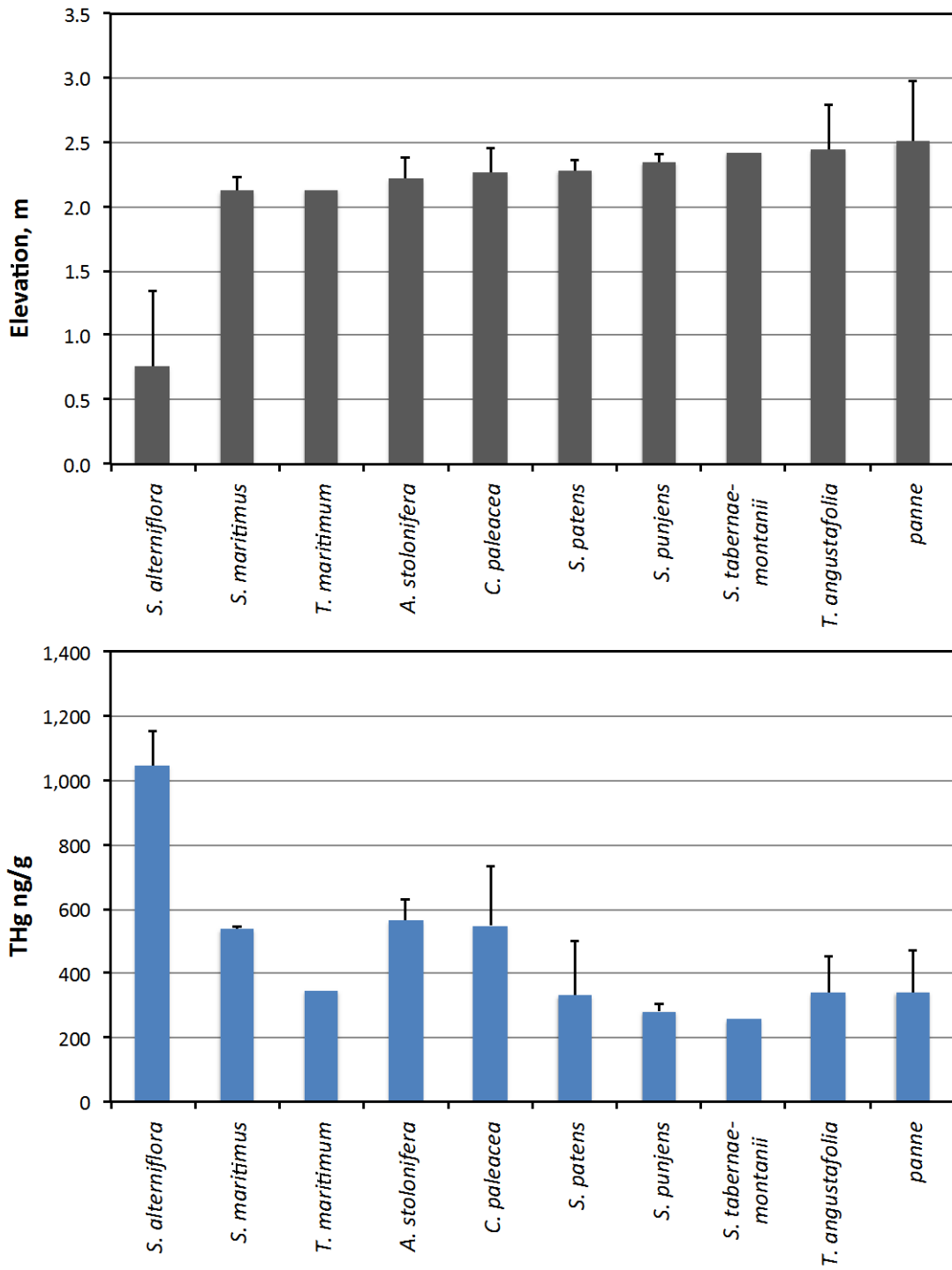


Figure 11-2.25. Average elevation (top) by dominant plant species in Mendall Marsh, and average total Hg concentration in surface (0-3 cm) soils. Elevations taken from LIDAR.

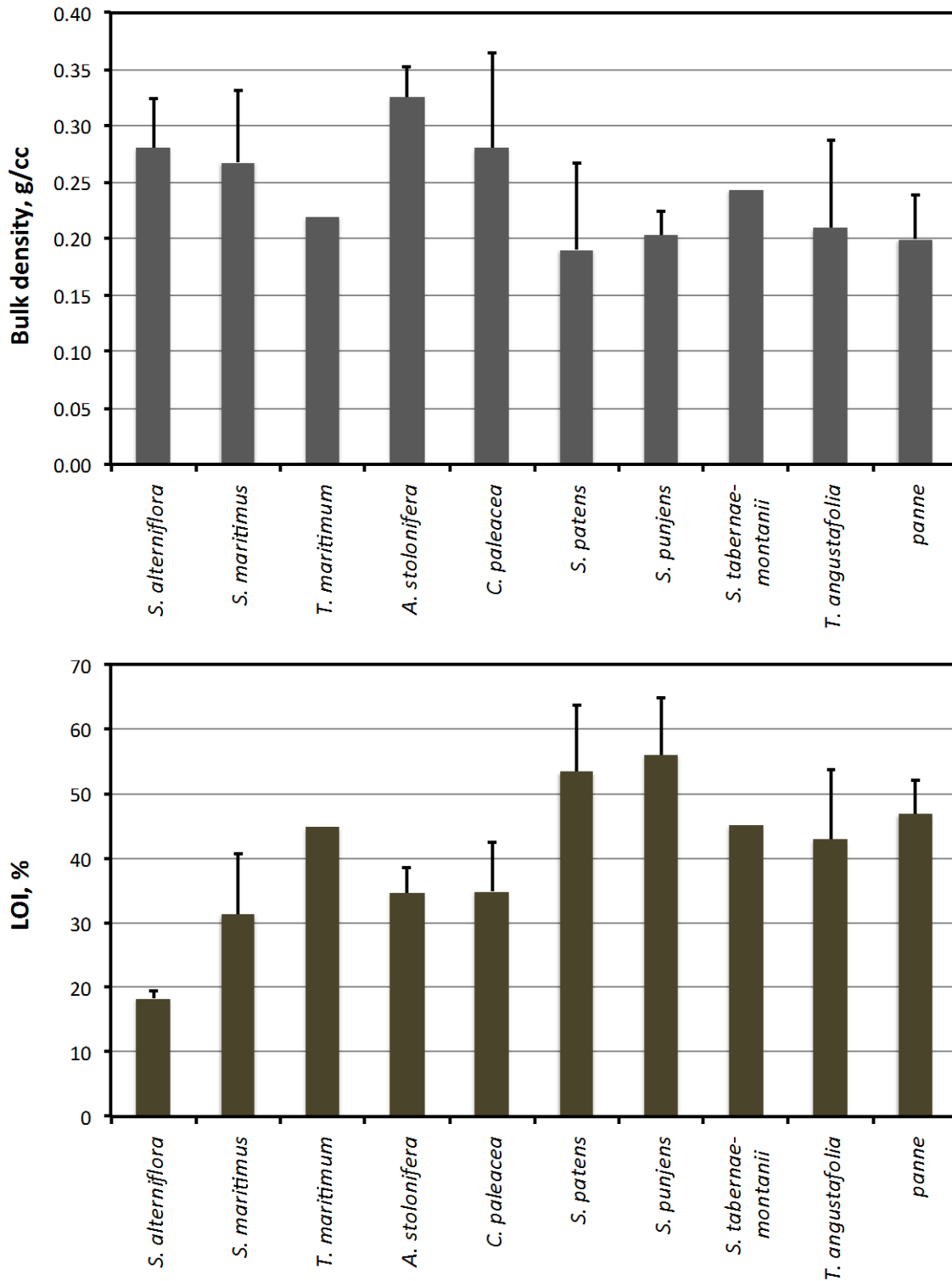


Figure 11-2.26 Average bulk density (top) and organic carbon content (% LOI) by dominant plant species in Mendall Marsh. Elevations increase from left to right, as per Figure 11-2.24.

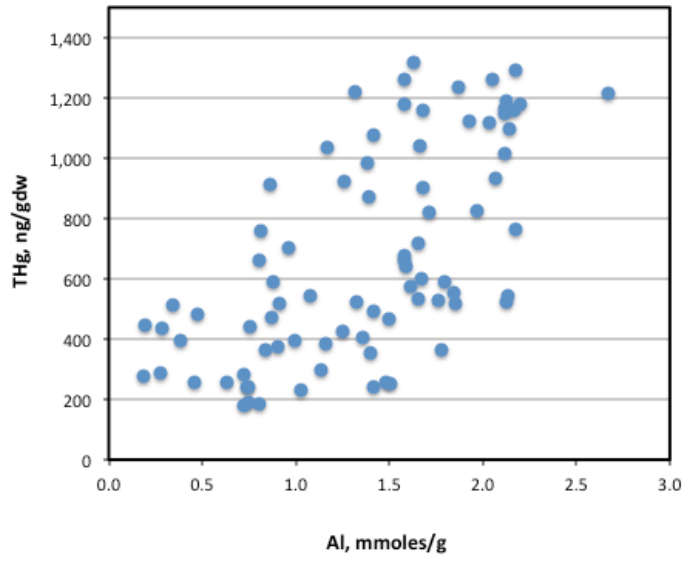
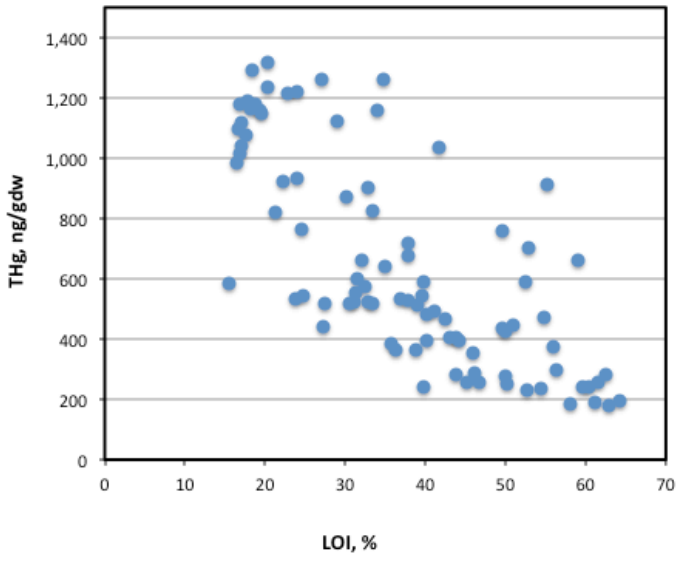
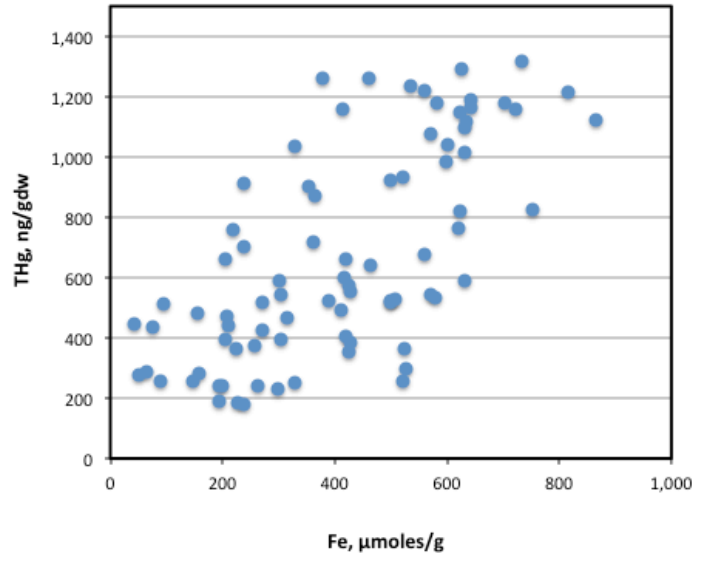
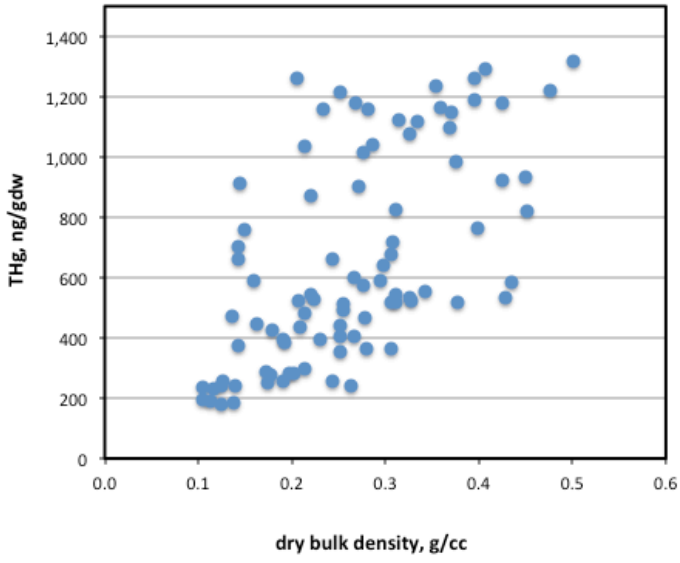


Figure 11-2.27. Correlates of total bulk phase Hg in Mendall Marsh surface soils. Data include all marsh surface soils data (0-3 cm) from 2009-2011.

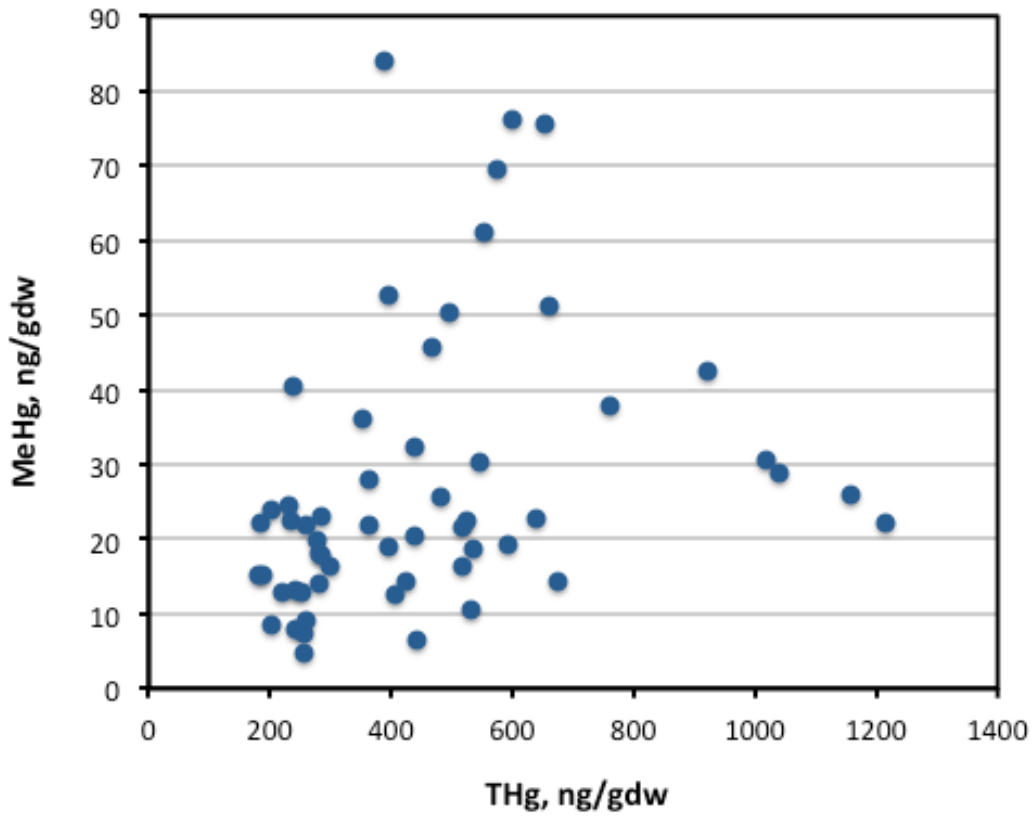


Figure 11-2.27b. Correlation between total bulk phase Hg and methyl Hg in Mendall Marsh surface soils. Data include all marsh surface soils data (0-3 m) from 2009-2011. Within surface marsh soils, total Hg accounts for about 40% of the variability in bulk methyl Hg, based on linear regression of the log transformed variables.

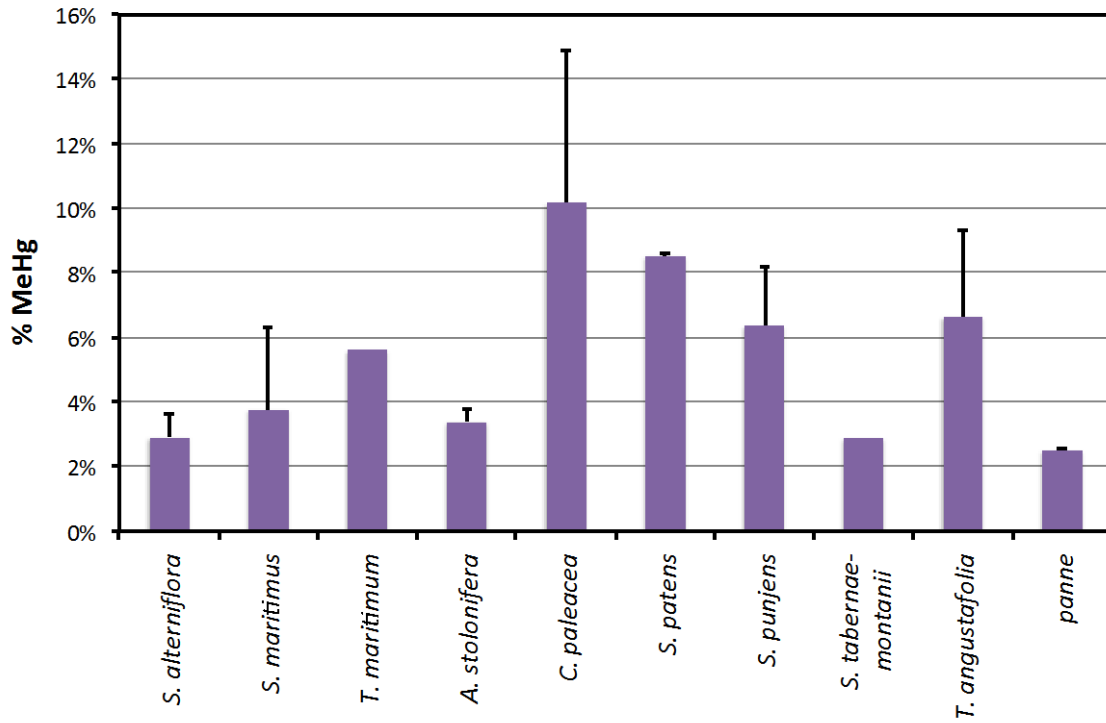
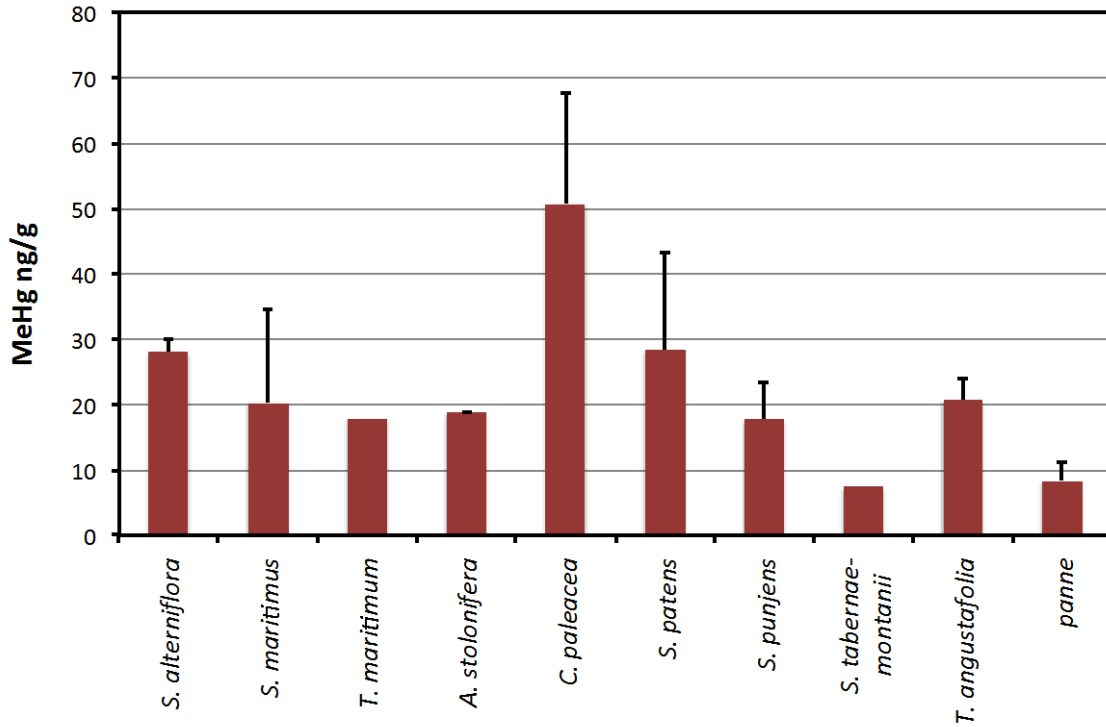
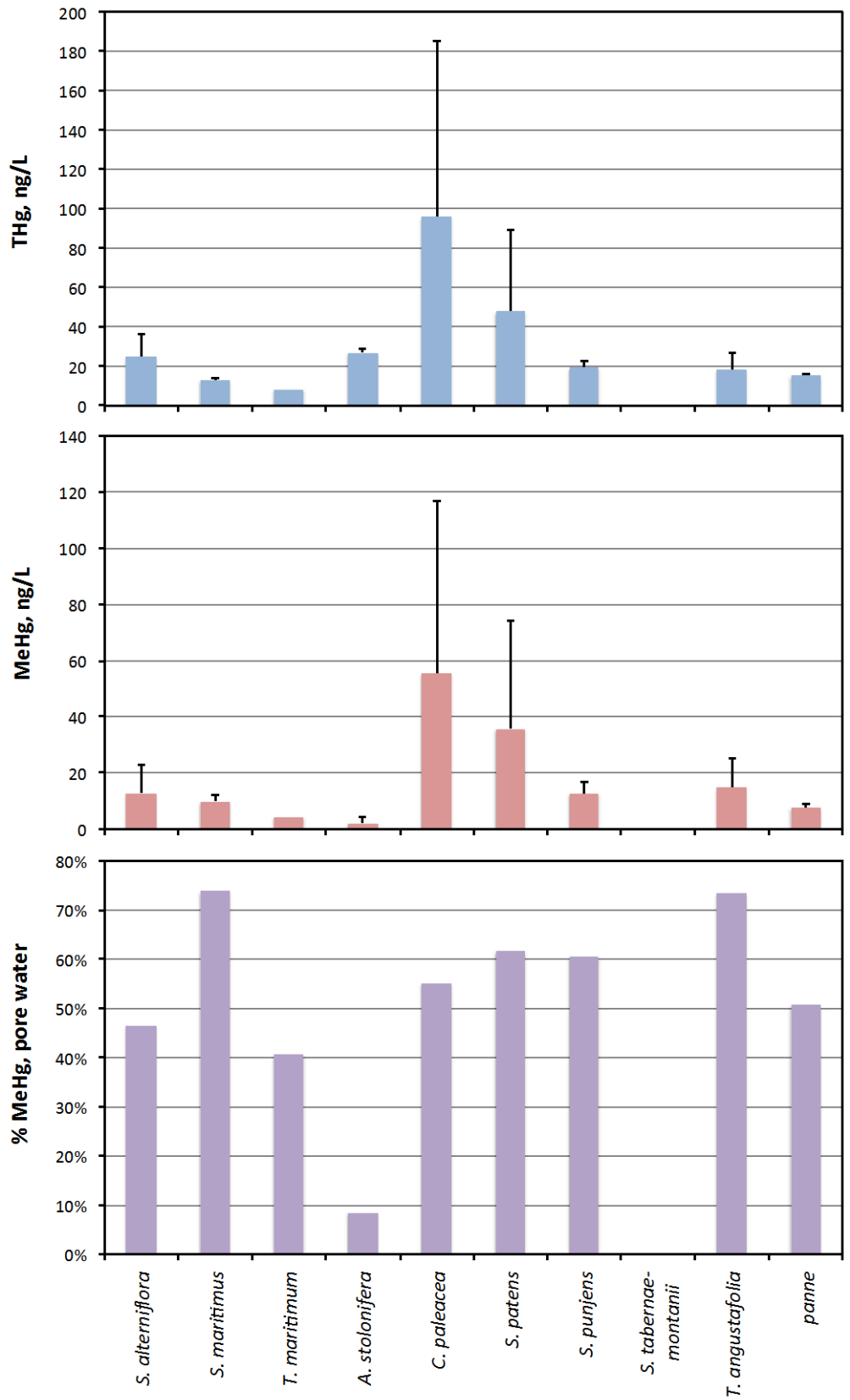


Figure 11-2.28. Average methyl Hg (top) and % methyl Hg (bottom) by dominant plant species in Mendall Marsh. Elevations increase from left to right.

Figure 11-2.29. Average pore water concentrations of total Hg (top), methyl Hg (middle) and % methyl Hg (bottom) by dominant plant species in Mendall Marsh. Elevations increase from left to right.



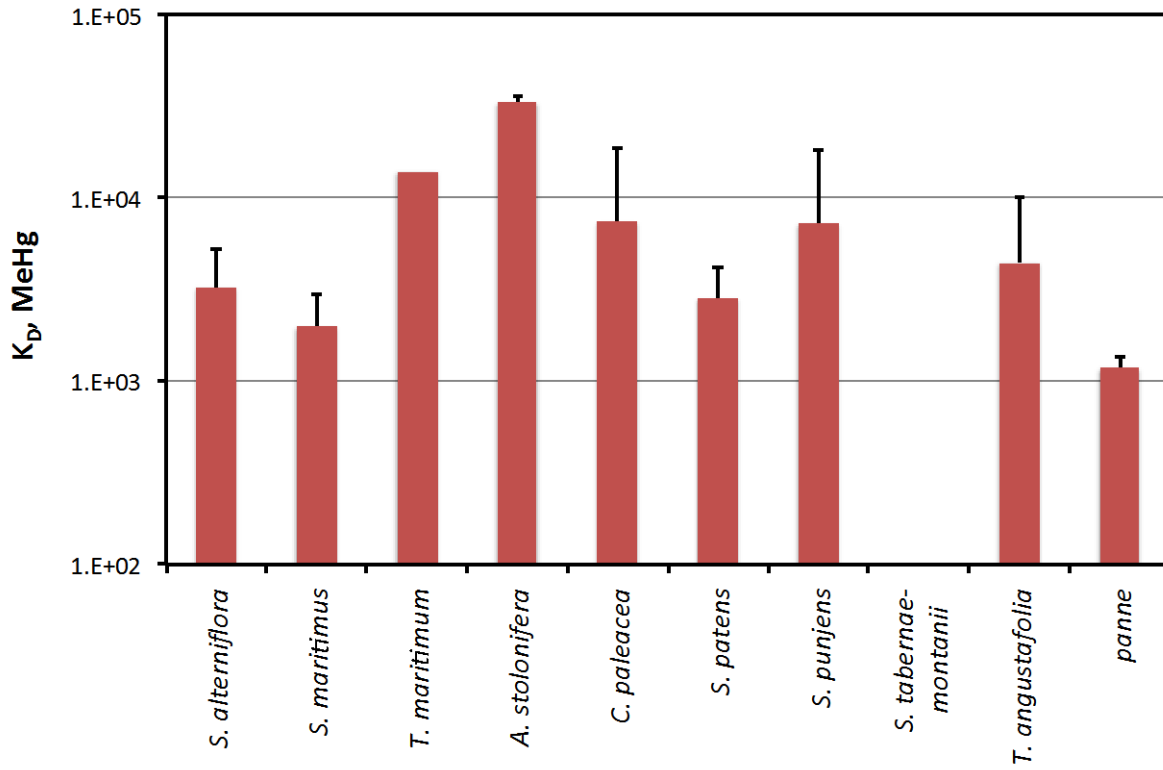
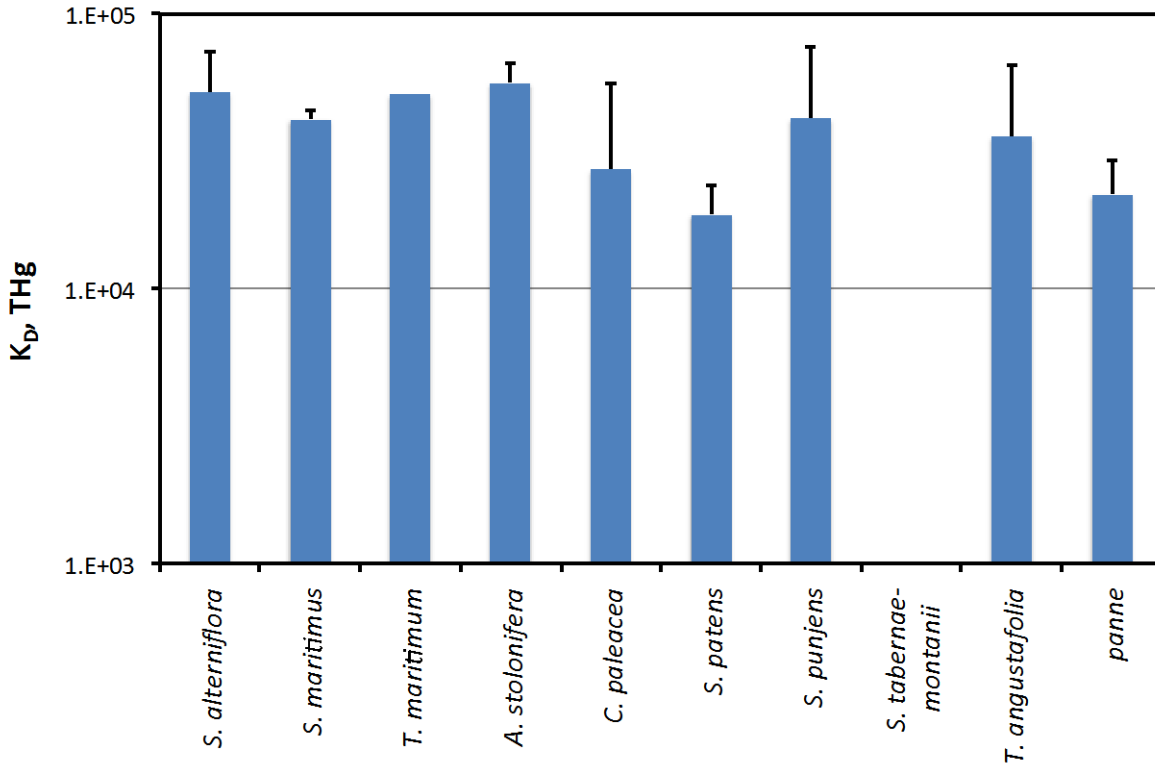


Figure 11-2.30. Average sediment:water partition coefficients for total Hg (top) and methyl Hg (bottom) by dominant plant species in Mendall Marsh. Elevations increase from left to right.

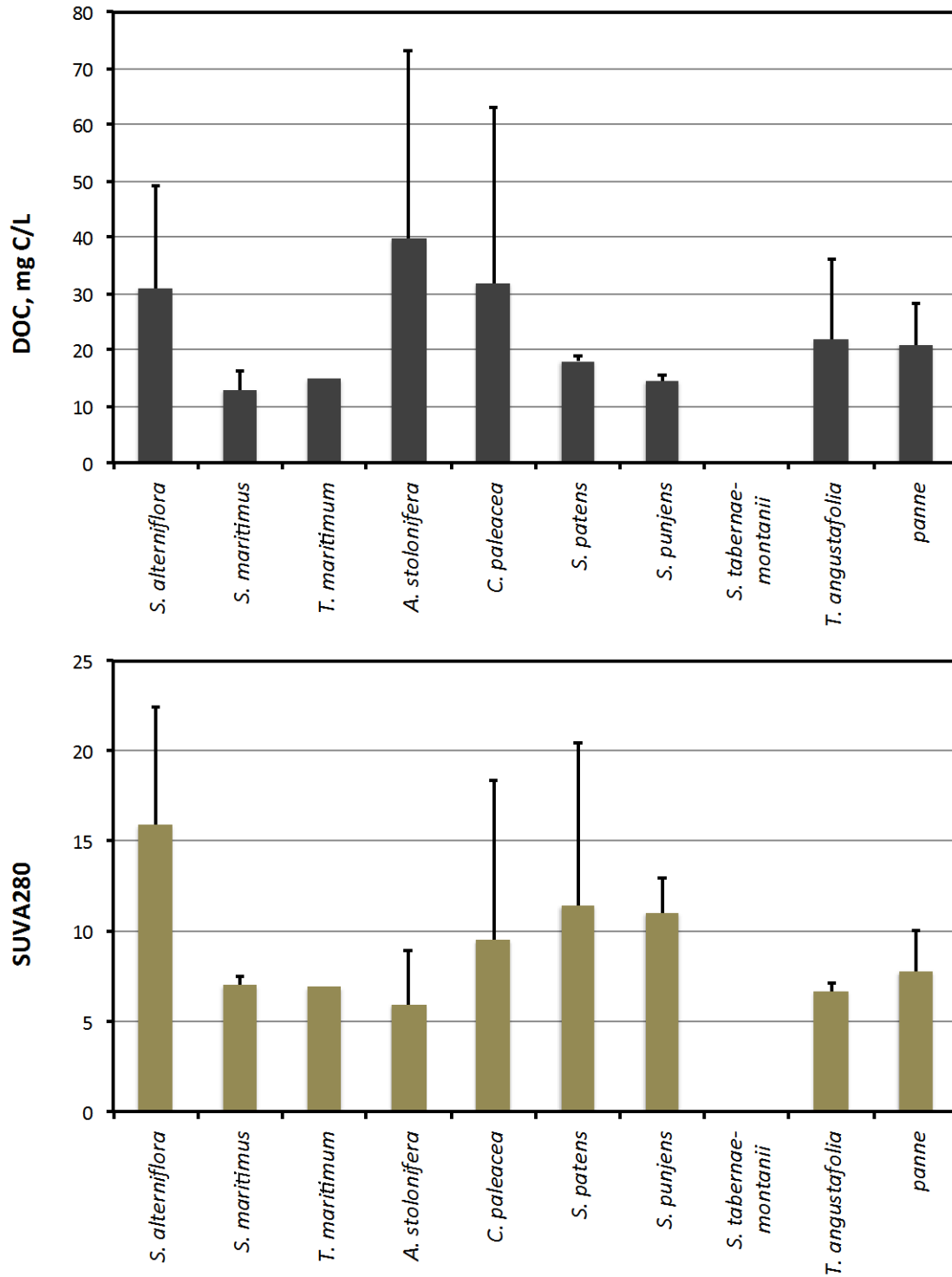


Figure 11-2.31. Average pore water DOC (top) and specific UV280 absorbance (bottom) by dominant plant species in Mendall Marsh. Elevations increase from left to right.

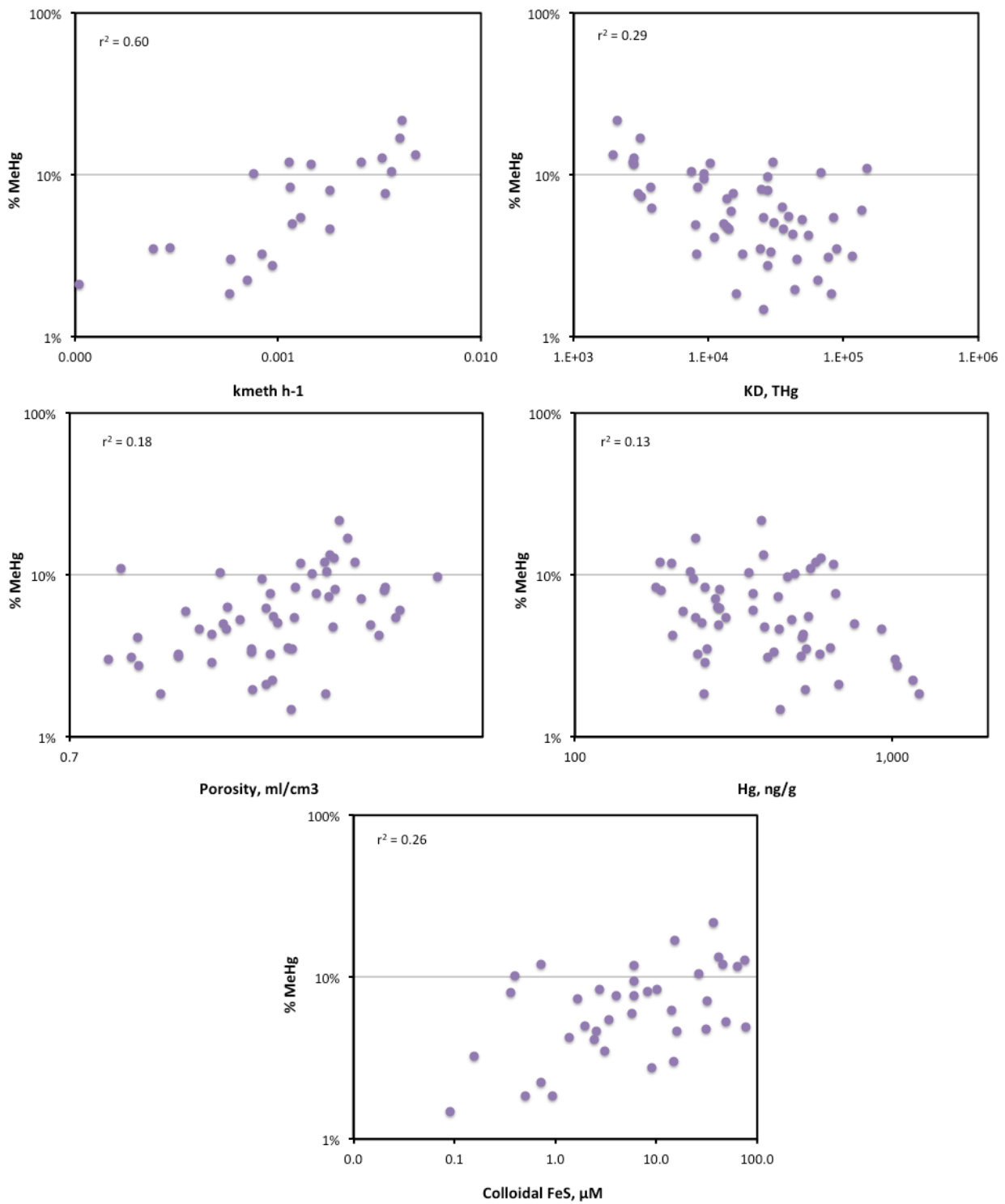


Figure 11-2.32a Significant correlates of % methyl Hg in Mendall Marsh surface (0-3 cm) soils. Data include all surface marsh surface soils data from 2009-2011. Variables were log transformed in some cases to achieve normality. See definition of colloidal FeS in text.

**Table 11-2.1. Dominant plants of Mendall Marsh. Plant names taken from USDA plant database. For more detail and images, see reports from Aram Calhoun.**

Latin name	Common name	Other names	Growth habit
<i>Agrostis stolonifera</i>	Creeping bentgrass		gramminoid
<i>Calystegia sepium</i>	False bindweed	Wild morning glory	forb
<i>Carex paleacea</i>	Salt marsh sedge	Chaffy sedge	gramminoid
<i>Eleocharis uniglumis</i>	Spikerush	Creeping spikerush, Saltmarsh spikerush	gramminoid
<i>Festuca rubra</i>	Red fescue	Redtop, Seaside bentgrass	gramminoid
<i>Juncus balticus</i>	Mountain rush	Baltic rush; now <i>Juncus articus</i>	gramminoid
<i>Juncus gerardii</i>	Black grass	Saltmeadow rush	gramminoid
<i>Potentilla anserina</i>	Silverweed	Cinquefoil; now <i>Argentina anserina</i>	forb
<i>Schoenoplectus maritimus</i>	Cosmopolitan bulrush	was <i>Scirpus</i> , <i>Bulboscheonus</i>	gramminoid
<i>Schoenoplectus punjens</i>	Common three-square	was <i>Scirpus</i>	gramminoid
<i>Schoenoplectus tabernaemontanii</i>	Softstem bulrush	Also <i>Schoenoplectus lacustris</i>	gramminoid
<i>Solidago sempervirens</i>	Seaside goldenrod		forb
<i>Spartina alterniflora</i>	Smooth cordgrass	tall <i>Spartina</i>	gramminoid
<i>Spartina patens</i>	Salt hay grass	short <i>Spartina</i>	gramminoid
<i>Spartina pectinata</i>	Slough grass		gramminoid
<i>Symphotrichum novi-belgii</i>	New York aster		forb
<i>Triglochin maritimum</i>	Seaside arrow grass		gramminoid
<i>Typha angustifolia</i>	Narrow-leaved cattail		forb

## 2.4 Spatial Distributions Across The Penobscot System

This section provides summary graphics and discussion of the spatial distribution of measured variables, for the all of sediments and marsh soil sites sampled in the Penobscot system in this study, from 2009-2011. Spatial distributions are shown by site and season in the first subsection, and then averaged across sites and habitats in additional sections.

### 2.4.1 Bar plots for surface soils and pore waters by site and season

Bar graphs in Figures 11-2.33 to 11-2.40 show the concentrations of measured parameters in surface sediment/soils and pore waters by area and habitat for each season sampled, including all data from 2009-2011. Effectively, these data are site-specific values by season. Most data represent just one sampling date, although almost all measurements were made from composite or replicate samples. Graphs are arranged by increasing salinity from left to right.

*Hg and methyl Hg in surface sediments and soils.* Surface total Hg concentrations ranged from roughly 200 to 1200 ng/g dry wt., with a few exceptions (Figure 11-2.33). In the large Mendall marsh platforms, Hg concentrations generally ranged between 200 and 600 ng/g. Higher total Hg concentrations were measured in berms deposited along the edges of Mendall Marsh platforms, and in other wetland (W10, W17 and W26) mud flats, silty low marsh sites, and in the few bottom sediments examined (ES11, OB1 and the PB sites).

The distribution of methyl Hg and % methyl Hg in surface sediments and soils (Figure 11-2.33) was more variable (showed a wider range) than total Hg. The highest methyl Hg concentrations and % methyl Hg were found on the main Mendall Marsh platforms, although concentrations were highly variable, mostly among sites (rather than with season).

Total Hg and methyl Hg concentrations in pore waters were more variable across the system than were bulk concentrations (Figure 11-2.34). Methyl Hg as a fraction of total Hg (% methyl Hg) in pore waters was unusually high, with methyl Hg accounting for most of the Hg in pore waters in most marsh samples. High pore water concentrations of both total Hg and methyl Hg arise from both the elevated Hg concentrations in this contaminated system, but also in large measure low partition coefficients between solid and aqueous phases (Figure 11-2.35). See Section 3 for a comparison of these values with other ecosystems. As for solids, the % methyl Hg in pore waters was highest at the Mendall Marsh (W21) platform sites (Figure 11-2.34).

Plots 11-2.35 to 11-2.40 show distributions for a variety other parameters.

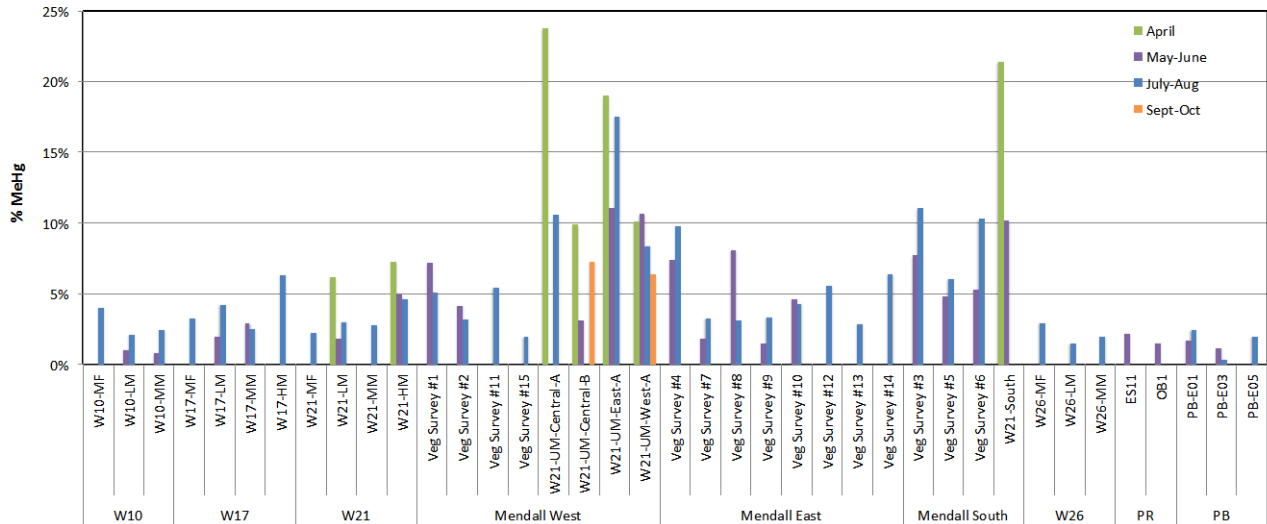
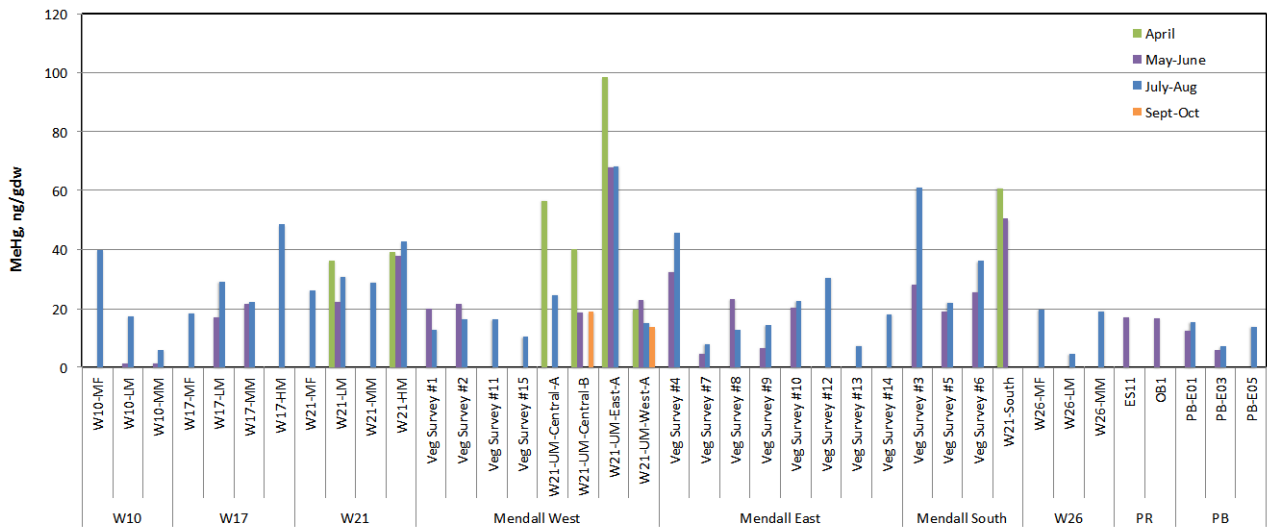
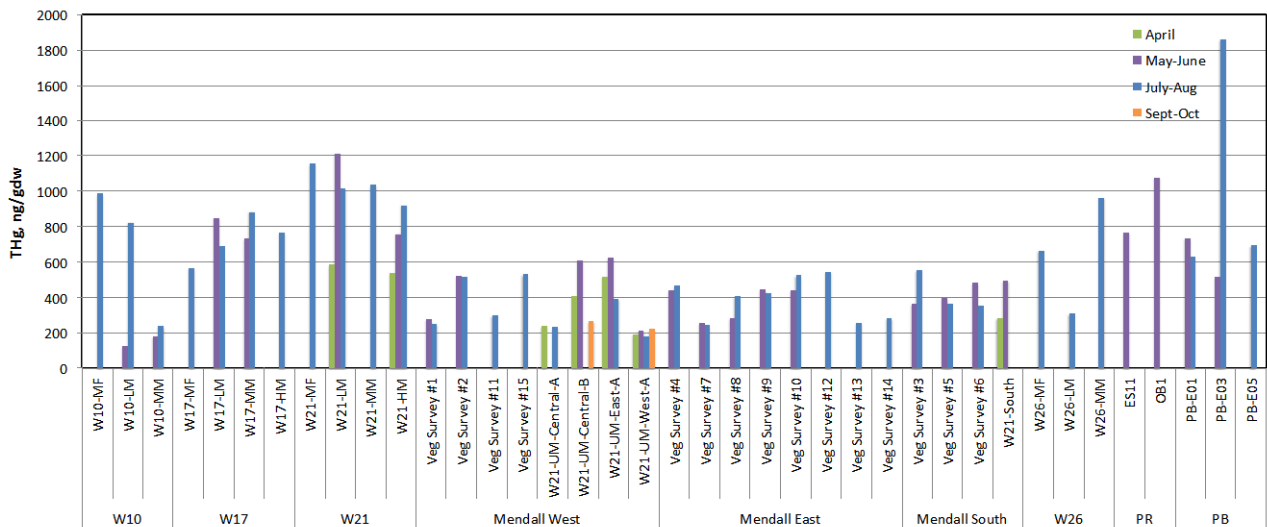


Figure 11-2.33. Total Hg, methyl Hg and methyl Hg as a % of total Hg for surface soils and sediments, broken down by season, for all sites sampled. Most bars represent one sample.

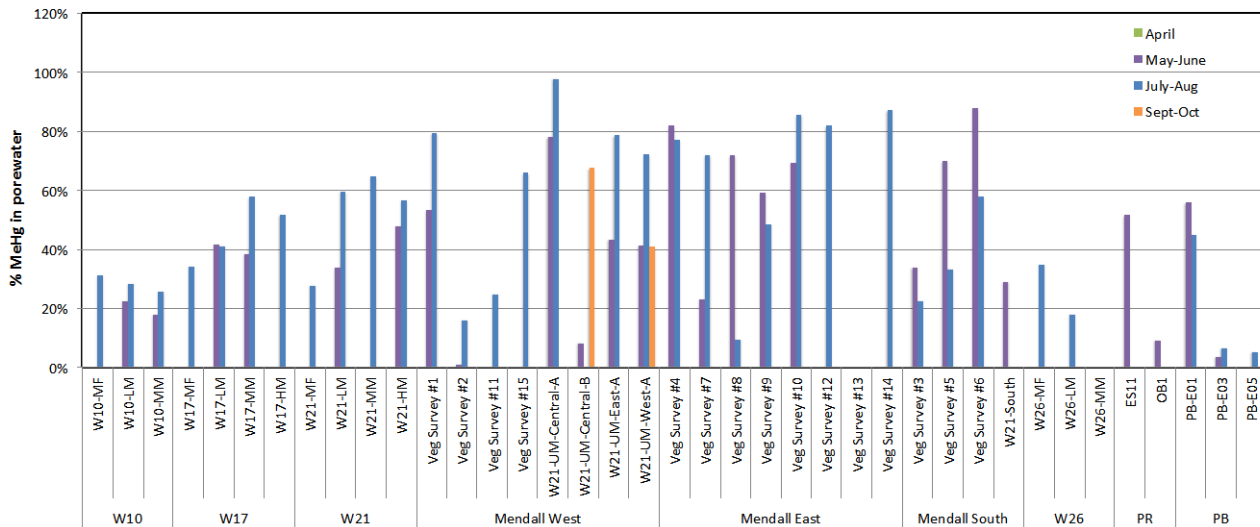
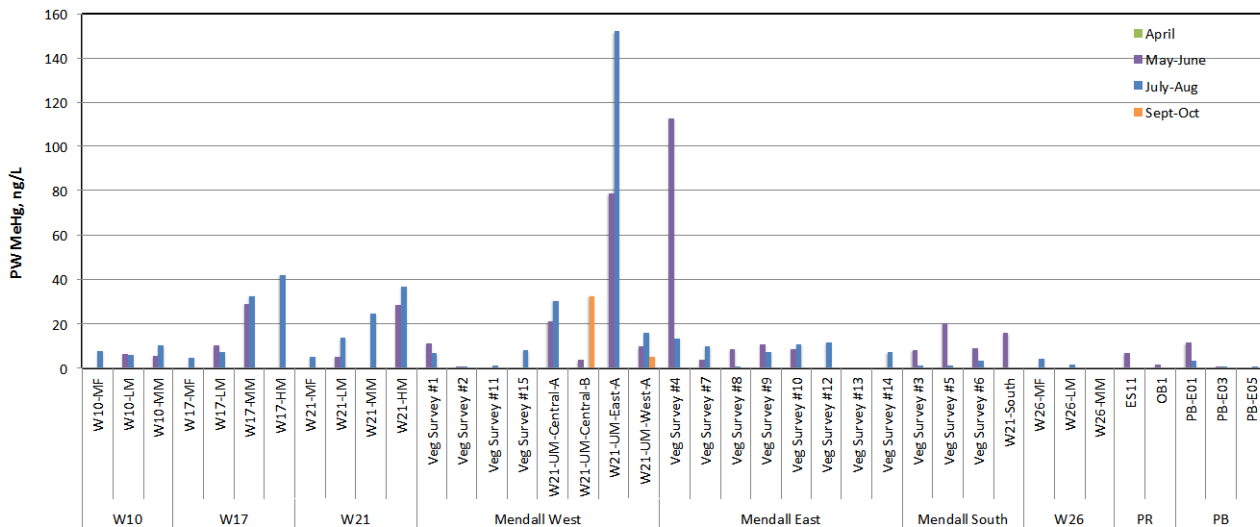
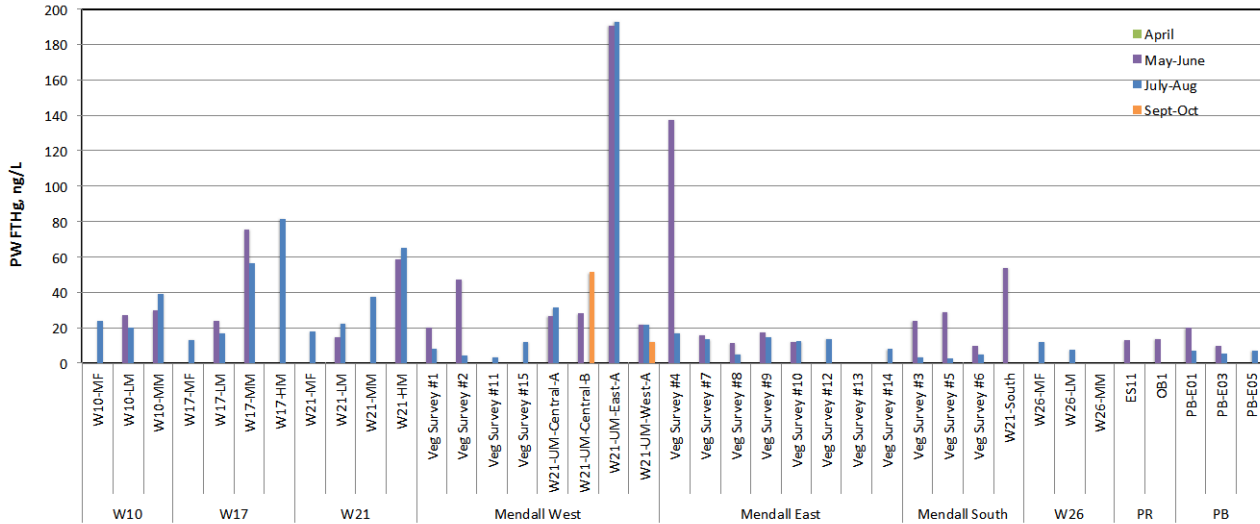


Figure 11-2.34. Total Hg, methyl Hg and methyl Hg as a % of total Hg for surficial pore waters, by season, for all sites sampled. Most bars represent one sample.

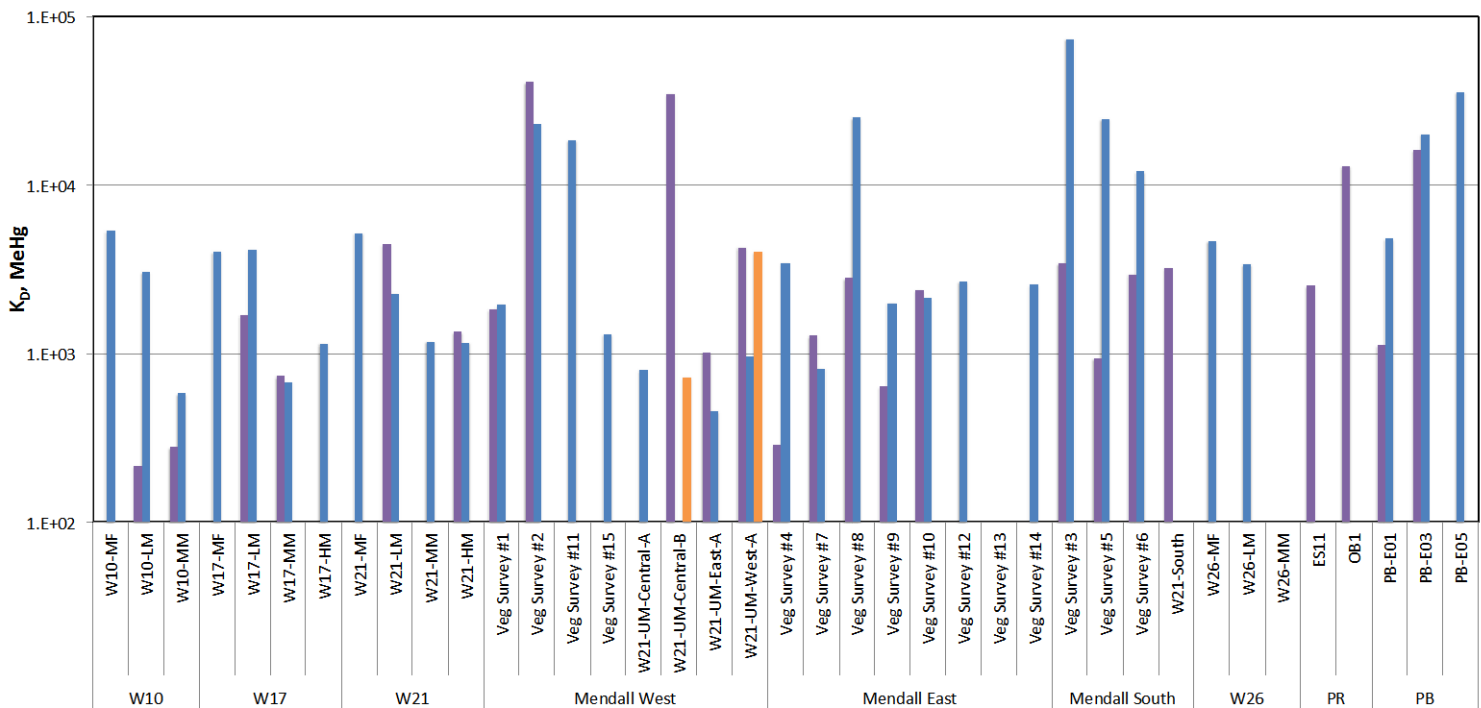
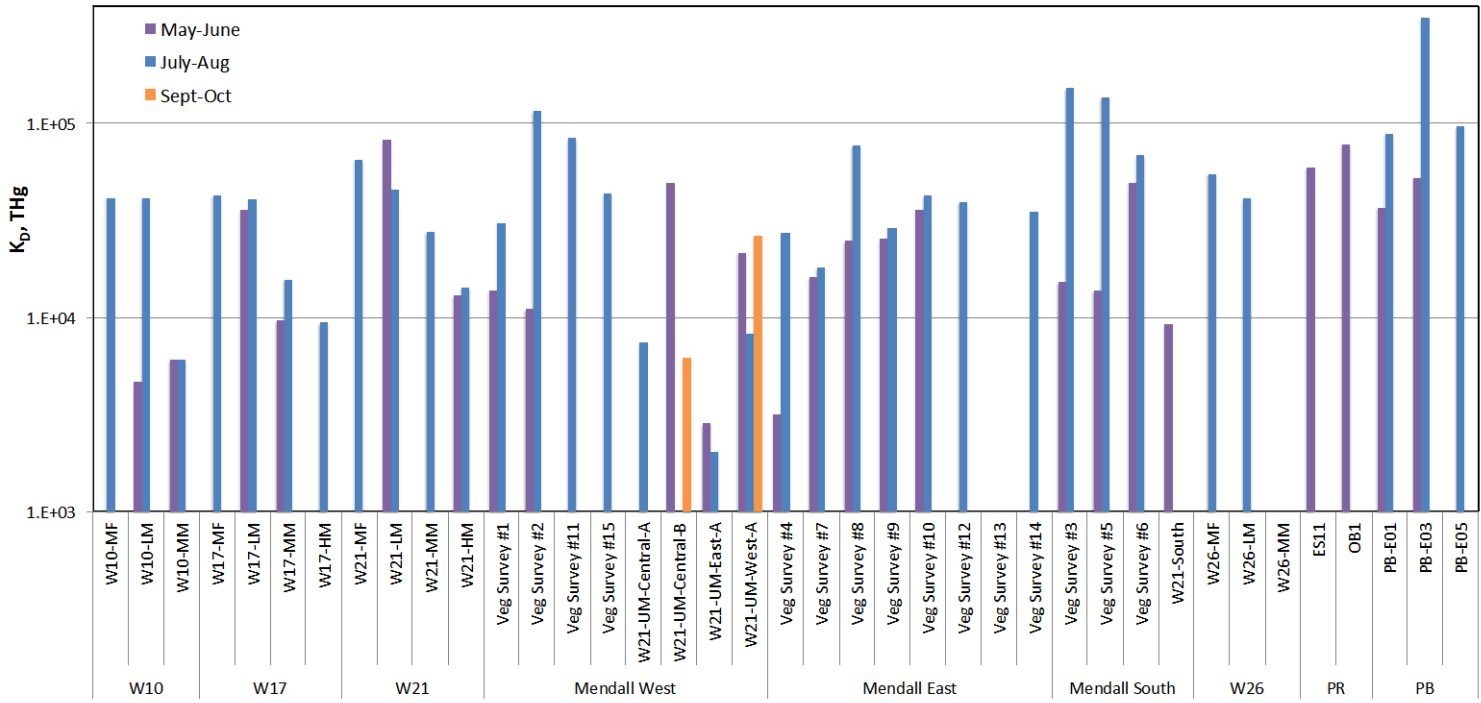


Figure 11-2.35. Partition coefficients for total Hg and methyl Hg and methyl Hg by season, for surface samples from all sites sampled.

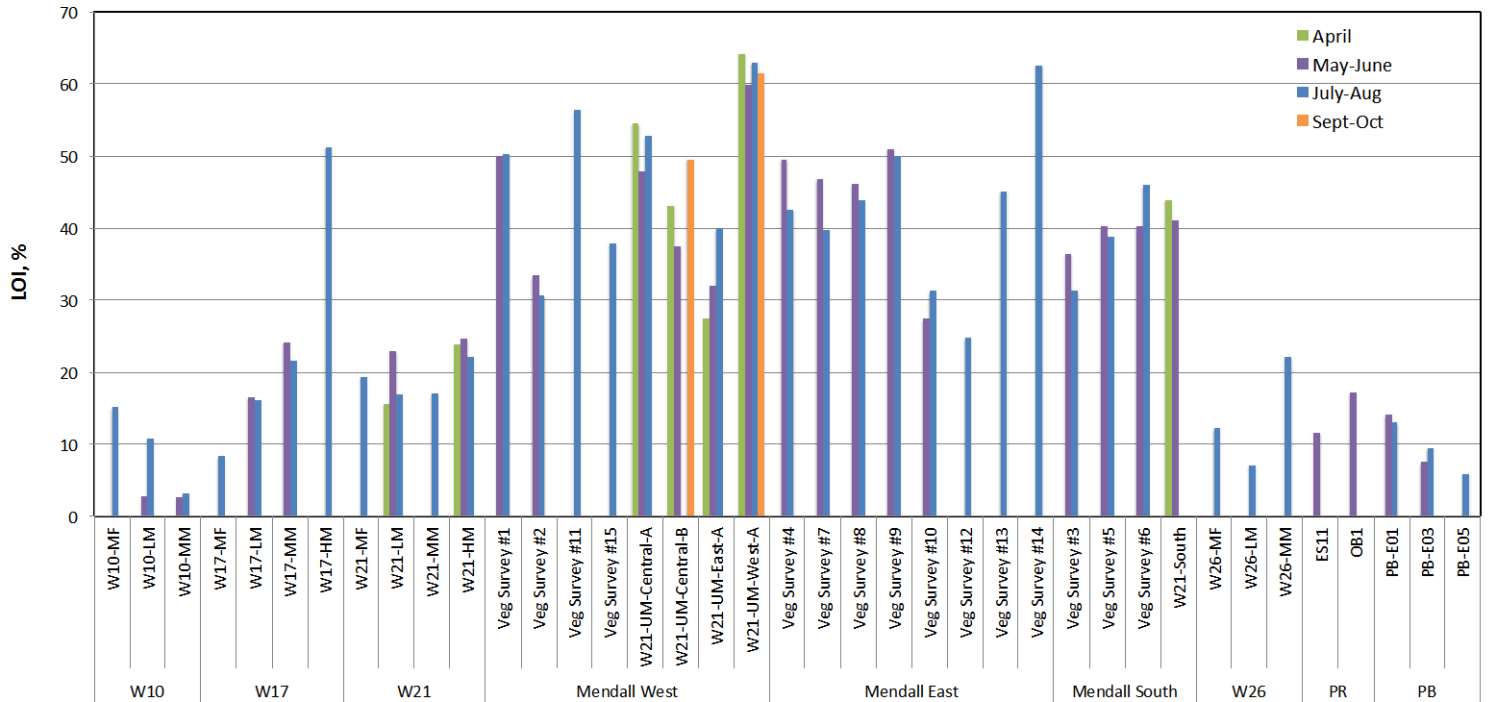
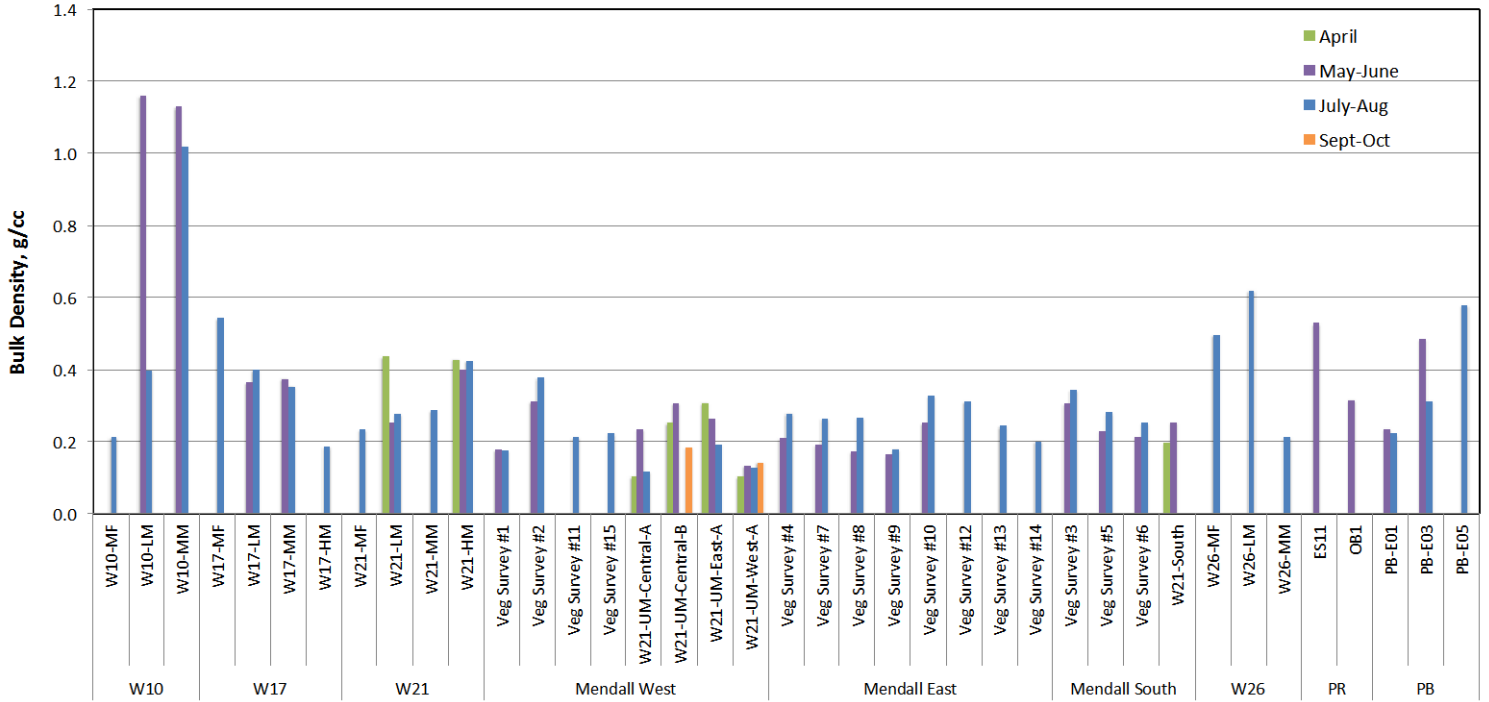


Figure 11-2.36. Sediment and soil bulk density (top) and loss on ignition (bottom) by season, for all sites sampled. Data are for top 0-3 cm. Most bars represent one composite sample.

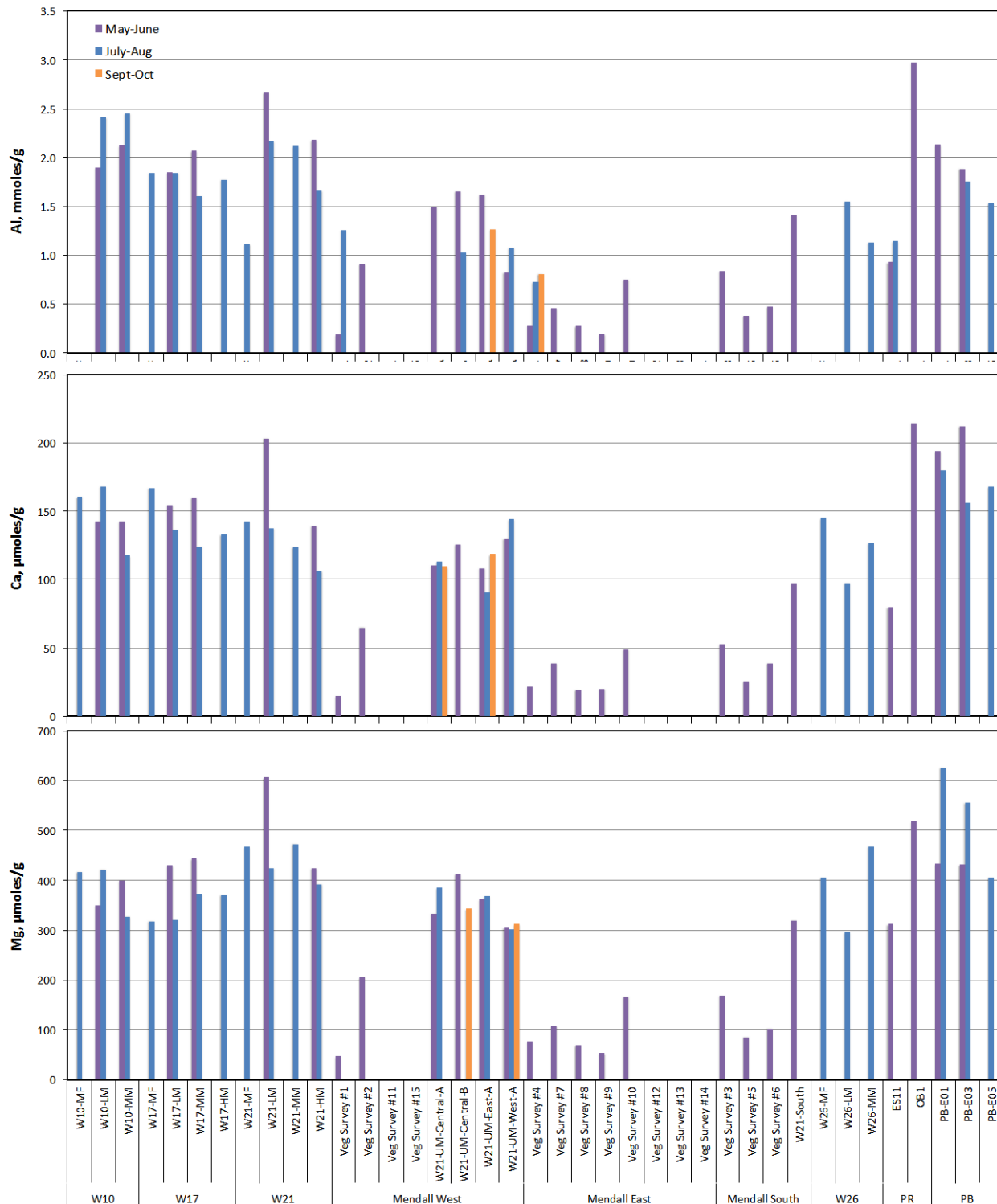


Figure 11-2.37. Selected crustal metal data for sediments and soils by season, for all sites by month sampled. Data are for top 0-3 cm. Most bars represent one composite sample.

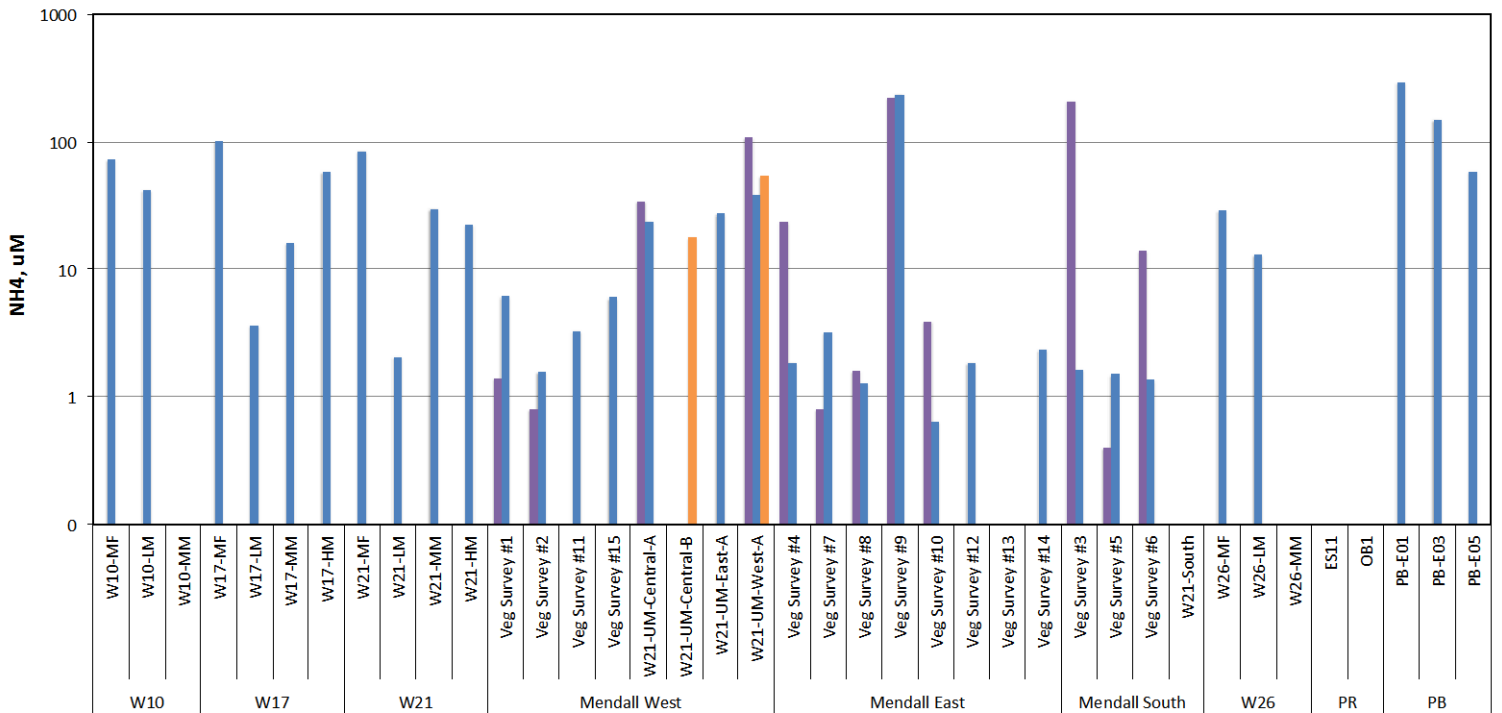
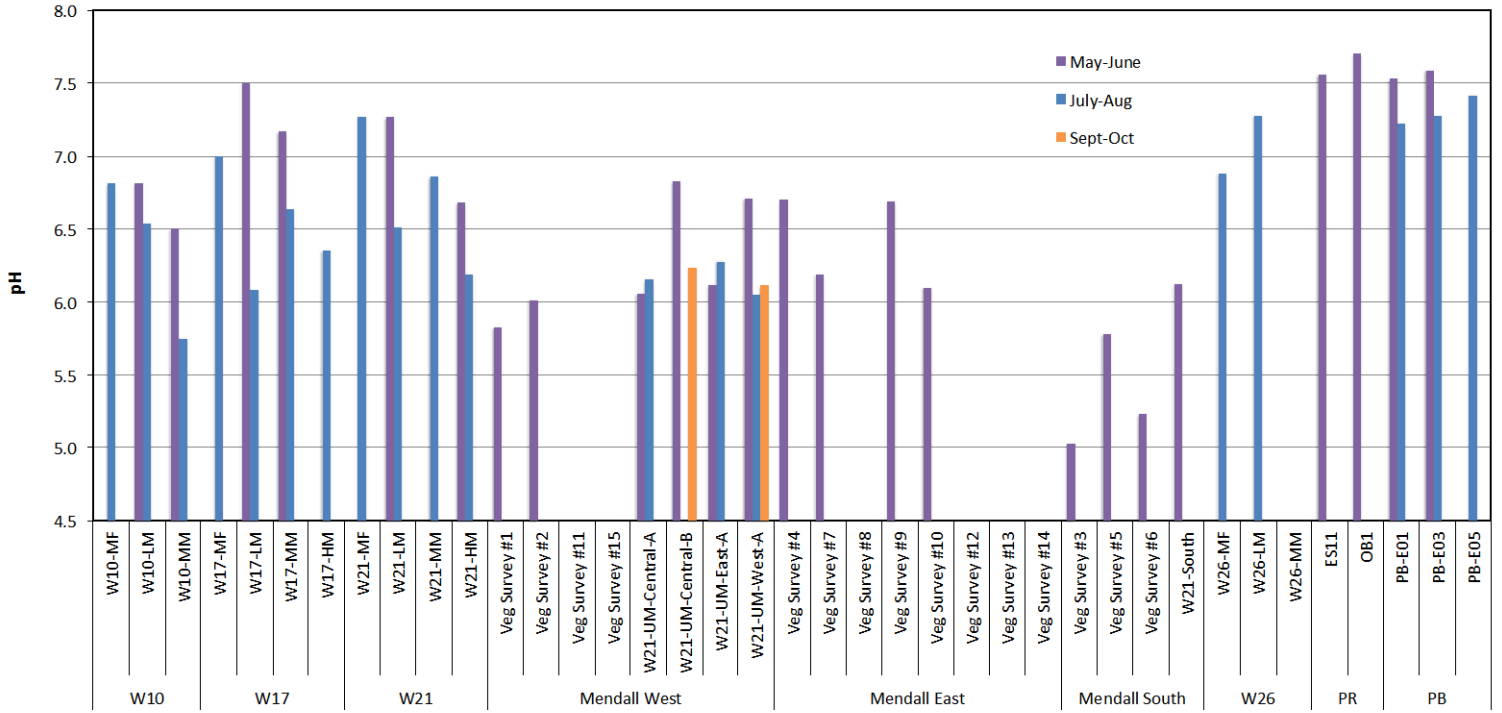


Figure 11-2.38. Surface pore water pH and ammonia by season, for all sites by month sampled. Most bars represent one composite sample. Note log scale for NH<sub>4</sub>.

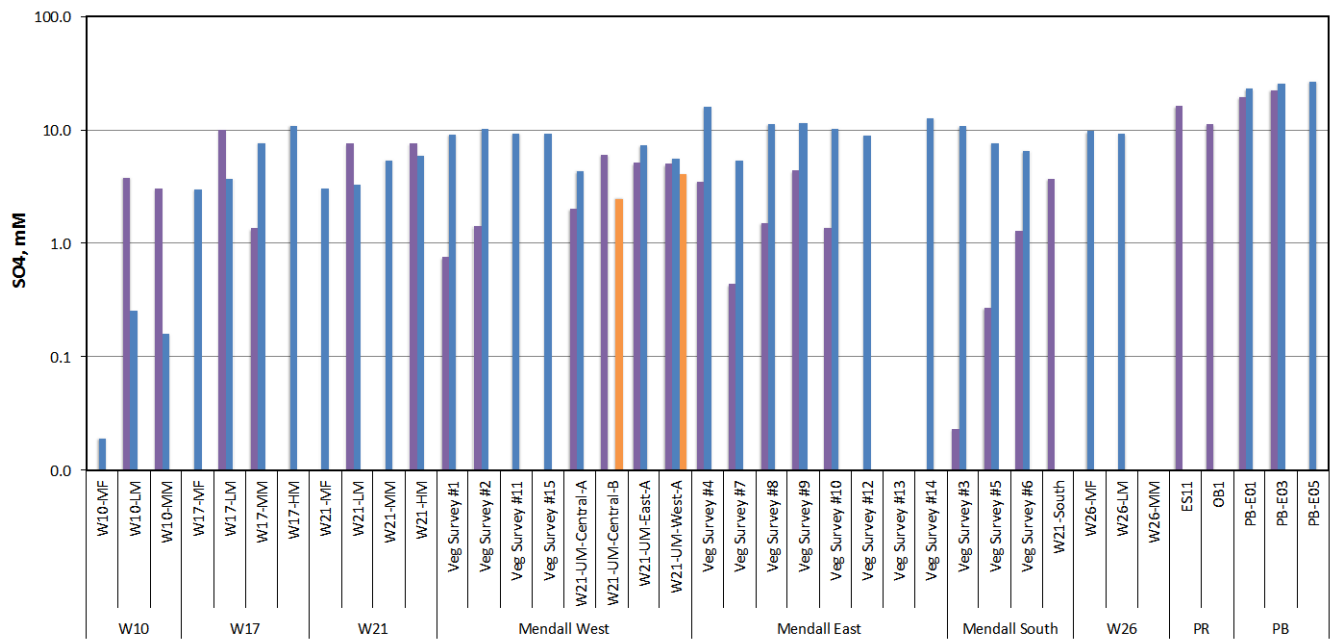
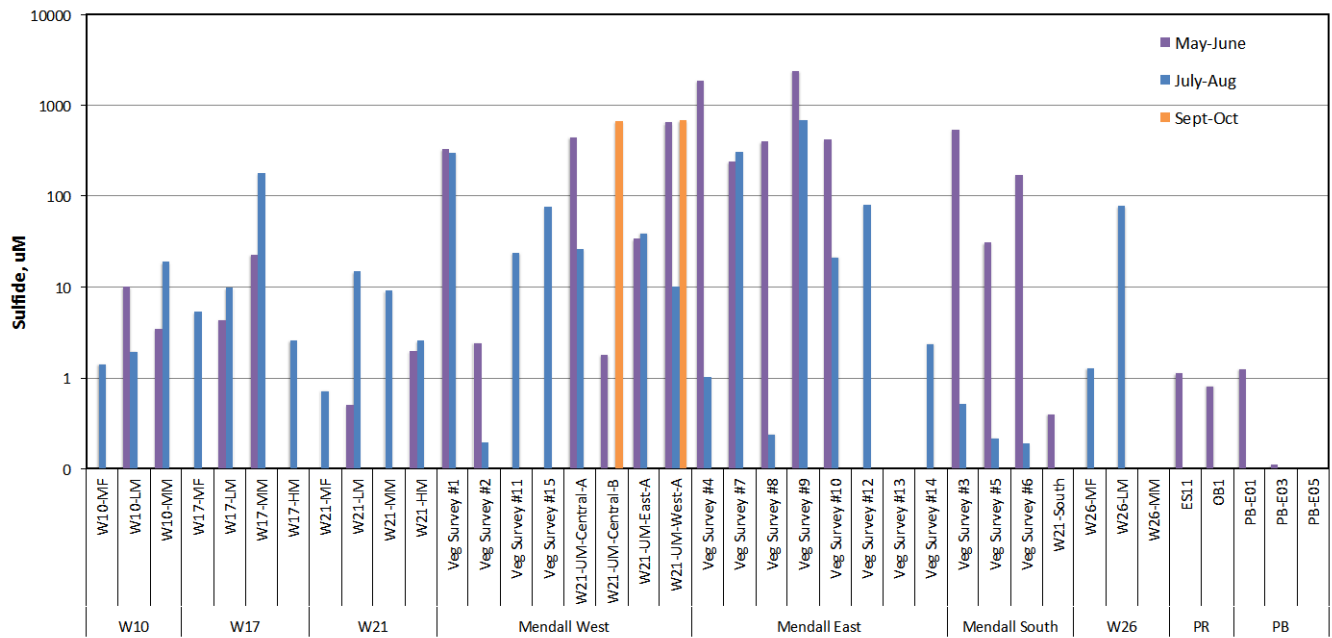


Figure11- 2.39. Surface pore water sulfide and sulfate by season, for all sites sampled. Most bars represent one composite sample. Note log scales.

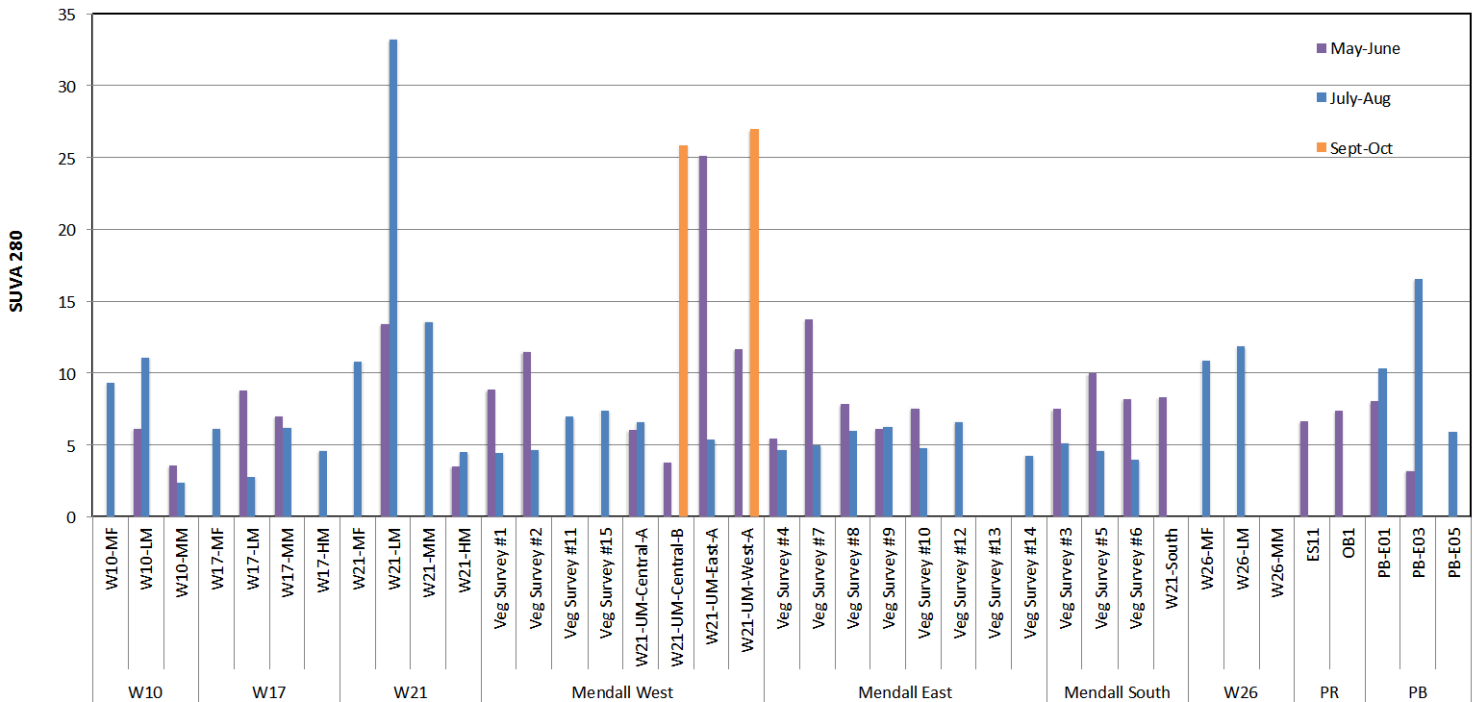
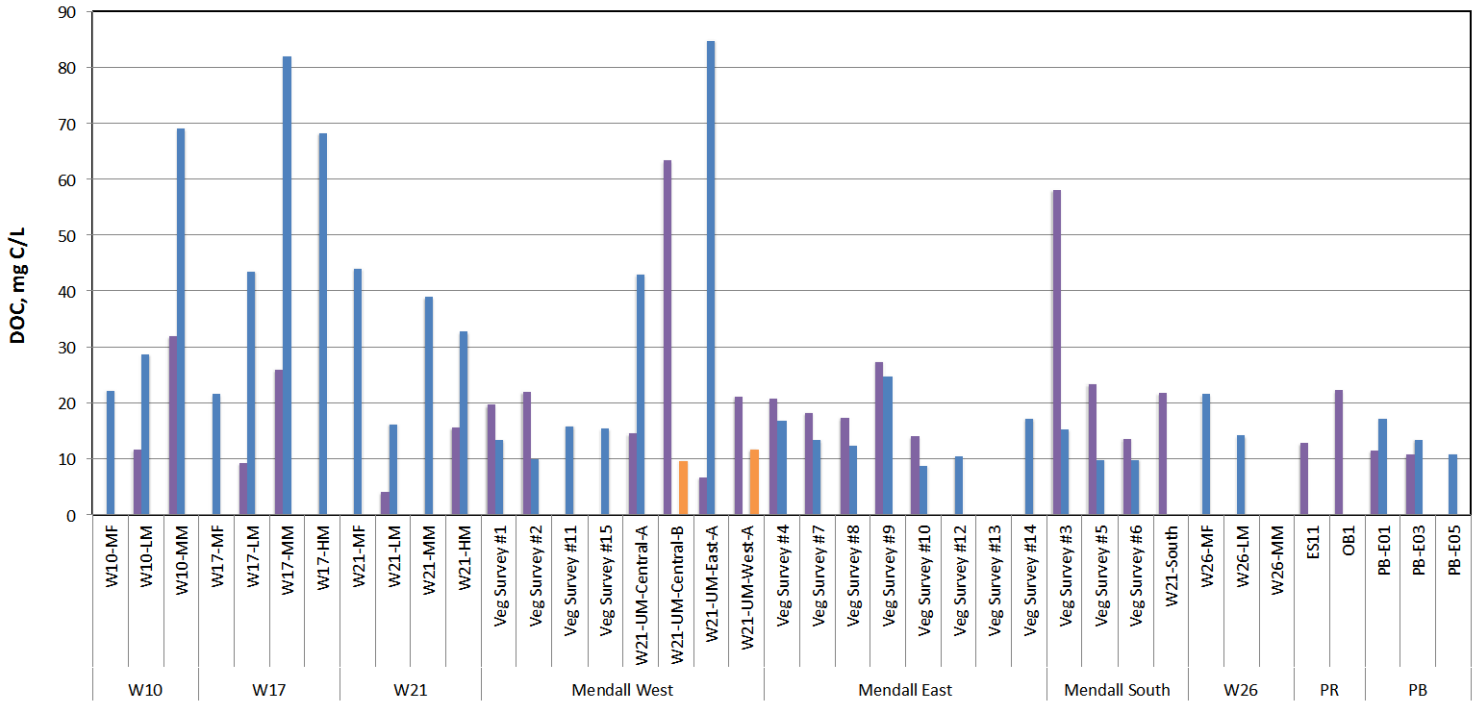
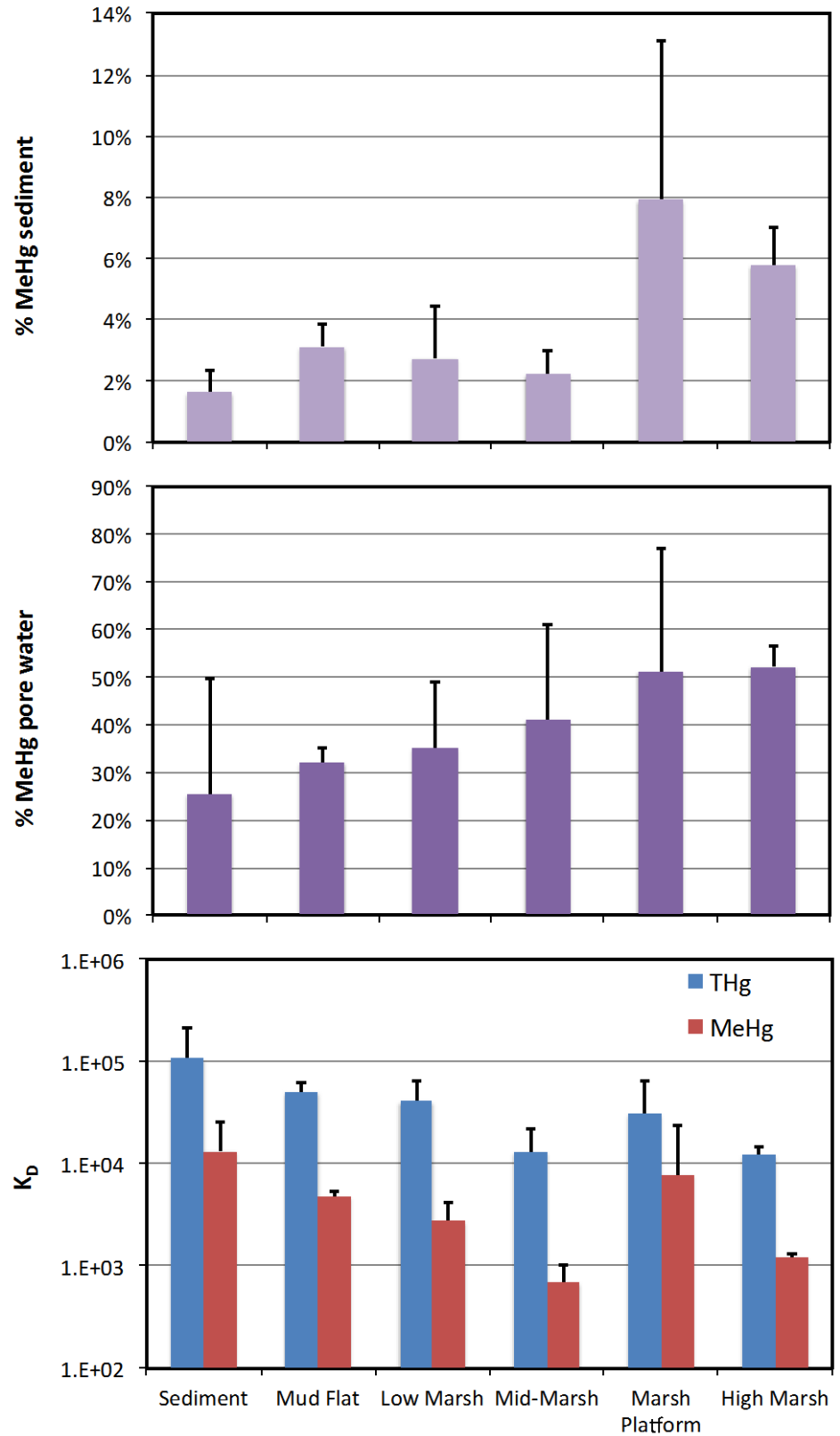


Figure 11-2.40. Surface pore water DOC and SUVA280 by season, for all sites sampled. Most bars represent one composite sample.

#### **2.4.2 Bar plots for surface soils and pore waters, averages by habitat type.**

Bar plots Figures 11-2.41 to 11-2.45 show average surface concentrations by habitat (across areas and seasons). Figure 2.41 highlights the higher % methyl Hg in both bulk and aqueous phases in high marsh and marsh platform soils, accompanied by lower sediment:water partition coefficients for total Hg, higher organic matter content and lower abundance of crustal metals (Figure 11-2.42), lower pH, higher sulfide and lower ammonium (Figure 11-2.43), and higher DOC (Figure 11-2.44).

Figure 11-2.41. Average % methyl Hg in bulk (top) and pore water (middle), and sediment:water partition coefficient by habitat type. Averages and standard deviations are based on all surface samples from all sites and sampling dates.



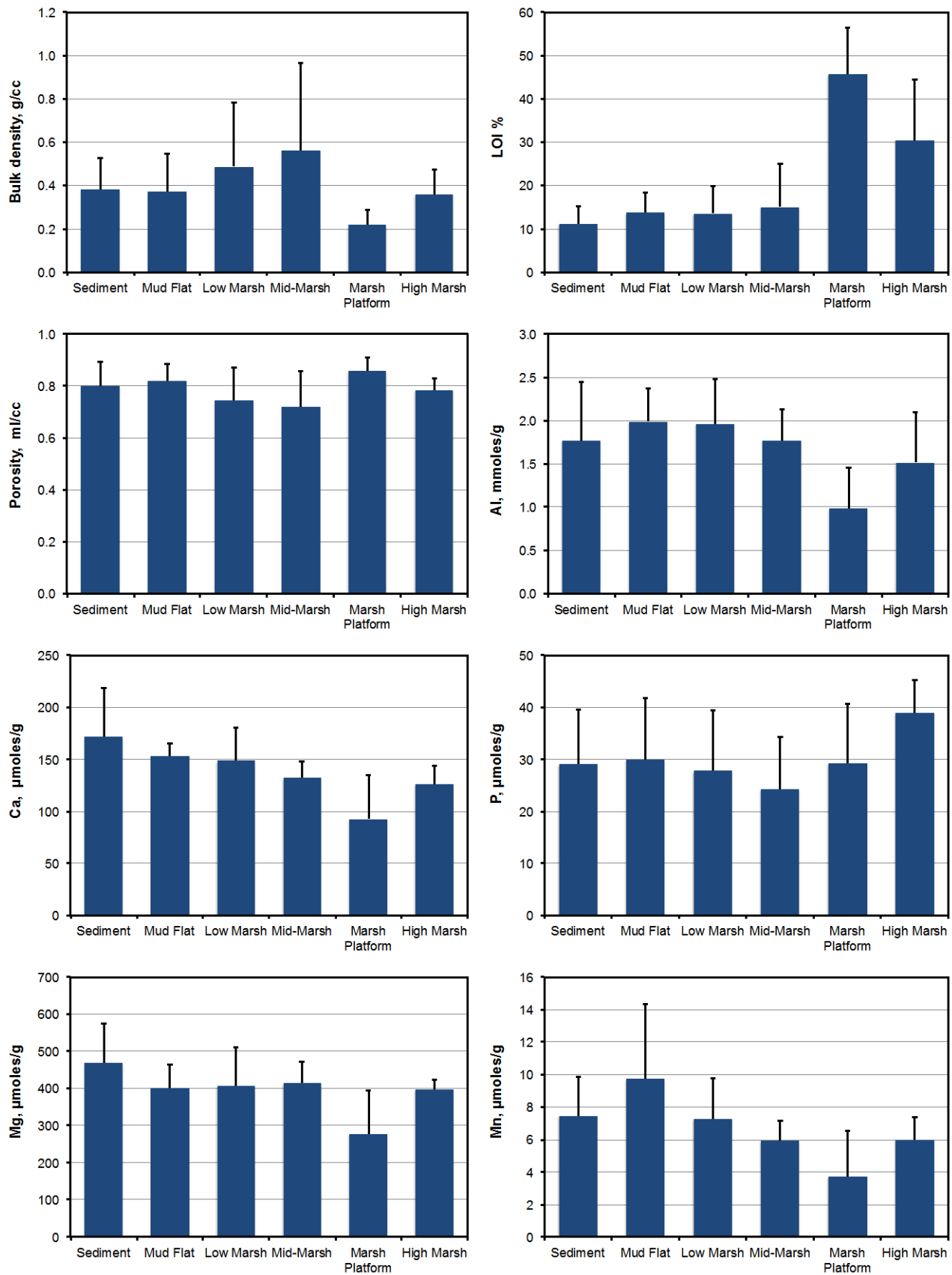
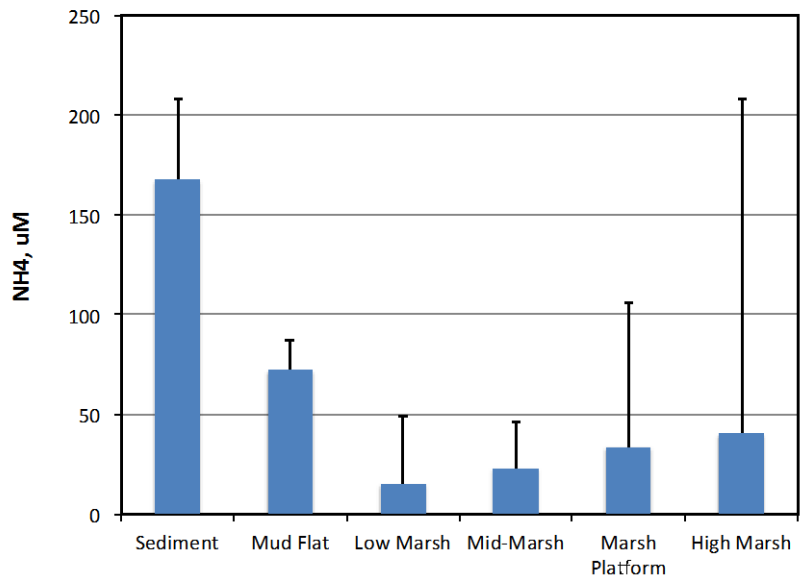
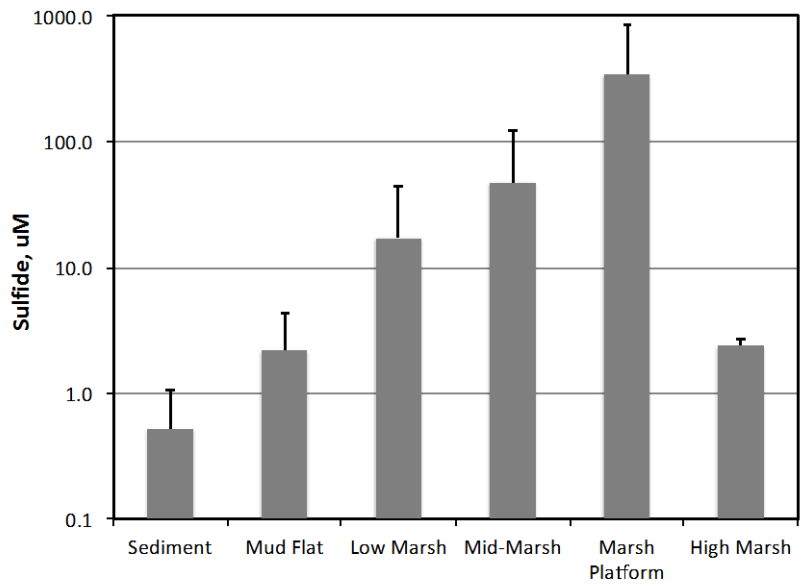
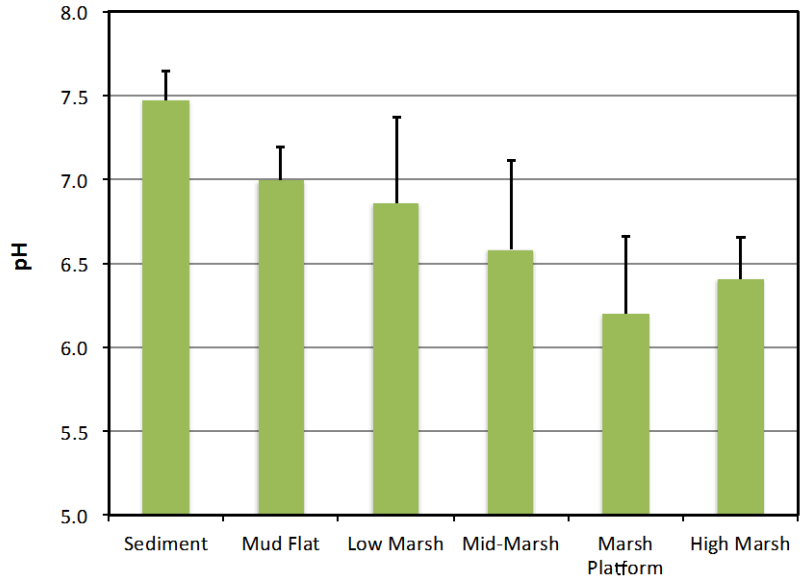


Figure 11-2.42. Sediment and soil physical and chemical parameters. Averages and standard deviations shown are based on all sites and sampling dates, for surface samples.

Figure 11-2.43. Sediment and soil pore water chemistry averages by habitat. Averages and standard deviations shown are based on all sites and sampling dates for surface samples.



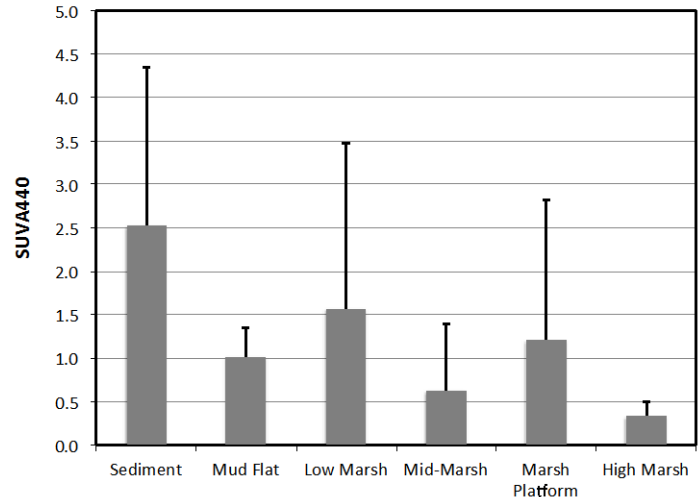
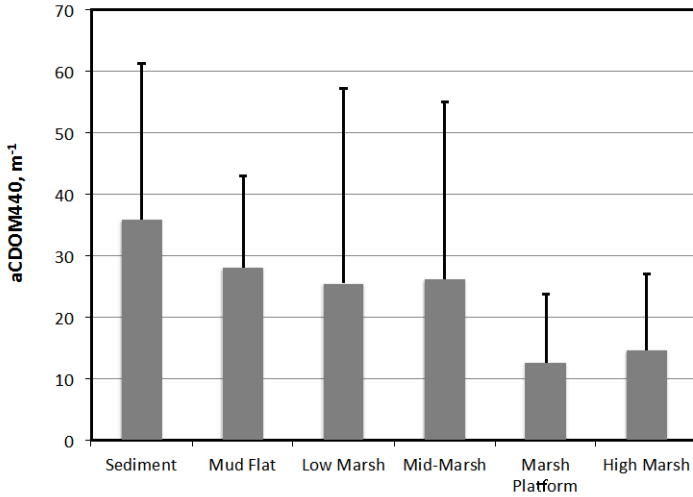
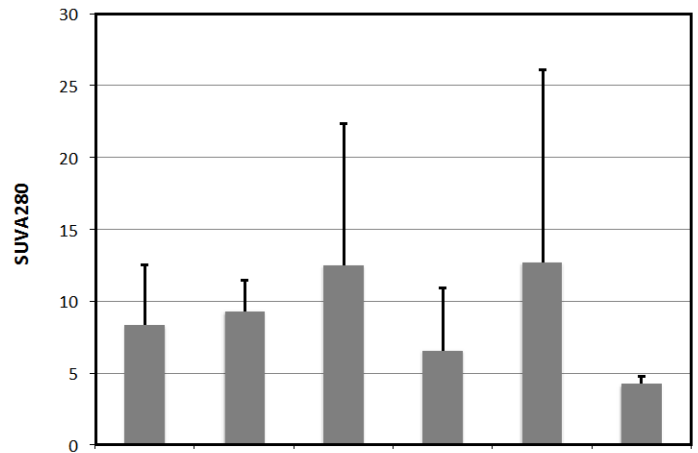
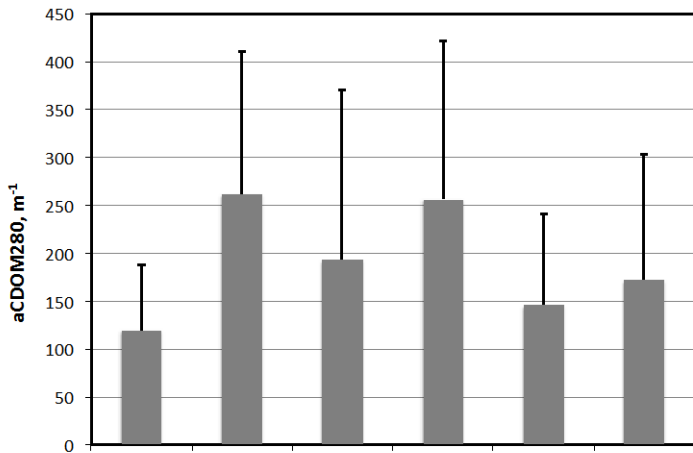
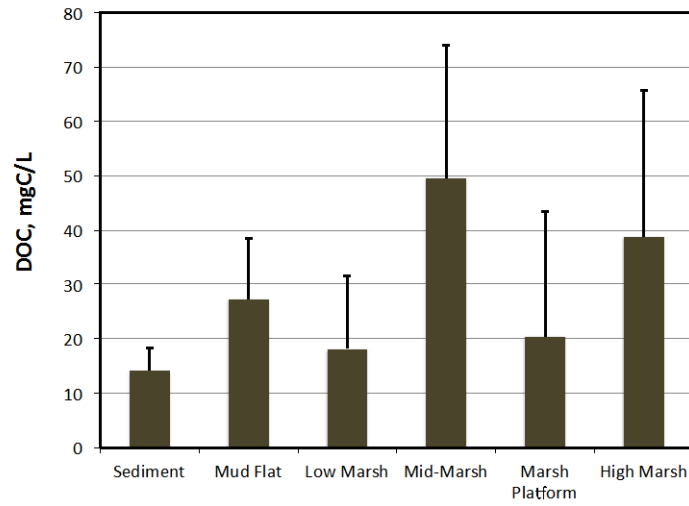


Figure 11-2.44. DOC concentration and character; averages by habitat. Averages and standard deviations shown are based on surface pore waters for all sites and sampling dates.

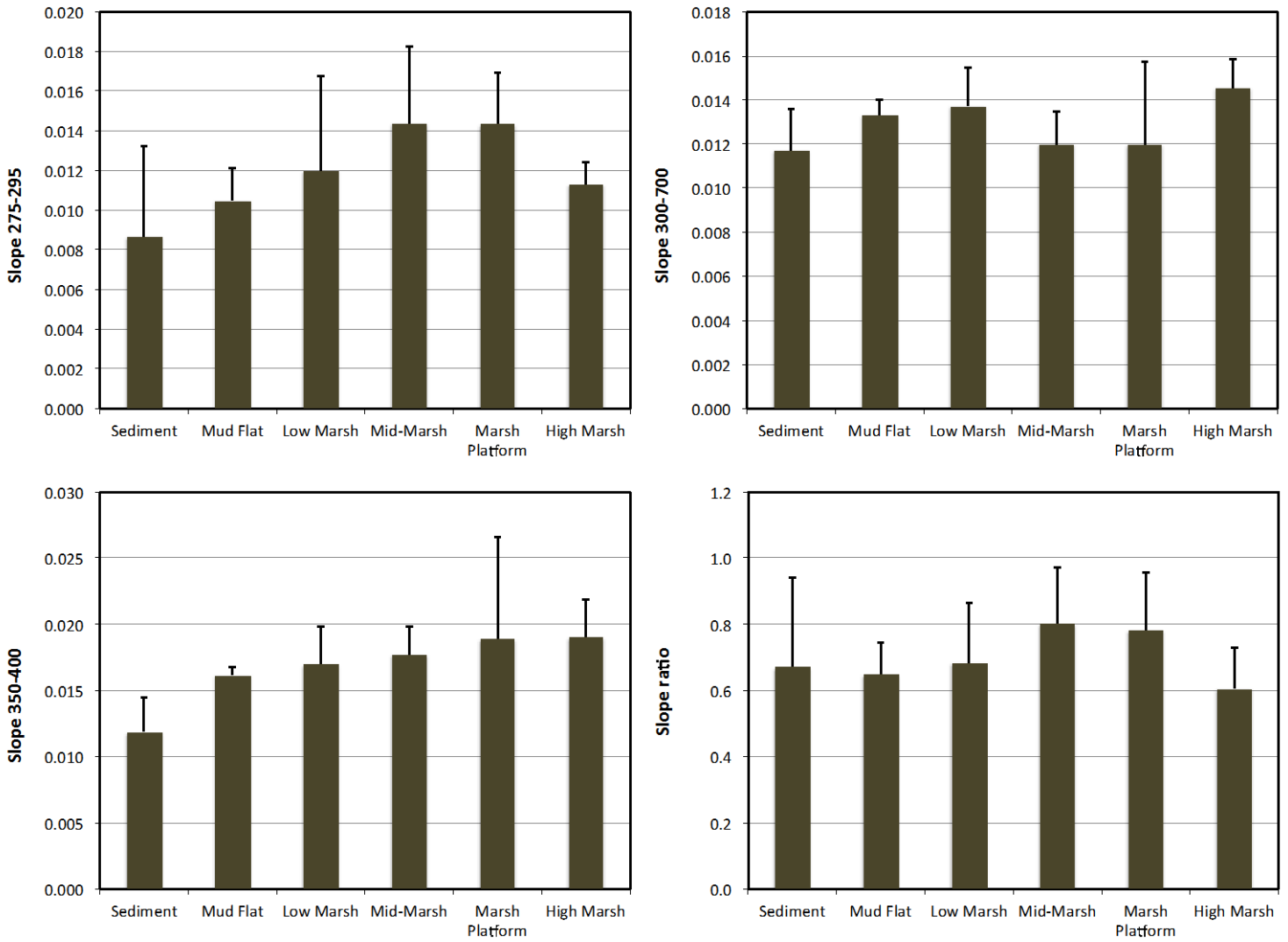


Figure 11-2.45. DOC spectral characteristics; averages by habitat. Averages and standard deviations shown are based on surface pore waters for all sites and sampling dates.

### **2.4.3 Bar plots for surface soils and pore waters, averages by site and elevation**

Plots Figures 11-2.46 to 11-2.50 show average values for surface sediments/soils and pore waters by site across all dates sampled, with standard errors.

Methyl Hg concentrations in porewaters and in the bulk phase were highest in the mesohaline marshes at sites W17 and W21/Mendall Marsh. Specifically, the marsh platforms, and mid to high marshes in these areas were the sites of most exceptional methyl Hg accumulation in soils and soil porewaters. Note that the complex of sites designated W21 is located at the edge of the west platform of Mendall Marsh, along the South Marsh River, including the mud flats adjacent to the marsh, the marsh bank, and the high berm at the edge of the marsh platform.

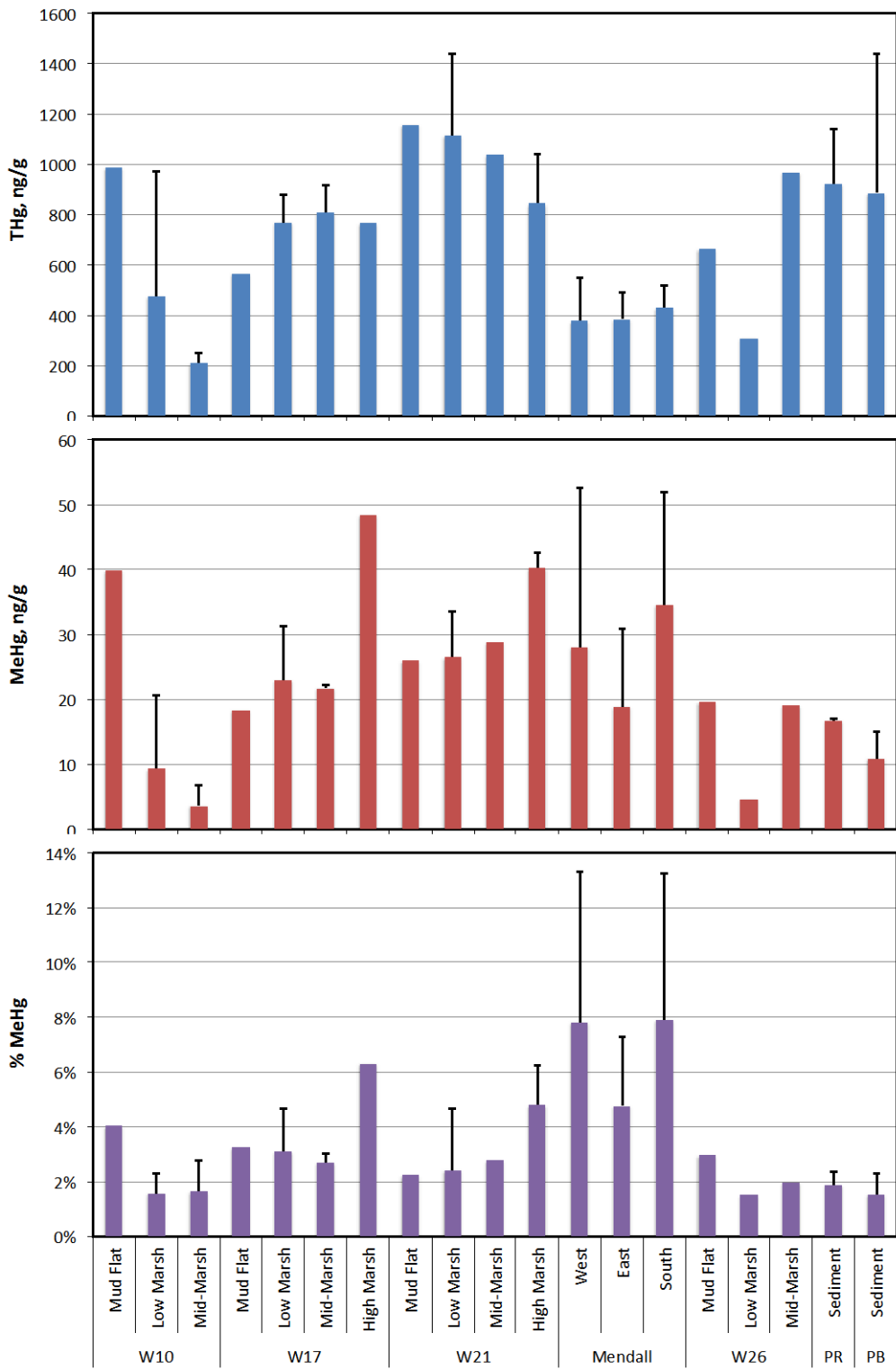


Figure 11-2.46. Average total Hg, methyl Hg and %methyl Hg by area and habitat. Bars are averages plus standard deviations for surface soils for all dates except April 2011.

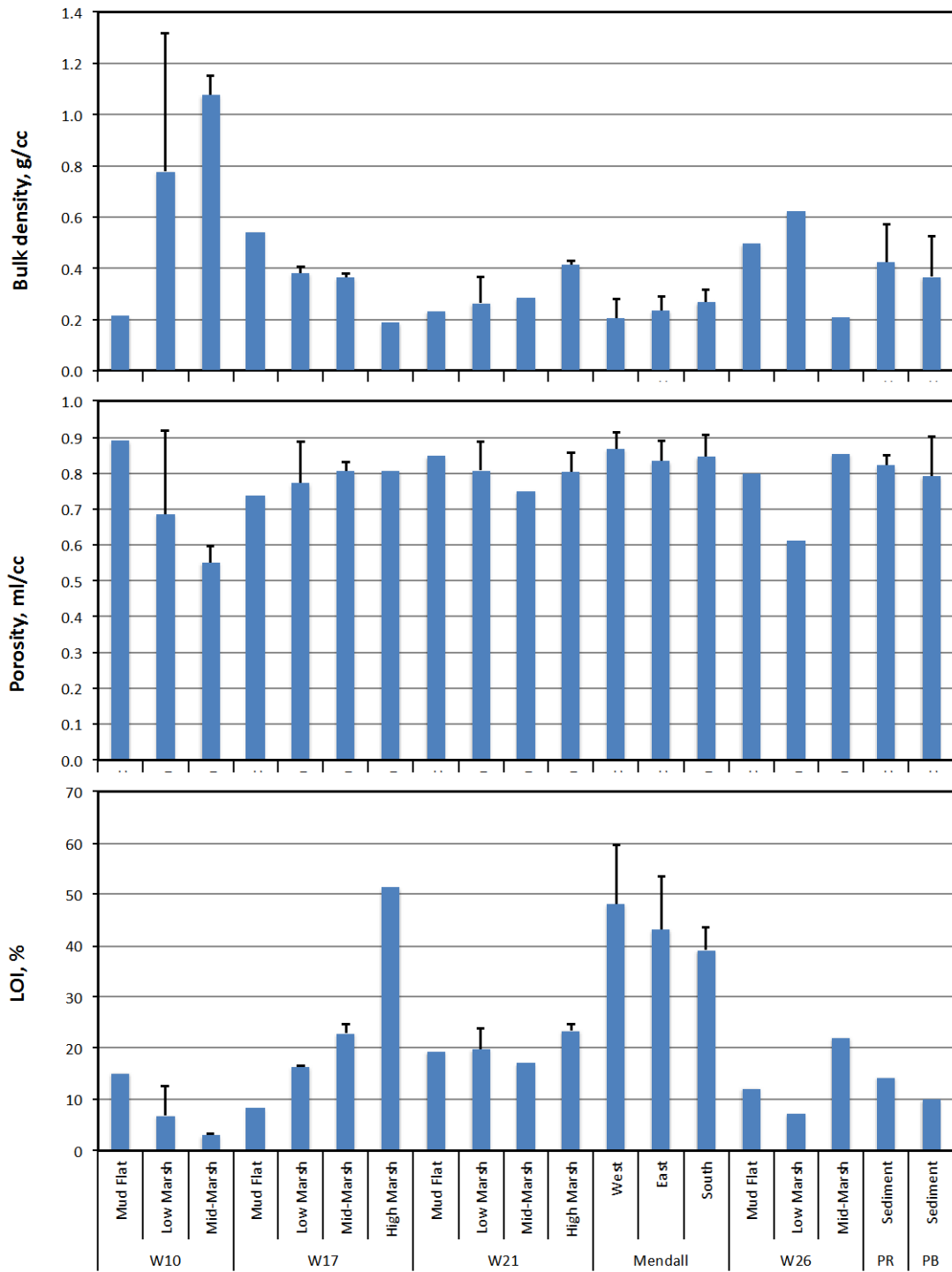


Figure 11-2.47. Average bulk density, porosity and % LOI by area and habitat. Bars are averages plus standard deviations for surface soils for all dates except April 2011.

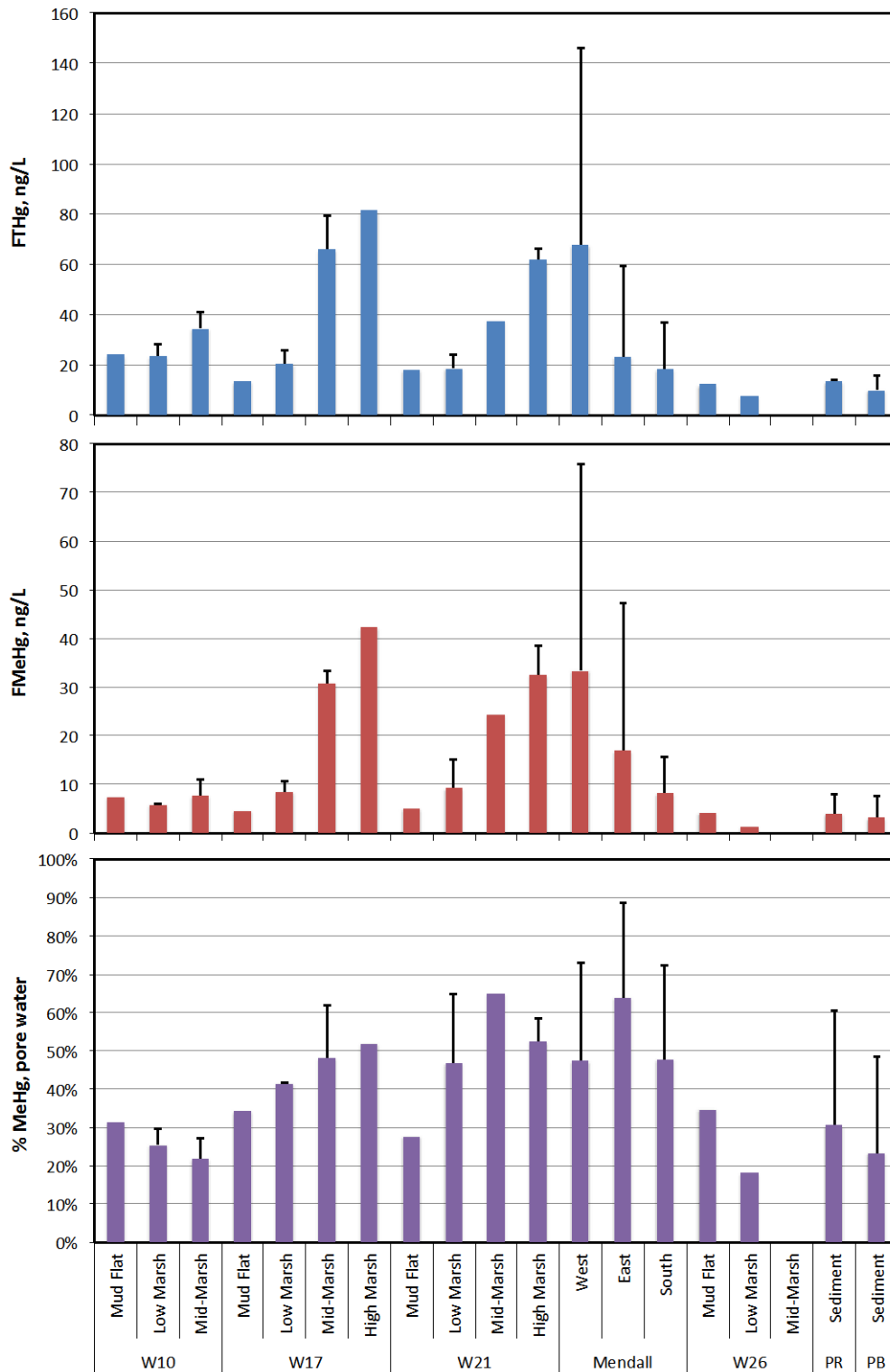


Figure 11-2.48. Average Hg, methyl Hg and % methyl Hg in surface pore waters area and habitat. Bars are averages plus standard deviations for surface soils for all dates except April 2011.

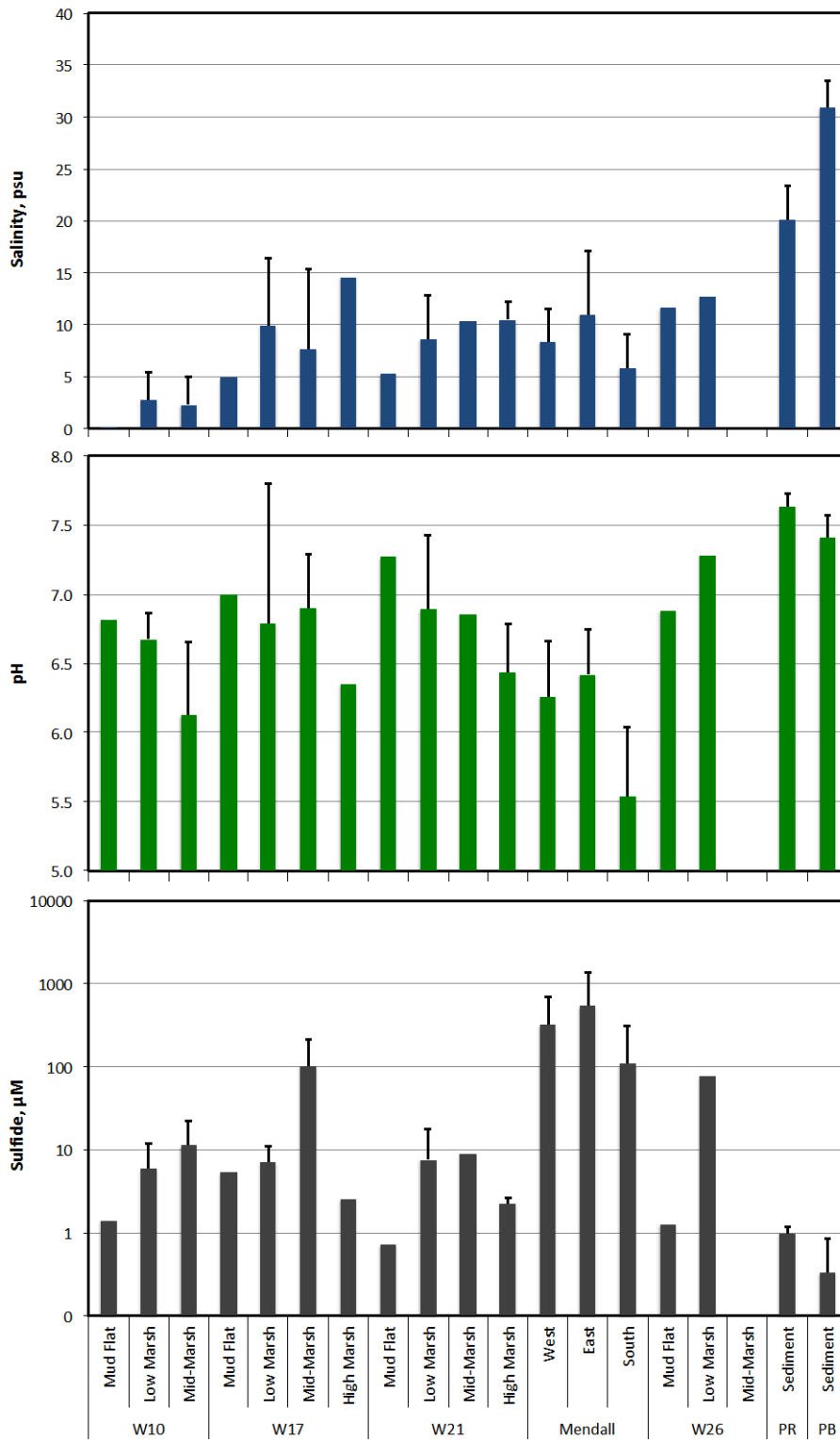


Figure 11-2.49. Average salinity, pH and sulfide in surface pore waters area and habitat. Bars are averages plus standard deviations for surface soils for all dates except April 2011.

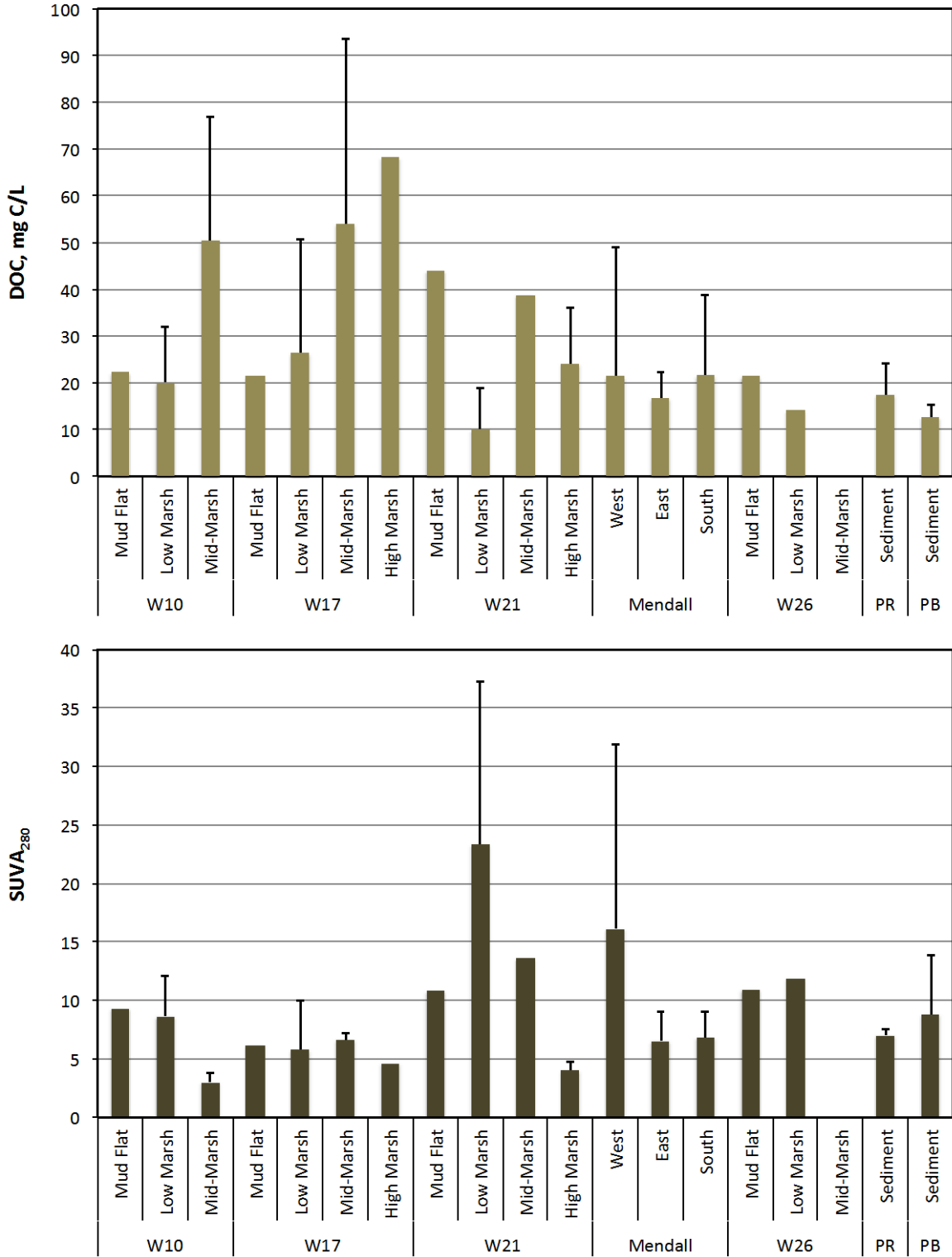


Figure 11-2.50. Average DOC and SUVA<sub>280</sub> in surface pore waters by area and habitat. Bars are averages plus standard deviations for surface soils for all dates except April 2011.

### SECTION 3. COMPARISON WITH OTHER ECOSYSTEMS

In order to put the behavior of mercury (Hg) in the Penobscot in context, we compared it to other ecosystems. Over the years, our group has studied Hg biogeochemistry in a wide variety of systems, spanning gradients in salinity, habitat, longitudinal and contamination intensity. Habitat types studied have mainly been bottom sediments and marsh habitats, known locations of *de novo* methyl Hg production.

A list of the ecosystems compared to the Penobscot is given in Table 11-3.1. All were sampled and analyzed using similar methods (although the methods have evolved over time). The biogeochemistry of methyl Hg production was examined with depth in sediments or soils in almost all of these studies. In the graphics shown below, points represent averages for any given site/date combination. The number of site/date combinations sampled in each study range from just a few to over 80, but averaged 20-40. For example, in the Chesapeake study, 12 sampling sites were occupied, from the top of Chesapeake Bay, along salinity gradient of the Bay, and onto the adjacent continental shelf and slope. Most of the sites were sampled 5 times over 5 cruises, yielding a total of about 50 site/date combinations. However, each data point represents the average of multiple (usually 3) sediment cores. In some of the comparisons below we used only the most surficial interval sampled. That depth varied from 2-5 cm depth. In others, all depths sampled were used, generally to 10-12 cm.

A useful way to evaluate Hg contamination levels is to normalize Hg concentrations in sediments or soils to organic carbon content. Within and across ecosystems, sediment total Hg concentrations are often well predicted by sediment organic matter (SOM) content, with the highest concentrations of Hg in fine-grained and organic sediments and soils (e.g. Hammerschmidt and Fitzgerald 2004; Sunderland et al. 2006; Ogrinc et al. 2007; Hollweg et al. 2010).

Figure 11-3.1 shows total Hg in sediments and soils plotted against loss on ignition (LOI, a measure of organic carbon content) for the set of comparison ecosystems. Hg concentrations rise with LOI through roughly 20% to 30% organic matter. Penobscot sediments and soils are elevated in Hg concentration relative to systems contaminated by atmospheric deposition, including Chesapeake sediments and marsh soils, which probably provide the most appropriate comparison. Two other estuarine study sites in the comparison set – Canal Creek, a contaminated tidal creek at Aberdeen Proving Grounds in the northern Chesapeake; and a contaminated salt marsh in New Jersey – contain much higher sediment and soil total Hg concentrations. In the Canal Creek study, we evaluated bottom sediments in the creek, while the NJ salt marsh study focused mainly on soils in a tidal *Phragmites* marsh. Note that in the Penobscot, especially in the marshes, total Hg concentrations are often lower at the surface of soils than at depth.

**Table 11-3.1: Characteristics of ecosystems used in comparisons with the Penobscot. Data are averages of all samples in the depth interval listed  $\pm$  1 standard deviation. ND = not determined.**

Study	Location	Description	Habitat(s) sampled	
L658	Ontario	Oligotrophic boreal lake	Bottom sediments	
MD Reservoirs	Maryland	Surface water impoundments	Bottom sediments	
South River	Virginia	Appalachian river	River shallow sediments	
Chesapeake/Shelf/Slope	Maryland, Virginia, offshore Atlantic	Chesapeake Bay, Mid-Atlantic Shelf and Slope	Bottom sediments	
Canal Creek	Upper Chesapeake Bay tidal creek	Estuarine Creek Sediment	Bottom sediments	
L658 Wetland	Ontario	Oligotrophic boreal lake	Adjacent wetland	
FL Everglades	Florida	Freshwater sawgrass and cattail marsh	Marsh soils	
Chesapeake salt marsh	Mid-Chesapeake Bay	Mesohaline mixed vegetation tidal marsh	Saltmarsh soils	
Penobscot	Coastal Maine	Macrotidal estuary	Bottom sediments, mud flats, marshes	
NJ salt marsh	Coastal NJ	Phragmites marsh	Saltmarsh soils	
Study	Salinity Range (psu)	Contamination Source	Years sampled	Surface interval sampled (cm)
L658	Freshwater	Atmospheric	2000-2012	0-2
MD Reservoirs	Freshwater	Atmospheric	2003-2005	0-4
South River	Freshwater	Fiber manufacturer	2009	0-5
Chesapeake/Shelf/Slope	2-35	Atmospheric and point sources	2006-2008	0-2
Canal Creek	<1-3	Point source	2009-2011	0-4
L658 Wetland	Freshwater	Atmospheric	2001-2007	0-4
FL Everglades	Freshwater	Atmospheric	1994-1998	0-4
Chesapeake salt marsh	5-15	Atmospheric	2007-2008	0-3
Penobscot	<1 - 33	Point source	2009-2012	0-3 and 0-5
NJ salt marsh	2-6	Point source	2011-present	0-5

**Table 11-3.1: Characteristics of ecosystems used in comparisons with the Penobscot. Data are averages of all samples in the depth interval listed  $\pm$  1 standard deviation. ND = not determined.**

Study	% LOI	Hg (ng/gdw)	Reference
L658	37 $\pm$ 15	104 $\pm$ 34	Harris et al. 2007
MD Reservoirs	10 $\pm$ 6	88 $\pm$ 61	Gilmour et al. <a href="http://www.dnr.state.md.us/irc/docs/00011581.pdf">http://www.dnr.state.md.us/irc/docs/00011581.pdf</a>
South River	9 $\pm$ 0.7	9803 $\pm$ 800	Gilmour et al. in review
Chesapeake/Shelf/Slope	6 $\pm$ 4	57 $\pm$ 52	Hollweg et al. 2009, 2010 and in review
Canal Creek	14 $\pm$ 2	3484 $\pm$ 3190	Gilmour et al. in review
L658 Wetland	ND	82 $\pm$ 32	Heyes et al. unpublished
FL Everglades	77 $\pm$ 27	117 $\pm$ 67	Gilmour et al. 1998; Orem et al. 2011; Aiken et al 2012
Chesapeake salt marsh	50 $\pm$ 11	125 $\pm$ 15	Mitchell et al. 2008, 2012
Penobscot	35 $\pm$ 18	515 $\pm$ 299	This study
NJ salt marsh	30 $\pm$ 6	39990 $\pm$ 15700	Underway

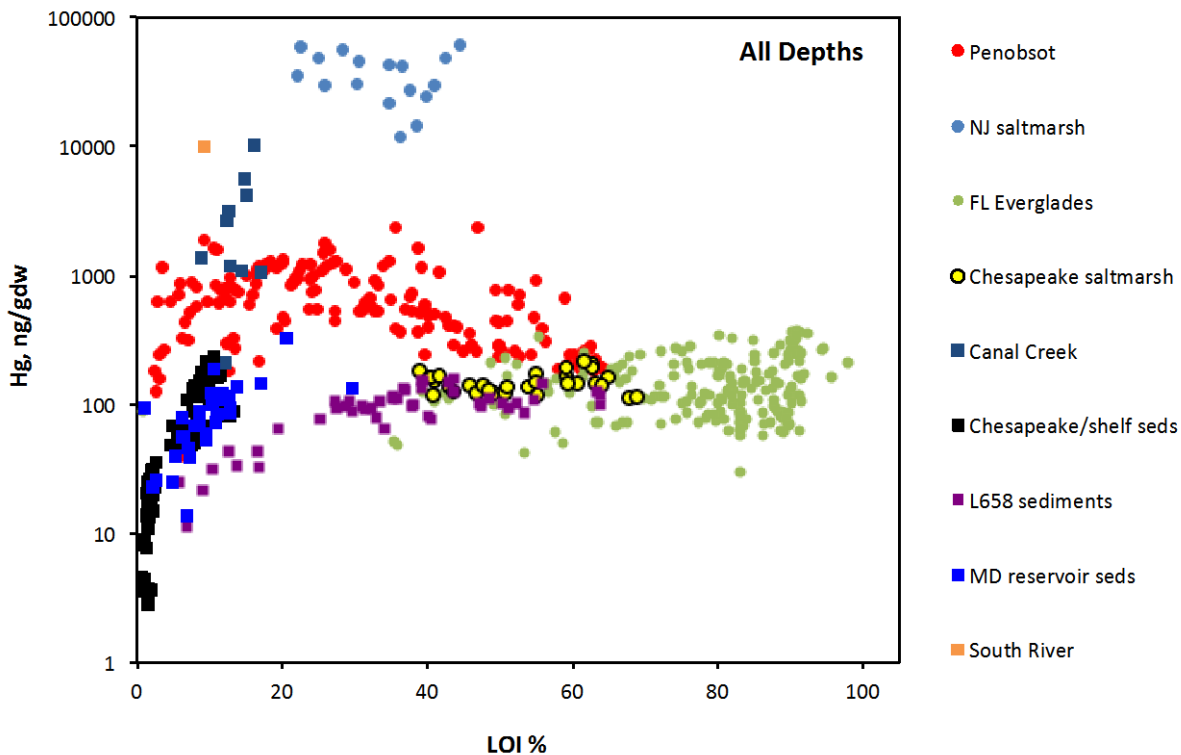


Figure 11-3.1. Total Hg concentrations in sediments or soils plotted vs. the organic carbon content (represented by % loss on ignition) for the comparison ecosystems. Each point represents the average value for a site/date/depth combination. Data for depths up to 12 cm are included.

Although total Hg concentrations in Penobscot sediment and soils are elevated, it is the methyl Hg concentrations in soils and soil pore waters (interstitial waters) that stand out. Both are extremely high relative to the other ecosystems examined in this comparison, and to almost all of the ecosystems for which data available in the literature, including freshwater and marine habitats.

One main driver of methyl Hg concentration in sediments and soils across ecosystems is inorganic Hg concentration. Methyl Hg commonly makes up about 1% of total Hg in sediments and wetland soils. A number of reviews have evaluated Hg vs. methyl Hg across ecosystems (e.g. Benoit et al. 2003; Munthe et al. 2007; Selin 2009; Wiener and Shields 2000; Wiener et al. 2006). In most of these syntheses, methyl Hg concentrations are well-correlated with total Hg at concentrations up to about 1-10 ppm. Above that concentration, the percentage of total Hg as methyl Hg (% methyl Hg) is generally lower, the explanation being that Hg bioavailability for methylation is lower in highly contaminated sediments.

Figure 11-3.2 shows methyl Hg vs. Hg in the solid phase in sediments and soils of the comparison ecosystems, and Figure 11-3.3 shows the averages and standard deviations for the study systems. Only surface data were included in this comparison, because methyl Hg production rates and concentrations commonly decrease with depth. Penobscot sediments, as especially marsh soils, exhibit a higher average % methyl Hg than all of these systems, and most of the highest values in the overall data set. Notably, all of the sites with higher Hg concentrations had lower % methyl Hg, including the highly contaminated NJ tidal *Phragmites* marsh. Many of the other high % methyl Hg habitats in this data set are wetlands. Marshes and wetlands often exhibit relatively high rates of net methyl Hg production and accumulation (e.g., St. Louis et al. 1994; Rudd 1995; Krabbenhoft et al. 1995; Gilmour et al. 1998; Mitchell et al. 2008a,b, 2009).

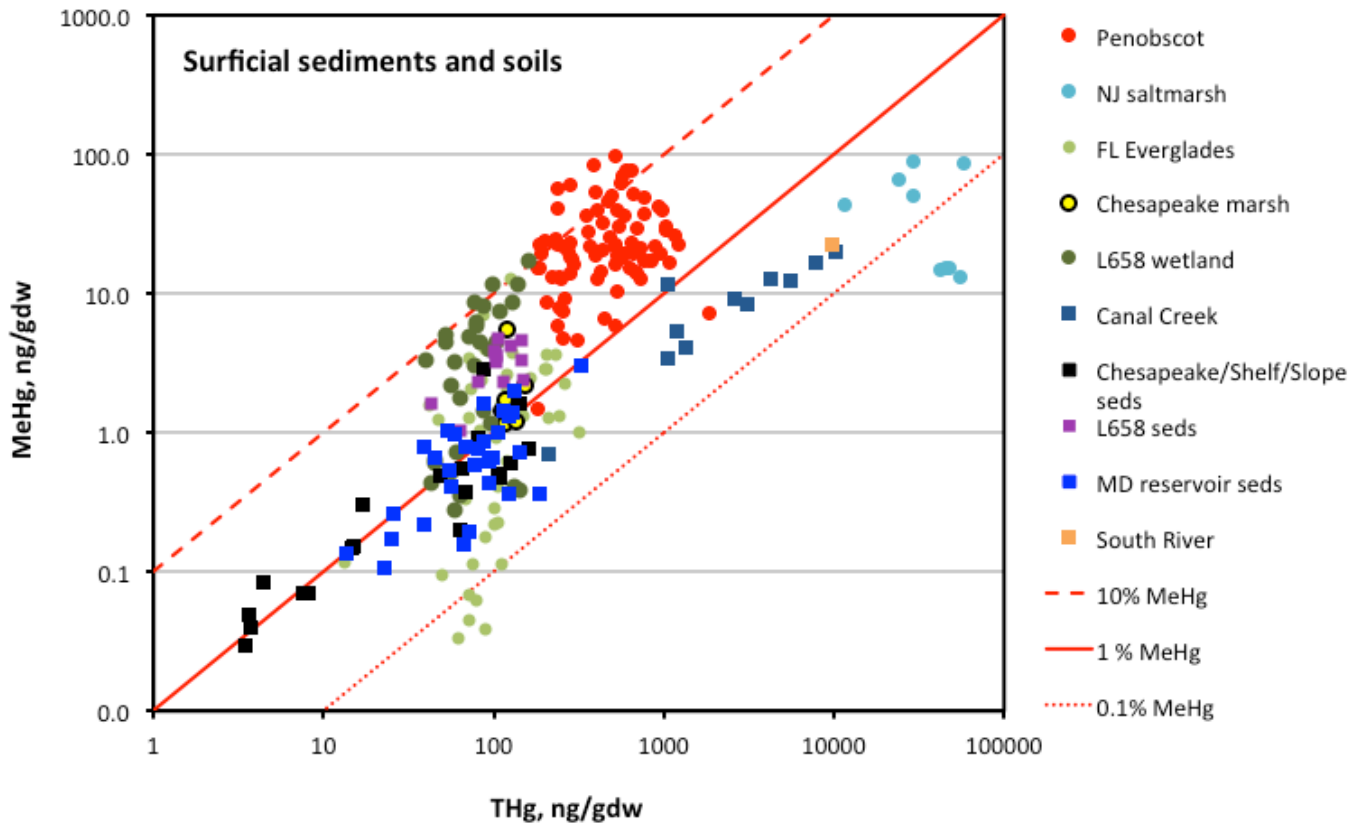


Figure 11-3.2. Methyl Hg concentrations in sediments or soils as a percentage of total Hg, for the comparison ecosystems. Each point represents the average value for a site/date combination. Only surface data were included in this comparison. The red lines show 0.1%, 1% and 10% of total Hg as methyl Hg. Data from marsh soils are shown as circles; bottom sediments as squares.

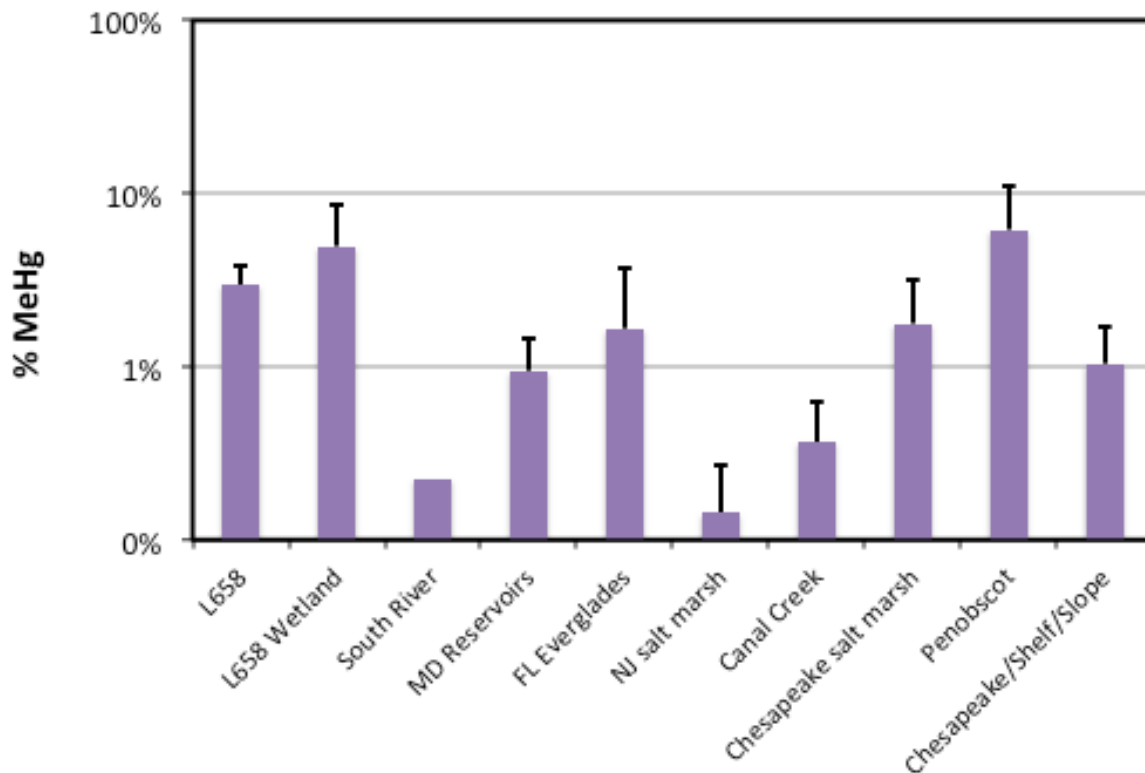


Figure 11-3.3. Average methyl Hg in sediments or marsh soils as a percentage of total Hg, for a wide variety of ecosystems. Bars are averages and standard deviations of all available data for surface soils. Ecosystems are generally arranged in order of increasing salinity left to right.

The marshes in the Penobscot system also stand out in terms of high total Hg and especially methyl Hg concentrations in pore waters. Figure 11-3.4 shows methyl Hg in pore water against total Hg in sediment or soil. Penobscot pore waters, specifically those in Mendall Marsh have the highest concentrations in a data set that includes soils with 100 times more total Hg (Figure 11-3.2). Methyl Hg in surficial pore waters at many of the Mendall marsh sites approached or exceeded 100 ng total Hg or methyl Hg/L. Assuming that methyl Hg in pore water is a linear correlate of total Hg in sediments, the Penobscot data fall well above the trend of most of the other sites.

Partitioning of Hg between the solid and aqueous phases appears to be a major control on Hg bioavailability for microbial methylation. Across and within ecosystems, the Hg  $K_D$  is a significant inverse correlate of % methyl Hg (Figure 11-3.5). These data, and experimental studies with Hg-methylating bacteria, suggest that Hg is most available for methylation in the filterable phase (Benoit et al. 1999, 2001; Golding et al. 2002, 2008; Schaefer et al. 2009; Graham et al. 2011, 2012). Filterable Hg can include (and indeed is generally dominated by) colloidal and nanoparticulate forms of Hg (e.g., Aiken et al.

2011; Han et al. 2005, 2006; Lee et al. 2011; Babiarz et al. 2001, 2012; Deonarine et al. 2009; Gerbig et al. 2010, 2011; Spencer et al. 2012 ).

In the Penobscot system, especially in marsh soils, Hg partitioning to sediments and soils is lower than in most other ecosystems (Figure 11-3.6; and marine data summarized in Fig. 6 in Hollweg et al. 2012; Hammerschmidt and Fitzgerald 2006; Liu et al. 2009; Sunderland et al. 2006; Ogrinc et al. 2007). Figure 11-3.7 compares the  $K_D$ s among ecosystems by plotting solid Hg vs. aqueous Hg (and solid methyl Hg vs. aqueous methyl Hg), with lines drawn for various  $K_D$  values. The other very low values (black squares) are for sandy sediments on the continental shelf.

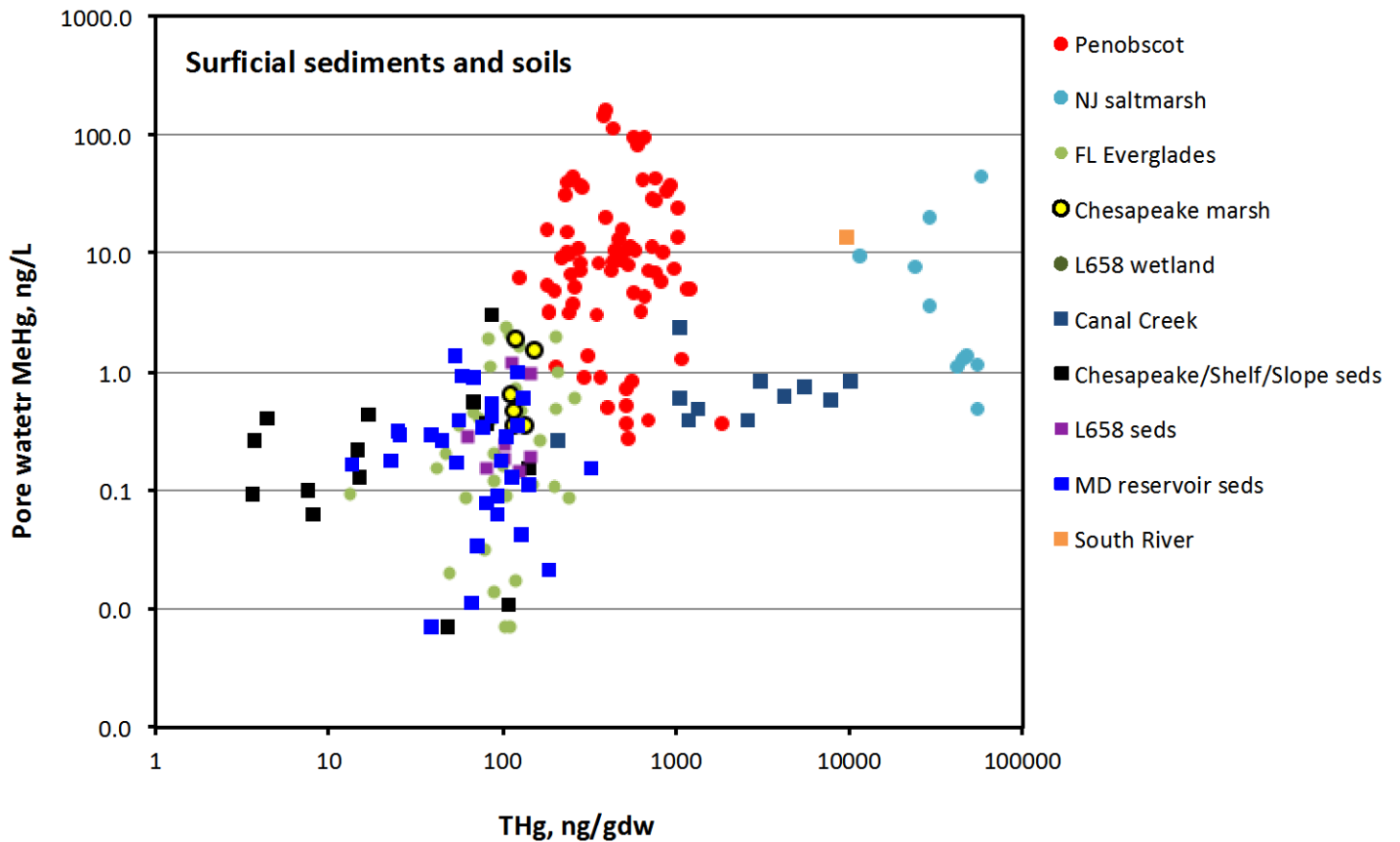


Figure 11-3.4. Pore water methyl Hg concentrations in surface sediments or soils vs. bulk phase total Hg for the comparison ecosystems. Data from marsh soils are shown as circles; bottom sediments as squares.

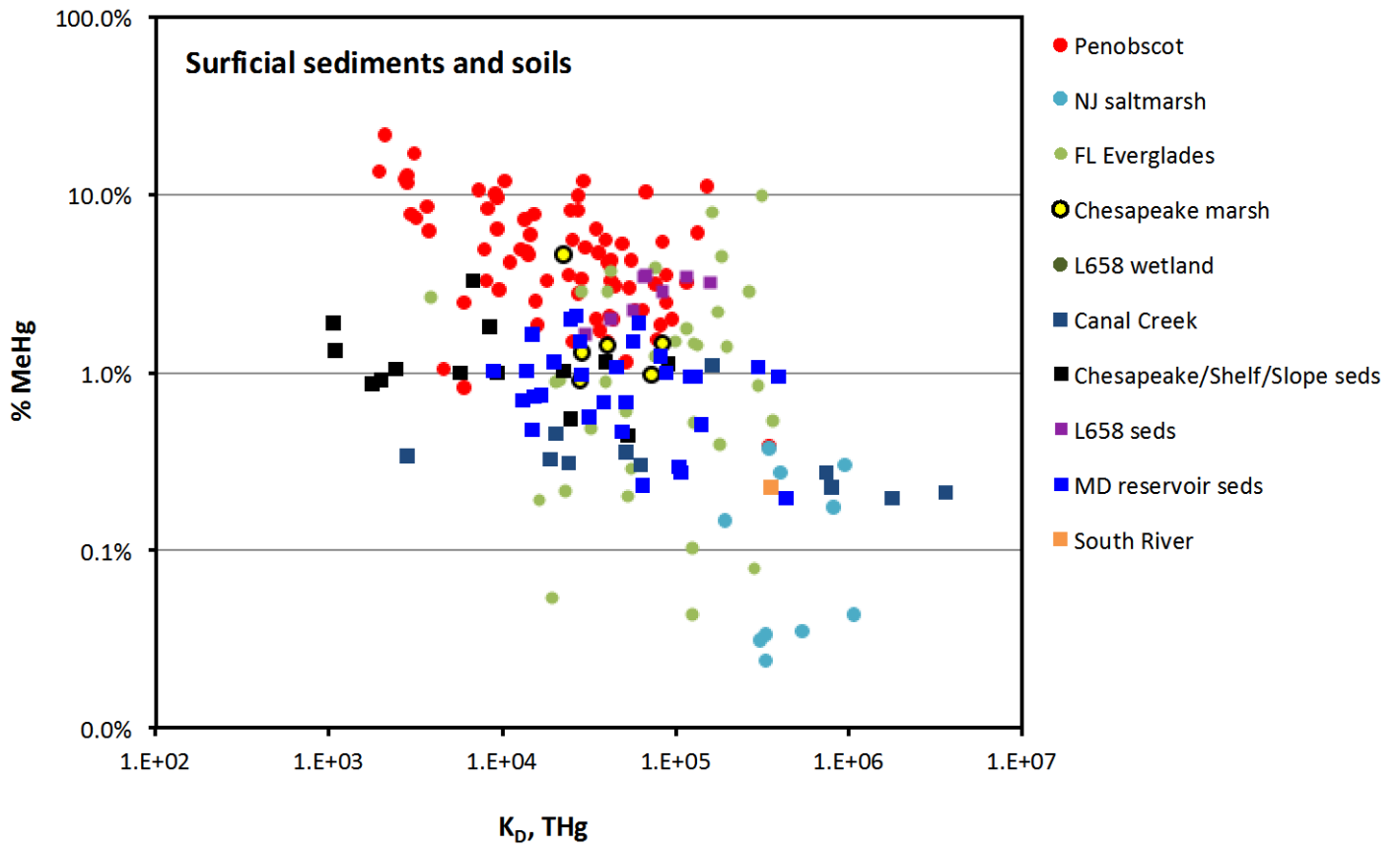


Figure 11-3.5. Methyl Hg as a percentage of total Hg in sediments is inversely correlated with the sediment:water partition coefficient ( $K_D$ ) for total Hg. Data for surface intervals only.

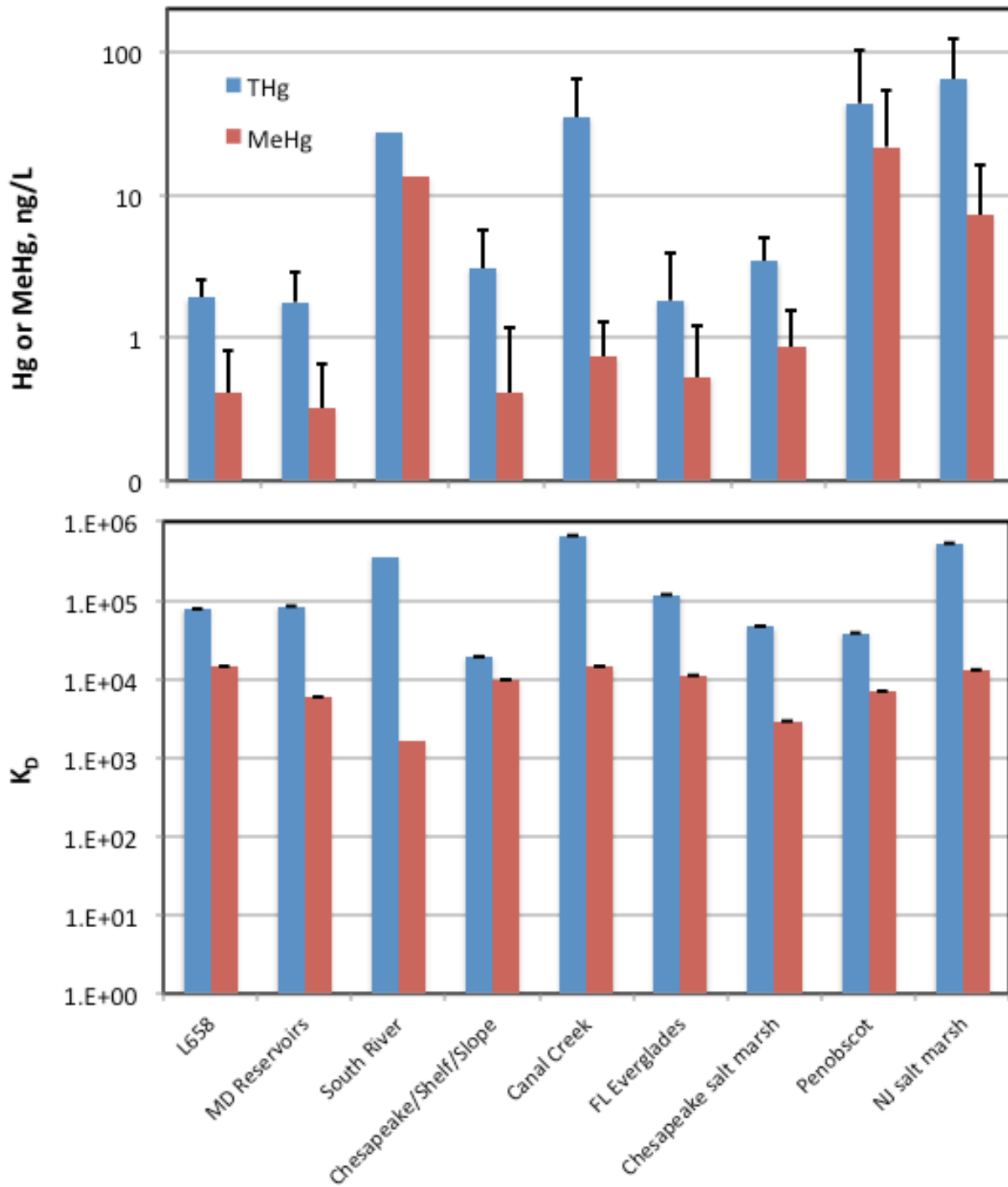


Figure 11-3.6. Top: average total Hg and methyl Hg concentrations in pore waters (with standard deviations) for the comparison ecosystems. Bottom: average sediment:water partition coefficients (K<sub>p</sub>) for total Hg and methyl Hg.

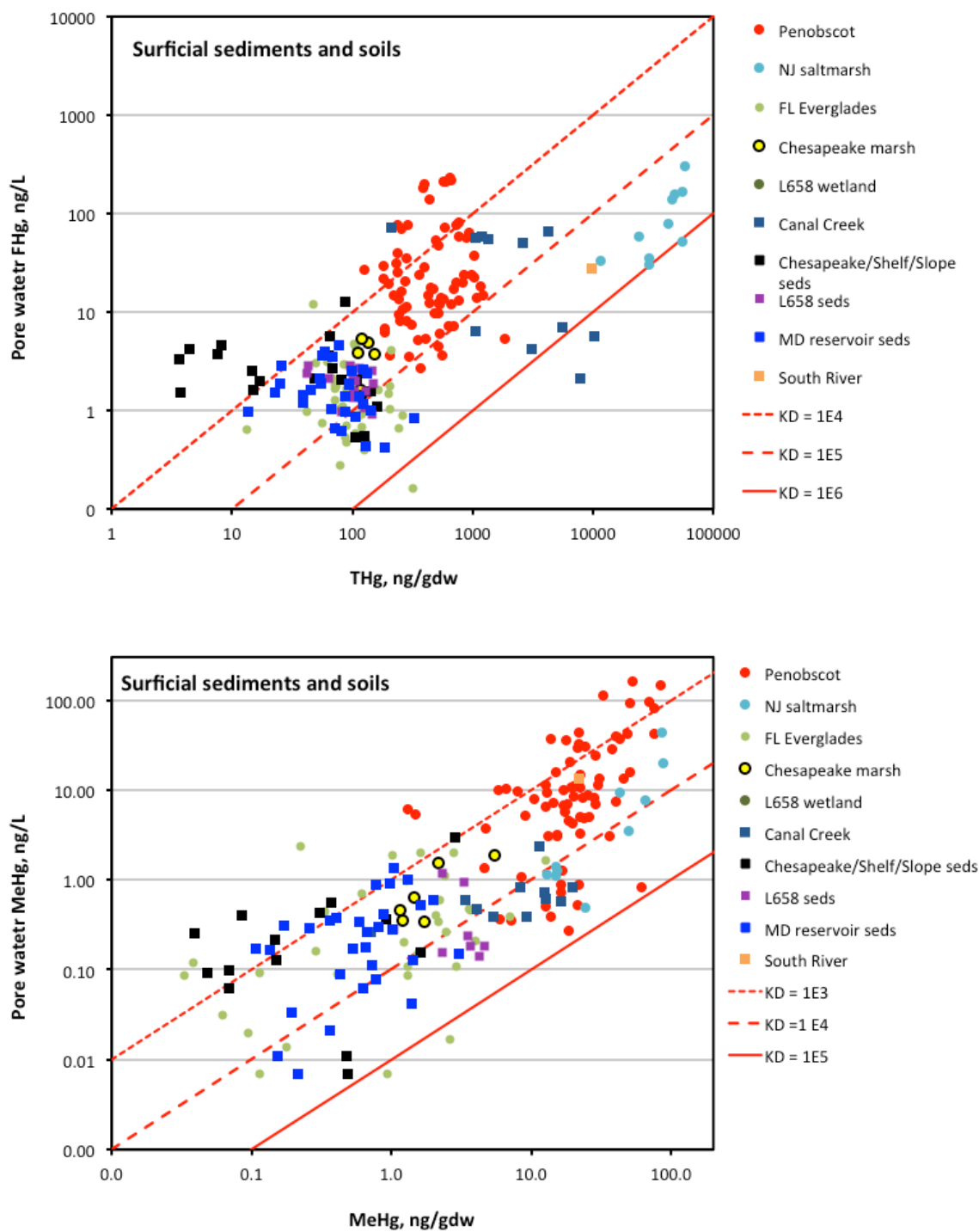


Figure 11-3.7. Top: pore water Hg (FHg = filtered Hg) concentrations in comparison to total Hg in sediments and soils, with lines showing sediment:water partition coefficients ( $K_D$ ) of  $10^4$ ,  $10^5$  and  $10^6$ , the range of  $K_D$  found in most of the published literature on Hg partitioning. Bottom: same for methyl Hg.

## SECTION 4. DISCUSSION - BIOGEOCHEMISTRY OF HG AND METHYL HG IN THE PENOBSCOT

Total mercury (Hg) levels in Penobscot River sediments and soils are elevated over background based on comparison with other ecosystems on the east coast of the U.S., normalized to organic carbon content (Figure 11-3.1). In this sample set, surface soils in Penobscot marshes were elevated 2-10 times above Chesapeake Bay marshes at the same organic carbon content.

Methyl Hg concentrations in Penobscot marsh soils are exceptionally high. In the set of ecosystems compared in Section 3, methyl Hg concentrations in Penobscot surface soils and surface pore waters stand out, even in comparison with more highly contaminated marshes (Figure 11-3.2).

This section provides a discussion of the potential controls on Hg biogeochemistry in the Penobscot system, with a focus on methyl Hg production and accumulation. For this evaluation, we used the data set of surface soils, sediments and pore waters for all of the study sites on all dates (n=85). The data set includes 44 primary variables, plus derived variables (like %methyl Hg or  $K_{DS}$ ). For statistics in this section, variables were evaluated for normalcy before running linear models, using SAS/JMP, and transformed (log transforms) as needed. Data appendices provide full data sets, transformations, simple statistics for all variables, and a correlation matrix of transformed variables.

Across all habitat types (wetland, sediment) total Hg levels in surface sediments and soils accounted for about 10% of the variability in methyl Hg in this sample set (Figure 11-4.1). That level is significant in this large data set (n=85,  $r = 0.33$ ,  $\alpha < 0.05$ ). Hg concentrations in surface sediments and soils were best correlated (positively) with variables indicative of mineral content (Table 11-4.1), and most negatively correlated with organic matter content and sulfide. Within individual habitat types, Hg is a stronger correlate of methyl Hg (for example see marsh soils in Section 2 of this chapter). Hg in marsh soils appears to derive from Hg in riverine silts, which wash into, deposit and accrete in Penobscot marshes.

While methyl Hg concentrations increase significantly with total Hg, % methyl Hg declined somewhat with total Hg concentration (Figure 11-4.2), as has often been observed in other contaminated ecosystems. While elevated levels of inorganic Hg in the Penobscot contribute to elevated levels of methyl Hg, other factors exacerbate methyl Hg production and contribute to the variability in methyl Hg across the system.

*Overview of other correlates with % methyl Hg.* In order to evaluate controls on methyl Hg other than total Hg concentration, correlates with % methyl Hg (methyl Hg normalized to Hg) were examined. The strongest positive predictors of % methyl Hg were soil organic content, soil porosity, methylation rate constant, pore water methyl Hg, and a measure of the colloidal FeS held in soil pore waters (see below for discussion) (Table 11-4.2). Unusually, % methyl Hg was positively correlated with pore water sulfide. % methyl Hg was negatively correlated with measures of sediment or soil mineral content (i.e. dry bulk density and the concentrations of crustal metals).

Scatterplot matrices of all variables against % methyl Hg are shown in Figures 11-4.3 to 11-4.10 for visualization.

Principal components analysis provides one way to visualize how parameters in the Penobscot data set cluster. Figure 11-4.11 shows a loading plot for the first two principal components of a PCA using all of the available variables. It shows that loss on ignition (LOI), pore water sulfide, methylation rate, SUVA<sub>280</sub> (a measure of DOC aromaticity), solid and pore water methyl Hg tend to co-vary. Measures of mineral content cluster with salinity, pH and sediment total Hg content. The reduced sulfur and extractable reduced Fe content of sediments cluster together, and somewhat separately. Dissolved organic carbon (DOC) and pore water Hg plotted in the same quadrant. A visualization of similar factors provides guidance for development of statistical (empirical) models.

*Methyl Hg production.* Methylation rate constants, measured via injection of enriched stable Hg isotope spikes into sediment and soil cores, were strong predictors of % methyl Hg (Figure 11-4.12, detailed in Figure 11-4.13). Other variables that were positively correlated with  $k_{\text{meth}}$  included pore water Hg concentration, and aromatic DOC (aCDOM<sub>280</sub>) (Figure 11-4.14). Bulk density, pH, and Hg  $K_D$  were negative correlates (Figure 11-4.12). Note the lack of inhibition of methylation by sulfide, and the lack of correlation with salinity.

Mitchell defined “hot spots and moments” of net methylation in a study of the distribution of methyl Hg production in peat lands (Mitchell et al. 2008). In his study, these were physical interfaces, where an upland/wetland connection provided runoff bearing sulfate and DOC into anoxic zones in the wetland during certain times of year. But the concept of methylation being favored at “hot spots and moments” applies more broadly to places and times where the activity of Hg-methylating bacteria is favored, and/or Hg is highly bioavailable for methylation.

Salt marshes appear to be one of those hot spots. Microbial activity in salt marshes, especially the activity of bacteria known to produce MeHg - sulfate-reducing bacteria – is notoriously high in these high sulfate systems. The physical movement of tidal waters brings fresh sulfate to soils frequently. Highly productive plant growth provides organic matter for microbial activity. In the Penobscot, %MeHg was highest in high organic matter soils with high porosity – sites favorable for microbial activity.

The Penobscot study may be the first detailed biogeochemical study of methyl Hg in marshes with salinities approaching seawater levels. Mitchell et al. (2008, 2012) studied methyl Hg in a mesohaline Chesapeake Bay salt marsh with somewhat lower maximum salinities and also found exceptional methyl Hg production and accumulation. Methylation rate constants, measured with the same methods reached 0.05 per day, %MeHg in soils approach 5% at maximum. However, in the Chesapeake marsh, a strong negative correlation between sulfide and both % MeHg and  $k_{\text{meth}}$  was observed.

*Pore water Hg concentrations and sediment:water partition coefficients* were strong predictors of methyl Hg concentration and % methyl Hg in sediments and soils (See Figure 11-4.6). Exceptionally low partition coefficients may be one driver of high methyl

Hg and high pore water methyl Hg in Penobscot marshes. Partition coefficients are calculated as the concentration of Hg in the bulk phase, in ng/kg, divided by the filterable concentration in pore water, in ng/L. Thus, higher  $K_D$ s mean less Hg in pore water and more in the solid phase. Partition coefficients can serve as an indicator of the bioavailability of Hg to bacteria for methylation. Methylation is thought to occur from Hg taken up from the aqueous phase. However, partitioning may provide more information on bioavailability than pore water concentration data do, reflecting how strongly Hg is bound in each phase.

As noted in Section 3, across and within ecosystems, the Hg  $K_D$  is a significant inverse correlate of % methyl Hg (Figure 11-3.5). Penobscot pore waters have exceptionally high Hg and methyl Hg concentrations and low  $K_D$ s (see Figures 11-3.6 and 11-3.7 for comparison with other ecosystems). Why are partition coefficients in the Penobscot system, especially in marshes, so low? Partitioning is effectively a competition for Hg between filterable and solid phase ligands. Many investigators have observed low partitioning in sediments with low solid phase organic matter or low solid phase-sulfide concentrations (Hammerschmidt and Fitzgerald 2004, 2006; Hammerschmidt et al. 2008; Hollweg et al. 2010; Ogrinc et al. 2007; Hollweg et al. 2010) where Hg binding sites in solids are limited. But neither is the case in Penobscot marshes, and neither solid AVS+CRS nor LOI correlate with Hg  $K_D$  in the Penobscot system (scatterplots of pairwise variable comparisons with  $K_D$ s are in Figures 11-4.15 to 11-4.17).

High concentrations of DOC in pore waters can help hold Hg in the filterable phase. DOC concentrations in Penobscot marsh soils are very high.  $K_D$  for both total Hg and methyl Hg correlated significantly with DOC across the Penobscot surface data set (Figure 11-4.14), but were weak.  $K_D$ s correlated better with a measure of the concentration of aromatic DOC ( $aCDOM_{280}$ ). With a coefficient of determination ( $r$ ) of 0.33 between total Hg and  $K_D$  and  $aCDOM_{280}$ , this class of DOC may contribute about 10% of the variability in Hg partitioning across the Penobscot data set.

*pH.* The partitioning of Hg to sediments rose with pH (Figure 11-4.15), and, concomitantly, % methyl Hg was higher at lower pHs. Both % methyl Hg (Figure 11-4.7) and  $k_{meth}$  (Figure 11-4.14) were strongly and negatively correlated with pH. Across the sediments and soils studied in the Penobscot, pH tended to be lowest in high marsh and marsh platform soils and tended to rise with salinity (Figure 11-2.49). Methylation proceeded best in the marsh soils where pH was generally lower. The mechanism for any direct effect of pH on Hg methylation is likely to be via an effect on Hg complexation in soil pore waters, and resultant impact on Hg bioavailability (Kelly et al. 2003; Golding et al. 2008).

*Sulfide.* The % methyl Hg in sediments and soils (Figure 11-4.7) and the concentration of methyl Hg in pore water were both positively correlated with sulfide. Partition coefficients for both total Hg and methyl Hg were strongly negatively correlated with sulfide. The coefficients of determinations ( $r$ ) between the total Hg and methyl Hg  $K_D$ s and sulfide were -0.47 and -0.54, some of the stronger correlations in the variable matrix.

In low organic matter sediments,  $K_D$  has been observed to positively correlate with pore water sulfide (e.g., Hammerschmidt et al. 2006; Hollweg et al. 2010). This has been attributed to HgS precipitation at higher sulfide concentrations. However, in organic soils, including the Penobscot data set (Figure 11-4.16), Hg  $K_D$  tends to decrease as sulfide increases. Figure 11-4.18 shows the  $K_D$  vs. sulfide comparison for the ecosystems discussed in Section 3. In sediments and marsh soils above about 15% to 20% organic content, sulfide appears to enhance the concentration of Hg in the filterable phase. Note that the Penobscot has some of the lowest  $K_D$ s at the highest sulfide concentrations among the ecosystems compared.

*Hg bioavailability and iron-sulfur chemistry.* This data set collected for the Penobscot is unique among published studies of Hg biogeochemistry in a number of ways. In addition to exceptional methyl Hg concentrations in pore waters and % methyl Hg in soils, Penobscot marshes are unusual among ecosystems previously studied in having high % methyl Hg at high sulfide concentrations. There is a large literature showing inhibition of methyl Hg production and accumulation by sulfide, starting with some of the earliest papers on methyl Hg in sediments (Craig and Bartlett 1978; Blum and Bartha 1980; also see Gilmour and Henry 1991; Gilmour et al. 2002; Gilmour et al. 1998; King et al. 2000, 2002; Benoit et al. 2001, 2003; Hammerschmidt et al. 2008; Orem et al. 2011). However, there are a few published exceptions especially at high salinity highly microbial active sites (King et al. 2002; Hollweg et al. 2009).

The fairly complete evaluation of FeS chemistry in soils in this study allowed us to look for oddities that might explain why we found high methyl Hg at high sulfide in the Penobscot. Although there are a number of Hg biogeochemical studies on coastal and marine sediments, including some with high sulfide, the Penobscot is probably the highest salinity saltmarsh for which Hg biogeochemistry has been studied in detail, including FeS and organic carbon chemistry.

One aspect that stands out in the Penobscot data set, especially in marsh soils, is the concomitant presence of both iron and sulfide in pore waters. This is unusual, because at equilibrium iron sulfide should precipitate, leaving effectively only Fe(II) or bisulfide in solution above a few micromolar in pore water (Berner 1970). However, Penobscot marsh pore waters sometimes carry up to 100  $\mu\text{M}$  of both Fe and sulfide together in 0.45  $\mu\text{m}$  filterable pore water.

The paradigm for metal sulfide precipitation in natural waters has changed in the last few years, with the realization that metal sulfide precipitation in natural waters and pore waters is often slowed by organic matter in solution. DOC can “cap” or coat metal sulfide particles, limiting their growth rate and their rate of precipitation from solution (e.g., Deonarine et al. 2011; Aiken et al. 2011). Effectively, metal sulfides – like  $\text{FeS}_2$  – are held in the aqueous phase as nanoparticles and colloids, and their removal to the bulk phase is delayed. The most recent work in this area suggests that the ability of DOC to impact metal sulfide precipitation may be dependent on the chemical “character” of the organic matter (Gerbig et al. 2011).

For this analysis, the concentration of “colloidal FeS” was calculated as the minimum of the concentration of Fe or sulfide in pore water, i.e. the concentration at which Fe and

sulfide occur together in the sample. Within the Penobscot data set, the coefficients of determination for FeS colloids with total Hg  $K_D$  and % methyl Hg were 0.57 and 0.40 respectively, some of the strongest correlations in the data set (Figure 11-4.19).

Among the ecosystems examined in Section 3, the co-occurrence of iron and sulfide in pore waters above  $\sim 10 \mu\text{M}$  was rare. When it did occur it was usually in marsh soils (Figure 11-4.20). The unique combination of exceptionally high % methyl Hg with colloidal FeS above  $\sim 10 \mu\text{M}$  in Penobscot soils is visually obvious in this figure.

Under the conditions found in Penobscot marsh pore waters, Hg should precipitate as HgS at equilibrium (Figure 11-4.21). However, the precipitation of HgS is also slowed by DOM (Ravichandran et al. 1999; Deonaraine et al. 2009; Aiken et al. 2011). In natural waters, HgS presumably precipitates as part of mixed metal sulfide complexes. The presence of “FeS colloids” in Penobscot pore waters may be an indicator that Hg is being held in solution as nanoparticulate or colloidal HgS, in association with DOC and probably other metals.

Mercuric sulfide nano-particles appear to be highly bioavailable for uptake and methylation by Hg-methylating sulfate reducing bacteria (Graham et al. 2012; Zhang et al. 2012). We demonstrated that under sulfidic conditions, DOC greatly enhances the bioavailability of Hg for methylation, presumably by limiting the size and growth of HgS nano-particles. More recently, Graham et al. showed that the impact of DOC on HgS bioavailability depends on its character, particularly its aromaticity and sulfur content (Graham et al. 2012 and in review).

The most likely explanation for the high levels of FeS, and the high bioavailability of Hg in Penobscot pore waters is probably the combination of available Fe, significant sulfide production, and high concentrations of highly aromatic DOC to hold it all as tiny particles in the aqueous phase. However, this is a new way of thinking about and modeling Hg complexation and bioavailability. Available data on highly sulfidic ecosystems are limited, and development of models will require more fieldwork in other sulfidic ecosystems. Equilibrium models for Hg speciation are clearly not sufficient for sulfidic systems, and bioavailability will need to be modeled using a non-equilibrium approach that includes multiple size phases. The Penobscot data set will be value in expanding models for Hg complexation and bioavailability.

*Summary of Penobscot methyl Hg biogeochemistry.* It is clear that Penobscot marsh soils are unusual in their capacity to produce and retain methyl Hg. To summarize, drivers of high methyl Hg in Penobscot marshes include elevated Hg in soils, low partitioning of Hg to solids resulting in high bioavailability for methylation, rapidly shifting redox conditions in surface marsh soils, and high rates of microbial activity. In these marshes, despite high levels of sulfide, it appears that Hg in Penobscot marsh soils is highly available for microbial methylation, perhaps through the formation of highly bioavailable DOM-associated HgS nanoparticles. Together, a combination of conditions leads to exceptional net accumulation of methyl Hg in surface marsh soils and pore waters.

Remediation approaches designed to limit Hg bioavailability for methylation, and/or the delivery of Hg-contaminated river silts to surface marsh soils may be most effective in reducing methyl Hg production in Penobscot marshes.

**Table 11-4.1: Correlation coefficients for pairwise comparisons of data set variables with total Hg in sediments and soils. Variables that were not normally distributed were log transformed prior to correlation analysis. Correlations are shown for variables where r is greater than 0.3 or less than – 0.3.**

Variable	r for total Hg
pw Mn	0.717
Fe-solid	0.709
Mn-solid	0.666
pw Fe	0.636
pw P	0.551
K-solid	0.550
Al-solid	0.540
F-PO <sub>4</sub>	0.535
Ext Fe(II)	0.507
Mg-solid	0.507
pH	0.427
Si-Solid	0.395
aCDOM440	0.383
Tot Ext Fe	0.377
K <sub>D</sub> total Hg	0.356
Salinity	0.351
Slope 300-700	0.344
Ca-solid	0.342
methyl Hg	0.329
Dry Bulk Density	0.320
pw Ca	0.316
% methyl Hg	-0.371
F-NO <sub>2</sub> NO <sub>3</sub>	-0.374
Slope 350-400	-0.408
Slope 275-295	-0.507
Sulfide	-0.548
LOI	-0.602

**Table 11-4.2. Correlation coefficients for pairwise comparisons of data set variables with % MeHg in sediments and soils. Variables that were not normally distributed were log transformed prior to correlation analysis. Correlations are shown for variables where r is greater than 0.3 or less than – 0.3.**

Variable	r with % methyl Hg
LOI	0.598
Filter-passing methyl Hg	0.487
Porosity	0.473
Colloidal FeS	0.457
% methyl Hg pw	0.424
k <sub>meth</sub>	0.404
pw Al	0.395
Sulfide	0.353
Filter-passing total Hg	0.347
S350-400	0.303
Mg-solid	-0.344
Salinity	-0.365
pw P	-0.369
F-PO <sub>4</sub>	-0.371
Total Hg	-0.371
pw Mn	-0.373
Ca-solid	-0.396
Mn-solid	-0.405
Wet Bulk Density	-0.407
Fe-solid	-0.422
Fe-solid 2	-0.422
Al-solid	-0.427
K-solid	-0.430
K <sub>D</sub> total Hg	-0.492
Si-Solid	-0.511
Dry Bulk Density	-0.536
pH	-0.540

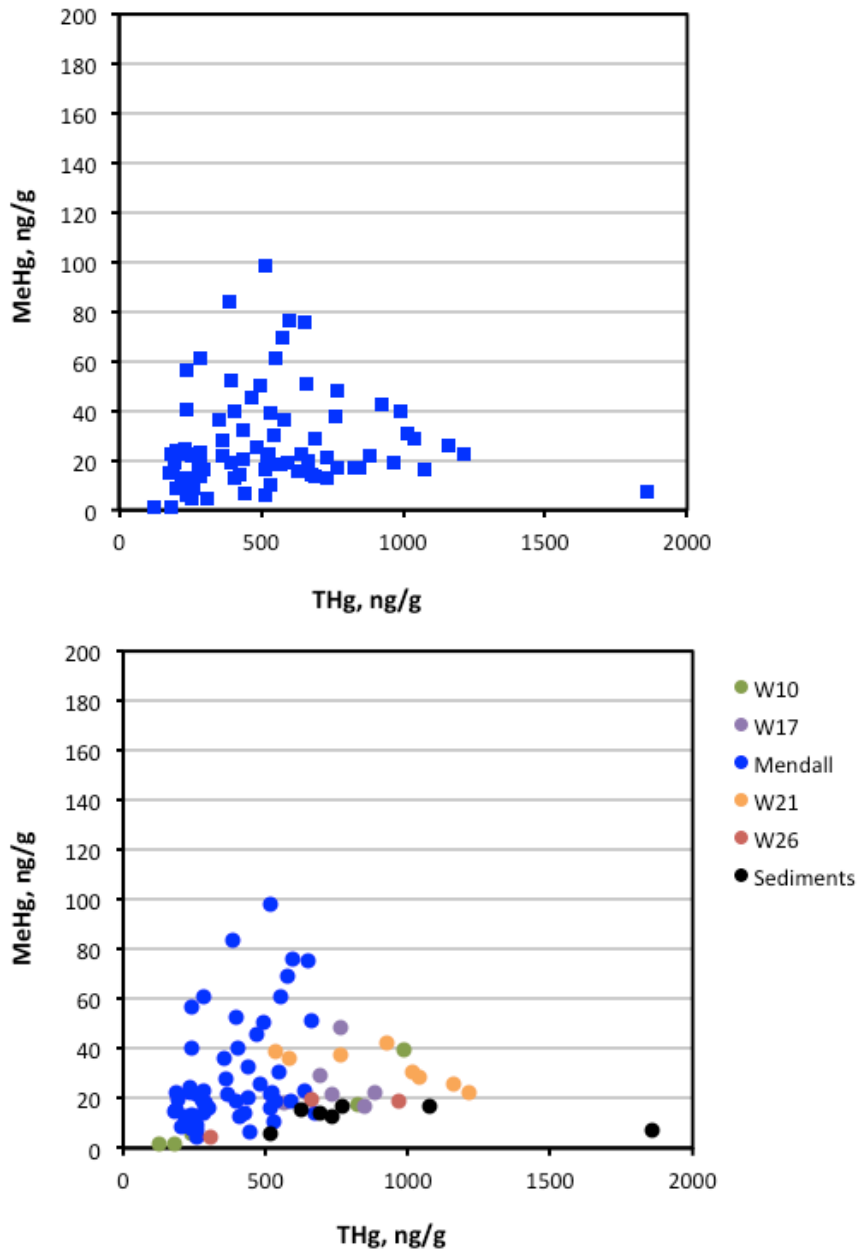
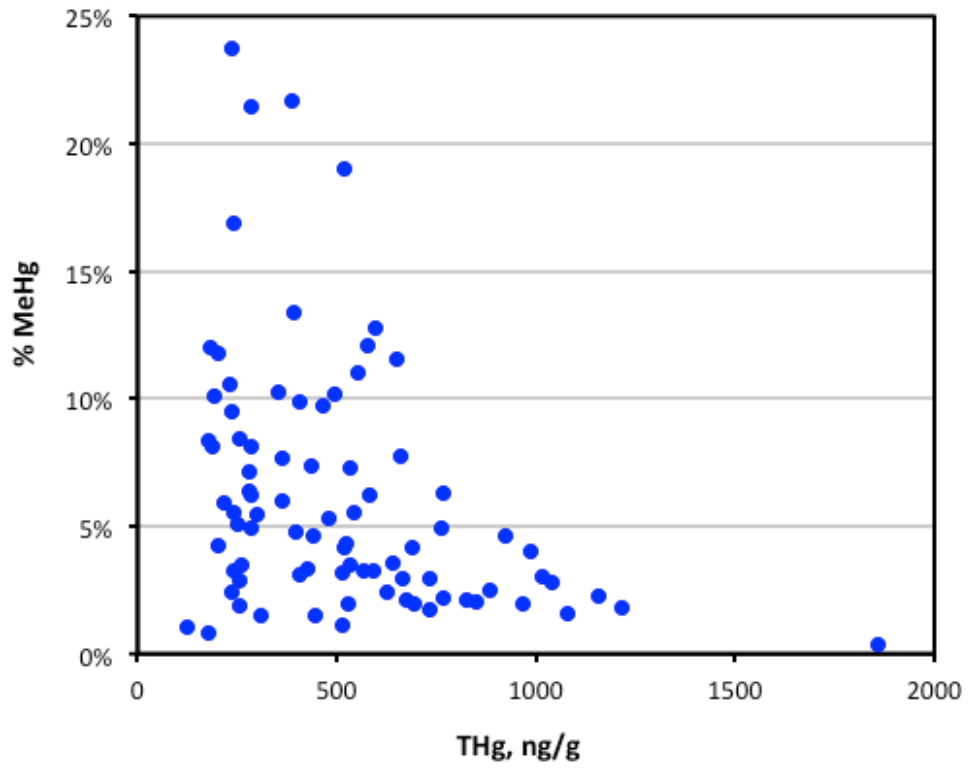


Figure 11-4.1. Hg accounts for about 10% of the variability in methyl Hg in surface sediments and soils across the Penobscot sites sampled. Data include all surface (0-3 cm) samples from all sites and dates 2009-2011. Top: all data (n=85). Bottom: Data identified by area.  $r = 0.33$  for the log transformed variables.



with total Hg.  $R = 0.37$  for the log transformed variables.

Figure 11-4.2. % methyl Hg in surface sediments and soils declines somewhat

## Multivariate

### Correlations

	%MeHg	Dry Bulk Density	Porosity	LOI	THg	kmeth
%MeHg	1.0000	-0.5336	0.4729	0.5928	-0.3745	0.3788
Dry Bulk Density	-0.5336	1.0000	-0.7649	-0.8480	0.3252	-0.3550
Porosity	0.4729	-0.7649	1.0000	0.5815	0.0251	0.1965
LOI	0.5928	-0.8480	0.5815	1.0000	-0.6036	0.1654
THg	-0.3745	0.3252	0.0251	-0.6036	1.0000	-0.0640
kmeth	0.3788	-0.3550	0.1965	0.1654	-0.0640	1.0000

There are 43 missing values. The correlations are estimated by REML method.

### Scatterplot Matrix

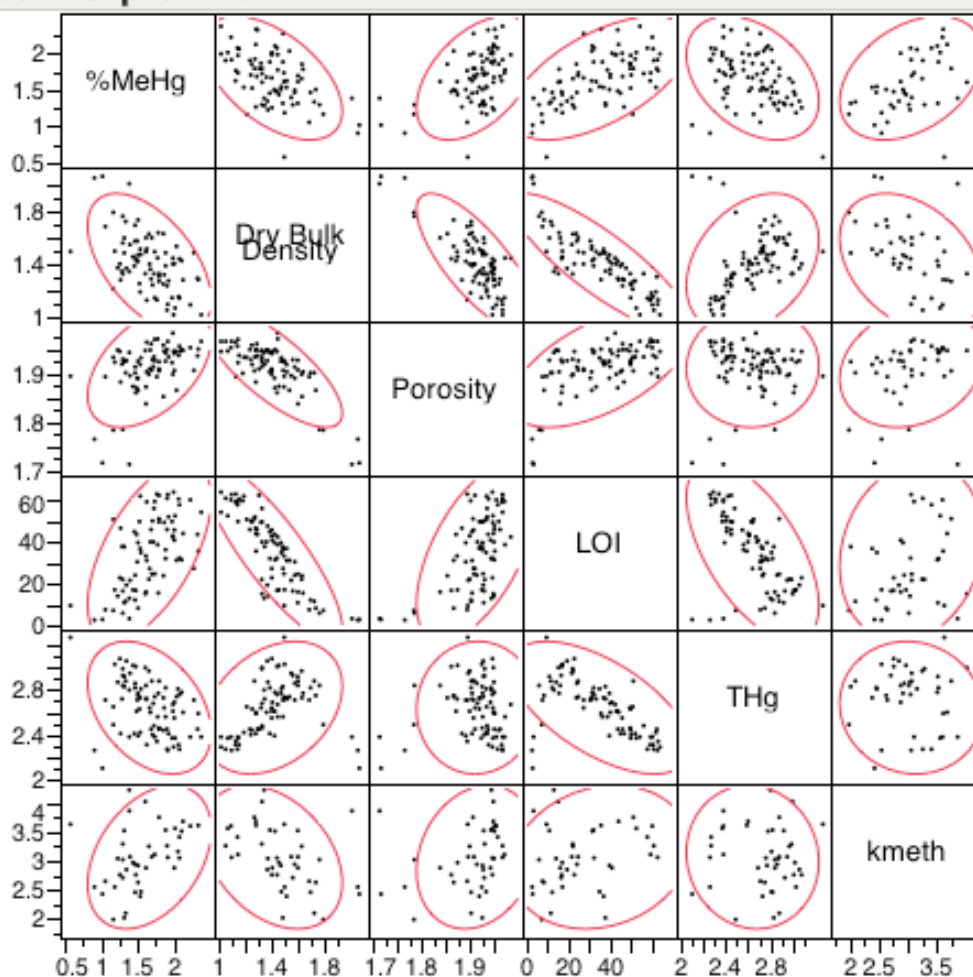


Figure 11-4.3. Scatterplot matrix for % methyl Hg in Penobscot surface sediments and soils, against bulk physical variables and total Hg and methyl Hg. Variables were log transformed as needed to achieve normality.

# Multivariate

## Scatterplot Matrix

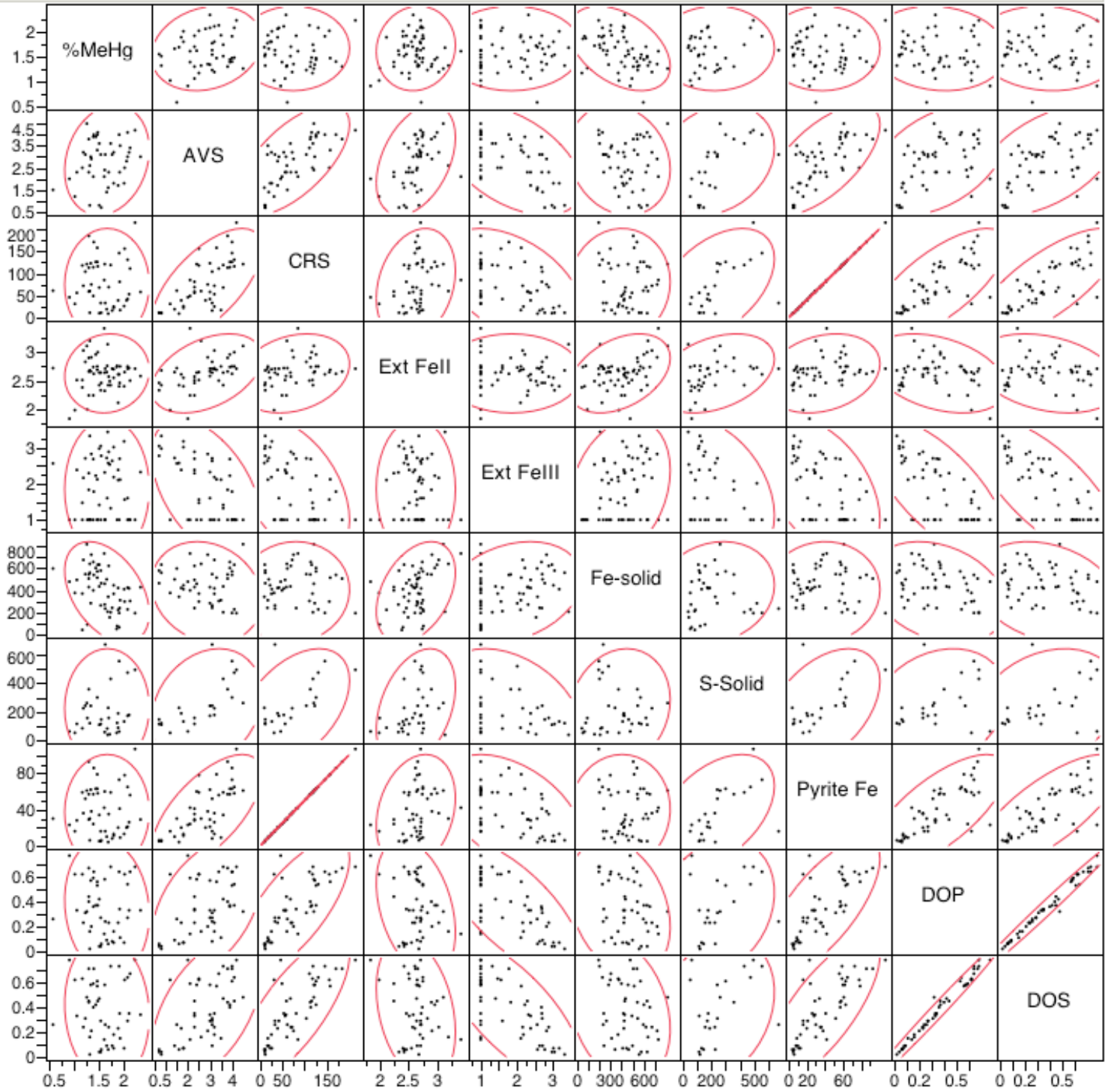


Figure 11-4.4. Scatterplot matrix for Penobscot surface sediments and soils, for solid S and Fe variables. Variables were log transformed as needed to achieve normality.

Multivariate

Scatterplot Matrix



Figure 11-4.5. Scatterplot matrix for % methyl Hg in Penobscot surface sediments and soils, against bulk phase metals. Variables were log transformed as needed to achieve normality.

## Multivariate

### Correlations

	%MeHg	FTHg	Fhgi	FMeHg	%MeHg pw	KD THg	KD Hgi	KD MeHg
%MeHg	1.0000	0.3793	0.1530	0.5122	0.4410	-0.5188	-0.3148	-0.1442
FTHg	0.3793	1.0000	0.8531	0.8540	0.2236	-0.8855	-0.7974	-0.7100
Fhgi	0.1530	0.8531	1.0000	0.5350	-0.2744	-0.6960	-0.8930	-0.4315
FMeHg	0.5122	0.8540	0.5350	1.0000	0.6397	-0.8145	-0.5463	-0.8579
%MeHg pw	0.4410	0.2236	-0.2744	0.6397	1.0000	-0.3091	0.1755	-0.5624
KD THg	-0.5188	-0.8855	-0.6960	-0.8145	-0.3091	1.0000	0.8600	0.7795
KD Hgi	-0.3148	-0.7974	-0.8930	-0.5463	0.1755	0.8600	1.0000	0.5413
KD MeHg	-0.1442	-0.7100	-0.4315	-0.8579	-0.5624	0.7795	0.5413	1.0000

There are 19 missing values. The correlations are estimated by REML method.

### Scatterplot Matrix

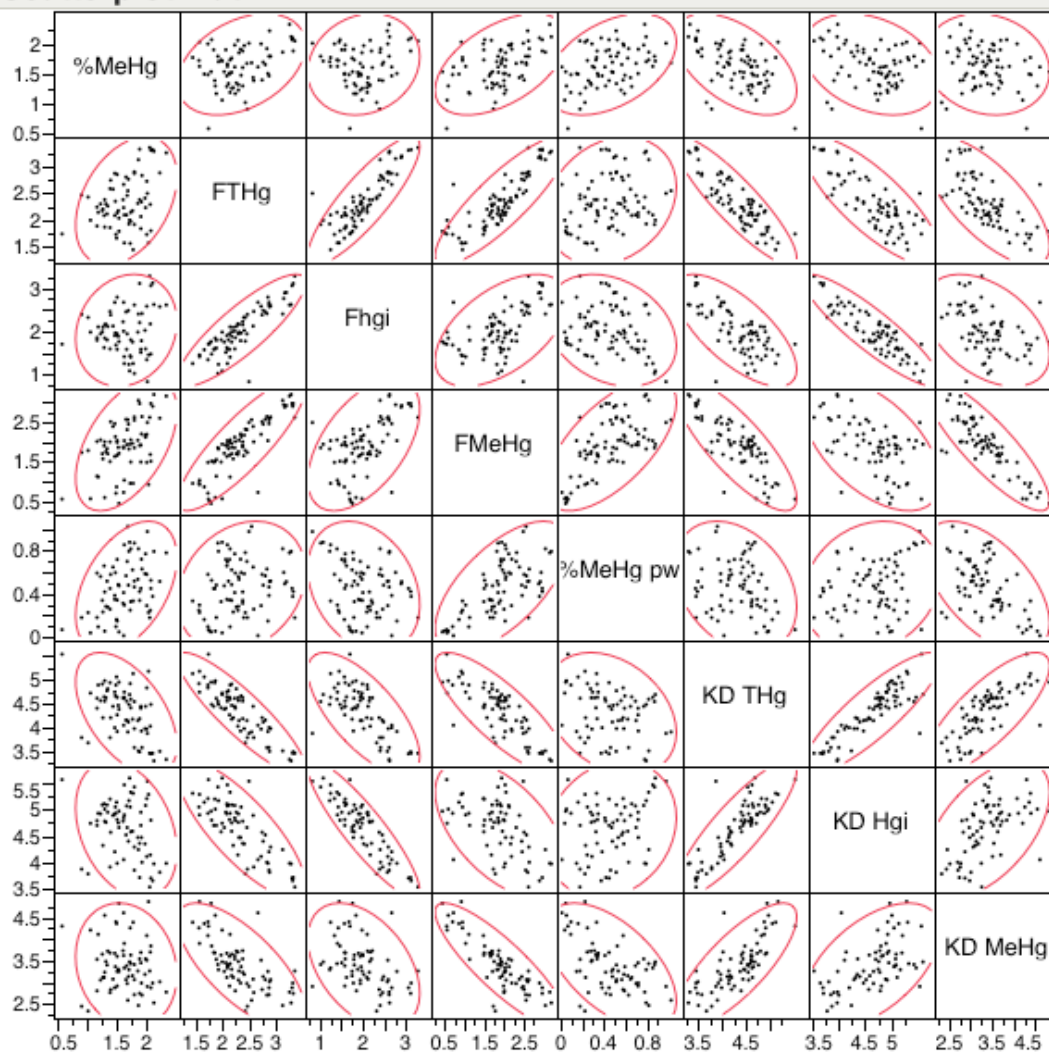


Figure 11-4.6. Scatterplot matrix for % methyl Hg in Penobscot surface sediments and soils, against pore water Hg variables. Variables were log transformed as needed to achieve normality.

## Multivariate

### Correlations

	%MeHg	pH	Sulfide	Salinity	pw Fe	Colloidal FeS
%MeHg	1.0000	-0.5227	0.3414	-0.3731	0.0370	0.4022
pH	-0.5227	1.0000	-0.3897	0.5830	0.1332	-0.4084
Sulfide	0.3414	-0.3897	1.0000	-0.4432	-0.6290	0.4126
Salinity	-0.3731	0.5830	-0.4432	1.0000	0.1688	-0.4643
pw Fe	0.0370	0.1332	-0.6290	0.1688	1.0000	0.3049
Colloidal FeS	0.4022	-0.4084	0.4126	-0.4643	0.3049	1.0000

There are 35 missing values. The correlations are estimated by REML method.

### Scatterplot Matrix

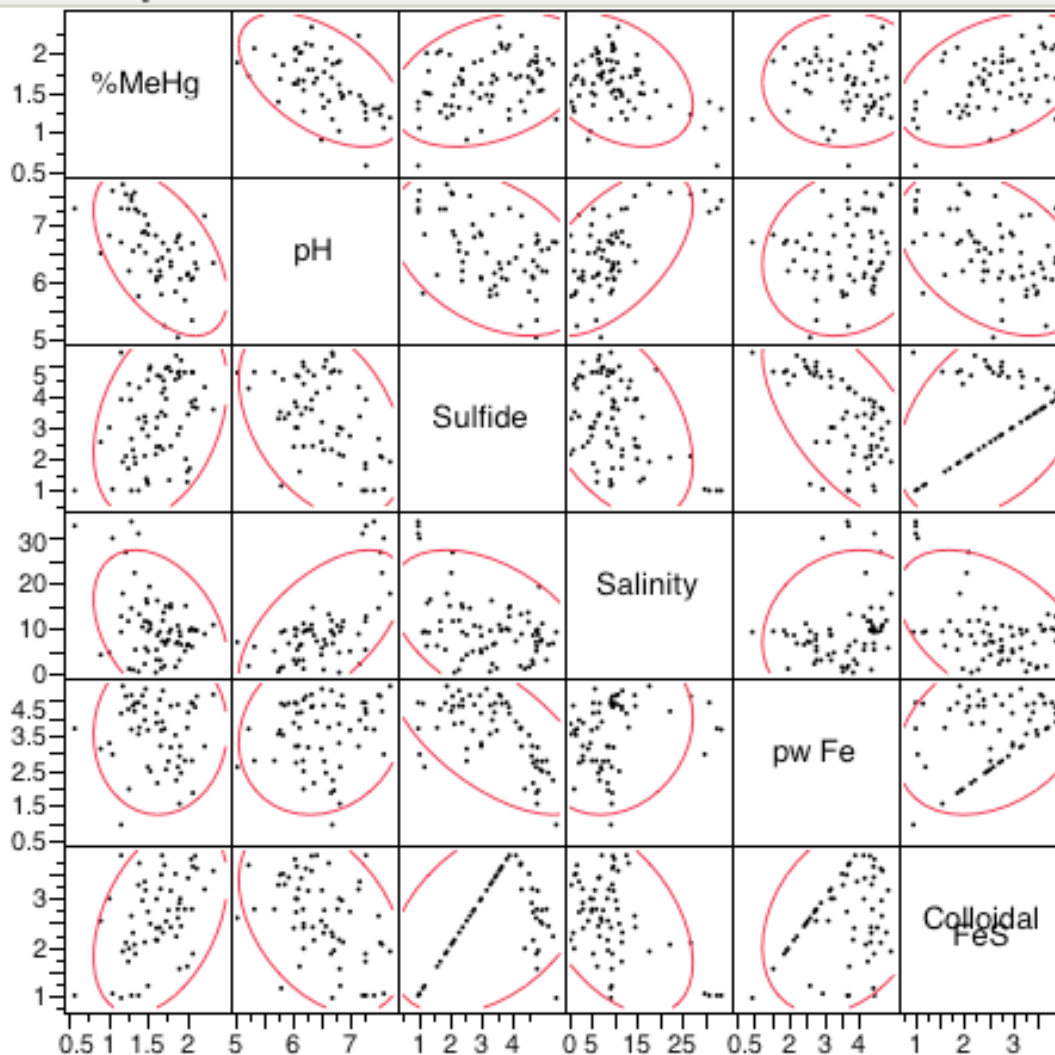


Figure 11-4.7. Scatterplot matrix for % methyl Hg in Penobscot surface sediments and soils, against pore pH, sulfide, salinity, Fe and colloidal FeS (see text for definition). Variables were log transformed as needed to achieve normality.

# Multivariate

## Scatterplot Matrix

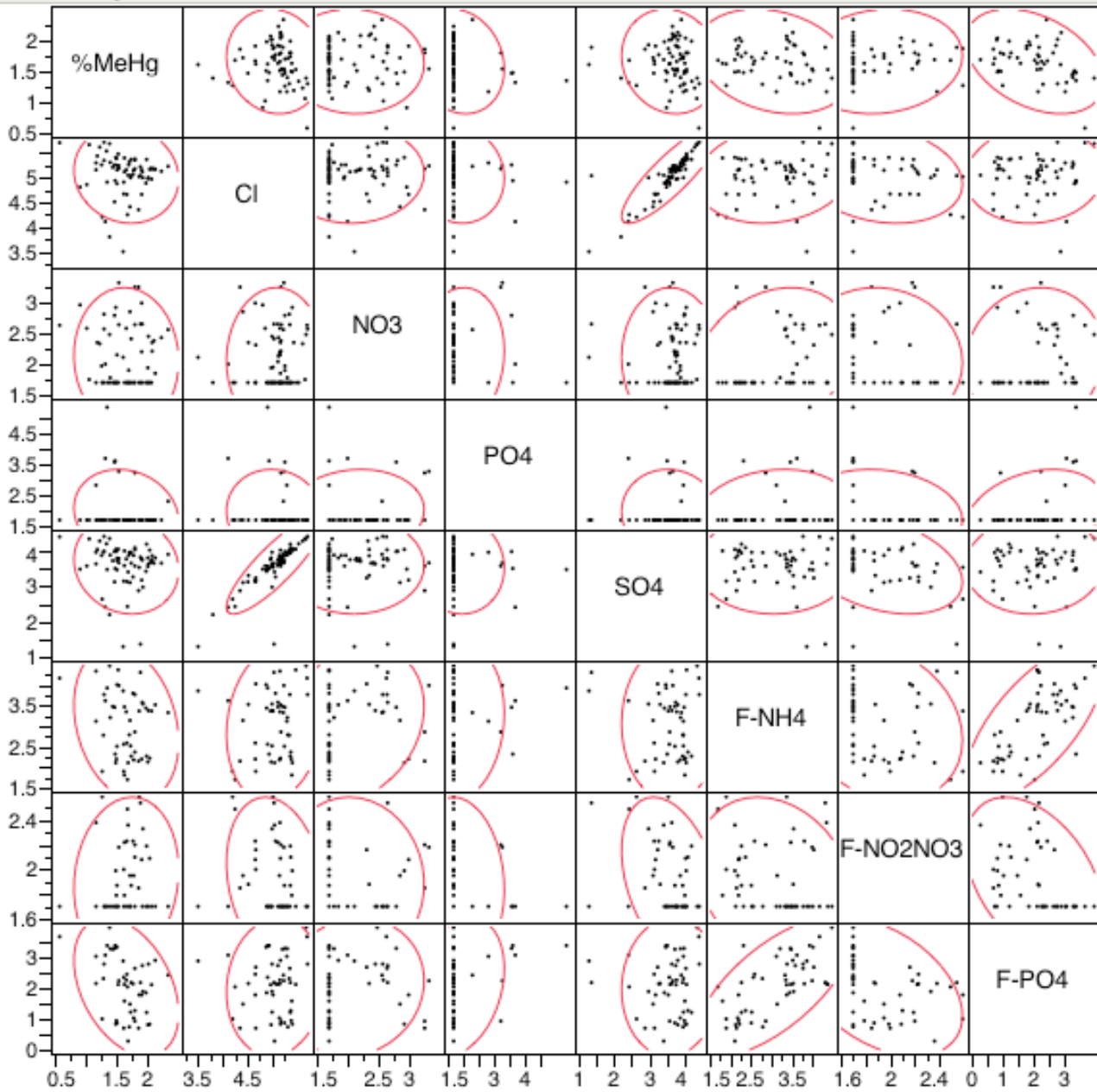


Figure 11-4.8. Scatterplot matrix for % methyl Hg in Penobscot surface sediments and soils, against pore water anions and nutrients. Variables were log transformed as needed to achieve normality.

Multivariate

Scatterplot Matrix

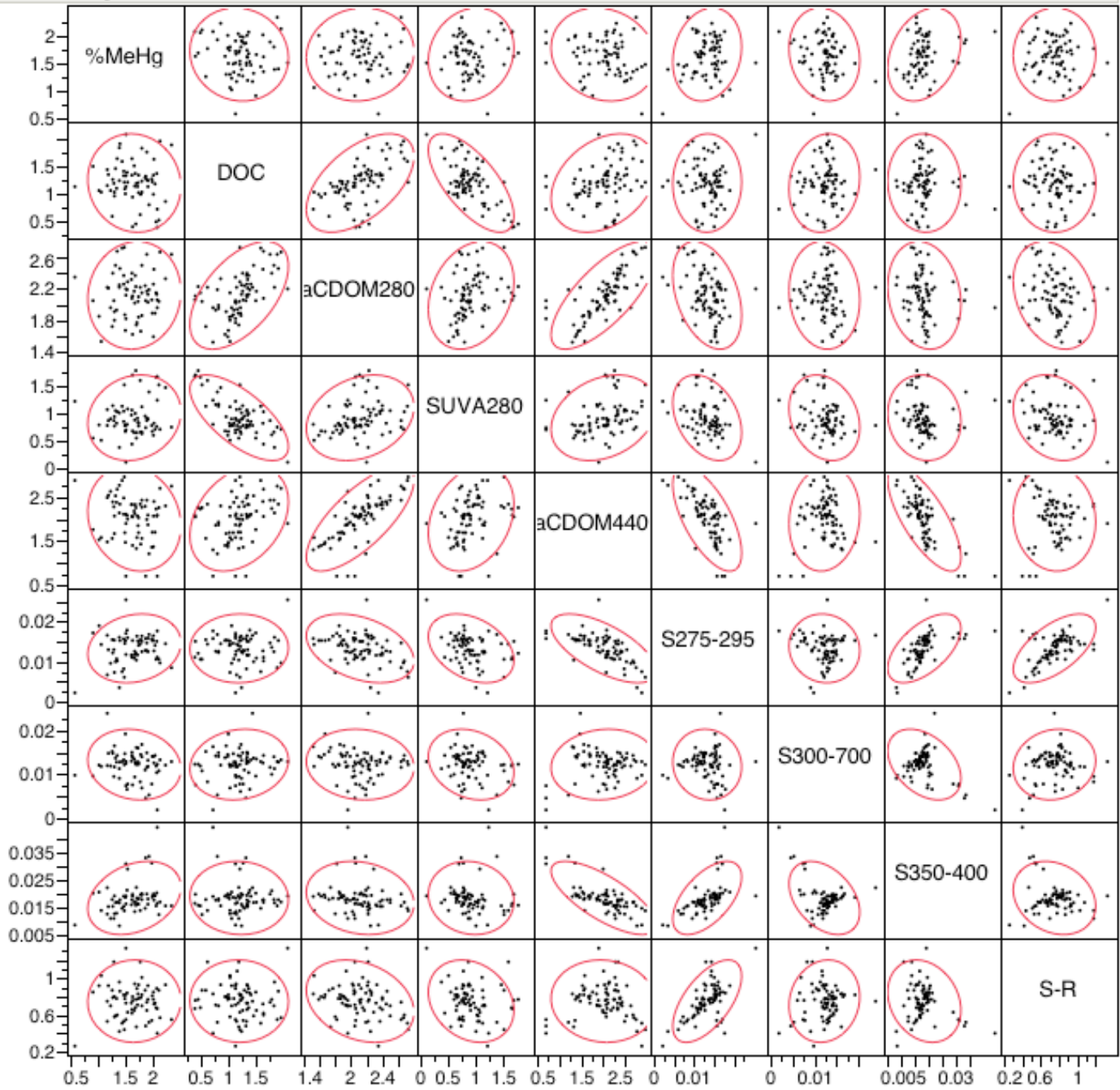


Figure 11-4.9. Scatterplot matrix for % methyl Hg in Penobscot surface sediments and soils, against pore water DOC and spectral characteristics. Variables were log transformed as needed to achieve normality.

## Multivariate

### Correlations

	%MeHg	pw Al	pw Ca	pw Fw	pw Mn	pw Na	pw P	pw S	pw Si
%MeHg	1.0000	0.3955	-0.1721	-0.0509	-0.3541	-0.1560	-0.3113	0.3177	-0.1560
pw Al	0.3955	1.0000	-0.6747	0.1029	-0.3142	-0.6271	-0.3174	-0.2672	-0.6271
pw Ca	-0.1721	-0.6747	1.0000	0.2073	0.4890	0.9648	0.6327	0.2847	0.9648
pw Fw	-0.0509	0.1029	0.2073	1.0000	0.6160	0.1878	0.4657	-0.6283	0.1878
pw Mn	-0.3541	-0.3142	0.4890	0.6160	1.0000	0.3542	0.7512	-0.0894	0.3542
pw Na	-0.1560	-0.6271	0.9648	0.1878	0.3542	1.0000	0.5456	0.2693	1.0000
pw P	-0.3113	-0.3174	0.6327	0.4657	0.7512	0.5456	1.0000	-0.1669	0.5456
pw S	0.3177	-0.2672	0.2847	-0.6283	-0.0894	0.2693	-0.1669	1.0000	0.2693
pw Si	-0.1560	-0.6271	0.9648	0.1878	0.3542	1.0000	0.5456	0.2693	1.0000

There are 80 missing values. The correlations are estimated by REML method.

### Scatterplot Matrix

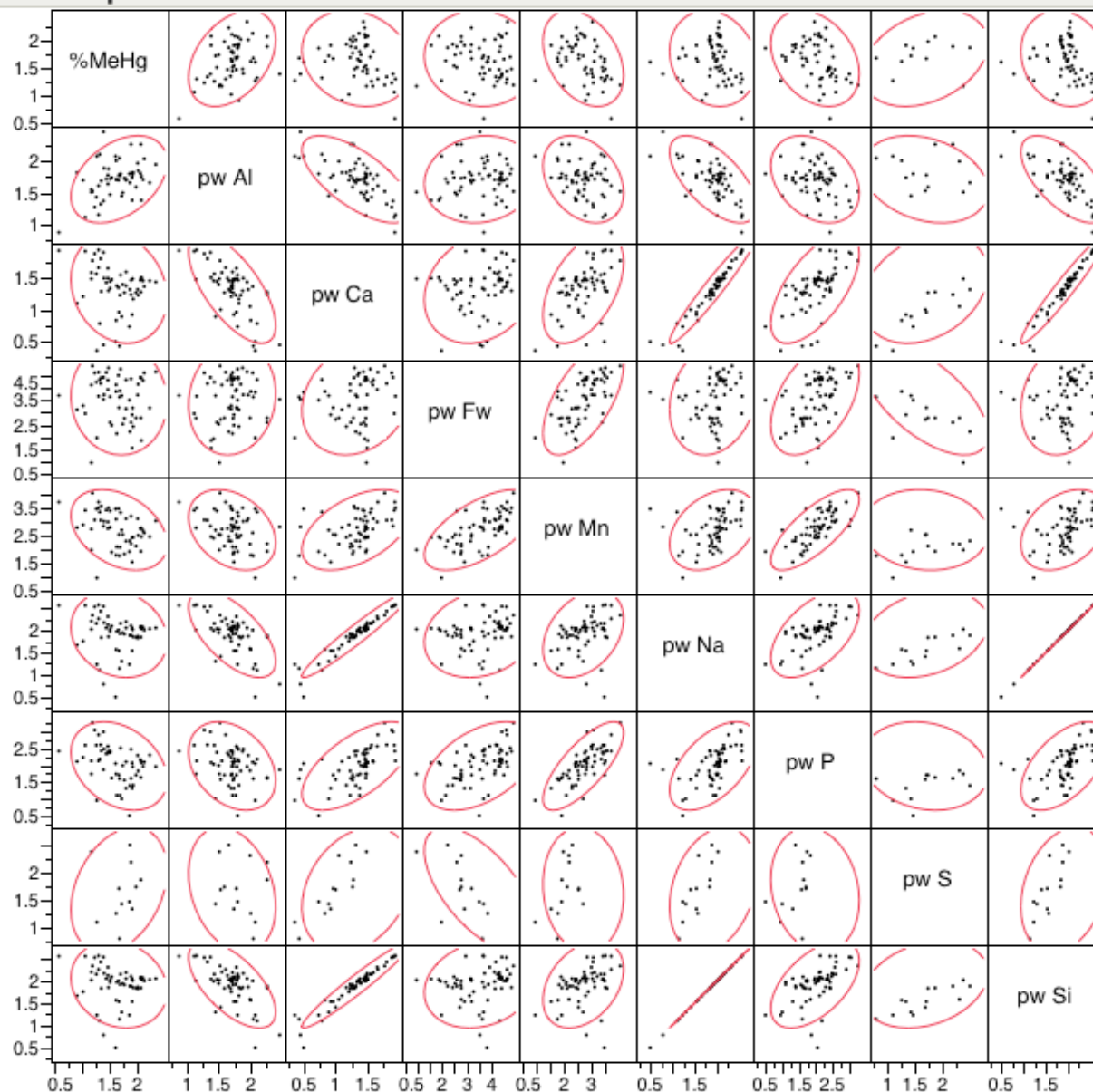


Figure 11-4.10. Scatterplot matrix for % methyl Hg in Penobscot surface sediments and soils, against pore water metal concentrations. Variables were log transformed as needed to achieve normality.

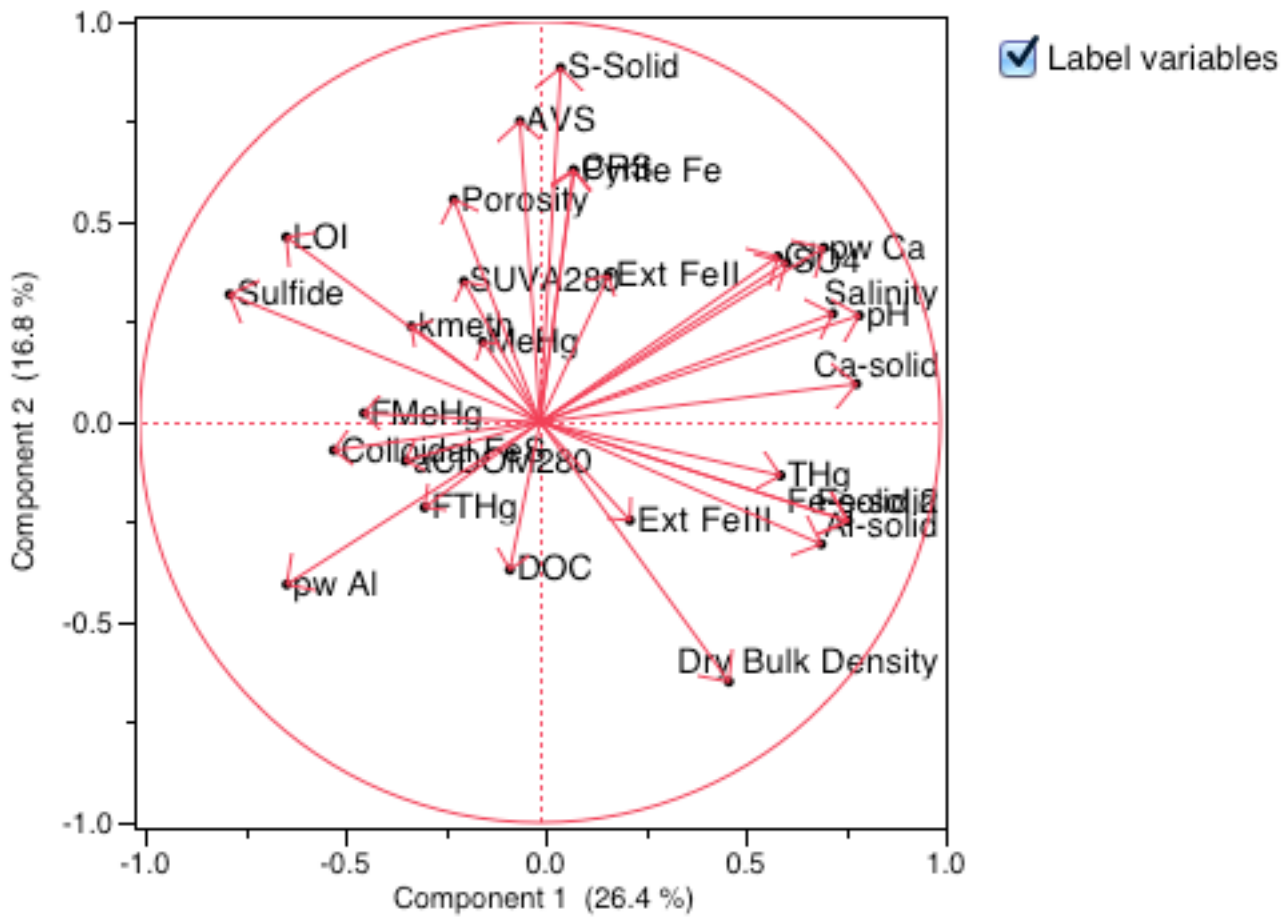


Figure 11-4.11 Loading plot for the first two principal components of a PC analysis of all measured variables for the surface interval data set.

## Multivariate

### Correlations

	kmeth	Dry Bulk Density	Wet Bulk Density	Porosity	LOI	THg	MeHg	%MeHg
kmeth	1.0000	-0.2889	-0.1121	0.2273	0.0376	0.0644	0.3705	0.3224
Dry Bulk Density	-0.2889	1.0000	0.8601	-0.7647	-0.8481	0.3239	-0.3129	-0.5327
Wet Bulk Density	-0.1121	0.8601	1.0000	-0.5371	-0.7075	0.1016	-0.3414	-0.4062
Porosity	0.2273	-0.7647	-0.5371	1.0000	0.5817	0.0235	0.4974	0.4721
LOI	0.0376	-0.8481	-0.7075	0.5817	1.0000	-0.6027	0.1778	0.5923
THg	0.0644	0.3239	0.1016	0.0235	-0.6027	1.0000	0.3254	-0.3745
MeHg	0.3705	-0.3129	-0.3414	0.4974	0.1778	0.3254	1.0000	0.7548
%MeHg	0.3224	-0.5327	-0.4062	0.4721	0.5923	-0.3745	0.7548	1.0000

There are 43 missing values. The correlations are estimated by REML method.

### Scatterplot Matrix

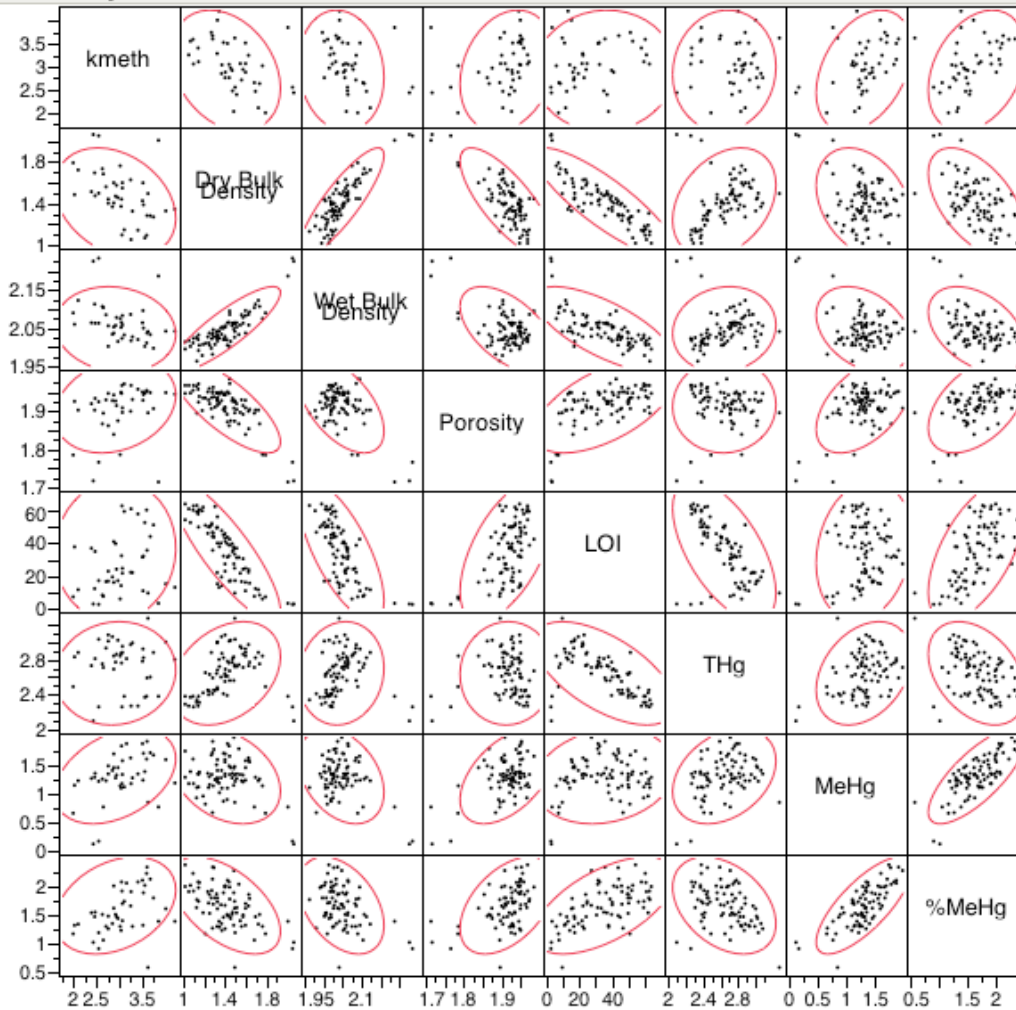


Figure 11-4.12. Scatterplot matrix for the methylation rate constant ( $k_{\text{meth}}$ ) in Penobscot surface sediments and soils, against soil physical parameters, organic content and bulk Hg. Variables were log transformed as needed to achieve normality.

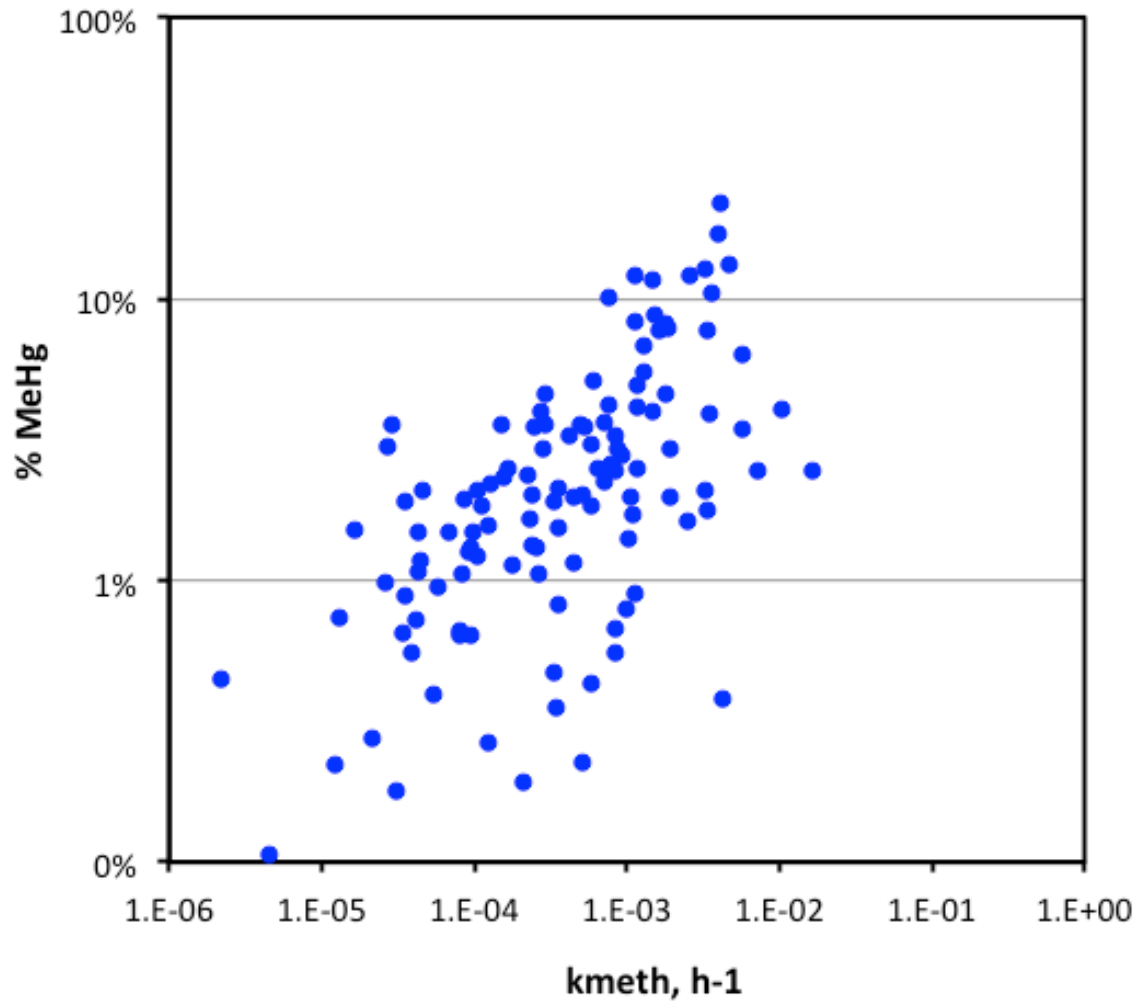


Figure 11-4.13. Relationship between % methyl Hg in sediments and soils, and the measured methylation rate constant. Unlike Figure 11-4.11 (which is surface intervals only), this figure includes data from all dates and depths.

## Multivariate

### Correlations

	kmeth	pH	Sulfide	Salinity	FTHg	KD THg	DOC	aCDOM280
kmeth	1.0000	-0.4120	0.1297	-0.0659	0.3558	-0.3341	0.1675	0.3892
pH	-0.4120	1.0000	-0.4501	0.5696	-0.3339	0.4841	-0.1184	-0.2579
Sulfide	0.1297	-0.4501	1.0000	-0.4387	0.1455	-0.3991	-0.0415	0.2233
Salinity	-0.0659	0.5696	-0.4387	1.0000	-0.2386	0.3950	-0.1443	-0.2720
FTHg	0.3558	-0.3339	0.1455	-0.2386	1.0000	-0.8831	0.1134	0.3719
KD THg	-0.3341	0.4841	-0.3991	0.3950	-0.8831	1.0000	-0.0510	-0.2684
DOC	0.1675	-0.1184	-0.0415	-0.1443	0.1134	-0.0510	1.0000	0.5417
aCDOM280	0.3892	-0.2579	0.2233	-0.2720	0.3719	-0.2684	0.5417	1.0000

There are 45 missing values. The correlations are estimated by REML method.

### Scatterplot Matrix

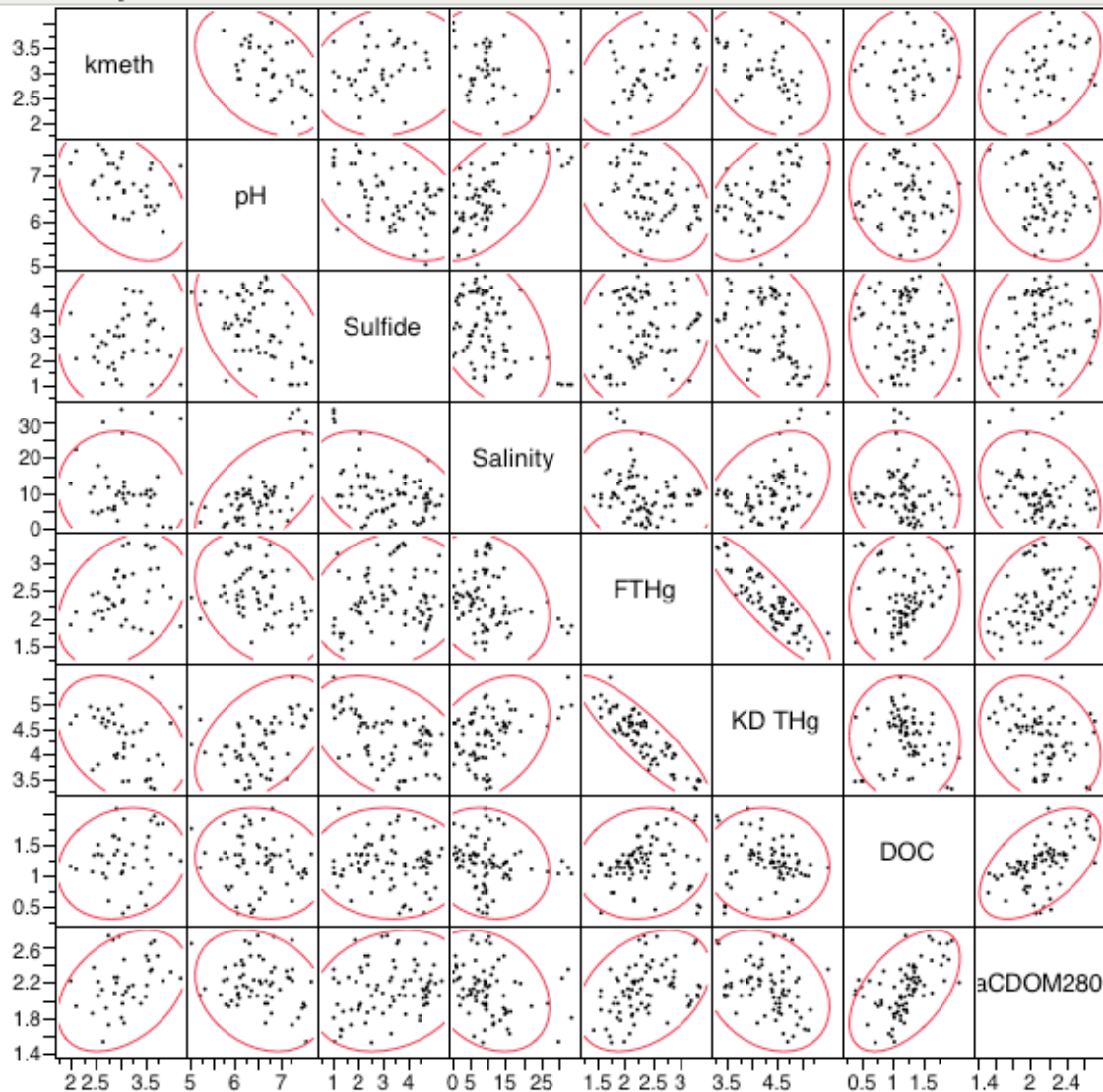


Figure 11-4.14. Scatterplot matrix for the methylation rate constant ( $k_{\text{meth}}$ ) in Penobscot surface sediments and soils, against selected pore water parameters. Variables were log transformed as needed to achieve normality.

## Multivariate

### Correlations

	KD THg	KD MeHg	Dry Bulk Density	LOI	CRS	Fe-solid	Al-solid	pH	Sulfide	Salinity
KD THg	1.0000	0.7723	0.1405	-0.2804	0.0508	0.2878	0.1418	0.3003	-0.4692	0.4021
KD MeHg	0.7723	1.0000	0.0541	-0.0920	-0.1510	0.2129	0.0678	0.0815	-0.5350	0.2957
Dry Bulk Density	0.1405	0.0541	1.0000	-0.8469	-0.1834	0.4224	0.5093	0.2298	-0.4771	0.1227
LOI	-0.2804	-0.0920	-0.8469	1.0000	-0.0564	-0.6047	-0.6455	-0.4169	0.5373	-0.2674
CRS	0.0508	-0.1510	-0.1834	-0.0564	1.0000	-0.2219	-0.2133	0.2233	0.2874	-0.0091
Fe-solid	0.2878	0.2129	0.4224	-0.6047	-0.2219	1.0000	0.9122	0.4370	-0.6988	0.2511
Al-solid	0.1418	0.0678	0.5093	-0.6455	-0.2133	0.9122	1.0000	0.4503	-0.5530	0.1331
pH	0.3003	0.0815	0.2298	-0.4169	0.2233	0.4370	0.4503	1.0000	-0.3404	0.5747
Sulfide	-0.4692	-0.5350	-0.4771	0.5373	0.2874	-0.6988	-0.5530	-0.3404	1.0000	-0.4274
Salinity	0.4021	0.2957	0.1227	-0.2674	-0.0091	0.2511	0.1331	0.5747	-0.4274	1.0000

There are 47 missing values. The correlations are estimated by REML method.

### Scatterplot Matrix

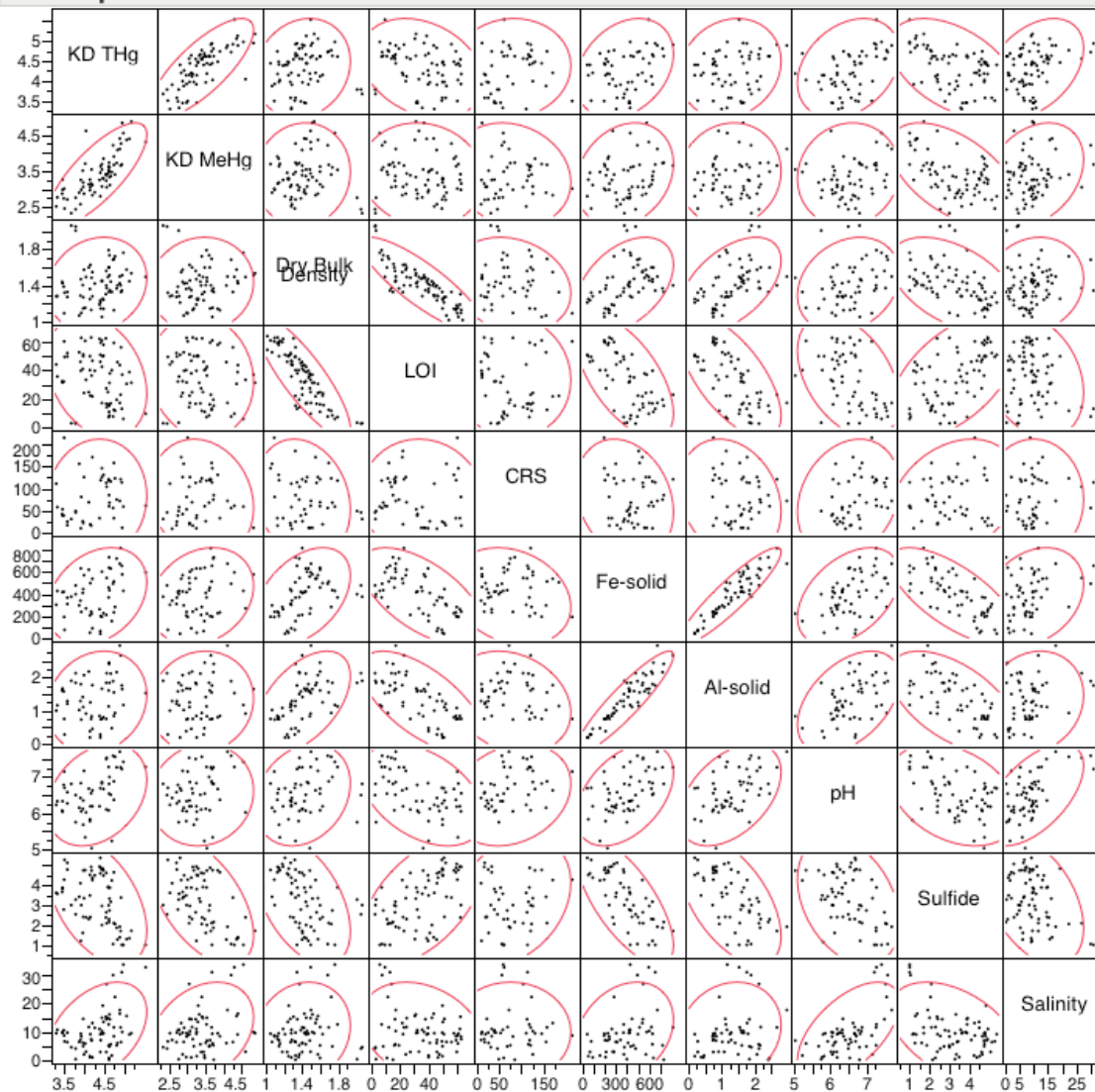


Figure 11-4.15. Scatterplot matrix for total Hg and methyl Hg  $K_D$ s for Penobscot surface sediments and soils, against soil physical parameters, and pore water pH, sulfide and salinity. Pore water metal concentrations. Variables were log transformed as needed to achieve normality.

## Multivariate

### Correlations

	KD THg	KD MeHg	DOC	aCDOM280	SUVA280	aCDOM440	S275-295	S300-700	S350-400	S-R
KD THg	1.0000	0.7686	-0.1432	-0.3320	-0.1282	-0.0265	-0.2028	0.2304	-0.2249	-0.0916
KD MeHg	0.7686	1.0000	-0.1863	-0.3178	-0.0663	-0.0510	-0.1388	0.2198	-0.1533	-0.0433
DOC	-0.1432	-0.1863	1.0000	0.5437	-0.6739	0.3221	0.0201	0.1229	-0.0392	-0.0128
aCDOM280	-0.3320	-0.3178	0.5437	1.0000	0.2536	0.7320	-0.3699	-0.0896	-0.1608	-0.2688
SUVA280	-0.1282	-0.0663	-0.6739	0.2536	1.0000	0.2726	-0.3502	-0.2234	-0.0966	-0.2217
aCDOM440	-0.0265	-0.0510	0.3221	0.7320	0.2726	1.0000	-0.6518	0.0939	-0.7351	-0.0613
S275-295	-0.2028	-0.1388	0.0201	-0.3699	-0.3502	-0.6518	1.0000	-0.0671	0.5728	0.6083
S300-700	0.2304	0.2198	0.1229	-0.0896	-0.2234	0.0939	-0.0671	1.0000	-0.3857	0.1114
S350-400	-0.2249	-0.1533	-0.0392	-0.1608	-0.0966	-0.7351	0.5728	-0.3857	1.0000	-0.2213
S-R	-0.0916	-0.0433	-0.0128	-0.2688	-0.2217	-0.0613	0.6083	0.1114	-0.2213	1.0000

There are 11 missing values. The correlations are estimated by REML method.

### Scatterplot Matrix

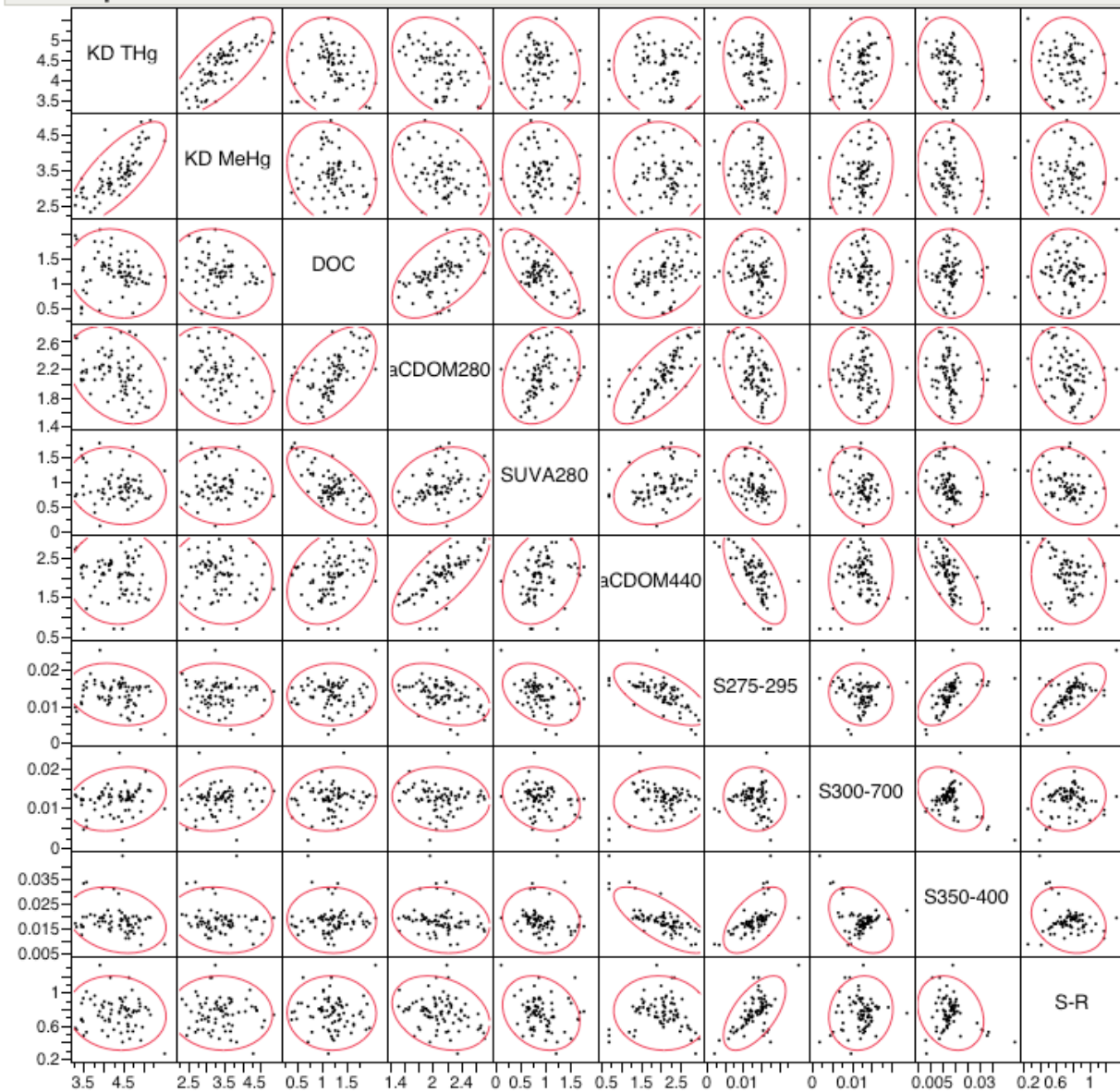


Figure 11-4.16. Scatterplot matrix for total Hg and methyl Hg  $K_D$ s for Penobscot surface sediments and soils, against pore water DOC concentrations and spectral parameters. Variables were log transformed as needed to achieve normality.

## Multivariate

### Correlations

	KD THg	KD MeHg	pw Al	pw Ca	pw S	Colloidal FeS	pw Fe
KD THg	1.0000	0.7696	-0.5135	0.2492	-0.0332	-0.5678	0.0306
KD MeHg	0.7696	1.0000	-0.3838	0.2308	-0.1381	-0.5526	0.0173
pw Al	-0.5135	-0.3838	1.0000	-0.6791	-0.3769	0.4814	0.1009
pw Ca	0.2492	0.2308	-0.6791	1.0000	0.8270	-0.3364	0.2071
pw S	-0.0332	-0.1381	-0.3769	0.8270	1.0000	-0.1802	0.3726
Colloidal FeS	-0.5678	-0.5526	0.4814	-0.3364	-0.1802	1.0000	0.2860
pw Fe	0.0306	0.0173	0.1009	0.2071	0.3726	0.2860	1.0000

There are 68 missing values. The correlations are estimated by REML method.

### Scatterplot Matrix

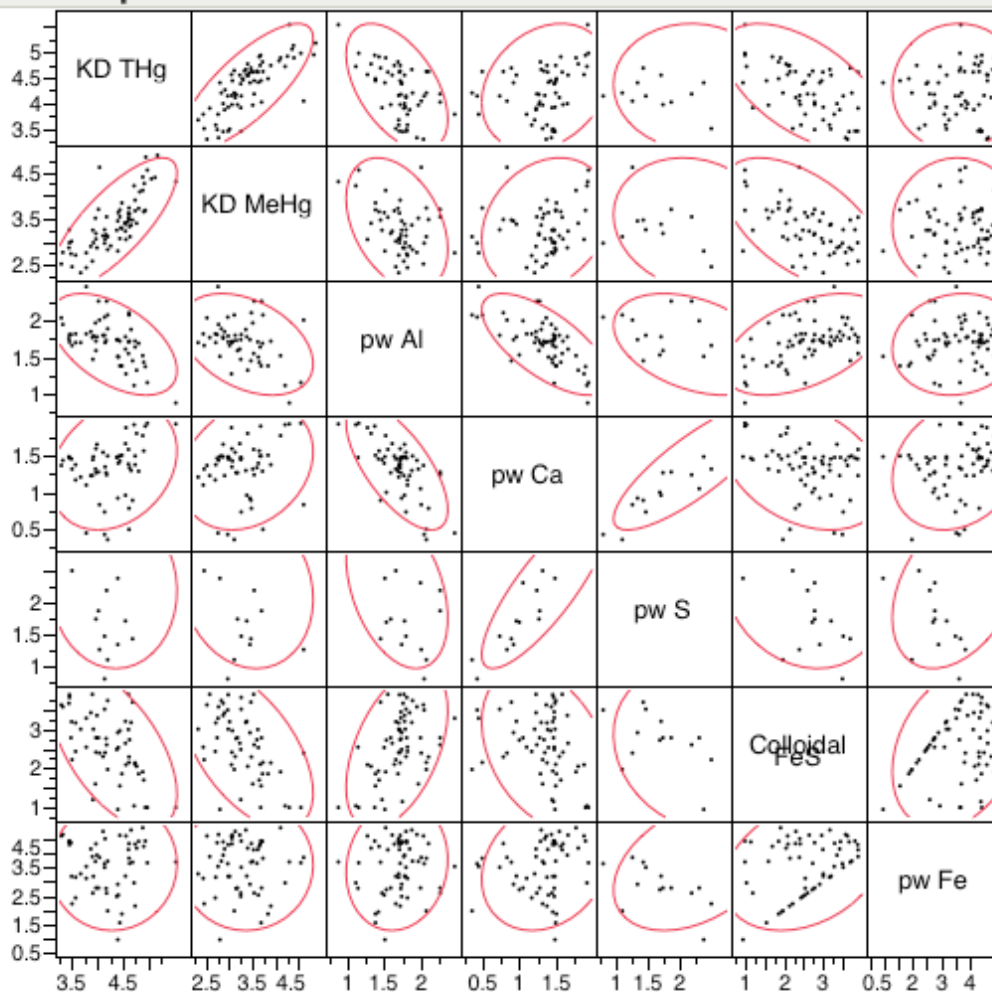


Figure 11-4.17. Scatterplot matrix for total Hg and methyl Hg  $K_D$ s for Penobscot surface sediments and soils, against pore water metals and colloidal FeS. Variables were log transformed as needed to achieve normality.

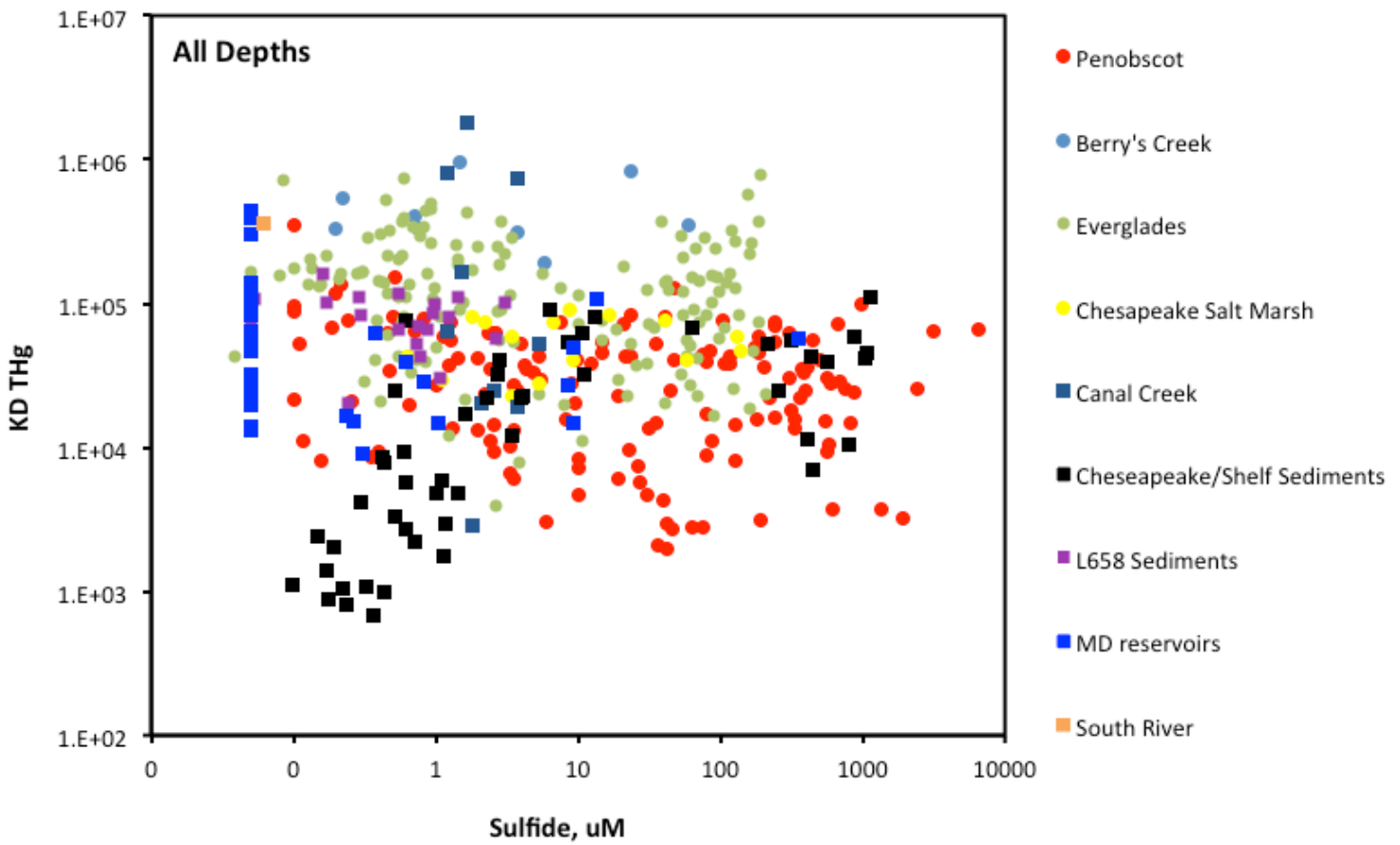


Figure 11-4.18. Sediment:water partition coefficients vs. pore water sulfide for the ecosystems compared in Section 3. Each point represents the average value for a site/date/depth combination. Data for depths up to 12 cm are included.

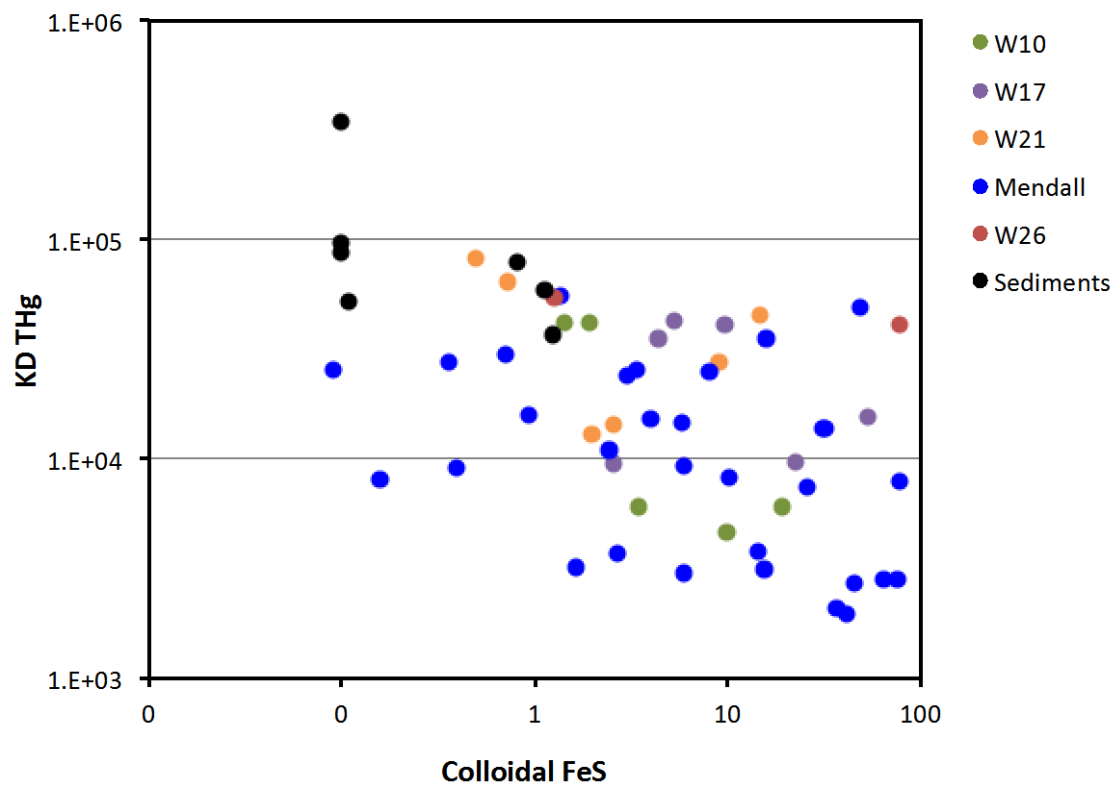
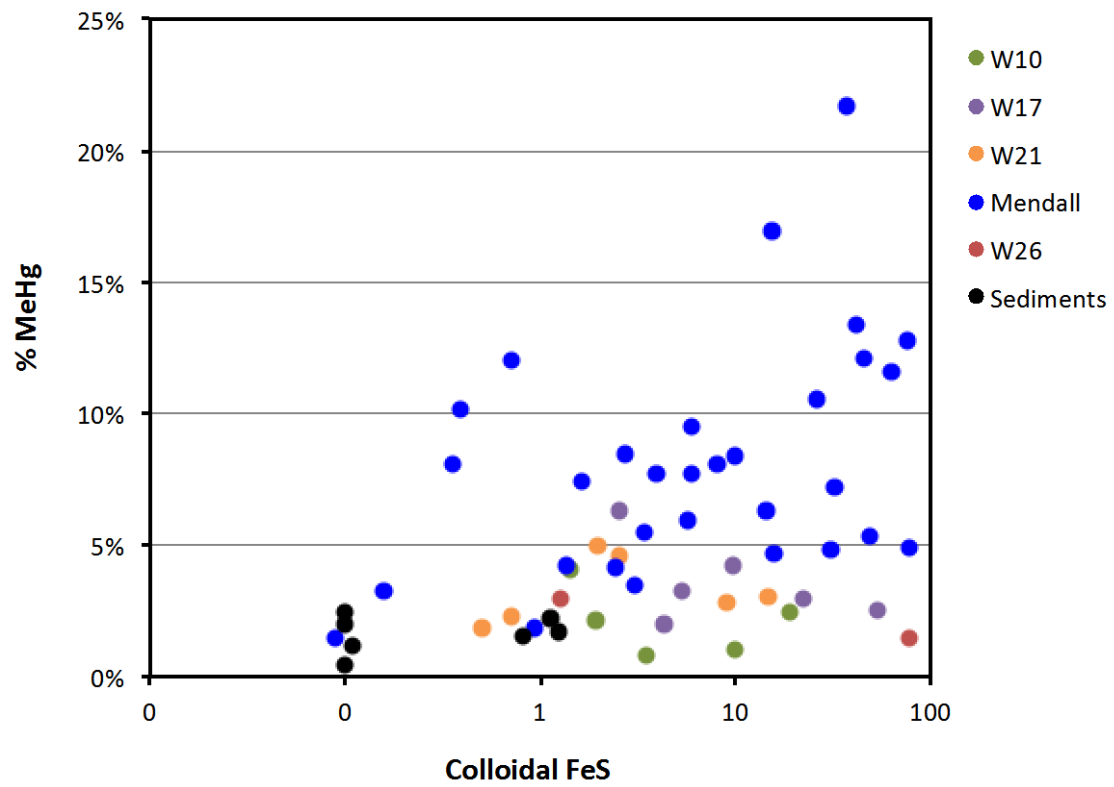


Figure 11-4.19. Relationship between colloidal FeS in pore waters, and % methyl Hg in sediments and soils (top) and the  $K_D$  for total Hg (bottom). Data shown are for surface samples only.

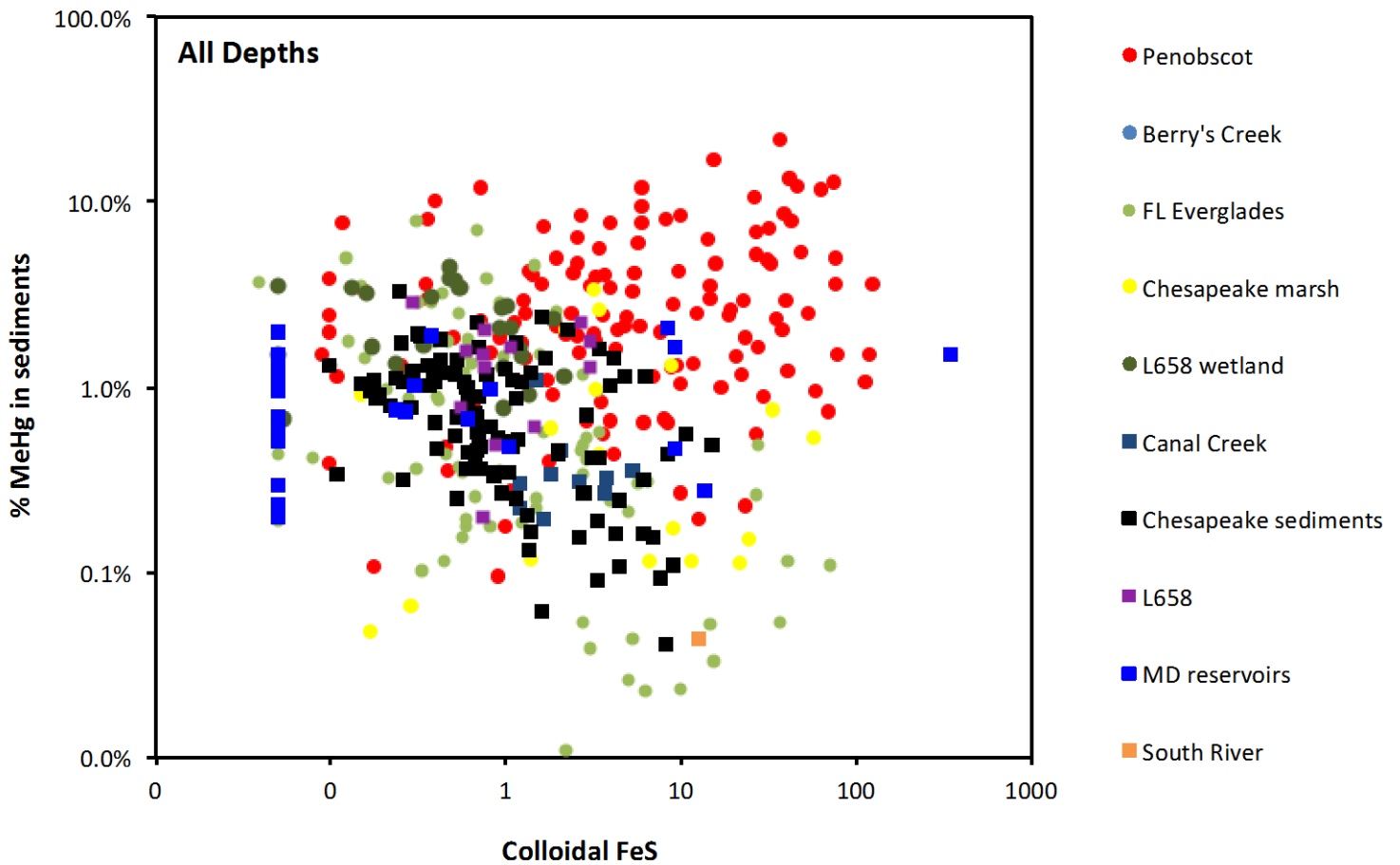


Figure 11-4.20. Relationship between the calculated concentration of colloidal FeS in pore water (see text) and % methyl Hg in sediment and soils for the ecosystems compared in Section 3. Each point represents the average value for a site/date/depth combination. Data for depths up to 12 cm are included.

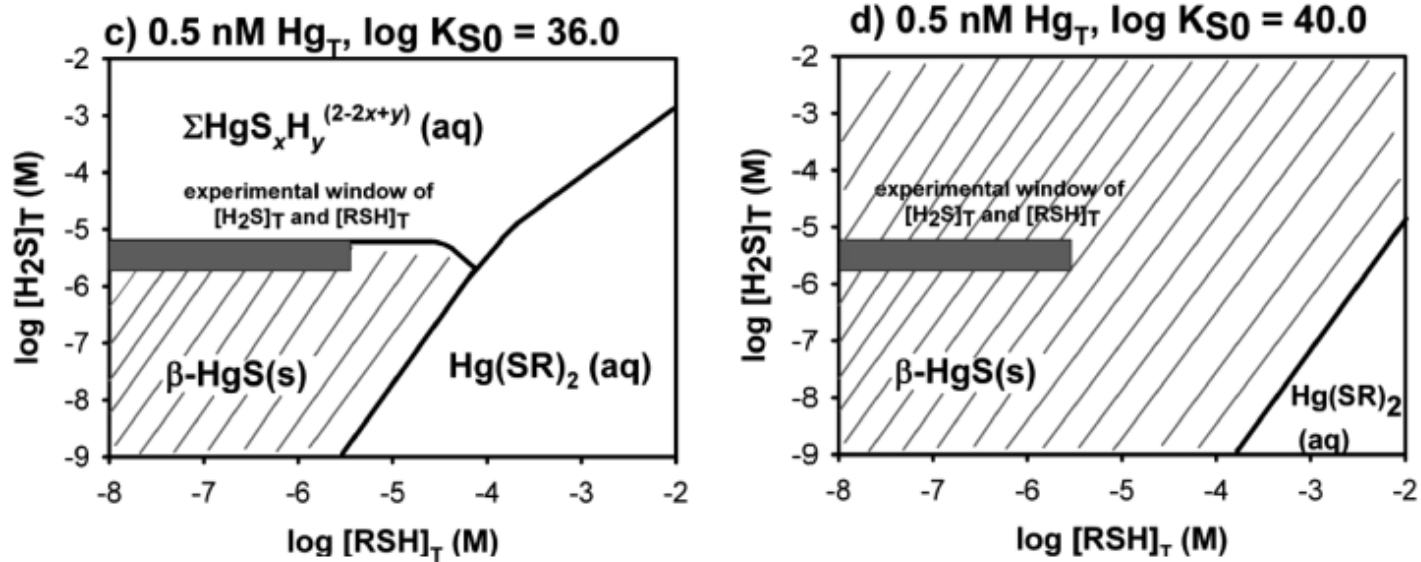


Fig 114.21. Phase diagram for 0.5 nM Hg (100 ng/l) across gradients of dissolved sulfide and DOM thiol concentrations, under controlled conditions in artificial solution. From Graham et al. 2012.

## SECTION 5. REFERENCES

- Aiken, G.R., C.C. Gilmour, D.P. Krabbenhoft, W. Orem. 2011. Dissolved Organic Matter in the Florida Everglades: Implications for Ecosystem Restoration. *Critical Reviews in Environmental Science & Technology*. 41:217-248.
- Aiken, G.R., H. Hsu-Kim, J.N. Ryan. 2011. Influence of Dissolved Organic Matter on the Environmental Fate of Metals, Nanoparticles, and Colloids. *Environmental Science & Technology*. 45:3196-3201.
- Babiarz, C., S. Hoffmann, A. Wieben, J. Hurley, A. Andren, M. Shafer, D. Armstrong. 2012. Watershed and discharge influences on the phase distribution and tributary loading of total mercury and methylmercury into Lake Superior. *Environmental Pollution*. 161:299-310.
- Babiarz, C.L., J.P. Hurley, S.R. Hoffmann, A.W. Andren, M.M. Shafer, D.E. Armstrong. 2001. Partitioning of total mercury and methylmercury to the colloidal phase in freshwaters. *Environmental Science & Technology*. 35:4773-4782.
- Benoit, J.M., C.C. Gilmour, A. Heyes, R.P. Mason, C.L. Miller. 2003. Geochemical and biological controls over methylmercury production and degradation in aquatic ecosystems, p. 262-297. In Cai Y, Braids OC (ed.), *Biogeochemistry of Environmentally Important Trace Elements*, vol. ACS Symposium Series, vol. 835. American Chemical Society, Washington, DC.
- Benoit, J.M., C.C. Gilmour, R.P. Mason. 2001. Aspects of bioavailability of mercury for methylation in pure cultures of *Desulfobulbus propionicus* (1pr3). *Applied and Environmental Microbiology*. 67:51-58.
- Benoit, J.M., C.C. Gilmour, R.P. Mason. 2001. The influence of sulfide on solid phase mercury bioavailability for methylation by pure cultures of *Desulfobulbus propionicus* (1pr3). *Environmental Science & Technology*. 35:127-132.
- Benoit, J.M., C.C. Gilmour, R.P. Mason, A. Heyes. 1999. Sulfide controls on mercury speciation and bioavailability to methylating bacteria in sediment pore waters. *Environmental Science & Technology*. 33:951-957.
- Berner, R.A. 1970. Sedimentary pyrite formation. *American Journal of Science*. 268:1-23.
- Blum, J.E. and R. Bartha. 1980. Effect of salinity on methylation of mercury. *Bulletin of Environmental Contamination and Toxicology*. 25:404-408.
- Brouwer, H. and T.P. Murphy. 1994. Diffusion method for the determination of acid-volatile sulfides (AVS) in sediment. *Environmental Toxicology and Chemistry*. 13:1273-1275.

- Chin, Y.P., G. Aiken, E. Oloughlin. 1994. Molecular-weight, polydispersity, and spectroscopic properties of aquatic humic substances. *Environmental Science & Technology*. 28:1853-1858.
- Craig, P.J. and P.D. Bartlett. 1978. Role of hydrogen-sulfide in environmental transport of mercury. *Nature*. 275:635-637.
- Deonaraine, A. and H. Hsu-Kim. 2009. Precipitation of Mercuric Sulfide Nanoparticles in NOM-Containing Water: Implications for the Natural Environment. *Environmental Science & Technology*. 43:2368-2373.
- Deonaraine, A., B.L.T. Lau, G.R. Aiken, J.N. Ryan, H. Hsu-Kim. 2011. Effects of Humic Substances on Precipitation and Aggregation of Zinc Sulfide Nanoparticles. *Environmental Science & Technology*. 45:3217-3223.
- Fossing, H. and B.B. Jorgensen. 1989. Measurement of bacterial sulfate reduction in sediments - evaluation of a single-step chromium reduction method. *Biogeochemistry*. 8:205-222.
- Gerbig, C., J. Ryan, G. Aiken, C. Kim, J. Stegemeier, J. Moreau. 2010. Identification of metacinnabar in mixed mercury, sulfide, and dissolved organic matter solutions through chromatographic concentration and EXAFS. *Geochimica et Cosmochimica Acta*. 74:A324-A324.
- Gerbig, C.A., C.S. Kim, J.P. Stegemeier, J.N. Ryan, G.R. Aiken. 2011. Formation of Nanocolloidal Metacinnabar in Mercury-DOM-Sulfide Systems. *Environmental Science & Technology*. 45:9180-9187.
- Gilmour, C.C. and E.A. Henry. 1991. Mercury methylation in aquatic systems affected by acid deposition. *Environmental Pollution*. 71:131-169.
- Gilmour, C.C., E.A. Henry, R. Mitchell. 1992. Sulfate stimulation of mercury methylation in fresh-water sediments. *Environmental Science & Technology*. 26:2281-2287.
- Gilmour, C.C., G.S. Riedel, M.C. Ederington, J.T. Bell, J.M. Benoit, G.A. Gill, M.C. Stordal. 1998. Methylmercury concentrations and production rates across a trophic gradient in the northern Everglades. *Biogeochemistry*. 40:327-345.
- Golding, G.R., C.A. Kelly, R. Sparling, P.C. Loewen, J.W.M. Rudd, T. Barkay. 2002. Evidence for facilitated uptake of Hg(II) by *Vibrio anguillarum* and *Escherichia coli* under anaerobic and aerobic conditions. *Limnology and Oceanography*. 47:967-975.
- Golding, G.R., R. Sparling, C.A. Kelly. 2008. Effect of pH on intracellular accumulation of trace concentrations of Hg(II) in *Escherichia coli* under anaerobic conditions, as measured using a mer-lux bioreporter. *Applied and Environmental Microbiology*. 74:667-675.

- Graham, A.M., G.R. Aiken, C.C. Gilmour. 2012. Dissolved Organic Matter Enhances Microbial Mercury Methylation Under Sulfidic Conditions. *Environmental Science & Technology*. 46:2715-2723.
- Hammerschmidt, C.R. and W.F. Fitzgerald. 2004. Geochemical controls on the production and distribution of methylmercury in near-shore marine sediments. *Environmental Science & Technology*. 38:1487-1495.
- Hammerschmidt, C.R. and W.F. Fitzgerald. 2006. Methylmercury cycling in sediments on the continental shelf of southern New England. *Geochimica Et Cosmochimica Acta*. 70:918-930.
- Hammerschmidt, C.R. and W.F. Fitzgerald. 2008. Sediment-water exchange of methylmercury determined from shipboard benthic flux chambers. *Marine Chemistry*. 109:86-97.
- Hammerschmidt, C.R., W.F. Fitzgerald, P.H. Balcom, P.T. Visscher. 2008. Organic matter and sulfide inhibit methylmercury production in sediments of New York/New Jersey Harbor. *Marine Chemistry*. 109:165-182.
- Hammerschmidt, C.R., W.F. Fitzgerald, C.H. Lamborg, P.H. Balcom, P.T. Visscher. 2004. Biogeochemistry of methylmercury in sediments of Long Island Sound. *Marine Chemistry*. 90:31-52.
- Han, S.H. and G.A. Gill. 2005. Determination of mercury complexation in coastal and estuarine waters using competitive ligand exchange method. *Environmental Science & Technology*. 39:6607-6615.
- Han, S.H., G.A. Gill, R.D. Lehman, K.Y. Choe. 2006. Complexation of mercury by dissolved organic matter in surface waters of Galveston Bay, Texas. *Marine Chemistry*. 98:156-166.
- Harris, R.C., J.W.M. Rudd, M. Amyot, C.L. Babiarz, K.G. Beaty, P.J. Blanchfield, R.A. Bodaly, B.A. Branfireun, C.C. Gilmour, J.A. Graydon, A. Heyes, H. Hintelmann, J.P. Hurley, C.A. Kelly, D.P. Krabbenhoft, S.E. Lindberg, R.P. Mason, M.J. Paterson, C.L. Podemski, A. Robinson, K.A. Sandilands, G.R. Southworth, V.L.S. Louis, M.T. Tate. 2007. Whole-ecosystem study shows rapid fish-mercury response to changes in mercury deposition. *Proceedings of the National Academy of Sciences of the United States of America*. 104:16586-16591.
- Helms, J.R., A. Stubbins, J.D. Ritchie, E.C. Minor, D.J. Kieber, K. Mopper. 2008. Absorption spectral slopes and slope ratios as indicators of molecular weight, source, and photobleaching of chromophoric dissolved organic matter. *Limnology and Oceanography*. 53:955-969.
- Hollweg, T.A., C.C. Gilmour, R.P. Mason RP. 2010. Mercury and methylmercury cycling in sediments of the mid-Atlantic continental shelf and slope. *Limnology and Oceanography*. 55:2703-2722.

- Hollweg, T.A., C.C. Gilmour, R.P. Mason. 2009. Methylmercury production in sediments of Chesapeake Bay and the mid-Atlantic continental margin. *Marine Chemistry*. 114:86-101.
- Krabbenhoft, D.P., J.M. Benoit, C.L. Babiarz, J.P. Hurley, A.W. Andren. 1995. Mercury cycling in the Allequash Creek watershed, Northern Wisconsin. *Water Air and Soil Pollution*. 80:425-433.
- Kelly, C.A., J.W.M. Rudd, M.H. Holoka. 2003. Effect of pH on mercury uptake by an aquatic bacterium: implications for Hg cycling. *Environmental Science & Technology*. 37: 2941-2946.
- Lee, S., S. Han, G.A. Gill. 2011. Estuarine mixing behavior of colloidal organic carbon and colloidal mercury in Galveston Bay, Texas. *Journal of Environmental Monitoring*. 13:1703-1708.
- Lichte, F.E., A.L. Meier, J.G. Crock. 1987. Determination of the rare-earth elements in geological-materials by inductively coupled plasma mass-spectrometry. *Analytical Chemistry*. 59:1150-1157.
- Liu, B., L.A. Schaider, R.P. Mason, M.S. Bank, N.N. Rabalais, P.W. Swarzenski, J.P. Shine, T. Hollweg, D.B. Senn. 2009. Disturbance impacts on mercury dynamics in northern Gulf of Mexico sediments. *Journal of Geophysical Research-Biogeosciences*. 114.
- Lovley, D.R. and E.J.P. Phillips. 1986. Organic-matter mineralization with reduction of ferric iron in anaerobic sediments. *Applied and Environmental Microbiology*. 51:683-689.
- Mitchell, C.P.J., B.A. Branfireun, R.K. Kolka. 2009. Methylmercury dynamics at the upland-peatland interface: Topographic and hydrogeochemical controls. *Water Resources Research*. 45.
- Mitchell, C.P.J., B.A. Branfireun, R.K. Kolka. 2008. Spatial characteristics of net methylmercury production hot spots in peatlands. *Environmental Science & Technology*. 42:1010-1016.
- Mitchell, C.P.J. and C.C. Gilmour. 2008. Methylmercury production in a Chesapeake Bay salt marsh. *Journal of Geophysical Research-Biogeosciences*. 113.
- Munthe, J., R.A. Bodaly, B.A. Branfireun, C.T. Driscoll, C.C. Gilmour, R. Harris, M. Horvat, M. Lucotte, O. Malm. 2007. Recovery of mercury-contaminated fisheries. *Ambio*. 36:33-44.
- Ogrinc, N., M. Monperrus, J. Kotnik, V. Fajon, K. Vidimova, D. Amouroux, D. Kocman, E. Tessier, S. Zizek, M. Horvat. 2007. Distribution of mercury and methylmercury in deep-sea surficial sediments of the Mediterranean Sea. *Marine Chemistry*. 107:31-48.

- Orem, W., C. Gilmour, D. Axelrad, D. Krabbenhoft, D. Scheidt, P. Kalla, P. McCormick, M. Gabriel, G. Aiken. 2011. Sulfur in the South Florida Ecosystem: Distribution, Sources, Biogeochemistry, Impacts, and Management for Restoration. *Critical Reviews in Environmental Science and Technology*. 41:249-288.
- Ravichandran, M., G.R. Aiken, J.N. Ryan, M.M. Reddy. 1999. Inhibition of precipitation and aggregation of metacinnabar (mercuric sulfide) by dissolved organic matter isolated from the Florida Everglades. *Environmental Science & Technology*. 33:1418-1423.
- Rudd, J.W.M. 1995. Sources of methyl mercury to fresh-water ecosystems - a review. *Water Air and Soil Pollution*. 80:697-713.
- Schaefer, J.K. and F.M.M. Morel. 2009. High methylation rates of mercury bound to cysteine by *Geobacter sulfurreducens*. *Nature Geoscience*. 2:123-126.
- Selin, N.E. 2009. Global Biogeochemical Cycling of Mercury: A Review. *Annual Review of Environment and Resources*. 34:43-63.
- Solorzano, L. 1969. Determination of ammonia in natural waters by phenolhypochlorite method. *Limnology and Oceanography*. 14:799-801.
- Spencer, R.G.M., K.D. Butler, G.R. Aiken. 2012. Dissolved organic carbon and chromophoric dissolved organic matter properties of rivers in the USA. *Journal of Geophysical Research-Biogeosciences*. 117.
- St. Louis, V.L., J.W.M. Rudd, C.A. Kelly, K.G. Beaty, N.S. Bloom, R.J. Flett. 1994. Importance of wetlands as sources of methyl mercury to boreal forest ecosystems. *Canadian Journal of Fisheries and Aquatic Sciences*. 51:1065-1076.
- Stookey, L.L. 1970. Ferrozine - a new spectrophotometric reagent for iron. *Analytical Chemistry*, 42:779-781.
- Sunderland, E.M., F. Gobas, B.A. Branfireun, A. Heyes. 2006. Environmental controls on the speciation and distribution of mercury in coastal sediments. *Marine Chemistry*. 102:111-123.
- Weishaar, J.L., G.R. Aiken, B.A. Bergamaschi, M.S. Fram, R. Fujii, K. Mopper. 2003. Evaluation of specific ultraviolet absorbance as an indicator of the chemical composition and reactivity of dissolved organic carbon. *Environmental Science & Technology*. 37:4702-4708.
- Wiener, J.G., B.C. Knights, M.B. Sandheinrich, J.D. Jeremiason, M.E. Brigham, D.R. Engstrom, L.G. Woodruff, W.F. Cannon, S.J. Balogh. 2006. Mercury in soils, lakes, and fish in Voyageurs National Park (Minnesota): Importance of atmospheric deposition and ecosystem factors. *Environmental Science & Technology*. 40:6261-6268.

Wiener, J.G. and P.J. Shields. 2000. Mercury in the Sudbury River (Massachusetts, USA): pollution history and a synthesis of recent research. *Canadian Journal of Fisheries and Aquatic Sciences*. 57:1053-1061.